Aus der

Urologischen Klinik und Poliklinik

des Klinikums der Universität München

Ludwig-Maximilians-Universität München

Direktor: Professor Dr. med. Christian G. Stief

Pathogenese und Management urologischer Infektionen

Habilitationsschrift

Zur Erlangung der Venia legendi

Im Fach

Urologie

vorgelegt von

Dr. med. Giuseppe Magistro

geboren in Fürstenfeldbruck

München 2020

Der kumulativen Habilitationsschrift liegen folgende Originalarbeiten zugrunde:

1. **Magistro G**, Westhofen T, Stief CG, Weinhold P. A matched-pair analysis of patients with medium-sized prostates (50cc) treated for male LUTS with HoLEP or TURP. Low Urin Tract Symptoms. 2019 Oct 1 **JIF: 1.701**

2. Marcon J, Schubert S, Stief CG, **Magistro G**. In vitro efficacy of phytotherapeutics suggested for prevention and therapy of urinary tract infections. Infection. 2019 May 8 **JIF: 2.927**

3. **Magistro G**, Bregenhorn P, Krauß B, Nörenberg D, D'Anastasi M, Graser A, Weinhold P, Strittmatter F, Stief CG, Staehler M. Optimized management of urolithiasis by coloured stent-stone contrast using dual-energy computed tomography (DECT). BMC Urol. 2019 Apr 30;19(1):29 **JIF: 1.583**

4. **Magistro G**, Magistro C, Stief CG, Schubert S. A simple and highly efficient method for gene silencing in Escherichia coli. J Microbiol Methods. 2018 Oct 5;154:25-32 **JIF: 1.701**

5. **Magistro G**, Magistro C, Stief CG, Schubert S. The high-pathogenicity island (HPI) promotes flagellum-mediated motility in extraintestinal pathogenic Escherichia coli. PLoS One. 2017 Oct 10;12(10) **JIF: 2.766**

6. Herlemann A, Wegner K, Roosen A, Buchner A, Weinhold P, Bachmann A, Stief CG, Gratzke C, **Magistro G**. "Finding the needle in a haystack": oncologic evaluation of patients treated for LUTS with holmium laser enucleation of the prostate (HoLEP) versus transurethral resection of the prostate (TURP). World J Urol. 2017 May 17 **JIF: 2.743**

7. Smati M*, **Magistro G* (contributed equally)**, Adiba S, Wieser A, Picard B, Schubert S, Denamur E. Strain-specific impact of the high-pathogenicity island on virulence in extra-intestinal pathogenic *Escherichia coli*. Int J Med Microbiol. 2017 Jan;307(1):44-56 **JIF: 3.298**

8. **Magistro G**, Wagenlehner FM, Grabe M, Weidner W, Stief CG, Nickel JC. Contemporary Management of Chronic Prostatitis/Chronic Pelvic Pain Syndrome. Eur Urol. 2016 Feb;69(2):286-97 **JIF: 16.265**

Inhaltsverzeichnis

1. Wissenschaftlicher und klinischer Hintergrund

Die Harnwegsinfektion (HWI) stellt eine der häufigsten bakteriellen Infektion des Menschen überhaupt dar. In der urologischen Praxis nimmt sie einen Spitzenplatz der häufigsten Diagnosen ein (1). In der stationären Krankenversorgung repräsentiert die HWI mit 22.4% neben postoperativen Wundinfektionen (22.7%) und Pneumonien (21.5%) eine der relevantesten Infektionskrankheiten (2). In Deutschland wird von 155.000 neu auftretenden nosokomialen HWIs pro Jahr berichtet (3). Aufgrund ihres daraus resultierenden Beitrages zu Morbidität, Mortalität und steigenden finanziellen Kosten haben sich HWIs weltweit zu einem bedeutenden Problem von sozioökonomischer Relevanz entwickelt. Allein in den vereinigten Staaten von Amerika belaufen sich die jährlichen Ausgaben auf etwa 2.4 Milliarden US - Dollar. Das Management der HWI fordert dabei 1.3 Millionen Konsultationen in Notaufnahmen und ca. 2.8 Millionen Arztbesuche im ambulanten Sektor (4, 5).

Die antimikrobielle Behandlung durch den Einsatz von Antibiotika ist ohne jeden Zweifel einer der bedeutendsten Meilensteine der modernen Medizin. Bereits zu Beginn des Antibiotikazeitalters erinnerten Nobelpreisträger wie der deutsche Wissenschaftler Paul Ehrlich daran, dass wir lernen müssen mit den neuen „magischen Kugeln“ die Krankheitserreger zu treffen. Der Entdecker des Penicillins, Sir Alexander Fleming, machte frühzeitig auf das Problem der Resistenzentwicklung bei nicht gewissenhaftem Einsatz der neuen Substanzen aufmerksam. Diese mahnenden Worte bewahrheiteten sich leider in den folgenden Jahren. Mit der Einführung neuer Antibiotika ließen die entsprechenden Resistenzen nicht lange auf sich warten. Durch den übermäßigen Gebrauch und Missbrauch sehen wir uns heute weltweit mit einer der größten Herausforderung der modernen Medizin in Form von multiresistenten Infektionserregern konfrontiert. Manche Berichte stellen sogar ein post-antibiotisches Zeitalter als realistische Bedrohung des 21. Jahrhunderts dar (6). Vorhersagen zu den drohenden ökonomischen Konsequenzen durch die antimikrobelle Resistenzentwicklung legen nahe, dass im Jahr 2050 etwa 10 Millionen Menschen an Infektionen durch multiresistente Erreger versterben werden, was um 2 Millionen die Todesfälle verursacht durch

onkologische Erkrankungen übersteigen wird (7). Wenn wir nicht heute unsere Praxis grundlegend überdenken, könnte die Infektiologie somit die Onkologie als Todesursache Nummer 1 ablösen. Die antibiotische Behandlung von Infektionserkrankungen gestaltete sich in der Vergangenheit als ein sicheres und effektives Vorgehen. Doch wenn wir unsere aktuelle Praxis nicht entscheidend ändern, werden in naher Zukunft keine wirksamen Therapieoptionen mehr zur Verfügung stehen. Das optimierte Management von Infektionskrankheiten wird von 4 Säulen getragen, nämlich die Entwicklung neuer Antibiotika, neue alternative antimikrobielle Strategien, effektive Hygiene - und Präventionsmaßnahmen und das Konzept des rationalen Einsatzes von Antibiotika („*Antimicrobial Stewardship*“) (8, 9). Obwohl in den letzten Jahren durch die Einführung neuer Antibiotikasubstanzen und Kombinationen wie etwa das Zoliflodacin, Ceftolozan / Tazobactam, Ceftazidim / Avibactam und Merpenem / Vaborbactam Erfolge verzeichnet werden konnten, ist dies sicherlich nicht die endgültige Lösung des Problems (10, 11). Neue vielversprechende und innovative Konzepte wie die sogenannte Anti - Virulenztherapie zielen darauf ab, die potenten Virulenzfaktoren der pathogenen Mikroorganismen zu adressieren. Dadurch werden virulente Erreger zu attenuierten Bakterien, die durch die Wirtsantwort effektiv eliminiert werden können ohne dass es dabei zu einer schädigenden Infektion kommt. Hierzu ist es notwendig, die Pathomechanismen des entsprechenden Erregerspektrums zu analysieren und die potentiellen Zielstrukturen zu identifizieren.

Im Hinblick auf die HWI wird in 75% der unkomplizierten Fälle und in 65% der komplizierten HWI die Spezies *Escherichia coli* (*E. coli*) als häufigster Erreger isoliert (4). Es handelt sich grundsätzlich um gramnegative, sporenlose, fakultativ anaerobe Stäbchenbakterien, die als Kommensale den humanen Gastrointestinaltrakt kolonisieren. Im Rahmen der Diversifizierung der Spezies gelang es *E. coli* unter bestimmtem Selektionsdruck sich an variable Nischen zu adaptieren. Ein vielfältiges Repertoire an Fitness - und Virulenzfaktoren wurde entwickelt, wodurch diese Subtypen pathogenes Potential erlangten. Neben HWIs umfasst das Infektionsspektrum intestinale Infektionen und Durchfallerkrankungen, Pneumonien, operative Wundinfektionen, bakterielle Peritonitis, Neugeborenen - Meningitis und septische Krankheitsbilder (12). Die Spezies *E. coli* lässt sich demnach entsprechend einer klinischen Klassifikation in 3 Pathotypen

unterteilen: kommensale, intestinal pathogene und extraintestinal pathogene *E. coli* (13-15).

Die häufigste durch extraintestinal pathogene *E. coli* (ExPEC) verursachte Infektion ist die HWI. Diese Isolate werden als uropathogene *E. coli* (UPEC) subsumiert. Ein vielseitiges Armamentarium an hoch effektiven Fitness - und Virulenzfaktoren befähigt UPEC erfolgreich den Harntrakt zu kolonisieren und Infektionen zu verursachen. Dieses Arsenal umfasst Invasine, Adhäsine, Toxine, Protektine, Autotransporter, Eisenaufnahmesysteme, Sekretionssysteme, Flagellen und Lipopolysaccharid (13, 16, 17). Eine der essentiellsten Funktionen besteht in der suffizienten Deckung des Eisenbedarfs der Mikroorganismen. Bis auf wenige Ausnahmen (*Treponema pallidum, Lactobacillus* spp*., Borrelia burgdoferi*) sind Bakterien ohne adäquate Zufuhr von Eisen nicht lebensfähig (18). Die Eisenhomöostase ist sowohl für Säugetiere als auch Mikroorganismen von zentraler Bedeutung (19, 20). Aufgrund der strikten Regulation des Eisenstoffwechsels im menschlichen Körper ist die frei verfügbare Eisenkonzentration (ca. 10^{-18}M) physiologisch so gering, dass die erforderliche Eisenkonzentration für replizierende Bakterien (ca. 10^{-6} bis 10^{-7}M) ungefähr 11 bis 12 Logstufen höher ausfällt. Diese effiziente Entzugsstrategie beeinträchtigt enorm die Entwicklung von Infektionserkrankungen und wird daher auch als antimikrobielle Abwehrstrategie („*nutritional immunity*“) betrachtet (18, 20). UPEC haben im Gegenzug ein hoch diffiziles System zur Eisenaufnahme entwickelt, um über spezielle Transportsysteme dreiwertiges Eisen oder eisenbeladene Haemproteine suffizient zu verwerten (18, 21-25). Besonders hervorzuheben ist eine Strategie, die dem Wirt über die Sekretion niedermolekularer Verbindungen, sogenannter Siderophore (griechisch für Eisenfänger), mit höchster Affinität gebundenes dreiwertiges Eisen entziehen kann. UPEC verfügt über bis zu 4 Siderophorsysteme, die sich anhand der chemischen Struktur in Ihrer Bindungsaffinität unterscheiden. Diese Siderophore umfassen die Katecholate Enterobactin und Salmochelin, das Hydroxamat Aerobactin und das Phenolat Yersiniabactin (Ybt). Jedes dieser Systeme besteht aus einem (i) Syntheseapparat, (ii) einem Export- und Internalisierungspfad und einem (iii) spezifischem Rezeptor an der Außenmembran.

Die vorliegende Habilitationsschrift beinhaltet experimentelle Forschungsergebnisse zum Beitrag der Siderophorsysteme für die Virulenz der UPEC im Rahmen der Pathogenese von HWIs. Diese Erkenntnisse sind hilfreich für die Entwicklung alternativer antimikrobieller Ansätze. Zudem werden potentielle antimikrobielle Strategien verfolgt, die die Pathogenität der Harnwegserreger limitieren und somit als Optionen zur Therapie und Prophylaxe von HWIs in Frage kommen. In weiteren Arbeiten werden klinische Resultate der operativen Behandlung des benignen Prostatasyndroms (BPS) mit dem Referenzverfahren der transurethralen Resektion der Prostata (TURP) oder neueren Laser - basierten Methoden wie der Holmium:YAG Laser Enukleation der Prostata (HoLEP) vorgestellt.

2.1 Beitrag der Siderophorsysteme zur Virulenz extraintestinal pathogener *E. coli* (ExPEC

Im ersten angeführten Projekt des Habilitanden wurde in einem Kooperationsprojekt die Rolle des Siderophores Yersiniabactin (Ybt) im Tiermodell untersucht (26). Das Yersiniabactin - System ist auf einem Gencluster namens High - Pathogenicity Island (HPI) lokalisiert, das bei *Enterobacteriacea* wie zum Beispiel *E. coli*, *Pseudomonas* spp., *Klebsiella* spp. , *Serratia* spp. , *Salmonella* spp., *Citrobacter* spp. und *Enterobacter* spp. identifiziert werden kann (27-30). Vor allem unter den UPEC liegt es mit einer hohen Prävalenz von über 70% vor. Das mobile Gencluster der HPI ist strukturell aus 11 Genen zusammengesetzt, die in 4 Operons organisiert sind. Das Siderophor zeigt eine hohe Bindungsaffinität zu dreiwertigem Eisen mit einer Dissoziationskonstante K_d von $4x10^{-36}$ M, mit einem Optimum für neutrale bis leicht alkalische *ph* Bedingungen (31, 32). Erste Ergebnisse zeigten für diverse Isolate in verschiedenen Tiermodellen die tragende Rolle der HPI auf (33-37). Allerdings konnte aufgrund der heterogenen Datenlage keine einheitliche Beurteilung abschließend getroffen werden. Daher wurden in der vorgestellten Arbeit 3 etablierte Prototypen, isoliert aus Pyelonephritiden (CFT073, 536) und Zystitiden (NU14), genauer untersucht. Zunächst wurde unter *in vitro* Bedingungen die Transkription wichtiger Gene in allen Isolaten mittels *real - time* PCR untersucht. Die Genexpression von *ybtA*, einem spezifischen HPI - Transkriptionsfaktor, *irp2*, einem Ybt-Synthesegen, und *fyuA*, dem spezifischen Rezeptor für Ybt, wurde unter Eisenmangelbedingungen (Abb. 1A) und im Infektionsmodell (Abb. 1B) in der Zellkultur (Urothelzelllinie HCV29) analysiert. Es zeigte sich ein Anstieg der Transkriptionsrate der Indikatorgene, wobei jeweils der stärkste Anstieg für das Synthesegen *irp2* zu verzeichnen war. Ein entsprechendes Resultat wurde unter Infektionsbedingungen in der Zellkultur bestätigt. Überraschend war die deutliche Aktivität des Pyelonephritisisolates CFT073, das aufgrund von Mutationen der HPI bisher als inaktiv angesehen wurde. Somit konnte eine Aktivierung der HPI unter Eisenmangel und während Infektionsprozessen demonstriert werden.

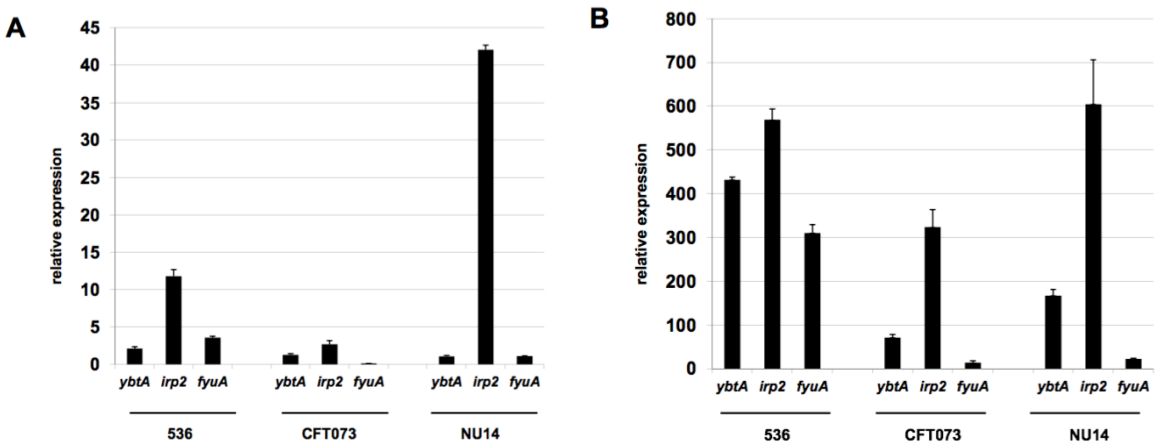

Abbildung 1. Transkriptionsanalysen der HPI-gene *ybtA*, *irp2* und *fyuA* unter Eisenmangel (A) und im Zellkulturmodell der HWI (B).

Nun galt es den Beitrag der HPI weiter zu untersuchen in Hinblick auf Siderophorproduktion und Wachstum unter Eisenmangel. Dazu wurden Knockout - Mutanten für alle Isolate generiert. Die Mutationen wurden gezielt für die Gene *ybtA*, *irp2* und *fyuA* konstruiert. Mittels Luziferase - Reporter Assay kann indirekt die Siderophorproduktion von Ybt quantifiziert werden (Abb. 2). Ybt - positive Stämme sind NU14 und 536 aufgrund einer intakten HPI, während die mutierte HPI im Stamm CFT073 bekanntermaßen nicht mehr zur Synthese befähigt ist. Erwartungsgemäß führt die Inaktivierung des Synthesegens *irp2* in beiden Stämmen NU14 und 536 zu keiner nachweisbaren Siderophorproduktion. Das gleiche konnte für die Mutante des Transkriptionsfaktor YbtA beobachtet werden, der für die volle Aktivierung der HPI unentbehrlich zu sein scheint. Interessanterweise resultierte die Inaktivierung des spezifischen Ybt - Rezeptors zu einer signifikanten Reduktion der Ybt - Produktion (p<0.05). Die entsprechenden Revertanten der *irp2* und *ybtA* Mutanten zeigten erneut eine volle Syntheseleistung wie in den Wildtyp - Stämmen NU14 und 536, wodurch gemäß Koch’schen Postulates die Funktionseinbuße auf die gezielte Mutation zurückgeführt werden kann.

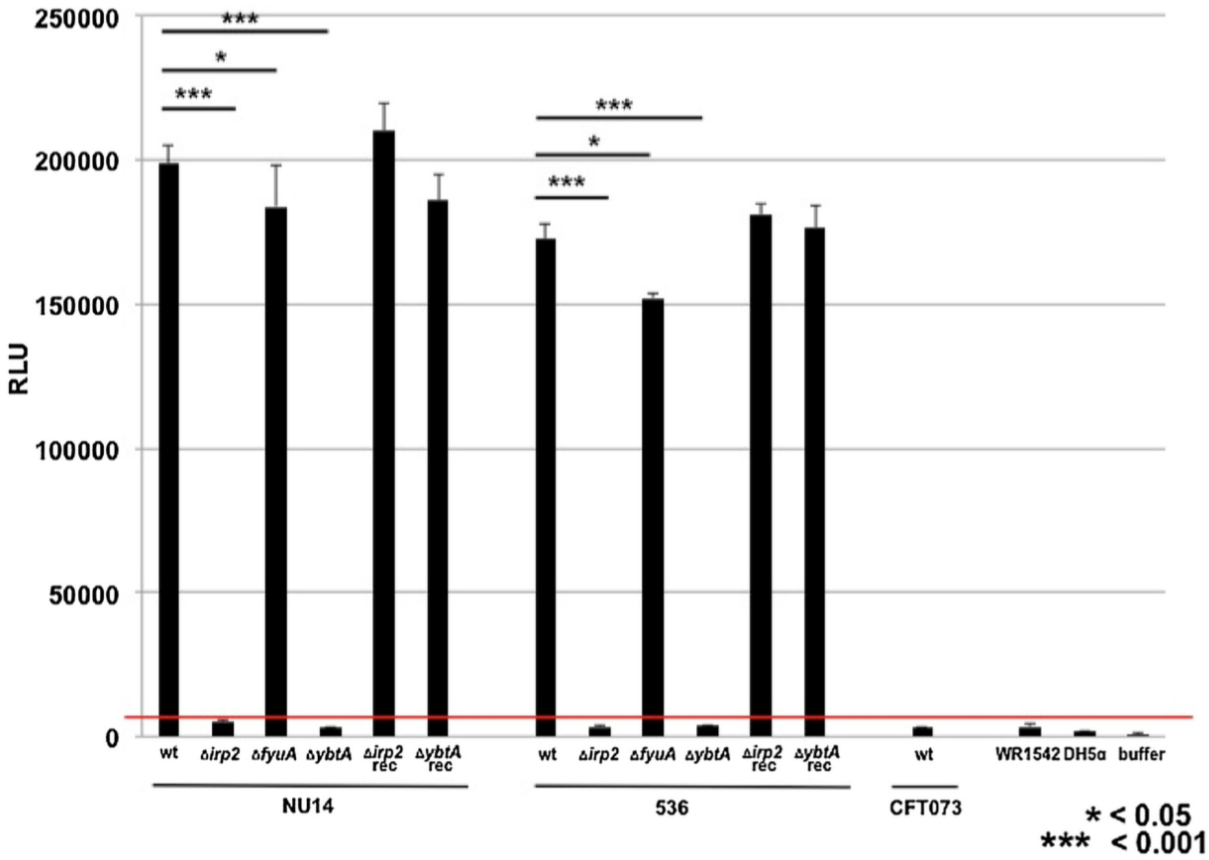

Abbildung 2. Luziferase - Reporter Assay zur Quantifizierung der Ybt - Produktion unter Eisenmangel. RLU: relative light units

Die Bedeutung einer intakten HPI für das Wachstum unter Eisenmangel kann in Wachstumsversuchen *in vitro* adäquat evaluiert werden (Abb. 3). In den Ybt - positiven Stämmen NU14 und 536 resultierte die gezielte Inaktivierung durch Mutation des Synthesegens *irp2* zu einem relevanten Wachstumsdefizit, welches durch Komplementierung des Zielgens *irp2* wieder reversibel war.

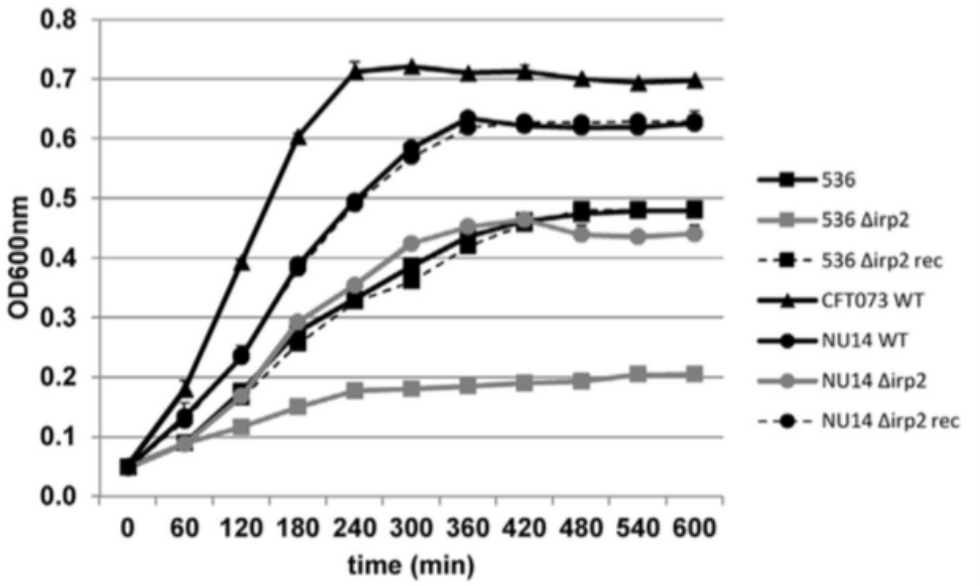

Abbildung 3. Wachstumskurven unter Eisenmangel für die UPEC Stämme 536, NU14 und CFT073. Die *irp2* - Mutanten für die Ybt - positiven Stämme NU14 und 536 zeigen ein deutliches Wachstumsdefizit.

Die Rolle der HPI für Pathogenität der UPEC wurde schließlich im murinen Modell der Sepsis evaluiert. Die Wildtyp - Stämme 536, NU14 und CFT073 wurden nach Kultivierung subkutan mit einem Inokulum von 10^9 Kolonie bildenden Einheiten in 4 Wochen alten weiblichen Mäusen injiziert, um eine Sepsis im Tiermodell auszulösen (externer genehmigter Tierversuchsantrag: AE-LU-002/12/INV MED.02/OUTROS 04). Das Überleben der Mäuse über 7 Tage wurde mit Kaplan - Meir Kurven dokumentiert (Abb. 4). Das Pyelonephritisisolat 536 stellte sich als hoch virulenter Stamm heraus, der innerhalb von 20 Stunden alle infizierten Mäuse tötete, gefolgt von Stamm CFT073, der nach 2 Tagen zum Tod durch Sepsis führte („*fast killers*“). Etwa 90% der infizierten Mäuse erlagen nach 4 Tagen einer Sepsis ausgelöst durch das Zystitisisolat NU14 („*slow killer*“). Dieser bemerkenswerte Phänotyp wurde weiter für den weniger virulenten Stamm NU14 analysiert, indem diverse Mutanten hinsichtlich Letalität untersucht wurden (Abb. 5). Im Vergleich zum Wildtyp wurde in einer kompletten HPI - Mutante, in der die gesamte HPI deletiert wurde, nur 10% der Mäuse getötet (p<0.00001). Die Rezeptor - Mutante war ebenfalls attenuierter als der Wildtyp - Stamm, da nur 50% der infizierten Mäuse einer Sepsis erlagen (p<0.001). Die Inaktivierung des Transkriptionsfaktors YbtA resultierte in einer 60%igen Letalität im Vergleich zum Wildtyp (p=0.015). Noch deutlicher war der

Effekt der *irp2* - Synthesemutante. Keine der infizierten Mäuse starb über den Beobachtungszeitraum von 7 Tagen. Zusätzliche HPI - Mutationen im Pyelonephritisisolates CFT073 zeigten bei ohnehin schon mutierter HPI keinen Effekt (nicht gezeigt). Die Beobachtung, dass eine komplette Deletion der HPI im Stamm 536 keinen relevanten Effekt auf die Letalität einer Sepsis aufzeigt, wurde vom Kooperationspartner bereits in einer früheren Arbeit publiziert (38).

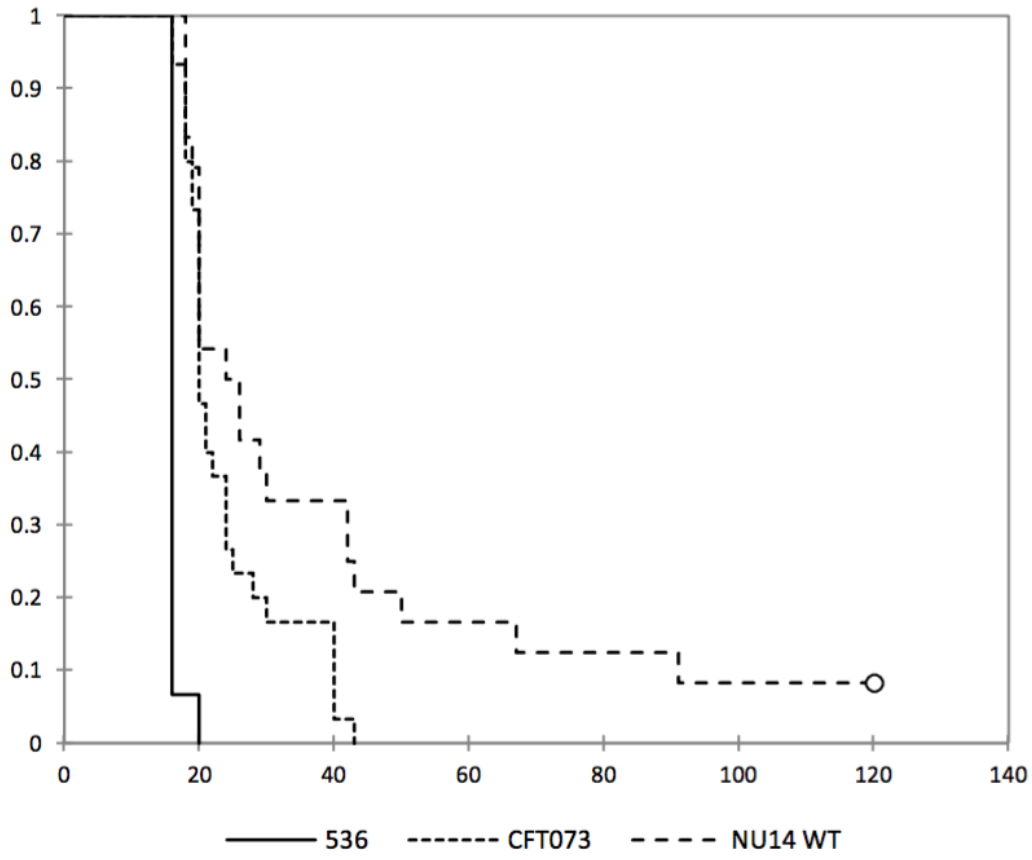

Abbildung 4. Kaplan - Meir Kurven der Sepsisletalität für die UPEC - Stämme 536, NU14 und CFT073. Es läßt sich grundsätzlich ein Unterschied in der Virulenz der Wildtyp - Stämme feststellen ("*fast killers* vs. *slow killers*")

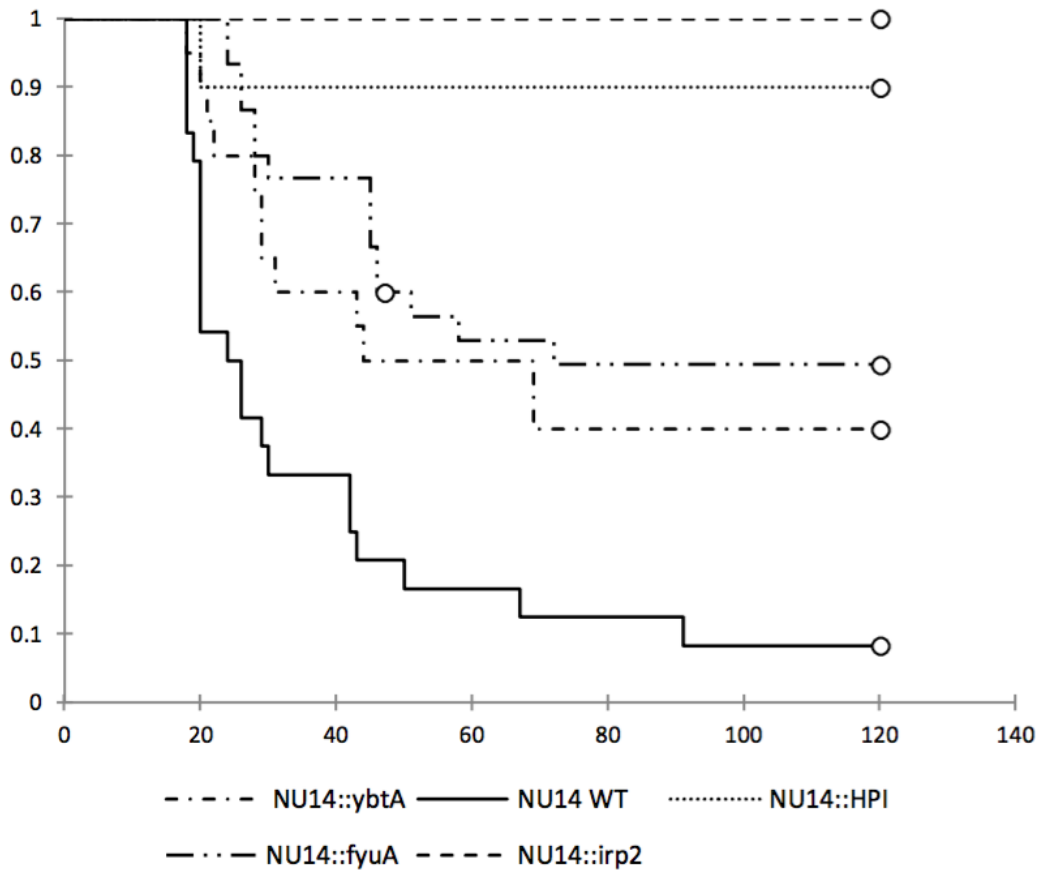

Abbildung 5. Kaplan - Meir Kurven der Sepsisletalität in unterschiedlichen HPI - Mutanten des Stammes NU14. Je größer der Einfluss durch die Mutation auf die Ybt - Synthese, desto größer der Effekt auf die Virulenz.

Zusammenfassend konnte funktionell eine bedeutende Rolle für das Ybt - System in UPEC demonstriert werden. Allerdings wurde ein stamm - spezifischer Einfluss für die experimentelle Virulenz aufgedeckt. Obwohl die HPI funktionell vergleichbaren regulatorischen Mustern folgt in diversen Isolaten, scheint doch in Abhängigkeit des genetischen Hintergrundes ein markanter Unterschied für die Virulenz vorzuliegen.

Das zweite Forschungsprojekt untersuchte nun die Interaktion der HPI mit anderen Pathomechanismen der UPEC, die nicht mit der primären Funktion als Eisenaufnahmesystem assoziiert sind (39). In einer bereits vom Habilitanden vorab publizierten Arbeit wurde die Multifunktionalität der Siderophorsysteme der ExPEC veranschaulicht. Es konnte demonstriert werden, dass die spezifischen Außenmembran-

Rezeptoren FyuA für die HPI, als auch der spezifische Rezeptor IroN für das Siderophor Salmochelin an der effektiven Biofilmbildung der ExPEC beteiligt sind (40). Für die erfolgreiche Kolonisierung des Harntraktes ist es erforderlich sich Zugang zu günstigeren Nischen zu verschaffen, um den Nährstoffbedarf zu decken und der feindlichen Immunantwort zu entgehen. Dies setzt die Motilität der pathogenen Erreger voraus, die beispielsweise durch den Flagellenapparat gewährleistet wird. Die Bedeutung der Flagellen - vermittelten Motilität für die Pathogenität der ExPEC wurde mehrfach belegt (41-43). Ziel des Projektes war es, die Interaktion zwischen der HPI und des Flagellenapparates in ExPEC molekular zu analysieren. Der erste Schritt bestand in der Herstellung von spezifischen HPI - Mutanten im Zystitisisolat NU14, das physiologisch durch eine hohe Flagellenaktivität charakterisiert ist. Es wurden eine *irp2* - Synthesemutante und eine Knockout - Mutante für den Transkriptionsregulator *ybtA* konstruiert und auf Schwärmagarplatten die Motilität anhand der Schwärmfront motiler Bakterien quantifiziert (Abb. 6). Obwohl unter den standardisierten Versuchsbedingungen ein Eisenüberschuss vorlag, zeigten beiden Mutationen ein signifikantes Defizit. Dieses war stärker für die Synthesemutante ausgeprägt (p<0.001) als für die *ybtA* – Knockout - Mutante (p<0.05).

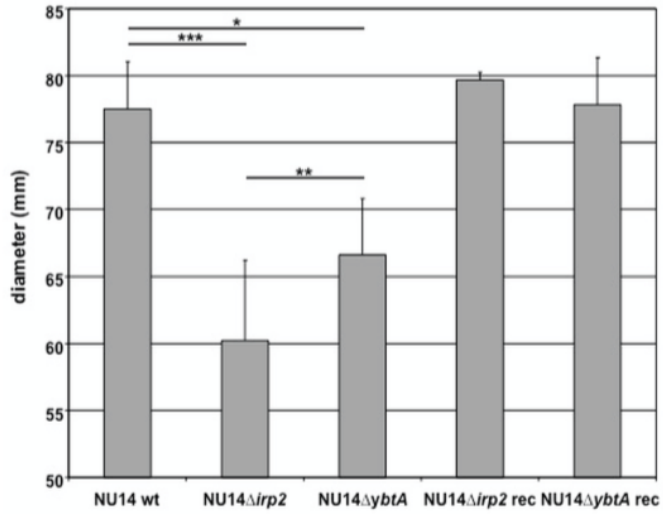

Abbildung 6. Einfluss von HPI - Mutationen auf die Flagellen - vermittelte Motilität.

Dieser Effekt wurde unterstrichen durch die „*gain of function*“ Mutationen im UPEC - Stamm CFT073 und dem apathogenen K12 *E. coli* Laborstamm DH5α. Beide sind

grundsätzlich Ybt - negative Stämme, die durch Transformation eines Plasmides mit kompletter funktioneller HPI zur Ybt - Synthese fähig sind. Die zusätzliche Produktion von Ybt steigerte signifikant die Motilität beider *E. coli* (Abb. 7).

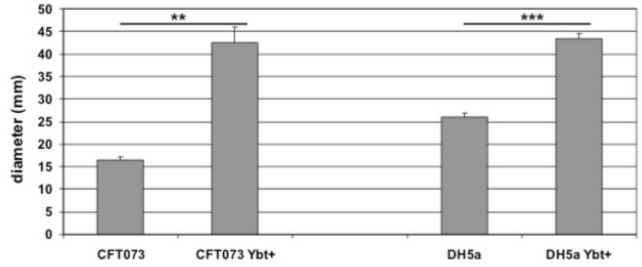

Abbildung 7. Die zusätzliche Produktion des Siderophores Ybt steigert signifikant die Motilität in Ybt - negativen pathogenen und apathogenen *E. coli* Stämmen.

Dadurch konnte der erste Beweis erbracht werden, dass die HPI positiv die Flagellen - vermittelte Motilität beeinflusst. Umgekehrt hatten Mutationen des Flagellenaparates keine Auswirkungen auf die Funktionalität der HPI. Grundsätzlich werden Siderophorsysteme unter Eisenüberschuss unterdrückt durch den Eisenhauptregulator Fur. Allerdings scheint dieser Regulationsmechanismus für die Interaktion von HPI und Flagellen umgangen zu werden (Abb. 8). Auf Transkriptionsebene konnten keine Unterschiede auf die Genexpression unter Eisenmangel und Eisenreichtum verifiziert werden (Abb. 8A). Exzessive Eisenzufuhr hatte während des Schwärmvorgangs keine hemmenden Wirkungen auf die Motilität und die HPI - Genexpression. Diese konnten sogar durch Zufuhr von 10µM an dreiwertigem Eisen signifikant gesteigert werden (Abb. 8B-D). Dieser Effekt beschreibt erstmalig eine Beteiligung eines Eisenaufnahmesystems, das nicht der hierarchischen Eisenhomöostase in Bakterien unterliegt. Um diesen Mechanismus weiter molekular zu untersuchen, wurden transkriptionelle *lacZ* Reporterfusionen für den Promoterbereich des Transkriptionsregulator *ybtA* generiert, der die zentrale Schnittstelle der HPI - Regulation repräsentiert. Die gewonnenen Ergebnisse demonstrierten eindeutig, dass dieser Effekt die Verfügbarkeit aller drei *ybtA* - Bindungsregionen voraussetzt. Während unter Eisenüberschuss die zu erwartende Repression der *ybtA* - Aktivierung verifiziert werden konnte, wie es bisher für alle Siderophore bestätigt wurde, ist diese Hemmung bei schwärmenden Bakterien tatsächlich aufgehoben. Der exakte Mechanismus dieses Phänomens konnte in diesem Projekt nicht

im Detail geklärt werden und bedarf weiterer molekularer Untersuchungen. Die hier präsentierten Ergebnisse unterstreichen um ein weiteres die Multifunktionalität der Siderophorsysteme in ExPEC. Die Flagellen - vermittelte Motilität wird durch zusätzliche Aktivierung der HPI über den Transkriptionsregulator optimiert und umgeht dabei die bisher bekannten Regulationsmechanismen des Eisenstoffwechsels in Bakterien.

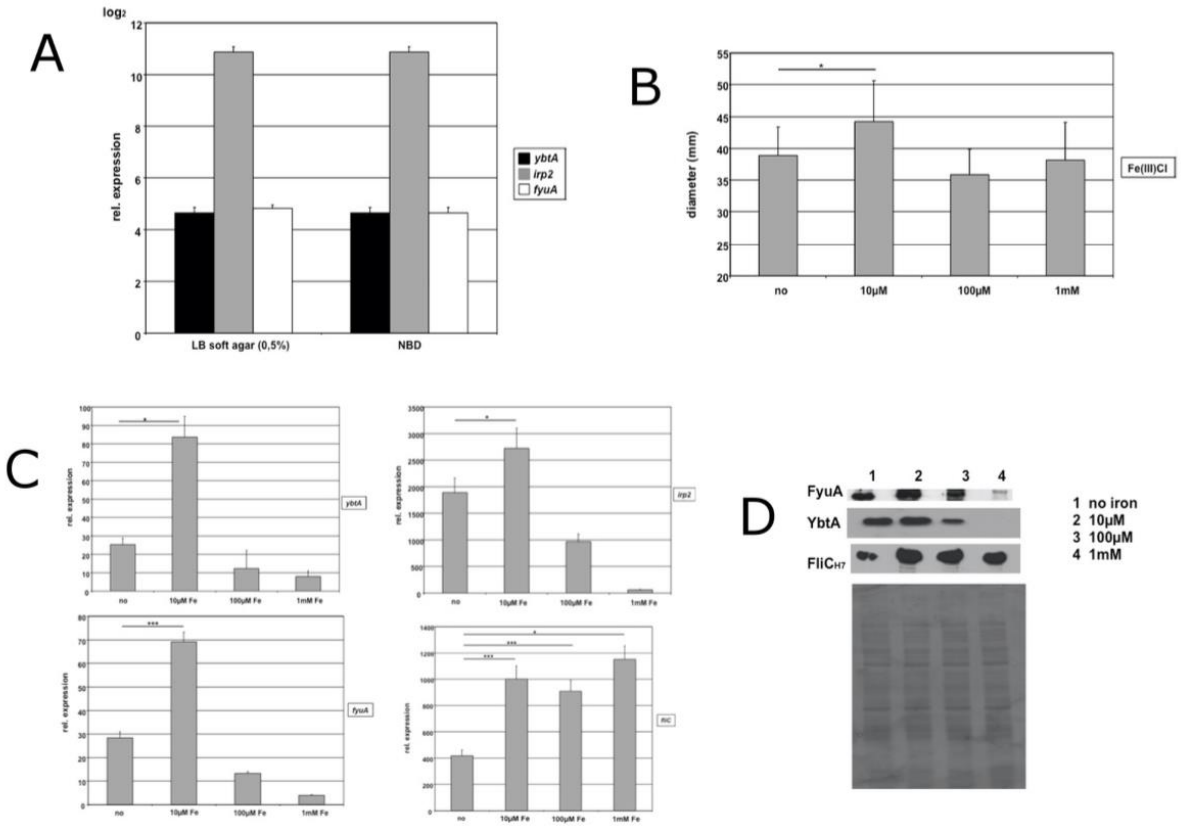

Abbildung 8. Einfluss der Eisenkonzentration auf die Interaktion zwischen HPI und Flagellen. (A) Real -time PCR von HPI - Genen zeigt keinen Unterschied unter Eisendefizit und eisenreichhaltigen Bedingungen. (B) Die Motilität kann unter Zugabe von 10µM an dreiwertigem Eisen signifikant gesteigert werden. (C) Genexpression von HPI-Genen unter exzessiver Eisenzufuhr. (D) Western - Blot der Proteine FyuA (Rezeptor), YbtA (Transkriptionsregulator) und des Flagellins (Strukturprotein der H7 Flagellen) unter unterschiedlicher Zugabe von dreiwertigem Eisen.

Die hier erhobenen Daten basierten auf der Herstellung von Knockout - Mutationen der HPI. Wir waren interessiert, inwieweit eine Modulierung dieses Mechanismus über den Regulator YbtA möglich ist. Dies war die Fragestellung eines Folgeprojektes, das über

Gene - Silencing einen modulierenden Effekt ermöglichen sollte (44). Über den Vorgang der RNA - Interferenz wurde erfolgreich eine Methode etabliert, die generell als Protokoll für Knock - Downs in *E. coli* nützlich ist (45). Über ein induzierbares Expressionsplasmid wird eine 400 Nukleotid lange *antisense* RNA im Zielstamm synthetisiert, die absolute Komplementarität zum Zielgen aufweisen sollte. Dabei gilt es die *antisense* RNA so zu entwerfen, dass die -10 Region des Promoters inklusive der *Shine - Dalgarno* Sequenz abgedeckt wird, sowie die ersten 300 Basenpaare des Zielgens (Abb. 9). Die *antisense* RNA bindet über Watson - Crick Paarung an die *messenger* RNA des frisch transkribierten Zielgens und blockiert wahrscheinlich dadurch als doppelsträngiger RNA- Komplex die Initiierung des Translationsprozesses. Die Daten belegten eindeutig, dass der Transkriptionsprozess nicht beeinflusst wurde, während die Translation einer entscheidenden Beeinträchtigung unterliegt.

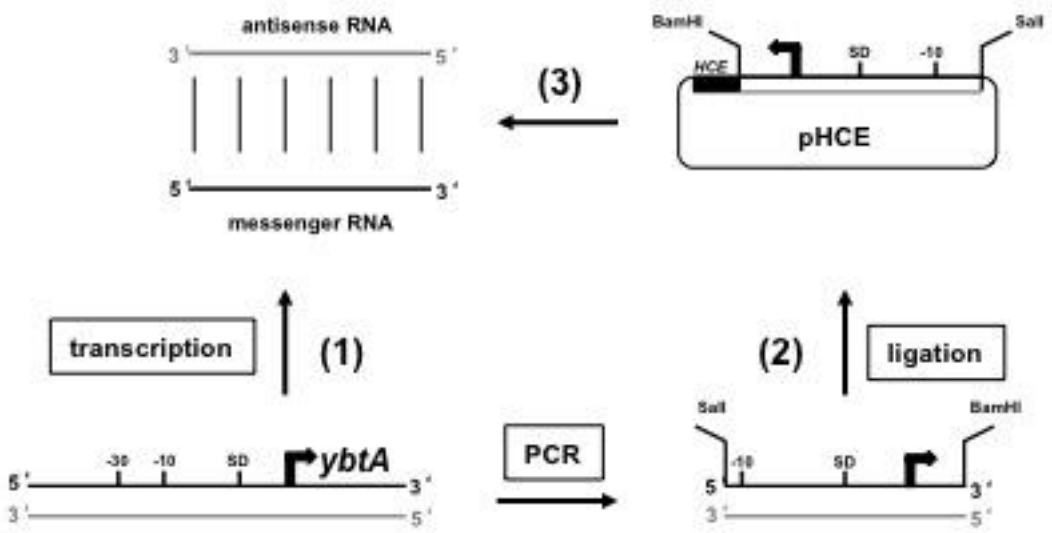

Abbildung 9. Rationale des *Gene - Silencing* Protokolls. (1) Die Transkription des Zielgens führt zur Abschrift in Form einer spezifischen *messenger* RNA. (2) Ein PCR Template für die *antisense* RNA wird in ein Expressionsplasmid kloniert (3) und wird als *antisense* RNA mit der *messenger* RNA, zu der sie absolut komplementär ist, hybridisieren (4). Als doppelsträngige RNA wird dadurch die Translation inhibiert.

Das etablierte Protokoll wurde erstmalig für die oben beschriebene Interaktion zwischen HPI und Flagellenaparat eingesetzt. Durch Verwendung eines induzierbaren Expressionsplasmides konnten wir durch steigende Konzentration eines Induktors den *Silencing* - Effekt auf *ybtA* modulieren (Abb. 10). Das hier vorgestellte Protokoll wurde für weitere Gene in *E. coli* erfolgreich eingesetzt und kann somit als nützliches Instrument

zur Analyse der Genregulation eingesetzt werden.

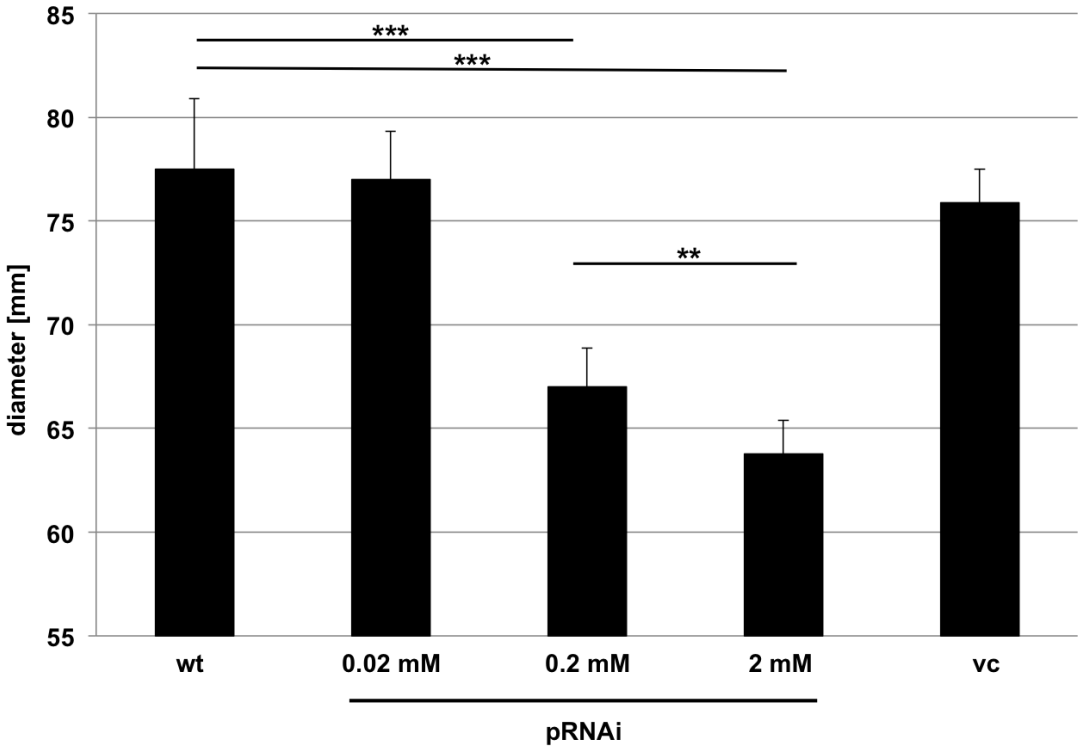

Abbildung 10. *Gene - Silencing* der HPI. Durch steigende Konzentration eines Induktors kann entsprechend die Konzentration spezifischer *ybtA antisense* RNA gesteigert werden, wodurch die Motilität in *E. coli* zunehmend reduziert wird.

2.2 Der Einsatz von Phytotherapeutika für die Prävention und Therapie von HWIs

Das zunehmende Aufkommen multiresistenter Infektionserreger stellt eines der größten Herausforderungen für das Management von Infektionskrankheiten weltweit dar. Aktuellen Schätzungen zufolge sterben jährlich etwa 700.000 Menschen durch Infektionen ausgelöst durch multiresistente Erreger (7). HWIs konnten für eine lange Zeit sicher und wirksam mit Antibiotika behandelt werden, doch dies gestaltet sich zunehmend problematisch im ambulanten und stationären Sektor. Die Entwicklung neuer antibiotischer Substanzen, die Einführung alternativer antimikrobieller Strategien, der rationale Einsatz von Antibiotika (*Antibiotic Stewardship*) und Hygiene - und Präventionsmaßnahmen werden als die entscheidenden Säulen betrachtet, um das antimikrobielle Management zu optimieren. Aufgrund der seit Jahren stagnierenden Entwicklung neuer Antibiotikaklassen besteht ein besonderes Interesse in der Etablierung neuer antimikrobieller Ansätze. Ein Vielzahl nicht - antibiotische Alternativen wurden bereits evaluiert und haben zum Teil bereits Einzug in internationale Leitlinienempfehlungen erhalten (46-48). In einer systematischen *in vitro* Analyse wurden die potentiellen Wirksubstanzen in bereits erhältlichen phytopharmazeutischen Präparaten hinsichtlich Speziesspezifität untersucht. Eine repräsentative Stammsammlung aus 40 Isolaten von komplizierten und unkomplizierten HWIs, die 8 unterschiedliche Spezies umfasst, wurde in verschiedenen Virulenzassays evaluiert. Es wurde der Einfluss auf bakterielles Wachstum, Mannose - sensitive Agglutination und Flagellen - vermittelte Motilität beurteilt. D - Mannose inhibierte bereits in niedrigster Konzentration die adhäsiven Fähigkeiten der Typ 1 - Fimbrien positiven Isolate (Tabelle 1). Ein bakteriostatischer Effekt konnte nicht festgestellt werden. Ebenso blockierten Proanthocyanidine wie sie in Cranberry - Präparaten vorkommen effizient die Agglutination der Bakterien, allerdings war dies sehr konzentrationsabhängig entsprechend der untersuchten Isolate. Während für *Enterobacter cloacae* bereits niedrigste Wirkspiegel suffizient waren, benötigte man für UPEC deutlich höhere Wirkspiegel.

	Escherichia coli	*Klebsiella pneumo-niae*	*Serratia marces-cens*	*Entero-bacter cloacae*
Supplements (concentration, %)				
D-mannose				
0.2%	+++	+++	+++	+++
2%	+++	+++	+++	+++
10%	+++	+++	+++	+++
Cranberry (PAC)				
0.1%	---	---	---	+++
1%	---	---	+++	+++
10%	+++	+++	+++	+++
AITC				
0.1%	+++	---	---	+++
1%	+++	+++	+++	+++
10%	+++	+++	+++	+++
BITC				
0.1%	---	---	---	---
1%	---	---	+++	---
10%	+++	+++	+++	---
PITC				
0.1%	---	---	---	---
1%	---	+++	+++	---
10%	+++	+++	+++	---
AITC:BITC:PITC (Angocin®)				
0.1%	+++	---	---	+++
1%	+++	+++	+++	+++
10%	+++	+++	+++	+++

In this qualitative assay, the agglutination is determined microscopically
+++ positive inhibition; — no inhibition

Tabelle 1. Hemmung der Typ 1 - Fimbrien vermittelten Agglutination

Allyl - Isothiocyanate hemmten nicht nur signifikant die Motilität in UPEC, *Klebsiella pneumoniae* und *Proteus mirabilis* (Abb. 11), sondern hatten auch einen ausgeprägten bakteriostatischen Effekt für die getesteten Stämme.

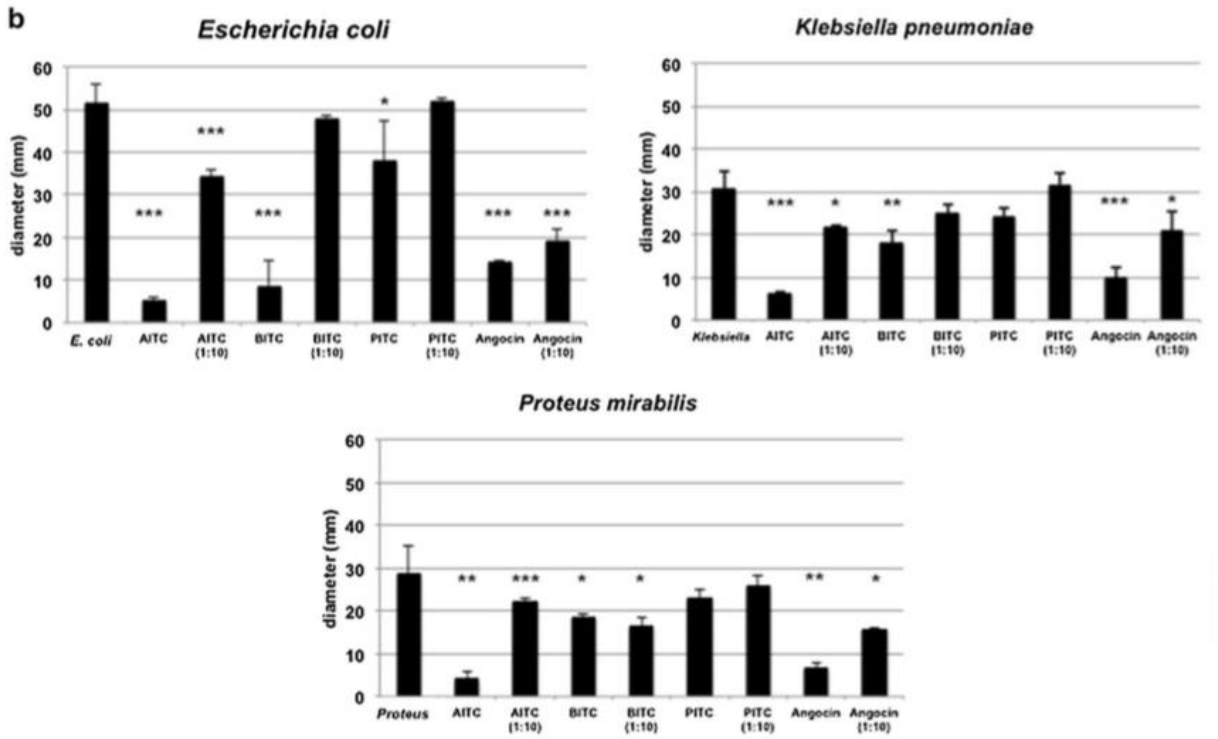

Abbildung 11. Einfluss der Thiocyanate auf die Flagellen vermittelte Motilität. Allyl - Isothiocyanat (AITC), Benzyl - Isothiocyanat (BITC), Phenylethyl - Isothiocyanat (PITC), Angocin® (38% AITC: 50% BITC: 12% PITC). *$p < 0.05$, **$p < 0.01$, ***$p < 0.001$

Rosmarinextrakte wirkten inhibierend in allen untersuchten Isolaten hinsichtlich Wachstumshemmung, allerdings waren für *Morganella morganii* höhere Konzentrationen notwendig und im Falle von *Serratia marcescens* war die Substanz in den applizierten Dosierungen unwirksam. Die hier erhobenen Ergebnisse konnten deutlich die *in vitro* Wirksamkeit von Phytopharmaka und niedermolekularen Verbindungen wie Mannoside demonstrieren. Dabei konnten wir eine entscheidende Spezies - Spezifität und Dosis - Wirkungsbeziehung feststellen. Daher sind diese Verbindungen potentiell in multimodalen Konzepten zur Therapie und Prophylaxe von HWIs denkbar und so sie erregerorientiert eingesetzt werden, lässt sich deren Einsatz entsprechend optimieren. Der wahre klinischer Wert dieses Ansatzes erfordert die Durchführung randomisierter, placebo - kontrollierter klinischer Studien, die aktuell noch ausstehend sind. Dieser Ansatz zielt auf die Manipulation der Pathomechanismen von Harnwegserreger ab und stellt einen interessanten Ansatz im Sinne einer Anti - Virulenztherapie dar. Ähnliches gilt für die

Entwicklung von Impfstoffen die gegen hochexprimierte Virulenzfaktoren gerichtet sind, wie dies erfolgreich in einem Nebenprojekt des Habilitanden aufgezeigt werden konnte (49, 50).

2.3 Management der chronischen Prostatitis / chronisches Beckenschmerzsyndrom (CBSS)

Das optimierte Management von Infektionserkrankungen basiert unter anderem auf dem rationalen Einsatz antimikrobieller Substanzen. Die chronische Prostatitis oder chronische Beckenschmerzsyndrom (englisch; *chronic pelvic pain syndrome*, CPPS) wurde vor der offiziellen Einführung der National Institutes of Health (NIH) - Klassifikation als Prostatodynie oft antimikrobiell mit Tetrazyklinen oder Makroliden behandelt, obwohl eine bakterielle Genese der Beschwerden nie erbracht wurde. Diese Praxis entsprach keiner evidenzbasierten Grundlage und war zumeist von Therapieversagen und Nebenwirkungen der protrahierten antibiotischen Behandlung geprägt. In der hier vorliegenden klinischen Arbeit wurde eine systematische Literaturrecherche (Abb. 12) durchgeführt, um im Expertengremium Empfehlungen zum praktischen Management des CBSS zu formulieren (51). Im Jahre 1999 wurden von der NIH eine Konsensus - Definition und ein Klassifikationssystem für das Prostatitis - Syndrom verabschiedet (Tabelle 2). Demnach wird unterschieden zwischen einer akuten bakteriellen Prostatitis (Kategorie I), einer chronisch bakteriellen Prostatitis (Kategorie II), eines inflammatorischen Beckenschmerzsyndroms (Kategorie IIIA), eines nicht - inflammatorischen Beckenschmerzsyndroms (Kategorie IIIB) und der asymptomatischen Prostatitis (Kategorie IV).

Kategorie	Nomenklatur
I	**Akute bakterielle Prostatitis**
II	**Chronische bakterielle Prostatitis**
III	**Chronisches Beckenschmerzsyndrom (CBSS)**
III A	**Inflammatorisch**
III B	**Nicht - inflammatorisch**
IV	**Asymptomatische Prostatitis**

Tabelle 2. NIH - Klassifikation des Prostatitis - Syndroms

Epidemiologischen Daten zu Folge liegt die Prävalenz von prostatitisähnlichen Beschwerden zwischen 2.2% und 9.7% (52). Dabei kann tatsächlich in weniger als 10% der Fälle ein ursächlicher Harnwegserreger isoliert werden. In über 90% der Fälle handelt es sich somit um das CBSS. Sowohl die diagnostische Abklärung als auch die Behandlung sind weiterhin eine große Herausforderung in der täglichen Praxis. Ziel dieses Projektes war es daher, einen klinischen Leitfaden für die Diagnostik und Behandlung des CBSS zu erarbeiten.

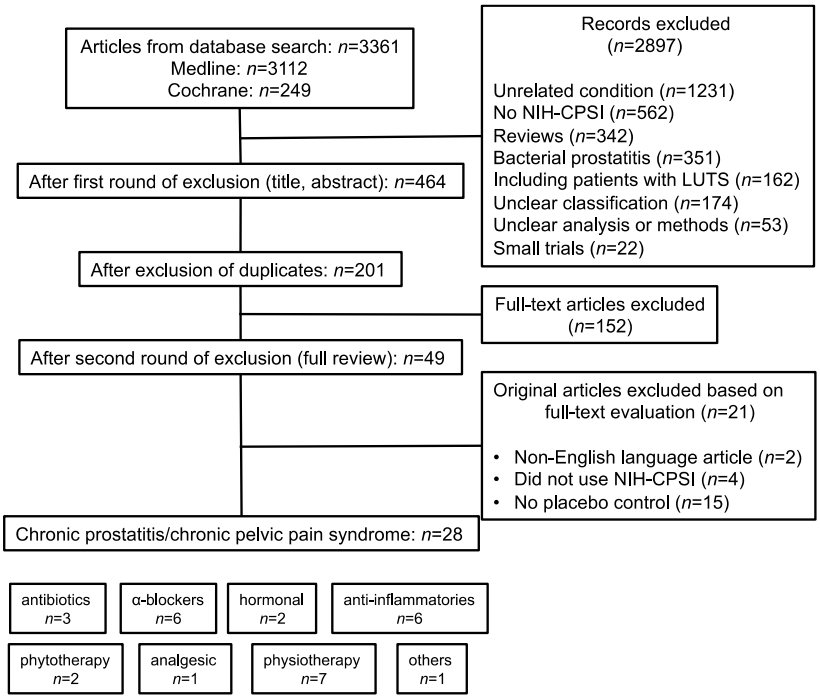

Abbildung 12. Flow - Chart zur systematischen Literaturrecherche gemäß *Preferred Reporting Items for Systematic Reviews and Meta-analysis Statement* (PRISMA).

Das CBSS ist charakterisiert durch Schmerzen / Missempfindungen im Beckenbereich, Beschwerden des unteren Harntraktes (obstruktiv, irritativ) und / oder sexueller Dysfunktion für mindestens 3 Monate in den vorausgegangenen 6 Monaten. Differenzialdiagnosen für Beschwerden im Beckenbereich wie HWIs, Tumorerkrankungen, anatomische Unregelmäßigkeiten, gastrointestinale Ursachen, orthopädische Erkrankungen und neurologische Störungen sollten ausgeschlossen werden. Die diagnostische Abklärung (Abb. 13) beinhaltet neben einer ausführlichen Anamnese die Verwendung von objektiven validierten Fragebögen wie dem NIH -Chronic Prostatitis Symptom Index (NIH - CPSI). Weiterhin ist eine körperliche Untersuchung von

Abdomen, äußerem Genitale, Perineum und der Prostata fester Bestandteil. Als Goldstandard der mikrobiologischen Diagnostik soll eine 4 - oder 2 -Gläser Probe durchgeführt werden. Nur diese erlaubt akkurat einen bakteriellen Nachweis zu erbringen und gemäß der Anzahl an Leukozyten zwischen inflammatorischem und nicht - inflammtorischem CBSS zu differenzieren. Nur der bakterielle Nachweis in der mikrobiologischen Diagnostik indiziert die antimikrobielle Behandlung. Labormedizinische Untersuchungen, bildgebende Verfahren und weitere apparative Diagnostik sollten je nach individuellem Beschwerdebild des Patienten veranlasst werden.

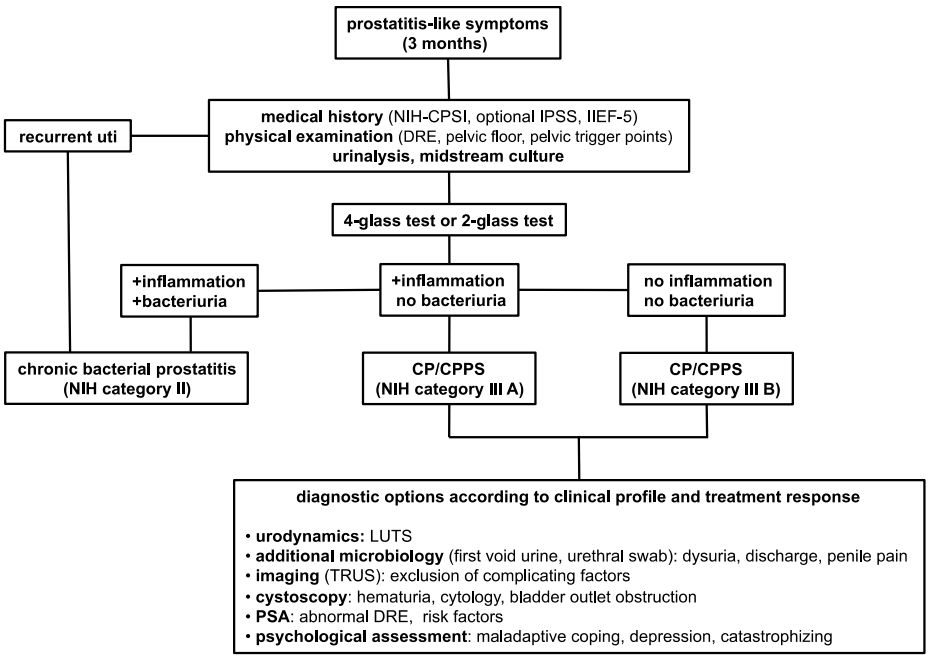

Abbildung 13. Diagnostischer Algorithmus des Prostatitis - Syndroms.

Eine Vielzahl randomisierter kontrollierter Studien wurde eingeschlossen und bereits vorab in aktuellen Meta - Analysen hinsichtlich Behandlung des CBSS evaluiert. Das ernüchternde Resultat veranschaulichte, dass keine effektive Monotherapie zur Behandlung zur Verfügung steht. Als vielversprechend stellte sich ein multimodales symptomorientiertes Vorgehen gemäß UPOINTS heraus (Abb. 14). Dieses Akronym umfasst die häufigsten Domänen an Beschwerden, die von CBSS Patienten angegeben werden (U - urinary; P - psychosocial; O - organ specific; I - infection; N - neurologic; T - tenderness; S - sexual dysfunction). Entsprechend den positiven Domänen in der diagnostischen Abklärung erschließt sich ein multimodales Konzept, das in der ersten

klinischen Evaluierung mit einer Ansprechrate von bis zu 84% die bisherigen Ansätze deutlich übertrifft. Zusammenfassend bietet die Arbeit auf Grundlage der aktualisierten Datenlage einen wertvollen Leitfaden für die klinische Praxis zum strukturierten Management des CBSS.

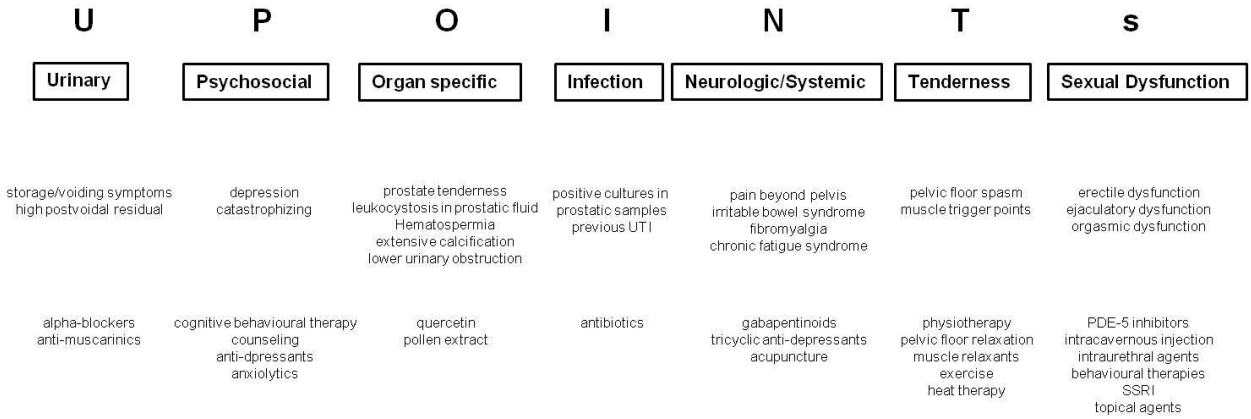

Abbildung 14. Multimodales symptomorientiertes Behandlungskonzept nach UPOINTS.

2.4 Onkologische und funktionelle Evaluation der Holmium Laser Enukleation der Prostata (HoLEP) im Vergleich zur transurethraler Resektion der Prostata (TURP)

Symptome des unteren Harntraktes (englisch; *lower urinary tract symptoms*, LUTS) sind einer der häufigsten Beschwerden des alternden Mannes. Nach der HWI stellt es eine der am meisten gestellten Diagnosen in der klinischen Praxis dar. Aufgrund der demographischen Entwicklung der letzten Jahrzehnte und der enormen finanziellen Belastung für Gesundheitssysteme weltweit erlangte diese „Volkskrankheit“ mehr und mehr an sozioökonomischer Relevanz (1). Die anfallenden Behandlungskosten belaufen sich beispielsweise in den Vereinigten Staaten von Amerika auf etwa 8 Milliarden US - Dollar pro Jahr (53). Als relevante Einflussfaktoren für das Beschwerdeausmaß und die Prävalenz des BPS konnten die Prostatagröße und das fortschreitende Alter identifiziert werden (54-56). Moderate bis schwere LUTS werden gemäß Prävalenzstudien in der Altersgruppe über 70 Jahren mit 33% bis 40% angegeben (57-60). Je nach Ausprägung der Beschwerden und Leidensdruck der Patienten können grundsätzlich konservative, medikamentöse und operative Behandlungsoptionen angeboten werden. Als operatives Referenzverfahren wird gemäß Leitlinienempfehlungen weiterhin die TURP für Prostatagrößen zwischen 30 und 80 ccm geführt (61, 62). Die HoLEP konnte sich Dank der guten klinischen Ergebnisse als attraktive Ergänzung zum Behandlungsspektrum etablieren, insbesondere für vergrößerte Prostaten > 80 ccm. In einem ersten klinischen Projekt wurde die Eignung der HoLEP als Behandlungsoption für die moderat vergrößerte Prostata evaluiert, wie sie bisher mit dem Referenzverfahren der TURP vornehmlich gemäß Leitlinienempfehlungen operiert wird. Aus einem Patientenkollektiv von 2011 operierten Patienten mit BPS, die von 2013 bis 2017 in der Urologischen Abteilung des Klinikums der Universität München behandelt wurden, wurde eine *matched - pair* Analyse vorgenommen. Dabei wurden alle Patienten auf eine Prostatagröße von 50 ccm *gematched* und hinsichtlich perioperativer Parameter, früh-funktioneller Ergebnisse und Sicherheitsprofil untersucht. In die finale Auswertung wurden 98 Patienten nach TURP und 97 Patienten, die mit HoLEP operiert wurden, eingeschlossen. Die demographischen Daten beider Kohorten zeigten bis auf Unterschiede im Gesamt – prostataspezifischen Antigen (PSA) und der PSA - Dichte keine relevanten Differenzen und waren somit vergleichbar. Die perioperativen und funktionellen Parameter legten deutliche Vorteile zu

Gunsten der HoLEP offen (Tabelle 3). Diese war ertragreicher in Hinblick auf das absolut entfernte Adenomgewicht (40 gr vs. 20 gr; $p < 0.001$), als auch auf den prozentualen abladierten Anteil bezogen auf das ursprüngliche Prostatavolumen (75.4% vs. 47.3%; $p < 0.001$). Dabei ergab sich eine um 6.5 min mediane längere OP - Zeit für die HoLEP ($p = 0.006$). Der mediane operative Hämoglobinverlust war für beide Verfahren sehr niedrig (< 1 g/dl), aber ausgeprägter nach der HoLEP (1 g/dl vs. 0.65 g/dl; $p = 0.016$). Urodynamische Parameter wurden nach beiden Verfahren signifikant verbessert, wobei es keinen Unterschied gab für die Reduktion des postmiktionellen Restharns, aber einen signifikant stärkeren Anstieg des maximalen Harnstrahls (Qmax) nach der HoLEP (12 ml/s vs. 8.5 ml/s; $p = 0.028$).

Klinische Ergebnisse			
	TURP (n=98)	**HoLEP** (n=97)	***p*-Wert**
Δ IPSS Median IQR	 7 3 - 14	 11 5.5 - 17	**0.007**
Δ QoL Median IQR	 2 1 - 3	 2 1 - 4	0.383
Entferntes Gewebe (g) Median IQR	 20 18 - 30	 40 30 – 49.5	**<0.001**
Entfernter Prostataanteil (%) Median IQR	 47.3 40 – 54.7	 75.4 64 – 81.2	**<0.001**
OP-Zeit (min) Median IQR	 55.5 48 – 70.5	 62 51 - 85	**0.006**
Abfall Hämoglobin (g/dl) Median IQR	 0.65 0.03 – 1.3	 1 0.4 – 1.5	**0.016**
Δ Qmax (ml/s) Median IQR	 8.5 5 – 18.25	 12 7 - 23	**0.028**
Δ PVR (ml) Median IQR	 66.5 6.5 - 140	 62 0 - 145	0.957

Tabelle 3. Perioperative und postoperative Resultate. IQR = Interquartilen - Bereich; IPSS = International Prostate Symptom Index; QoL = Quality of Life; Qmax = Maximaler Harnstrahl; PVR = Postmiktionelles Restharnvolumen. Ein *p*-Wert < 0.05 gilt als statistisch signifikant.

Das Sicherheitsprofil gemäß Clavien - Dindo Klassifikation beider Verfahren erschien allgemein günstig, allerdings konnten insgesamt signifikant weniger Komplikationen nach HoLEP festgestellt werden als nach der TURP (6% vs. 16%; $p = 0.041$) (Tabelle 4).

Tabelle 4. Operationsbedingte Komplikationen nach Clavien - Dindo Klassifikation. Ein *p*-Wert < 0.05 gilt als statistisch signifikant.

Komplikationen			
	TUR-P (n=98)	**HoLEP** (n=97)	***p*-Wert**
Komplikationen gesamt; *N* (%)	**16** (16%)	**6** (6%)	**0.041**
Clavien Dindo I	**5** (5%)	**2** (2%)	0.446
Harnverhalt	5	2	0.446
Clavien Dindo II	**3** (3%)	**1** (1%)	0.622
Blasentamponade	2	1	1.000
Fieber	1	0	1.000
Clavien Dindo III	**8** (8%)	**3** (3%)	0.215
Clavien Dindo IIIa	0	0	-
Clavien Dindo IIIb	8	3	0.215
Harnverhalt	1	0	1.000
Blasentamponade	2	1	1.000
Blutung	1	0	1.000
Harnröhrenstriktur	4	2	0.683

Zusammenfassend konnten beide Verfahren als sichere und effiziente Behandlungsoptionen für mäßig vergrößerte Prostaten bestätigt werden. Jedoch war die HoLEP in dieser Indikation dem Referenzverfahren der TURP bezüglich Abtragungsrate und urodynamischen Ergebnissen überlegen. Zudem ist es das komplikationsärmere Verfahren. Daher sollte HoLEP als größenunabhängiges Verfahren nicht nur als Enukleationstechnik für große Drüsenvolumina > 80 ccm in Betracht gezogen werden, sondern kann als zumindest gleichwertige Option neben der TURP bei kleineren Adenomen eingesetzt werden.

Da es sich beim BPS um eine benigne Entität handelt, gilt es für die präoperative Diagnostik den erhobenen Verdacht auf ein Prostatakarzinom etwa durch digitale rektale Untersuchung, laborchemische Methoden wie die Messung des PSA oder bildgebende Verfahren wie die multi-parametrische Magnet – Resonanz - Tomographie (MRT) abzuklären. Jedoch ist die diagnostische Methodik klinisch nicht für Patienten mit deutlich vergrößerter Prostata validiert worden. Um das präoperative Assessment dieser

speziellen LUTS - Population zu optimieren und das Risiko der Überdiagnose und Übertherapien zu reduzieren, ist eine onkologische Evaluation dieses Patientengutes sinnvoll. Im zweiten klinischen Projekt zum BPS wurden onkologische Parameter von Patienten evaluiert, die aufgrund des BPS operativ mit HoLEP oder einer TURP behandelt wurden (63). Diese retrospektive monozentrische Studie schloss 518 Patienten ein, die in der Urologischen Klinik der Universität München von Januar 2013 bis Dezember 2014 mit HoLEP (n=289) oder TURP (n=229) operiert wurden. Die demographischen, klinisch - pathologischen und onkologischen Charakteristika beider Kohorten sind in Tabelle 5 dargestellt.

Parameter	**HoLEP** (n=289)	**TURP** (n=229)	***p*-Wert**
Alter (Jahre)			**0.007**
Median	71	69	
IQR	65 - 76	61 - 75	
Gesamt PSA (ng/mL)			**<0.001**
Median	5.5	2.3	
IQR	3.5 - 8.8	1.2 - 4.4	
Prostatavolumen (ccm)			**<0.001**
Median	80	41	
IQR	67.3 - 100	30 - 55	
PSA Dichte (ng/mL/ccm)			**0.001**
Median	0.063	0.050	
IQR	0.042 - 0.104	0.030 - 0.095	
≤0.15	253/283 (89%)	204/221 (92%)	0.265
>0.15	30/283 (11%)	17/221 (8%)	
Preoperative Prostatabiopsie, n (%)			**<0.001**
ja	100/289 (35%)	35/229 (15%)	
nein	189/289 (65%)	194/229 (85%)	
Entferntes Prostatagewicht (g)			**<0.001**
Median	60	20	
IQR	42.8 - 80	15 - 35	
Entfernter Prostataanteil (%)			**<0.001**
Median	71	50	
IQR	60.4 - 85	39 - 62.8	
Histopathologie, n (%)			0.593
BPH	242/289 (84%)	189/229 (83%)	
HGPIN	2/289 (1%)	2/229 (1%)	
ASAP	2/289 (1%)	0/229 (0%)	
iPCa	43/289 (15%)	38/229 (17%)	

pT-Stadium, n (%) pT1a pT1b	 38/43 (88%) 5/43 (12%)	 29/38 (76%) 9/38 (24%)	0.152
Gleason Score, n (%) ≤6 7 8-10	 37/43 (86%) 4/43 (9%) 2/43 (5%)	 32/38 (84%) 5/38 (13%) 1/38 (3%)	0.779
iPCa trotz negative praoperativer Prostatabiopsie, n (%)	17/43 (40%)	3/38 (8%)	**0.007**

Tabelle 5. Demographische, klinisch - pathologische und onkologische Charakteristika beider Kohorten. IQR = Interquartilen - Bereich; PSA = Prostate spezifisches Antigen; BPH = Benigne Prostata Hyperplasie; HGPIN = high-grade prostatic intraepithelial neoplasia; ASAP = atypical small acinar proliferation; iPCa = Inzidentelles Prostatakarzinom;

Hervorzuheben sind das deutlich vergrößerte Prostatavolumen in der HoLEP - Kohorte (80 ccm vs. 41 ccm; $p<0.001$), als auch sämtlich erhobenen PSA - Parameter, die ebenfalls signifikant höher ausfielen. Das Resektionsgewicht und die Desobstruktionsrate waren in der HoLEP - Gruppe signifikant ausgeprägter, wie es für dieses Enukleationsverfahren bereits bekannt ist. Interessanterweise wurden mehr Patienten vor einer HoLEP stanzbioptisch auf das Vorliegen eines möglichen Prostatakarzinoms abgeklärt als vor einer TURP (35% vs. 15%; $p<0.001$). Die Rate an falsch - negativen Biopsien lag hierbei signifikant höher für die HoLEP (40%) als für die TURP (8%) ($p=0.007$). Die Detektionsrate für ein inzidentelles Prostatakarzinom nach HoLEP (15%) oder TURP (17%) war vergleichbar ($p>0.05$). In der univariaten und multivariaten logistischen Regressionsanalyse konnten neben dem Patientenalter als bereits bekannter Prädiktor auch die PSA - Dichte (>0.15 ng/ml/ccm) als neuer Parameter für das Vorliegen eines inzidentellen Prostatakarzinoms identifiziert werden (Abb. 15).

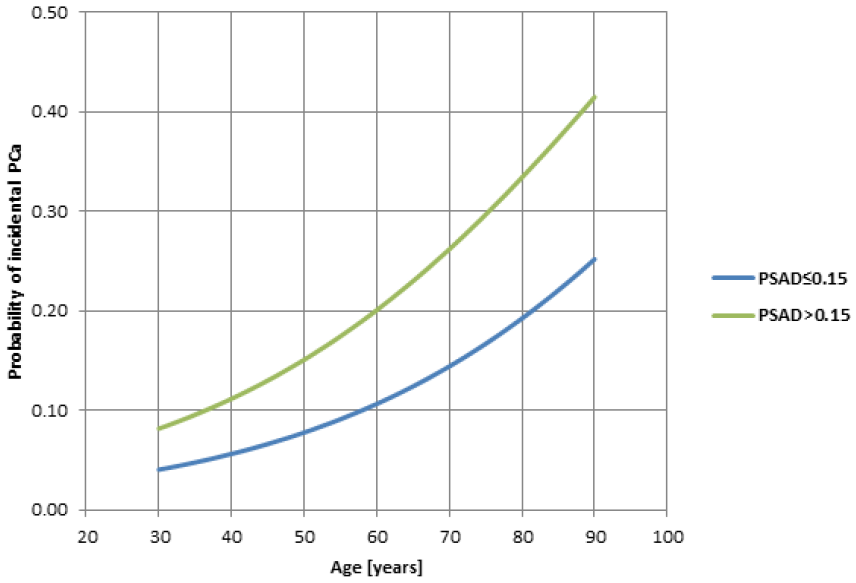

Abbildung 15. Prädiktoren für das Vorliegen eines inzidentellen Prostatakarzinoms. Eine PSA - Dichte >0.15 in älteren Patienten resultiert in einer höheren Wahrscheinlichkeit für ein inzidentelles Prostatakarzinom.

Zusammenfassend konnten wir zeigen, dass die Operationstechnik keinen Einfluss auf die Detektionsrate für ein inzidentelles Prostatakarzinom aufweist. Als neuen Prädiktor konnten wir in Patienten mit deutlich vergrößerter Prostata die PSA - Dichte identifizieren. Die signifikant höhere Rate an falsch - negativen Stanzbiopsien und die deutlich höhere Anzahl an präoperativen Prostatabiopsien in der HoLEP - Kohorte verdeutlichen, dass LUTS - Patienten mit stark vergrößerter Prostata ein besonderes Kollektiv darstellen, dass nicht optimal mit bekannten diagnostischen Standards onkologisch abgeklärt wird.

Zusammenfassung

Der primäre Schwerpunkt der Habilitationsarbeit liegt in der molekularen Untersuchung von Pathogenitätsmechanismen der ExPEC. Das tiefere Verständnis ist eine wichtige Grundlage, um potente alternative antimikrobielle Strategien gegen HWIs zu entwickeln. Wir konnten klar aufzeigen, dass die Eisenaufnahmesysteme der ExPEC einen essentiellen Beitrag zur Virulenz leisten im Tiermodell. Der Aspekt der Multifunktionalität von Siderophorsystemen konnte in der vorliegenden Habilitationsschrift und durch Vorarbeiten des Habilitanden weiter verfolgt werden. Neben ihrer Hauptfunktion als Eisenlieferant, sind sie Bestandteil eines komplexen regulatorischen Netzwerkes, das die Virulenz - und Fitnesseigenschaften der ExPEC zu optimieren vermag. Die Außenmembranrezeptoren unterstützen zusätzlich die Biofilmbildung, unterstützen Invasionsvorgänge und die Flagellen - vermittelte Motilität wird durch Siderophorsysteme wie der HPI verbessert. Im Sinne des Konzeptes der Anti -Virulenztherapie ergibt sich die Gelegenheit einen Virulenzfaktor therapeutisch zu modulieren, um damit das pathogene Potential auf mehreren Ebenen zu schwächen. Siderophorsysteme und deren Elemente sind pathogen - spezifisch, wirken antigen, besitzen spezifische Rezeptoren an der Membranoberfläche und zeigen eine verstärkte Expression unter Infektionsvorgängen. Damit sind sie attraktive Kandidaten für die Vakzinentwicklung. In Vorarbeiten des Habilitanden ist dies bereits in der Form eines Multi – Epitop - Vakzins erfolgreich demonstriert worden (49, 50). Dabei wurde ein maßgeschneiderter Impfstoff entwickelt, der immunogene Domänen diverser Siderophorrezeptoren umfasst, und eine effektive Immunprotektion gegen ExPEC Infektionen im Tiermodell vermitteln konnte. Eine weitere attraktive Option liefert der Einsatz von Phytopharmaka mit antimikrobieller Wirkung. Wir konnten im Rahmen einer systematischen *in vitro* Evaluation die Dosisabhängigleit und Spezies – Spezifität bereits erhältlicher Präparate aufzeigen, die unter Berücksichtigung das aktuelle Management in multimodalen Ansätzen weiter optimieren lassen. Jedoch ist die klinische Evaluierung dieser Strategie in randomisierten, kontrollierten klinischen Studien noch ausstehend. Ein weiterer Aspekt zum optimierten Management von urologischen Infektionserkrankungen legt den Fokus auf den rationalen und gezielten Einsatz von Antibiotika. Das Prostatitis - Syndrom ist ein Beispiel, das für einen

exzessiven Missbrauch an antimikrobiellen Substanzen verantwortlich ist. In über 90% der Fälle liegt keine bakterielle Genese vor, weshalb die antibiotische Behandlung hier nicht zielführend ist. Anhand klinischer Evidenz wurde ein praktischer Leitfaden zum strukturierten Management dieser Entität erarbeitet.

Neben HWIs ist die Volkskrankheit des BPS eine der häufigsten Anlässe für den urologischen Arztbesuch. Die hier vorgestellte Habilitationsschrift verdeutlicht zum einen, dass die HoLEP als größenunabhängiges Verfahren eine sichere und effektive Option zur Behandlung moderat vergrößerter Prostaten bietet. Zum anderen wird unterstrichen, dass BPS - Patienten mit deutlich vergrößerter Prostata durch den aktuellen diagnostischen Standard zur präoperativen Abklärung einer Malignität der Prostata nur unzureichend erfasst werden. Ein optimiertes Assessment ist sinnvoll, um das Risiko der Überdiagnose und Übertherapie zu vermeiden.

Abkürzungsverzeichnis

AITC	= Allyl - Isothiocyanat
BITC	= Benzyl - Isothiocyanat
BPS	= Benignes Prostatasyndrom
CBBS	= Chronisches Beckenschmerzsyndrom
E. coli	= *Escherichia coli*
ExPEC	= extraintestinale pathogene *E. coli*
HoLEP	= Holmium Laser Enukleation der Prostata
HPI	= High - Pathogenicity Island
HWI	= Harnwegsinfektion
IPSS	= International Prostate Symptom Index
IQR	= Interquartilen-Bereich
K_d	= Dissoziationskonstante
LUTS	= Lower Urinary Tract Symptoms
NIH – CPSI	= National Institutes of Health – Chronic Prostatits Symptom Index
PITC	= Phenylethyl - Isothiocyanat
PSA	= Prostataspezifisches Antigen
PVR	= Postmiktionelles Restharnvolumen
Qmax	= Maximaler Harnstrahl
QoL	= Quality of Life
RLU	= Relative Light Units
RNA	= Ribonucleic Acid
TURP	= Transurethrale Resektion der Prostata
UPEC	= uropathogene *E. coli*
Ybt	= Yersiniabactin

Referenzen

1. Vuichoud C, Loughlin KR. Benign prostatic hyperplasia: epidemiology, economics and evaluation. Can J Urol. 2015;22 Suppl 1:1-6.
2. RKI Robert Koch-Institut. Deutsche Daten im Rahmen der ersten euro- päischen Prävalenzerhebung zum Vorkommen nosokomialer Infektio- nen und zur Antibiotikaanwendung. Epidemiologisches Bulletin 2012; 26: 239–240.
3. Piechota H. [Prevention of Catheter-Associated Urinary Tract Infections]. Aktuelle Urol. 2016;47(3):220-8.
4. Flores-Mireles AL, Walker JN, Caparon M, Hultgren SJ. Urinary tract infections: epidemiology, mechanisms of infection and treatment options. Nat Rev Microbiol. 2015;13(5):269-84.
5. Stamm WE, Norrby SR. Urinary tract infections: disease panorama and challenges. J Infect Dis. 2001;183 Suppl 1:S1-4.
6. World Health Organization (WHO); Antimicrobial Resistance - Global Report on Surveillance. 2014.
7. O'Neill J. Antimicrobial Resistance:Tackling a crisis for the health and wealth of nations. The Review on Antimicrobial Resistance, chaired by Jim O'Neill; December 2014.
8. Magistro G. Urological Infections: "The Time for Change is Now". Eur Urol Focus. 2018.
9. Magistro G, Stief CG. Vaccine Development for Urinary Tract Infections: Where Do We Stand? Eur Urol Focus. 2018.
10. Giacobbe DR, Mikulska M, Viscoli C. Recent advances in the pharmacological management of infections due to multidrug-resistant Gram-negative bacteria. Expert Rev Clin Pharmacol. 2018;11(12):1219-36.
11. Taylor SN, Marrazzo J, Batteiger BE, Hook EW, 3rd, Sena AC, Long J, et al. Single-Dose Zoliflodacin (ETX0914) for Treatment of Urogenital Gonorrhea. The New England journal of medicine. 2018;379(19):1835-45.
12. Russo TA, Johnson JR. Medical and economic impact of extraintestinal infections due to Escherichia coli: focus on an increasingly important endemic problem. Microbes Infect. 2003;5(5):449-56.
13. Kaper JB, Nataro JP, Mobley HL. Pathogenic Escherichia coli. Nat Rev Microbiol. 2004;2(2):123-40.
14. Vila J, Saez-Lopez E, Johnson JR, Romling U, Dobrindt U, Canton R, et al. Escherichia coli: an old friend with new tidings. FEMS Microbiol Rev. 2016.
15. Russo TA, Johnson JR. Proposal for a new inclusive designation for extraintestinal pathogenic isolates of Escherichia coli: ExPEC. J Infect Dis. 2000;181(5):1753-4.
16. Johnson JR. Virulence factors in Escherichia coli urinary tract infection. Clin Microbiol Rev. 1991;4(1):80-128.
17. Subashchandrabose S, Mobley HL. Virulence and Fitness Determinants of Uropathogenic Escherichia coli. Microbiol Spectr. 2015;3(4).
18. Andrews SC, Robinson AK, Rodriguez-Quinones F. Bacterial iron homeostasis. FEMS Microbiol Rev. 2003;27(2-3):215-37.
19. Hentze MW, Muckenthaler MU, Andrews NC. Balancing acts: molecular control of mammalian iron metabolism. Cell. 2004;117(3):285-97.

20. Schaible UE, Kaufmann SH. Iron and microbial infection. Nat Rev Microbiol. 2004;2(12):946-53.
21. Chu BC, Garcia-Herrero A, Johanson TH, Krewulak KD, Lau CK, Peacock RS, et al. Siderophore uptake in bacteria and the battle for iron with the host; a bird's eye view. Biometals. 2010;23(4):601-11.
22. Nairz M, Schroll A, Sonnweber T, Weiss G. The struggle for iron - a metal at the host-pathogen interface. Cell Microbiol. 2010;12(12):1691-702.
23. Ratledge C, Dover LG. Iron metabolism in pathogenic bacteria. Annu Rev Microbiol. 2000;54:881-941.
24. Wandersman C, Delepelaire P. Bacterial iron sources: from siderophores to hemophores. Annu Rev Microbiol. 2004;58:611-47.
25. Skaar EP. The battle for iron between bacterial pathogens and their vertebrate hosts. PLoS Pathog. 2010;6(8):e1000949.
26. Smati M, Magistro G, Adiba S, Wieser A, Picard B, Schubert S, et al. Strain-specific impact of the high-pathogenicity island on virulence in extra-intestinal pathogenic Escherichia coli. Int J Med Microbiol. 2017;307(1):44-56.
27. Perry RD, Fetherston JD. Yersiniabactin iron uptake: mechanisms and role in Yersinia pestis pathogenesis. Microbes Infect. 2011;13(10):808-17.
28. Schubert S, Cuenca S, Fischer D, Heesemann J. High-pathogenicity island of Yersinia pestis in enterobacteriaceae isolated from blood cultures and urine samples: prevalence and functional expression. J Infect Dis. 2000;182(4):1268-71.
29. Schubert S, Rakin A, Karch H, Carniel E, Heesemann J. Prevalence of the "high-pathogenicity island" of Yersinia species among Escherichia coli strains that are pathogenic to humans. Infect Immun. 1998;66(2):480-5.
30. Bultreys A, Gheysen I, de Hoffmann E. Yersiniabactin production by Pseudomonas syringae and Escherichia coli, and description of a second yersiniabactin locus evolutionary group. Appl Environ Microbiol. 2006;72(6):3814-25.
31. Perry RD, Balbo PB, Jones HA, Fetherston JD, DeMoll E. Yersiniabactin from Yersinia pestis: biochemical characterization of the siderophore and its role in iron transport and regulation. Microbiology. 1999;145 (Pt 5):1181-90.
32. Valdebenito M, Crumbliss AL, Winkelmann G, Hantke K. Environmental factors influence the production of enterobactin, salmochelin, aerobactin, and yersiniabactin in Escherichia coli strain Nissle 1917. Int J Med Microbiol. 2006;296(8):513-20.
33. Adiba S, Nizak C, van Baalen M, Denamur E, Depaulis F. From grazing resistance to pathogenesis: the coincidental evolution of virulence factors. PloS one. 2010;5(8):e11882.
34. Garcia EC, Brumbaugh AR, Mobley HL. Redundancy and specificity of Escherichia coli iron acquisition systems during urinary tract infection. Infect Immun. 2011;79(3):1225-35.
35. Lloyd AL, Henderson TA, Vigil PD, Mobley HL. Genomic islands of uropathogenic Escherichia coli contribute to virulence. J Bacteriol. 2009;191(11):3469-81.
36. Schubert S, Picard B, Gouriou S, Heesemann J, Denamur E. Yersinia high-pathogenicity island contributes to virulence in Escherichia coli causing extraintestinal infections. Infect Immun. 2002;70(9):5335-7.
37. Brumbaugh AR, Smith SN, Subashchandrabose S, Himpsl SD, Hazen TH, Rasko DA, et al. Blocking yersiniabactin import attenuates extraintestinal pathogenic Escherichia coli in cystitis and pyelonephritis and represents a novel target to prevent urinary tract infection. Infect Immun. 2015;83(4):1443-50.

38. Diard M, Garry L, Selva M, Mosser T, Denamur E, Matic I. Pathogenicity-associated islands in extraintestinal pathogenic Escherichia coli are fitness elements involved in intestinal colonization. J Bacteriol. 2010;192(19):4885-93.
39. Magistro G, Magistro C, Stief CG, Schubert S. The high-pathogenicity island (HPI) promotes flagellum-mediated motility in extraintestinal pathogenic Escherichia coli. PloS one. 2017;12(10):e0183950.
40. Magistro G, Hoffmann C, Schubert S. The salmochelin receptor IroN itself, but not salmochelin-mediated iron uptake promotes biofilm formation in extraintestinal pathogenic Escherichia coli (ExPEC). Int J Med Microbiol. 2015;305(4-5):435-45.
41. Lane MC, Alteri CJ, Smith SN, Mobley HL. Expression of flagella is coincident with uropathogenic Escherichia coli ascension to the upper urinary tract. Proc Natl Acad Sci U S A. 2007;104(42):16669-74.
42. Lane MC, Lockatell V, Monterosso G, Lamphier D, Weinert J, Hebel JR, et al. Role of motility in the colonization of uropathogenic Escherichia coli in the urinary tract. Infect Immun. 2005;73(11):7644-56.
43. Wright KJ, Seed PC, Hultgren SJ. Uropathogenic Escherichia coli flagella aid in efficient urinary tract colonization. Infect Immun. 2005;73(11):7657-68.
44. Magistro G, Magistro C, Stief CG, Schubert S. A simple and highly efficient method for gene silencing in Escherichia coli. J Microbiol Methods. 2018;154:25-32.
45. Fire A, Xu S, Montgomery MK, Kostas SA, Driver SE, Mello CC. Potent and specific genetic interference by double-stranded RNA in Caenorhabditis elegans. Nature. 1998;391(6669):806-11.
46. Beerepoot MA, Geerlings SE, van Haarst EP, van Charante NM, ter Riet G. Nonantibiotic prophylaxis for recurrent urinary tract infections: a systematic review and meta-analysis of randomized controlled trials. The Journal of urology. 2013;190(6):1981-9.
47. Bonkat GP, R.; Bartoletti,R.; Cai,T.; Bruyere, F.; Geerlings, S.E.; Köves,B.; Wagenlehner, F. EAU Guidelines on Urological Infections 2018.
48. Smith AL, Brown J, Wyman JF, Berry A, Newman DK, Stapleton AE. Treatment and Prevention of Recurrent Lower Urinary Tract Infections in Women: A Rapid Review with Practice Recommendations. The Journal of urology. 2018;200(6):1174-91.
49. Wieser A, Magistro G, Norenberg D, Hoffmann C, Schubert S. First multi-epitope subunit vaccine against extraintestinal pathogenic Escherichia coli delivered by a bacterial type-3 secretion system (T3SS). Int J Med Microbiol. 2012;302(1):10-8.
50. Wieser A, Romann E, Magistro G, Hoffmann C, Norenberg D, Weinert K, et al. A multiepitope subunit vaccine conveys protection against extraintestinal pathogenic Escherichia coli in mice. Infect Immun. 2010;78(8):3432-42.
51. Magistro G, Wagenlehner FM, Grabe M, Weidner W, Stief CG, Nickel JC. Contemporary Management of Chronic Prostatitis/Chronic Pelvic Pain Syndrome. European urology. 2015.
52. Krieger JN, Lee SW, Jeon J, Cheah PY, Liong ML, Riley DE. Epidemiology of prostatitis. International journal of antimicrobial agents. 2008;31 Suppl 1:S85-90.
53. Taub DA, Wei JT. The economics of benign prostatic hyperplasia and lower urinary tract symptoms in the United States. Curr Urol Rep. 2006;7(4):272-81.
54. Bosch JL, Bangma CH, Groeneveld FP, Bohnen AM. The long-term relationship between a real change in prostate volume and a significant change in lower urinary tract symptom severity in population-based men: the Krimpen study. European urology. 2008;53(4):819-25; discussion 25-7.

55. Parsons JK, Wilt TJ, Wang PY, Barrett-Connor E, Bauer DC, Marshall LM, et al. Progression of lower urinary tract symptoms in older men: a community based study. The Journal of urology. 2010;183(5):1915-20.
56. Roehrborn CG. BPH progression: concept and key learning from MTOPS, ALTESS, COMBAT, and ALF-ONE. BJU international. 2008;101 Suppl 3:17-21.
57. Berges RR, Pientka L. Management of the BPH syndrome in Germany: who is treated and how? European urology. 1999;36 Suppl 3:21-7.
58. Boeing H, Wahrendorf J, Becker N. EPIC-Germany--A source for studies into diet and risk of chronic diseases. European Investigation into Cancer and Nutrition. Ann Nutr Metab. 1999;43(4):195-204.
59. Riboli E, Kaaks R. The EPIC Project: rationale and study design. European Prospective Investigation into Cancer and Nutrition. Int J Epidemiol. 1997;26 Suppl 1:S6-14.
60. Rohrmann S, Katzke V, Kaaks R. Prevalence and Progression of Lower Urinary Tract Symptoms in an Aging Population. Urology. 2016.
61. AWMF-Reg.Nr:043-035: S2e Leitlinie-Therapie des Benignen Prostatasyndroms (BPS); 2012.
62. Gravas S, et al. EAU Guidelines on the
Management of Non-Neurogenic Male Lower Urinary Tract Symptoms (LUTS). 2018.
63. Herlemann A, Wegner K, Roosen A, Buchner A, Weinhold P, Bachmann A, et al. "Finding the needle in a haystack": oncologic evaluation of patients treated for LUTS with holmium laser enucleation of the prostate (HoLEP) versus transurethral resection of the prostate (TURP). World J Urol. 2017;35(11):1777-82.

Originalarbeiten (nach Erscheinungsdatum)

Received: 18 June 2019 | Revised: 14 July 2019 | Accepted: 27 August 2019
DOI: 10.1111/luts.12290

ORIGINAL ARTICLE

WILEY

A matched-pair analysis of patients with medium-sized prostates (50 cc) treated for male LUTS with HoLEP or TURP

Giuseppe Magistro | Thilo Westhofen | Christian G. Stief | Philipp Weinhold

Department of Urology, Ludwig-Maximilians-University of Munich, Munich, Germany

Correspondence
Giuseppe Magistro, Department of Urology, Ludwig-Maximilians-University, Marchioninistrasse 15, 81377 Munich, Germany.
Email: giuseppe.magistro@med.uni-muenchen.de

Abstract

Objectives: To evaluate perioperative parameters, early functional outcomes, and the safety profile in a matched-pair analysis of lower urinary tract symptom (LUTS) patients treated with holmium laser enucleation of the prostate (HoLEP) or transurethral resection of the prostate (TURP).

Methods: We conducted a retrospective, matched-pair analysis of 2011 men treated for LUTS in our institution from 2013 to 2017. In the final analysis, 197 patients (HoLEP n = 97; TURP n = 98) were matched for prostate size (50 cc), age, and body mass index, and both cohorts were compared for demographic parameters, clinical outcomes, and adverse events according to the Clavien-Dindo classification.

Results: The perioperative assessment revealed a significantly higher tissue retrieval percentage of 75.4% (interquartile range [IQR] 64-81.2) after HoLEP in comparison to 47.3% (IQR 40-54.7) after TURP (P <.001). A shorter surgery time was reported for TURP with a median time of 55.5 minutes (IQR 48-70.5), whereas the median time for HoLEP was 62 minutes (IQR 51-85) (P =.006). The median improvements in International Prostate Symptom Score (IPSS) were 11 points (IQR 5.5-17) and 7 points (IQR 3-14) for HoLEP and TURP, respectively (P =.007). Peak urinary flow rate (Q_{max}) increased more after HoLEP (12.0 mL/s; IQR 7-23) than after TURP (8.5 mL/s; IQR 5-18.25) (P =.028). With an overall incidence of adverse events of 6% (n = 6) compared to 16% (n = 16%), significantly fewer complications occurred after HoLEP than after treatment with TURP (P <.05).

Conclusions: HoLEP is not only an attractive alternative for the enucleation of larger prostates, but it must be considered a size-independent technique with the potential to outdo the current reference method TURP.

KEYWORDS
benign prostatic hyperplasia, holmium laser enucleation of the prostate (HoLEP), lower urinary tract symptoms, transurethral resection of the prostate (TURP)

1 | INTRODUCTION

With the growing body of clinical evidence, holmium laser enucleation of the prostate (HoLEP) gained its place among the established surgical procedures for the treatment of male lower urinary tract symptoms (LUTS) due to benign prostatic obstruction (BPO).[1-3] As for all the LUTS treatment approaches, one aspect is of utmost importance: Patient selection is key to address the individual clinical profile and patients' expectations with the ideal technique. We need to know

Giuseppe Magistro and Thilo Westhofen contributed equally to this work.

patients' characteristics in order to determine which patients will benefit the most from a specific surgical technique. However, with respect to current guideline recommendations, it appears that the position of HoLEP among the plethora of treatment modalities has not been conclusively defined yet. It is strongly recommended as a treatment option for moderate-to-severe LUTS with enlarged prostates >80 cc. But for this indication, guideline recommendations vary between open prostatectomy as a first-line therapy,[4] HoLEP as an equal first-line option with open prostatectomy[5] and HoLEP as a size-independent procedure.[6] So, the question arises as to which patients with which characteristics are best treated with HoLEP. Urologists need to know the true clinical benefits of each treatment option when counseling their patients. For larger prostates, randomized controlled trials (RCTs) and meta-analyses confirmed the efficacy and safety of HoLEP compared to open prostatectomy.[7-10] The LUTS improvements are at least equally effective, but a clear benefit was identified for perioperative parameters including the duration of hospital stay, shorter catheterization, and better hemostatic control. Meta-analyses comparing HoLEP with transurethral resection of the prostate (TURP) revealed that symptom improvements are even superior with HoLEP.[11,12] The incidence of treatment-related adverse events (AEs) comprising urethral strictures, stress urinary incontinence, and sexual dysfunction, including erectile and ejaculatory function, are comparable between HoLEP and TURP. But long-term data suggest that the re-treatment rates are higher after TURP than after HoLEP.[3]

The technical and clinical advantages of HoLEP become more obvious in larger prostates; but also for moderately enlarged prostates, where TURP has clearly set the benchmark for therapy, it is an attractive option. In the current study, we performed a matched-pair analysis of two representative cohorts that were treated with HoLEP or TURP for male LUTS. The main objective was to identify relevant differences between both procedures in this clearly defined patient population by assessing perioperative parameters, early functional outcomes, and the safety profile.

2 | METHODS

2.1 | Study design and surgical procedures

In this retrospective single-center study, we conducted a matched-pair analysis of patients who underwent surgical treatment for LUTS due to BPO. We analyzed perioperative parameters, early functional outcomes, and the safety profile of each procedure. Our matching endpoints were the prostate size of 50 cc, age (years), and the body mass index (BMI). A total of 2011 patients who were treated with HoLEP (n = 1062) or TURP (n = 949) from January 2013 to December 2017 at our institution were included for data collection by one investigator (M.K.). The data sets were then screened and matched for prostate size by a second investigator (T.W.) who was blinded to the procedure. Afterwards, the datasets were completed for the technique by a third investigator (G.M.), and both cohorts were finally established. This approach is supposed to avoid a potential bias effect during the matching process.

All HoLEP procedures were always performed with a three-lobe technique by two experienced surgeons with the VersaPulse 100 W Holmium Laser (Lumenis Ltd., Yokneam, Israel), using a frequency of 53 Hz and a power setting of 1.2 kJ. All TURPs were conducted with bipolar technique by four surgeons. All surgeons have great expertise with endoscopic procedures, including TURP and HoLEP, and perform at least 250 operations a year.

2.2 | Parameters

In the present study we evaluated prostate volume (PV; cc) measured by transrectal ultrasound (TRUS), International Prostate Symptom Score (IPSS), quality of life (QoL), peak urinary flow rate (Q_{max}; mL/s), postvoid residual urine volume (PVR; mL), total surgical time (minutes), resected prostate weight (g), and blood loss (g/dL). The short-term LUTS improvements and functional outcomes were determined 4 weeks after surgery, whereas the perioperative technical parameters were measured in the operating room directly after surgery. The drop in hemoglobin levels was studied 24 hours after the intervention. The tissue retrieval percentage (%) was defined as the proportion of removed tissue relative to the PV as determined by TRUS prior to surgery. Demographic parameters included age (year), BMI, total serum prostate-specific antigen (PSA; ng/mL; Elecsys Assay, Roche Diagnostics GmbH, Mannheim, Germany), and PSA density (ng/mL/cc). Treatment-related AEs were graded according to the Clavien-Dindo classification.[13]

2.3 | Statistical analysis

After the matching process, 98 patients for TURP and 97 patients for HoLEP were eligible for inclusion and final analysis. For descriptive statistics, continuous variables were presented as the mean (standard deviation, SD), and continuous variables were presented as percentages or absolute numbers. Univariate analyses were performed using Fisher's exact test, *t* test, and Mann-Whitney *U* test for categorical variables and continuous variables. Normal distribution of variables was determined with the Shapiro-Wilk test. A *P* value <.05 was considered statistically significant. All calculations were carried out using SPSS Statistics software, version 25.0 (SPSS Inc., Chicago, Illinois).

3 | RESULTS

3.1 | Baseline characteristics

In the present matched-pair analysis, a total of 195 patients were eligible for inclusion—98 patients in the TURP cohort and 97 patients treated with HoLEP (Table 1). The evaluation of the patients' baseline parameters revealed only differences for total PSA and PSA density. The total serum PSA was higher in the HoLEP group with a median of 3.27 ng/mL (interquartile range [IQR] 1.73-5.54) compared to the median of 2.3 ng/mL (IQR 1.38-3.5) in the TURP arm (*P* =.001). The median PSA density was also more elevated for HoLEP with a median of 0.07 ng/mL/cc (IQR 0.04-0.11) than TURP, which showed a median

value of 0.04 ng/mL/cc (IQR 0.03-0.07) (*P* =.002). All the other assessed variables showed that both cohorts were comparable. As this population was matched for prostate size, both populations showed a median size of 51 cc (*P* >.05). The median ages were 67.5 years (IQR 59-74) and 66 (IQR 59-73.5) for TURP and HoLEP, respectively (*P* >.05). No difference was found for median BMI between TURP (25.7; IQR 23.85-27.7) and HoLEP (25.62; IQR 23.37-27.92) (*P* >.05). LUTS determined by IPSS and QoL were also similar. The median IPSSs were 18.5 (IQR 16.25-25.75) for TURP patients and 20 (IQR 14-26.5) for patients treated with HoLEP (*P* >.05). The median score for QoL was 4 for both TURP (IQR 3-4.75) and HoLEP (IQR 3-4.5) (*P* >.05). Voiding parameters, including Q_{max} and PVR, were equally impaired in both cohorts. The medians for Q_{max} were 9.5 mL/s (IQR 8-14) in the TURP arm and 12 mL/s (IQR 9-15.5) for HoLEP (*P* >.05). The median value for PVR documented for TURP was 97 mL (IQR 52.75-172.5), and the HoLEP cohort presented with a median of 100 mL (IQR 55-165) (*P* >.05).

TABLE 1 Baseline characteristics

Characteristics	TURP (n = 98)	HoLEP (n = 97)	*P* value
Age (yr)			
Median	67.5	66	.869
IQR	59-74	59-73.5	
BMI			
Median	25.7	25.62	.982
IQR	23.85-27.7	23.37-27.92	
IPSS			
Median	18.5	20	.302
IQR	16.25-25.75	14-26.5	
QoL			
Median	4	4	.451
IQR	3-4.75	3-4.5	
PV (cc)			
Median	51	51	.612
IQR	41-58	43.5-59	
Total PSA (ng/mL)			
Median	2.3	3.27	**.001**
IQR	1.38-3.50	1.73-5.54	
PSA density (ng/mL/cc)			
Median	0.04	0.07	**.002**
IQR	0.03-0.07	0.04-0.11	
Q_{max} (mL/s)			
Median	9.5	12	.698
IQR	8-14	9-15.5	
PVR (mL)			
Median	97	100	.516
IQR	52.75-172.5	55-165	

Note: Bold values indicate statistically significant *P* values (*P* < .05).
Abbreviations: BMI, body mass index; HoLEP, holmium laser enucleation of the prostate; IPSS, International Prostate Symptom Index; IQR, interquartile range; PSA, prostate-specific antigen; PV, prostate volume; PVR, postvoid residual urine; Q_{max}, peak urinary flow rate; QoL, quality of life; TURP, transurethral resection of the prostate.

3.2 | Direct comparison of TURP vs HoLEP

The perioperative assessment revealed a higher efficiency of tissue removal with HoLEP (Table 2). The median weight of enucleated tissue was 40.0 g (IQR 30-49.5) compared to 20 g (IQR 18-30) after TURP (*P* <.001). Matched for prostate size the tissue retrieval percentage was also higher after HoLEP. About 75.4% (IQR 64-81.2) were removed, which was significantly more than the median value of

TABLE 2 Perioperative and postoperative outcome parameters after 4 wk

Clinical outcomes	TURP (n = 98)	HoLEP (n = 97)	*P* value
Δ IPSS			
Median	7	11	**.007**
IQR	3-14	5.5-17	
Δ QoL			
Median	2	2	.383
IQR	1-3	1-4	
Resected tissue (g)			
Median	20	40	**<.001**
IQR	18-30	30-49.5	
Resected tissue (%)			
Median	47.3	75.4	**<.001**
IQR	40-54.7	64-81.2	
Time (min)			
Median	55.5	62	**.006**
IQR	48-70.5	51-85	
Hemoglobin drop (g/dL)			
Median	0.65	1	**.016**
IQR	0.03-1.3	0.4-1.5	
Δ Q_{max} (mL/s)			
Median	8.5	12	**.028**
IQR	5-18.25	7-23	
Δ PVR (mL)			
Median	66.5	62	.957
IQR	6.5-140	0-145	

Note: Bold values indicate statistically significant *P* values (*P* < .05).
Abbreviations: HoLEP, holmium laser enucleation of the prostate; IPSS, International Prostate Symptom Index; IQR, interquartile range; PVR, postvoid residual urine; Q_{max}, peak urinary flow rate; QoL, quality of life; TURP, transurethral resection of the prostate.

47.3% (IQR 40-54.7) found in the TURP arm (*P* <.001). This might be the reason for the shorter surgery time observed for TURP. Here the procedure took about 55.5 minutes (IQR 48-70.5), whereas the median time for HoLEP was 62 minutes (IQR 51-85) (*P* =.006). Also, the median blood loss documented after the intervention was slightly elevated after HoLEP. The drop in hemoglobin level was 1.0 g/dL (IQR 0.4-1.5) after HoLEP compared to 0.65 g/dL for the patients treated with TURP (*P* =.016). The early functional outcomes 4 weeks after treatment were more pronounced after HoLEP than TURP. The median improvements were 11 points (IQR 5.5-17) and 7 points (IQR 3-14) for HoLEP and TURP, respectively (*P* =.007). The median changes in QoL were 2.0 points for both HoLEP (IQR 1-4) and TURP (IQR 1-3) (*P* >.05). Q_{max} increased more after HoLEP, with a median change of 12.0 mL/s (IQR 7-23), than after TURP with 8.5 mL/s (IQR 5-18.25) (*P* =.028). The median reduction was comparable in both patient cohorts. PVR was reduced by 62 mL (IQR 0-145) and 66.5 mL (IQR 6.5-140) after HoLEP and TURP, respectively (*P* >.05).

3.3 | Adverse events

The overall incidence of treatment-related AEs determined for both matched cohorts was statistically different. With an incidence of 6% (n = 6) compared to 16% (n = 16%), significantly fewer complications occurred with HoLEP than after treatment with TURP (*P* <.05) (Table 3). No differences of incidence for the specific Clavien-Dindo groups were revealed between both cohorts (all *P* >.05). In both treatment arms most of the relevant AEs were classified as Clavien-Dindo grade ≥ 2. The incidence of these complications was comparable between both procedures. Grade ≥ 2 AEs were reported in 68.8% and 66.7% for TURP and HoLEP, respectively (*P* >.05). The grade 3 complications requiring intervention within the first 4 weeks after TURP included urinary retention (n = 1), clot retention (n = 2), bleeding (n = 4), and four cases of an early bulbar urethral stricture. After HoLEP, one patient presented with clot retention and two patients developed a bulbar stricture.

TABLE 3 Treatment-related adverse events (AEs) according to Clavien-Dindo classification

Adverse events	TURP (n = 98)	HoLEP (n = 97)	*P* value
Overall AEs; N (%)	**16** (16%)	**6** (6%)	**.041**
Clavien-Dindo I	**5** (5%)	**2** (2%)	.446
Urinary retention	5	2	.446
Clavien-Dindo II	**3** (3%)	**1** (1%)	.622
Clot retention	2	1	1.000
Fever	1	0	1.000
Clavien-Dindo III	**8** (8%)	**3** (3%)	.215
Clavien-Dindo IIIa	0	0	-
Clavien-Dindo IIIb	8	3	.215
Urinary retention	1	0	1.000
Clot retention	2	1	1.000
Bleeding	1	0	1.000
Urethral stricture	4	2	.683

Note: Bold values indicate statistically significant *P* values (*P* < 0.05).
Abbreviations: HoLEP, holmium laser enucleation of the prostate; TURP, transurethral resection of the prostate.

4 | DISCUSSION

In the rapidly advancing field of surgical treatment modalities for male LUTS, one main objective becomes more and more important. We strive for tailored concepts to address the patients' clinical profile and their expectations. But a *one-size-fits-all* solution appears not to be attainable. A clearly defined patient selection may be key to identify specific features that will respond adequately to therapy. The true clinical benefits and risks of every technique need to be counterbalanced when evaluating and counseling our patients. For many years, the reference method TURP set the benchmark; and when prostate enlargement was too advanced, open prostatectomy proved to be a good choice. All the emerging new procedures have to stand up to the standard before they are considered valid treatment options. HoLEP has definitely come of age, and some even consider it the new gold standard.[14-18] After its introduction 20 years ago, numerous RCTs and meta-analyses confirmed the efficacy and safety of the procedure.[1,7-11,19-21]

In the present study, we reviewed our records of over 2000 procedures performed over the last 4 years and conducted a matched-pair analysis of patients with bothersome LUTS, who underwent TURP or HoLEP in our institution. As demonstrated above, both cohorts are clinically identical, except for their PSA parameters. Matched for a prostate size of 50 cc, our objective was to evaluate the outcomes of HoLEP for an indication where TURP has been considered the reference method for decades. RCTs comparing HoLEP with TURP in the past years included prostate sizes ranging from about 40 cc up to 80 cc.[22-32] HoLEP was always at least as effective as TURP in terms of relief of LUTS and urodynamic parameters, but with a more favorable safety profile. In this short-term analysis both cohorts presented with a good treatment response, but HoLEP turned out to be even superior to TURP in terms of improvements in IPSS, tissue removal, tissue retrieval percentage, and Q_{max}. This supports the trend revealed in meta-analyses toward an overall superiority of HoLEP.[11,12,20] A shorter operation time has always favored TURP, and this was also confirmed by our results. Although this difference was of statistical significance, with a median difference of 6.5 minutes it can be considered clinically irrelevant. The median time just for the enucleation step in our study was 31 minutes (25-45), which is significantly shorter than TURP. But this parameter was not included in the final analysis because there is no technical counterpart in TURP. The drop in hemoglobin levels in this study was lower than in most published RCTs,[27,31] and no blood transfusion was necessary at all. In

terms of hemostatic control our results favor TURP, but with a median reduction in hemoglobin levels of 1.0 g/dL in the HoLEP cohort, the clinical relevance of this observation has to be questioned. The safety assessment revealed a lower incidence of AEs in the short-term follow-up after HoLEP, which supports the results of published meta-analyses.[11,19,20] The typical spectrum of complications, including urinary retention, clot retention, bleeding, and urethral stricture, was also documented in our analysis.

Our data highlight the importance of the surgeon's expertise. The clinical outcomes presented in this study are favorable for both TURP and HoLEP in terms of efficacy and safety. But the results of this matched-pair analysis reaffirm the experience made by specialized centers. Even in the typical TURP territory, HoLEP is able to optimize the early and durable therapeutic effects with a more favorable safety profile. HoLEP is a size-independent procedure that needs to be recognized as a valid alternative in the spectrum of surgical procedures, not only as a transurethral enucleation option for larger prostates but also as a laser-based technique for small- and medium-sized prostates. The published data of a plethora of RCTs and meta-analyses of the last two decades is convincing and needs to be acknowledged. Nevertheless, there is still a considerable reservation among urologists to learn the procedure due to the notorious steep learning curve and the financial burden for the technical equipment. The favorable safety profile, available low-power systems, and reusable laser fibers make it still an attractive investment. Studies on the HoLEP learning curves suggest 20-30 cases under guidance and about 50 procedures for a self-taught learning curve to become comfortable with the technique.[2] For successful implementation of HoLEP as a new technique, mentoring programs are strongly recommended to overcome the obstacles of the first attempts.

In the current study, certain limitations have to be acknowledged. First, this is a retrospective, single-center analysis of 197 matched patients, although the matching process included over 2000 patients. Second, we present only short-term outcomes. The long-term evaluation is still ongoing, which will help to assess common long-term complications like stress urinary incontinence, storage symptoms, sexual dysfunction, and re-treatment rates. Nevertheless, we consider the report of our short-term results of clinical value as they convincingly demonstrate and confirm the potential of the HoLEP procedure.

In this first matched-pair analysis between HoLEP and TURP, it was our main objective to reveal the clinically relevant differences in a representative population of LUTS patients, who according to most international guidelines are treated best with TURP. Both procedures were efficient and safe, but in the direct comparison HoLEP showed a clear trend toward overall superiority.

Due to the growing body of good clinical evidence, HoLEP has gained a position among the established surgical options for the treatment of male LUTS. HoLEP is not only an attractive alternative for the enucleation of larger prostates, but it must be considered a size-independent technique with the potential to outdo the current reference method TURP.

COMPLIANCE WITH ETHICAL STANDARDS

Conflicts of Interest: The authors declare that they have no conflict of interest.

For this type of study formal consent is not required.

This article does not contain any studies with human participants or animals performed by any of the authors.

ORCID

Giuseppe Magistro https://orcid.org/0000-0001-9872-7766

REFERENCES

1. Elmansy HM, Kotb A, Elhilali MM. Holmium laser enucleation of the prostate: long-term durability of clinical outcomes and complication rates during 10 years of followup. *J Urol*. 2011;186(5):1972-1976.
2. Elzayat EA, Elhilali MM. Holmium laser enucleation of the prostate (HoLEP): long-term results, reoperation rate, and possible impact of the learning curve. *Eur Urol*. 2007;52(5):1465-1471.
3. Gilling PJ, Wilson LC, King CJ, Westenberg AM, Frampton CM, Fraundorfer MR. Long-term results of a randomized trial comparing holmium laser enucleation of the prostate and transurethral resection of the prostate: results at 7 years. *BJU Int*. 2012;109(3):408-411.
4. Nickel JC, Aaron L, Barkin J, Elterman D, Nachabe M, Zorn KC. Canadian Urological Association guideline on male lower urinary tract symptoms/benign prostatic hyperplasia (MLUTS/BPH): 2018 update. *Can Urol Assoc J*. 2018;12(10):303-312.
5. Gravas S, Cornu JN, Drake MJ, et al. EAU Guidelines on the Management of Non-Neurogenic Male Lower Urinary Tract Symptoms (LUTS). 2018.
6. AWMF-Reg.Nr:043–035. S2e Leitlinie-Therapie des Benignen Prostatasyndroms (BPS). 2012.
7. Kuntz RM, Lehrich K, Ahyai SA. Holmium laser enucleation of the prostate versus open prostatectomy for prostates greater than 100 grams: 5-year follow-up results of a randomised clinical trial. *Eur Urol*. 2008;53(1):160-166.
8. Li M, Qiu J, Hou Q, et al. Endoscopic enucleation versus open prostatectomy for treating large benign prostatic hyperplasia: a meta-analysis of randomized controlled trials. *PLoS One*. 2015;10(3):e0121265.
9. Lin Y, Wu X, Xu A, et al. Transurethral enucleation of the prostate versus transvesical open prostatectomy for large benign prostatic hyperplasia: a systematic review and meta-analysis of randomized controlled trials. *World J Urol*. 2016;34(9):1207-1219.
10. Naspro R, Suardi N, Salonia A, et al. Holmium laser enucleation of the prostate versus open prostatectomy for prostates >70 g: 24-month follow-up. *Eur Urol*. 2006;50(3):563-568.
11. Cornu JN, Ahyai S, Bachmann A, et al. A systematic review and meta-analysis of functional outcomes and complications following transurethral procedures for lower urinary tract symptoms resulting from benign prostatic obstruction: an update. *Eur Urol*. 2015;67(6):1066-1096.
12. Li S, Zeng XT, Ruan XL, et al. Holmium laser enucleation versus transurethral resection in patients with benign prostate hyperplasia: an updated systematic review with meta-analysis and trial sequential analysis. *PLoS One*. 2014;9(7):e101615.
13. Dindo D, Demartines N, Clavien PA. Classification of surgical complications: a new proposal with evaluation in a cohort of 6336 patients and results of a survey. *Ann Surg*. 2004;240(2):205-213.

14. Kuntz RM. Current role of lasers in the treatment of benign prostatic hyperplasia (BPH). *Eur Urol*. 2006;49(6):961-969.
15. Kuntz RM, Lehrich K, Ahyai S. Does perioperative outcome of transurethral holmium laser enucleation of the prostate depend on prostate size? *J Endourol*. 2004;18(2):183-188.
16. Michalak J, Tzou D, Funk J. HoLEP: the gold standard for the surgical management of BPH in the 21(st) century. *Am J Clin Exp Urol*. 2015;3(1):36-42.
17. van Rij S, Gilling PJ. In 2013, holmium laser enucleation of the prostate (HoLEP) may be the new 'gold standard. *Curr Urol Rep*. 2012;13(6):427-432.
18. Vincent MW, Gilling PJ. HoLEP has come of age. *World J Urol*. 2015;33(4):487-493.
19. Ahyai SA, Gilling P, Kaplan SA, et al. Meta-analysis of functional outcomes and complications following transurethral procedures for lower urinary tract symptoms resulting from benign prostatic enlargement. *Eur Urol*. 2010;58(3):384-397.
20. Tan A, Liao C, Mo Z, Cao Y. Meta-analysis of holmium laser enucleation versus transurethral resection of the prostate for symptomatic prostatic obstruction. *Br J Surg*. 2007;94(10):1201-1208.
21. Yin L, Teng J, Huang CJ, Zhang X, Xu D. Holmium laser enucleation of the prostate versus transurethral resection of the prostate: a systematic review and meta-analysis of randomized controlled trials. *J Endourol*. 2013;27(5):604-611.
22. Chen YB, Chen Q, Wang Z, et al. A prospective, randomized clinical trial comparing plasmakinetic resection of the prostate with holmium laser enucleation of the prostate based on a 2-year followup. *J Urol*. 2013;189(1):217-222.
23. Eltabey MA, Sherif H, Hussein AA. Holmium laser enucleation versus transurethral resection of the prostate. *Can J Urol*. 2010;17(6):5447-5452.
24. Fayad AS, Sheikh MG, Zakaria T, Elfottoh HA, Alsergany R. Holmium laser enucleation versus bipolar resection of the prostate: a prospective randomized study. Which to choose? *J Endourol*. 2011;25(8):1347-1352.
25. Gilling PJ, Mackey M, Cresswell M, Kennett K, Kabalin JN, Fraundorfer MR. Holmium laser versus transurethral resection of the prostate: a randomized prospective trial with 1-year followup. *J Urol*. 1999;162(5):1640-1644.
26. Gupta N, Sivaramakrishna, Kumar R, Dogra PN, Seth A. Comparison of standard transurethral resection, transurethral vapour resection and holmium laser enucleation of the prostate for managing benign prostatic hyperplasia of >40 g. *BJU Int*. 2006;97(1):85-89.
27. Kuntz RM, Ahyai S, Lehrich K, Fayad A. Transurethral holmium laser enucleation of the prostate versus transurethral electrocautery resection of the prostate: a randomized prospective trial in 200 patients. *J Urol*. 2004;172(3):1012-1016.
28. Mavuduru RM, Mandal AK, Singh SK, et al. Comparison of HoLEP and TURP in terms of efficacy in the early postoperative period and perioperative morbidity. *Urol Int*. 2009;82(2):130-135.
29. Rigatti L, Naspro R, Salonia A, et al. Urodynamics after TURP and HoLEP in urodynamically obstructed patients: are there any differences at 1 year of follow-up? *Urology*. 2006;67(6):1193-1198.
30. Shishido T, Enomoto K, Fujita N, et al. Comparison of clinical results between TUR-P and holmium laser enucleation of the prostate (HoLEP) based on the initial experience. *Nihon Hinyokika Gakkai Zasshi*. 2008;99(3):543-550.
31. Sun N, Fu Y, Tian T, et al. Holmium laser enucleation of the prostate versus transurethral resection of the prostate: a randomized clinical trial. *Int Urol Nephrol*. 2014;46(7):1277-1282.
32. Tan AH, Gilling PJ, Kennett KM, Frampton C, Westenberg AM, Fraundorfer MR. A randomized trial comparing holmium laser enucleation of the prostate with transurethral resection of the prostate for the treatment of bladder outlet obstruction secondary to benign prostatic hyperplasia in large glands (40 to 200 grams). *J Urol*. 2003;170(4 Pt 1):1270-1274.

How to cite this article: Magistro G, Westhofen T, Stief CG, Weinhold P. A matched-pair analysis of patients with medium-sized prostates (50 cc) treated for male LUTS with HoLEP or TURP. *Lower Urinary Tract Symptoms*. 2019;1–6. https://doi.org/10.1111/luts.12290

Infection
https://doi.org/10.1007/s15010-019-01315-4

ORIGINAL PAPER

In vitro efficacy of phytotherapeutics suggested for prevention and therapy of urinary tract infections

Julian Marcon[1] · Sören Schubert[2] · Christian G. Stief[1] · Giuseppe Magistro[1]

Received: 17 February 2019 / Accepted: 30 April 2019

Abstract

Purpose To analyse the therapeutic efficacy of various phytotherapeutics and their antimicrobial compounds with regard to strain specificity and dose dependence.

Methods A representative strain collection of 40 uropathogenic bacteria isolated from complicated and uncomplicated urinary tract infection was subjected to various virulence assays (bacterial growth, mannose-sensitive agglutination, and motility) to determine the therapeutic impact of various compounds with antimicrobial activity. We tested proanthocyanidins (PAC), D-mannose, rosemary extract (Canephron®), and isothiocyanates (Angocin®).

Results D-mannose efficiently blocked the adhesive properties of all type 1 fimbriae-positive isolates in low concentration (0.2%), but showed no bacteriostatic effect. PAC also actively blocked agglutination, but the concentration varied considerably among isolates. *Escherichia coli* required the highest concentration (10%), while *Enterobacter cloacae* responded to low concentrations (0.1%). Allyl isothiocyanates not only impaired agglutination in all tested isolates, but also had a dramatic impact on flagella-mediated motility in *Escherichia coli, Klebsiella pneumoniae,* and *Proteus mirabilis* ($p < 0.001$). The administration of rosemary extracts revealed a strong bacteriostatic effect in growth assays. All tested strains were strongly inhibited by the addition of 10 µg/ml or 1 µg/ml of purified rosemary extractions with the exception of *Serratia marcescens*. *Morganella morganii* responded only to 10 µg/ml.

Conclusion Phytotherapeutics and small-molecular compounds like mannosides have the potential to become an integral part in a multi-modal treatment concept for the treatment and prevention of urinary tract infections. Their efficiency can be optimised when strain specificities and therapeutic concentrations are taken into account.

Keywords Urinary tract infections · Phytotherapeutics · Prevention · Therapy · Uropathogenic *Escherichia coli* (UPEC)

Introduction

Antimicrobial resistance (AMR) has emerged as one of the most challenging and threatening problems to public health on a global scale. If we do not change our practice today, we might be on the verge of a pre-antibiotic era scenario. Projections predict an alarming trend, with AMR as the number #1 death cause in the near future [1]. This especially holds true for the management of urinary tract infections (UTI), which are among the most common bacterial infections in clinical practice [2, 3]. Its socio-economic relevance is mirrored by the staggering financial burden to health care systems worldwide. Annual societal costs of 2.4 billion US dollars are caused by 1.3 million emergency room visits and 6.8 million office visits in the US alone [4]. Uropathogenic *Escherichia coli* (UPEC) are the main causative pathogens isolated from about 80% of uncomplicated UTIs [5]. Globally, the resistance rates for the treatment of UPEC are seriously high. Resistance rates for common antibiotic drugs, such as ciprofloxacin, trimethoprim/sulfamethoxazole, and aminopenicillins, reached 45, 48.2, and 50.4%, respectively [6]. Once, the antibiotic treatment of UTI was considered an easy and safe matter, but the rising AMR renders the management more and more challenging.

Now, we need to endorse action plans to prevent this critical development. The four most important cornerstones include the design of novel antibiotic agents, the

✉ Giuseppe Magistro
Giuseppe.Magistro@med.uni-muenchen.de

[1] Department of Urology, Ludwig-Maximilians-University, Marchioninistrasse 15, 81377 Munich, Germany

[2] Max von Pettenkofer-Institut für Hygiene und Medizinische Mikrobiologie, Munich, Germany

Published online: 08 May 2019

development of alternative antimicrobial strategies, effective hygiene and preventive measures, and, finally, the concept of antimicrobial stewardship [7–11]. There has been a considerable developmental void for novel antibiotic agents in the last 3 decades. Consequently, we are in an urgent need for alternatives. Non-antibiotic approaches for the treatment or the prevention of UTI comprise a plethora of concepts. They are an integral part of current guideline recommendations now [12]. Hormonal agents, the use of probiotics, food supplements to modify the urine composition, the design of vaccines and immune-stimulatory compounds, intravesical instillations, and phytotherapeutics have been evaluated [13, 14].

Especially, the role of phytotherapeutics remains still elusive. Although certain underlying modes of action have been postulated, results have not been convincing in the clinical evaluation. For example, cranberry extracts have a proposed efficacy due to its high content of proanthocyanidins (PAC). These compounds interfere with the most prevalent and important adhesins of UPEC. Therefore, they appeared to be effective for the prevention of UTI when administered on a daily basis. In a first Cochrane review, it was concluded that cranberry products can significantly reduce the incidence of recurrent UTIs over 12 months (RR 0.65, 95% CI 0.46–0.90) [15]. However, a more recent Cochrane meta-analysis, including more clinical studies, withdrew the former recommendation due to the lack of positive trials [16]. The optimal formulations, dosages, or regimens have not been determined yet. Similarly, the spectrum of pathogens that might respond to treatment has not been identified. Exemplarily, not all uropathogenic bacteria express the potential targets addressed by proanthocyanidins.

This lack of information applies to almost all tested phytotherapeutics. This prompted us to evaluate the efficacy of various phytopharmaceuticals in a representative collection of different uropathogenic species isolated from complicated and uncomplicated UTIs. In this first in vitro study, we determined the impact of different compounds on relevant virulence features. When phytotherapeutics are considered, we need to first assure that the right targets are hit. These results are supposed to give first insights into the potential spectrum of pathogens appropriate for specific phytotherapeutic compounds.

Methods

Bacterial strains used in the present work were isolated from uncomplicated and complicated UTIs. The strain collection included *Escherichia coli, Klebsiella pneumoniae, Proteus mirabilis, Enterobacter cloacae, Serratia marcescens, Citrobacter freundii, Morganella morganii,* and *Pseudomonas aeruginosa*. We subjected five isolates of each species to different virulence assays.

In this study, we tested proanthocyanidins, D-mannose, rosemary extract, allyl isothiocyanate (AITC), benzyl isothiocyanate (BITC), and phenylethyl isothiocyanate (PITC). The composition of the phytomedical compound Angocin® consists of 38% AITC, 50% BITC and 12% PITC. Concentrations were applied as indicated. The purified substances were all purchased from Sigma-Aldrich Chemie GmbH, Taufkirchen, Germany.

Three relevant virulence mechanisms for the development of UTI were assessed. We investigated adhesive properties mediated by type 1 fimbriae, flagellum-mediated motility, and bacterial growth. All experimental settings were performed according to previously published protocols [17, 18]. Briefly, mannose-sensitive adhesion of bacteria was assayed by the ability to agglutinate yeast cells (*Saccharomyces cerevisiae*) on glass slides [19]. The outcome is evaluated microscopically by the presence of agglutinated cells or loose cells (Fig. 1). Motility was analysed using 0.3% Luria–Bertani soft agar plates. A late logarithmic phase culture (optical density at 600 nm = 1.0; OD_{600nm}) was stabbed into the middle of a soft agar plate and incubated at 37 °C. Motility was quantified by measuring the diameter of motile bacteria after 8 h of incubation (Fig. 2a). The soft agar plates were supplemented with 5 µM AITC, 7 µM BITC, and 8 µM PITC. Growth curves were assessed in triplicates of 50 ml cultures in 250 ml Erlenmeyer flasks. Overnight cultures were incubated in 50 ml fresh Luria–Bertani medium to a starting OD_{600nm} of 0.05 and the optical density was recorded every 20 min. We used a rich medium to ensure optimal growth conditions and focused on the exponential growth phase, which is known to represent the fastest growth kinetics.

The selection of assays and inhibitory compounds was the results of an exploratory screening in concert with the published literature. Published data are mainly restricted to single species. In this manuscript, we evaluated the impact on various strains of different origin. Our aim was to highlight clearly defined effects. Data with an inconsistent outcome were not presented. All experiments were performed

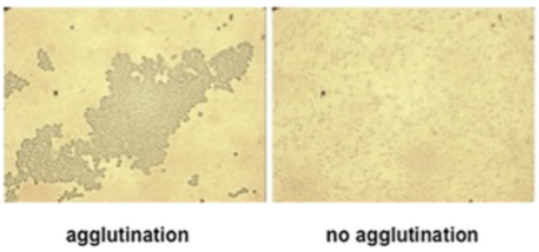

Fig. 1 Mannose-sensitive agglutination mediated by type 1 fimbriae. Microscopically examination of agglutinated cells

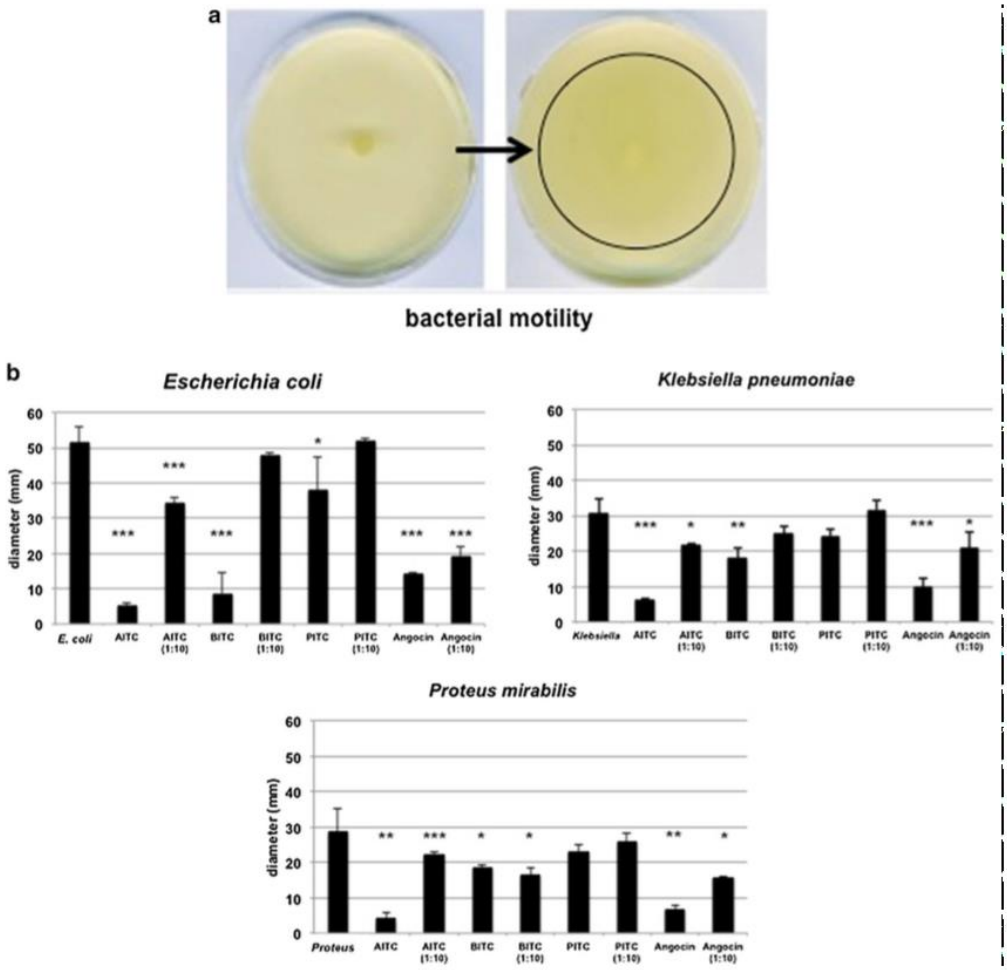

Fig. 2 Flagella-mediated motility. The front of swarming bacteria can be measured after spotting bacteria on the centre of a soft agar plate. Influence of isothiocyanates on the motility of uropathogenic bacteria. Allyl isothiocyanates had the strongest impact on flagella-mediated motility in *Escherichia coli, Klebsiella pneumoniae,* and *Proteus mirabilis*. Allyl isothiocyanate (AITC), benzyl isothiocyanate (BITC), phenylethyl isothiocyanate (PITC), Angocin® (38% AITC: 50% BITC: 12% PITC). $*p<0.05$, $**p<0.01$, $***p<0.001$

in duplicates and repeated at least three times. For statistical analysis, a paired *t* test or the Mann–Whitney *U* test was performed and results were considered statistically significant if the *p* value was lower than 0.05.

Results

Screening for anti-adhesive compounds

In our first screening, we investigated the response to various available phytotherapeutics and small molecules like D-mannose in an agglutination assay (Table 1). D-mannose in various concentrations (0.2%, 2%, 10%) was always able to inhibit agglutination of *E. coli*. Purified PAC, as the active compound in cranberry extracts, was able to interfere with agglutination only using the 10% solution. Among the isothiocyanates, only AITC efficiently blocked agglutination at low concentrations, whereas both BITC and PITC required higher doses of 10%. The combination of all isothiocyanates, as present in the phytomedical preparation Angocin®, displayed a strong inhibitory effect for every concentration applied. Various *Enterobacteriaceae* express type 1 fimbriae, but their role for the development of UTIs is unclear. We included additional type 1 fimbriae-positive isolates with the ability to agglutinate yeast cells. As observed for *E. coli*, D-mannose efficiently blocked agglutination in *Klebsiella pneumoniae, Serratia marcescens,* and *Enterobacter*

Table 1 Inhibition of agglutination mediated by type 1 fimbriae

	Escherichia coli	*Klebsiella pneumoniae*	*Serratia marcescens*	*Enterobacter cloacae*
Supplements (concentration, %)				
D-mannose				
0.2%	+++	+++	+++	+++
2%	+++	+++	+++	+++
10%	+++	+++	+++	+++
Cranberry (PAC)				
0.1%	---	---	---	+++
1%	---	---	+++	+++
10%	+++	+++	+++	+++
AITC				
0.1%	+++	---	---	+++
1%	+++	+++	+++	+++
10%	+++	+++	+++	+++
BITC				
0.1%	---	---	---	---
1%	---	---	+++	---
10%	+++	+++	+++	---
PITC				
0.1%	---	---	---	---
1%	---	+++	+++	---
10%	+++	+++	+++	---
AITC:BITC:PITC (Angocin®)				
0.1%	+++	---	---	+++
1%	+++	+++	+++	+++
10%	+++	+++	+++	+++

In this qualitative assay, the agglutination is determined microscopically

+++ positive inhibition; — no inhibition

cloacae, as well. However, their response to PAC and isothiocyanates differed considerably compared to *E. coli*. With regard to PAC, *Klebsiella pneumoniae* reacted similarly to *E. coli*. However, *Serratia marcescens* and *Enterobacter cloacae* were responsive to lower concentrations. Regarding the response to isothiocyanates, *Enterobacter cloacae* demonstrated inhibition with all dosages of AITC. However, neither BITC nor PITC showed an inhibitory effect. The mixed preparation of isothiocyanates blocked agglutination efficiently. *Klebsiella pneumoniae* and *Serratia marcescens* responded to AITC in higher concentrations. Only the highly concentrated blocking solution with 10% of BITC was efficient in *Klebsiella pneumoniae.* For *Serratia marcescens,* 1% of BITC was sufficient. In the case of PITC, the 1% blocking solution showed an inhibitory effect in *Klebsiella pneumoniae* and *Serratia marcescens.* Correspondingly, the 1% solution of the mixed isothiocyanate compound blocked agglutination activity. This first descriptive screening suggests that the overall response to anti-adhesive compounds depends on the specific species. A dose-dependant inhibitory effect can be observed, but this was different for every species.

Screening for substances interfering with motility

The ability to move to a more favourable niche is another relevant feature associated with bacterial virulence. Some uropathogens express the so-called flagella to ascend within the urinary tract [20]. Flagella-mediated motility can be assayed by spotting bacteria on a soft agar plate and by measuring the diameter of moving bacteria (Fig. 2a). We investigated the effect of isothiocyanates on motility in *E. coli*, *Klebsiella pneumoniae,* and *Proteus mirabilis* (Fig. 2b). *E. coli* displayed the strongest impairment by 5 µM of purified AITC, with a 90% reduction of motility ($p < 0.001$). For the 1:10 dilution, this effect was diminished to 33% ($p < 0.001$). The application of 7 µM BITC yielded a strong inhibitory effect, with an 83% decrease of motility ($p < 0.001$). Supplementation with 8 µM PITC led to a reduction of 25% ($p < 0.05$). The mixed preparation of

isothiocyanates decreased motility by 73% in its undiluted form and by 62% in a 1:10 dilution (both, $p < 0.001$). In *Klebsiella pneumoniae,* AITC was again the strongest inhibitor, showing a motility reduction of 79% ($p < 0.001$). BITC impaired motility by 41% ($p < 0.01$). PITC had no inhibitory effect at all. The Angocin®-like preparation impaired motility by 67% ($p < 0.001$). A similar pattern was also revealed for *Proteus mirabilis.* AITC and BITC decreased motility by 86% ($p < 0.01$) and 38% ($p < 0.05$), respectively. No impairment was detected using PITC. Mixed isothiocyanates reduced motility by 77% ($p < 0.01$). Isothiocyanates turned out to have a strong impact on flagella-mediated motility. The pattern was similar in various species, with AITC displaying the strongest inhibitory effect.

Screening for bacteriostatic agents

The next virulence assay evaluated the inhibitory effect on bacterial growth. We tested the influence of D-mannose and rosemary extracts in *E. coli, Proteus mirabilis, Enterobacter cloacae, Serratia marcescens, Citrobacter freundii, Morganella morganii,* and *Pseudomonas aeruginosa* (Fig. 3). We started to analyse the impact of D-mannose to rule out that our observations made for bacterial agglutination were due to a possible bacteriostatic effect. As depicted in Fig. 3, D-mannose did not affect bacterial growth of the screened isolates at all. The next step was the investigation of rosemary extracts, as they are proposed to mediate various antimicrobial effects [22]. The concentrations were 10 µg/ml and 1 µg/ml. With the only exception of *Serratia marcescens,* all included isolates were significantly impaired when the highest concentration of 10 µg/ml was applied. Even 1 µg/ml of rosemary extract was sufficient to inhibit bacterial growth in most strains, excluding *Serratia marcescens and Morganella morganii.* Again, our results do not speak for a consistent reaction to phytotherapeutics. Our observations rather suggest a differentiated response depending on the target and the concentration of the agent.

Discussion

One of the main questions to be answered is how to tackle the problem of AMR. To overcome this obstacle, we need to act on various levels. The development of novel antibiotic agents is one important mainstay, but it still remains a formidable task. Recently, the novel antibiotic zoliflodacin has been tested successfully for the oral treatment of urogenital gonorrhoea caused by antibiotic-resistant *Neisseria gonorrhoeae* in a phase 2 trial [23]. Novel antimicrobial combinations including ceftolozane/tazobactam, ceftazidime/avibactam, and meropenem/vaborbactam are additional examples that the efforts made in the last years are bearing fruits [24].

Another important aspect is the introduction of efficient vaccines and immune-stimulatory agents as a preventive measure. Uro-Vaxom® and Urovac®/StroVac® have been shown to reduce the UTI recurrence rate compared to placebo in clinical trials and meta-analyses [9, 25]. Newly designed vaccines, such as ExPEC4, are emerging and entering the stage of clinical evaluation [26]. The search for alternative antimicrobial compounds is attracting more and more attention. We strive for equally effective approaches without the risk of inducing antibiotic resistance mechanisms. The concept of anti-virulence treatment addresses the most important virulence factors of pathogens and turns them into strongly attenuated bacteria. Adhesion of the pathogen is one of the first essential steps in the pathogenesis of infectious diseases. In UPEC, up to 13 diverse fimbrial systems can be expressed [20]. Fimbriae are complex microbial structures on the surface with the ability to bind specifically to the host epithelium. Type 1 fimbriae are among the most important adhesins in UPEC. They mediate the first attachment to the urothelium by binding to mannosylated uroplakins. Mannose derivatives are known to block type 1 fimbriae [21]. They proved to be promising candidates for the treatment and prevention in the murine model of UTI [21, 27, 28]. Experimental data even suggest that the action of mannosides is not restricted to the urinary tract. They also appear to selectively deplete type 1 fimbriae-positive UPEC from the intestinal microbiota. These experimental results have also been confirmed in clinical trials. Daily administration of 2 g of D-mannose was equally effective as the antibiotic prophylaxis with nitrofurantoin regarding risk reduction of recurrent UTIs [29]. Our data support the concept of anti-virulence treatment using mannosides. No bacteriostatic or bactericidal effects were observed in the strains tested in this study. However, it was highly effective as a type 1 fimbriae-blocking compound. Our results in concert with published data suggest that, by the inactivation of relevant virulence factors of a pathogen, we are able to efficiently treat and prevent bacterial infections.

Phytotherapeutics might also contain antimicrobial compounds with therapeutic potential. As explained above for the use of cranberry products, they are not recommended due to the lack of positive trials. Our results demonstrate that PAC as the active compound is efficiently impairing the adhesive ability of bacteria. However, we clearly show that this effect is strain specificity and dose dependence. Only type 1 fimbriae-positive strains are responsive. With regard to UPEC, high concentrations were required for complete inhibition, whereas, in *Enterobacter cloacae,* low concentrations were sufficient. In clinical trials, the bacterial spectrum was rarely taken into consideration. With UPEC as the most common pathogen isolated from UTI, our data suggest that the concentration of PAC reached in the urine of patients with recurrent UTI might have been insufficient.

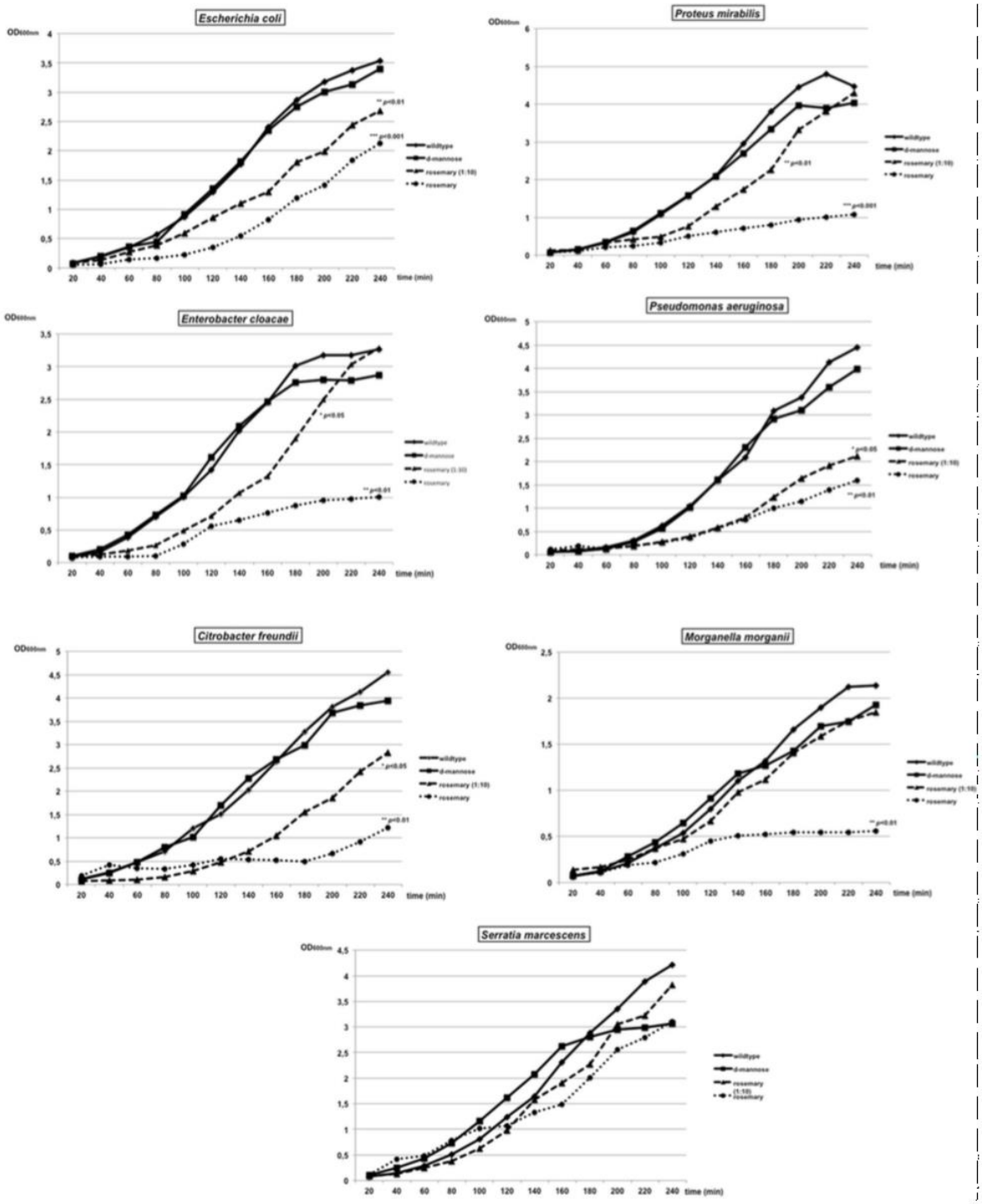

Fig. 3 Bacteriostatic effect of rosemary extracts. Impact of D-Mannose and rosemary extracts on the growth kinetics of various uropathogenic bacteria. OD_{600nm} (optical density at 600 nm). $*p<0.05$, $**p<0.01$, $***p<0.001$

Further RCTs are warranted to evaluate higher dosages of standardised PAC preparations. Phytotherapeutics containing rosemary extracts have recently been analysed in two RCTs for the treatment of uncomplicated cystitis [30, 31]. In the study by Wagenlehner et al., herbal treatment was non-inferior to the antibiotic therapy with fosfomycin, but higher rates of pyelonephritis were detected. Furthermore, Sabadash et al. reported that the addition of phytotherapeutics (Canephron®) to fluoroquinolones (ofloxacin) provided better relief of bothersome cystitis symptoms compared to fluoroquinolones only. Furthermore, they also reduced the rate of recurrent infection. The exact mechanism underlying this observation is not clear. Our results pinpoint towards a bacteriostatic effect of rosemary extracts, which again is strain specificity and dose dependence. All tested isolates responded to purified rosemary extracts except *Serratia marcescens*. For *Morganella morganii,* a bacteriostatic effect was also confirmed, but only at higher concentrations. Another interesting herbal combination containing nasturtium and horseradish indicated clinical efficacy for the treatment and prevention of recurrent UTIs [32, 33]. The high concentration of isothiocyanates is considered to play a relevant role for its therapeutic potential. We investigated the impact of isothiocyanates on flagella-mediated motility. Bacterial motility is another relevant virulence mechanism for the successful ascension and colonisation of the urinary tract [34–36]. Results of the present study provide evidence for a significant impact on motility. Especially, the addition of AITC showed the strongest reduction of bacterial motility in UPEC, *Klebsiella pneumoniae* and *Proteus mirabilis*. The antimicrobial properties of AITC also appear to have an activity against biofilms, which anticipates a potential impact on catheter-associated UTIs [37].

The main objective of the current study was to perform a systematic analysis of available phytotherapeutics with antimicrobial properties and their impact on specific virulence and fitness factors in a representative strain collection of uropathogenic bacteria. It was not the goal to decipher the exact mechanism underlying the effects observed in our assays on a molecular level. This study is descriptive in its nature. Nevertheless, this is the first analysis highlighting the strain specificity and dose dependence of phytotherapeutics. Not all species are responsive to the bioactive compounds in herbal therapeutics. The various therapeutic concentrations have to be considered, as well. These are two relevant aspects that have been largely neglected in clinical trials, which might be one reason for the failure of most studies. Here, we attempted to correlate the in vitro activity with the positive outcomes of clinical trials. Certain limitations of this study need to be acknowledged. This is a descriptive study analysing the antimicrobial activity under standardised in vitro conditions in a qualitative way. It was not the main goal to determine the minimum inhibitory concentrations under our laboratory in vitro settings. We have to admit that the pharmacokinetics of the substances used in this study is still unclear. We still do not know the dosage necessary to achieve a therapeutic concentration in the urinary tract. Further studies are warranted to clarify this essential aspect. Furthermore, our study does not claim to be exhaustive. We focused on Gram-negative bacteria only, but are aware that also Gram-positive pathogens like *Enterococcus spp.* are relevant uropathogenic bacteria. Accordingly, the phytotherapeutics tested in our analysis are not available in every country and more herbal combinations are on the market registered as food supplements. It is important to stress that no recommendation for clinical practice can be formulated based on these in vitro data. We believe that the therapeutic potential of standardised phytotherapeutics can be optimised when they are applied more specifically. Of course, RCTs are necessary to determine the true clinical value of this approach.

Conclusions

With the challenging problem of AMR still rising, we need to act on various levels to check its progress. Phytotherapeutics and small-molecular compounds like mannosides have the potential to become an integral part in a multi-modal treatment concept for the treatment and prevention of UTI.

Author contributions JM: project development, data collection and analysis, and manuscript writing. SS: supervision. CGS: project development and supervision. GM: project development, data collection and analysis, and manuscript writing.

Compliance with ethical standards

Conflict of interest The authors declare that they have no conflict of interest.

Human and animal rights This article does not contain any studies with human participants or animals performed by any of the authors.

References

1. O'Neill J. Antimicrobial resistance: tackling a crisis for the health and wealth of nations. Rev Antimicrob Resist. 2014;1:1–16.
2. Flores-Mireles AL, Walker JN, Caparon M, Hultgren SJ. Urinary tract infections: epidemiology, mechanisms of infection and treatment options. Nat Rev Microbiol. 2015;13:269–84.
3. Stamm WE, Norrby SR. Urinary tract infections: disease panorama and challenges. J Infect Dis. 2001;183:S1–4.
4. Litwin MS, Saigal CS, Yano EM, Avila C, Geschwind SA, Hanley JM, et al. Urologic diseases in America Project: analytical methods and principal findings. J Urol. 2005;173:933–7.
5. Foxman B. The epidemiology of urinary tract infection. Nat Rev Urol. 2010;7:653–60.

6. Tandogdu Z, Cek M, Wagenlehner F, Naber K, Tenke P, van Ostrum E, et al. Resistance patterns of nosocomial urinary tract infections in urology departments: 8-year results of the global prevalence of infections in urology study. World J Urol. 2014;32:791–801.
7. Grabe MJ, Resman F. Antimicrobial stewardship: what we all just need to know. Eur Urol Focus. 2018;5:46–9.
8. Magistro G. Urological infections: "the time for change is now". Eur Urol Focus. 2018;5:1.
9. Magistro G, Stief CG. Vaccine Development for urinary tract infections: where do we stand? Eur Urol Focus. 2018;5:39–41.
10. Naber KG, Wagenlehner FME. Novel antibiotics in the treatment of urinary tract infections. Eur Urol Focus. 2018;5:10–2.
11. Pilatz A, Veeratterapillay R, Koves B, Cai T, Bartoletti R, Wagenlehner F, et al. Update on strategies to reduce infectious complications after prostate biopsy. Eur Urol Focus. 2018;5:20–8.
12. Bonkat G, Bartoletti R, Cai T, Bruyere F, et al. EAU guidelines on urological infections. Edn. presented at the EAU Annual Congress Copenhagen 2018. ISBN 978-94-92671-01-1.
13. Beerepoot MA, Geerlings SE, van Haarst EP, van Charante NM, ter Riet G. Nonantibiotic prophylaxis for recurrent urinary tract infections: a systematic review and meta-analysis of randomized controlled trials. J Urol. 2013;190:1981–9.
14. Smith AL, Brown J, Wyman JF, Berry A, Newman DK, Stapleton AE. Treatment and prevention of recurrent lower urinary tract infections in women: a rapid review with practice recommendations. J Urol. 2018;200:1174–91.
15. Jepson RG, Craig JC. Cranberries for preventing urinary tract infections. Cochrane Database Syst Rev. 2008;10:CD001321.
16. Jepson RG, Williams G, Craig JC. Cranberries for preventing urinary tract infections. Cochrane Database Syst Rev. 2012;10:001321.
17. Magistro G, Hoffmann C, Schubert S. The salmochelin receptor IroN itself, but not salmochelin-mediated iron uptake promotes biofilm formation in extraintestinal pathogenic Escherichia coli (ExPEC). Int J Med Microbiol. 2015;305:435–45.
18. Magistro G, Magistro C, Stief CG, Schubert S. The high-pathogenicity island (HPI) promotes flagellum-mediated motility in extraintestinal pathogenic *Escherichia coli*. PLoS One. 2017;12:e0183950.
19. Schembri MA, Sokurenko EV, Klemm P. Functional flexibility of the FimH adhesin: insights from a random mutant library. Infect Immun. 2000;68:2638–46.
20. Nielubowicz GR, Mobley HL. Host-pathogen interactions in urinary tract infection. Nat Rev Urol. 2010;7:430–41.
21. Hannan TJ, Totsika M, Mansfield KJ, Moore KH, Schembri MA, Hultgren SJ. Host-pathogen checkpoints and population bottlenecks in persistent and intracellular uropathogenic Escherichia coli bladder infection. FEMS Microbiol Rev. 2012;36:616–48.
22. de Oliveira JR, de Jesus D, Figueira LW, de Oliveira FE, Pacheco Soares C, Camargo SE, et al. Biological activities of *Rosmarinus officinalis* L. (rosemary) extract as analyzed in microorganisms and cells. Exp Biol Med (Maywood). 2017;242:625–34.
23. Taylor SN, Marrazzo J, Batteiger BE, Hook EW 3rd, Sena AC, Long J, et al. Single-dose zoliflodacin (ETX0914) for treatment of urogenital gonorrhea. N Engl J Med. 2018;379:1835–45.
24. Giacobbe DR, Mikulska M, Viscoli C. Recent advances in the pharmacological management of infections due to multidrug-resistant Gram-negative bacteria. Expert Rev Clin Pharmacol. 2018;11:1219–36.
25. Aziminia N, Hadjipavlou M, Philippou Y, Pandian SS, Malde S, Hammadeh MY. Vaccines for the prevention of recurrent urinary tract infections: a systematic review. BJU Int. 2018;123:753–68.
26. Huttner A, Hatz C, van den Dobbelsteen G, Abbanat D, Hornacek A, Frolich R, et al. Safety, immunogenicity, and preliminary clinical efficacy of a vaccine against extraintestinal pathogenic Escherichia coli in women with a history of recurrent urinary tract infection: a randomised, single-blind, placebo-controlled phase 1b trial. Lancet Infect Dis. 2017;17:528–37.
27. Cusumano CK, Pinkner JS, Han Z, Greene SE, Ford BA, Crowley JR, et al. Treatment and prevention of urinary tract infection with orally active FimH inhibitors. Sci Transl Med. 2011;3:109ra15.
28. Klein T, Abgottspon D, Wittwer M, Rabbani S, Herold J, Jiang X, et al. FimH antagonists for the oral treatment of urinary tract infections: from design and synthesis to in vitro and in vivo evaluation. J Med Chem. 2010;53:8627–41.
29. Kranjcec B, Papes D, Altarac S. D-mannose powder for prophylaxis of recurrent urinary tract infections in women: a randomized clinical trial. World J Urol. 2014;32:79–84.
30. Wagenlehner FM, Abramov-Sommariva D, Holler M, Steindl H, Naber KG. Non-antibiotic herbal therapy (BNO 1045) versus antibiotic therapy (fosfomycin trometamol) for the treatment of acute lower uncomplicated urinary tract infections in women: a double-blind, parallel-group, randomized, multicentre, non-inferiority phase III trial. Urol Int. 2018;101:327–36.
31. Sabadash MS. Canephron® N in the treatment of recurrent cystitis in women of child-bearing age: a randomised controlled study. Clin Phytosci. 2017;3:9.
32. Albrecht U, Goos KH, Schneider B. A randomised, double-blind, placebo-controlled trial of a herbal medicinal product containing Tropaeoli majoris herba (Nasturtium) and Armoraciae rusticanae radix (Horseradish) for the prophylactic treatment of patients with chronically recurrent lower urinary tract infections. Curr Med Res Opin. 2007;23:2415–22.
33. Lau I, Albrecht U, Kirschner-Hermanns R. Phytotherapy in catheter-associated urinary tract infection: observational study recording the efficacy and safety of a fixed herbal combination containing Tropaeoli majoris herba and Armoraciae rusticanae radix. Urologe A. 2018;57:1472–80.
34. Lane MC, Alteri CJ, Smith SN, Mobley HL. Expression of flagella is coincident with uropathogenic *Escherichia coli* ascension to the upper urinary tract. Proc Natl Acad Sci USA. 2007;104:16669–74.
35. Lane MC, Lockatell V, Monterosso G, Lamphier D, Weinert J, Hebel JR, et al. Role of motility in the colonization of uropathogenic *Escherichia coli* in the urinary tract. Infect Immun. 2005;73:7644–56.
36. Wright KJ, Seed PC, Hultgren SJ. Uropathogenic *Escherichia coli* flagella aid in efficient urinary tract colonization. Infect Immun. 2005;73:7657–68.
37. Kaiser SJ, Mutters NT, Blessing B, Gunther F. Natural isothiocyanates express antimicrobial activity against developing and mature biofilms of Pseudomonas aeruginosa. Fitoterapia. 2017;119:57–63.

Magistro et al. BMC Urology (2019) 19:29
https://doi.org/10.1186/s12894-019-0459-3

BMC Urology

RESEARCH ARTICLE Open Access

Optimized management of urolithiasis by coloured stent-stone contrast using dual-energy computed tomography (DECT)

Giuseppe Magistro[1*], Patrick Bregenhorn[2], Bernhard Krauß[3], Dominik Nörenberg[3], Melvin D'Anastasi[3], Anno Graser[4], Philipp Weinhold[1], Frank Strittmatter[1], Christian G. Stief[1] and Michael Staehler[1]

Abstract

Background: We analysed in vitro the appearance of commonly used ureteral stents with dual-energy computed tomography (DECT) and we used these characteristics to optimize the differentiation between stents and adjacent stone.

Methods: We analysed in vitro a selection of 36 different stents from 7 manufacturers. They were placed in a self-build phantom model and measured using the SOMATOM® Force Dual Source CT-Scanner (Siemens, Forchheim, Germany). Each sample was scanned at various tube potentials of 80 and 150 peak kilovoltage (kVp), 90 and 150 kVp and 100 and 150 kVp. The syngo Post-Processing Suite software program (Siemens, Forchheim, Germany) was used for differentiation based on a 3–material decomposition algorithm (UA, calcium, urine) according to our standard stone protocol.

Results: Stents composed of polyurethane appeared blue and silicon-based stents were red on the image. The determined appearances were constant for various peak kilovoltage (kVp) values. The coloured stent-stone-contrast displayed on DECT improves monitoring, especially of small calculi adjacent to indwelling ureteral stents.

Conclusion: Both urinary calculi and ureteral stents can be accurately differentiated by a distinct appearance on DECT. For the management of urolithiasis patients can be monitored more easily and accurately using DECT if the stent shows a different colour than the adjacent stone.

Keywords: Urolithiasis, Stone disease, Dual-energy computed tomography, Stent-stone-contrast

Background

Urolithiasis is a common bothersome condition with a prevalence of 4–20% and an upward trend is reported in developed countries [1, 2]. Non-contrast enhanced computed tomography (NCCT) is the standard for diagnosing patients with acute flank pain [3]. Low-dose NCCT has emerged as the imaging technique of first choice in the acute setting. It provides both excellent sensitivity of 97% and specificity of 95% for the detection of urinary calculi [4]. NCCT determines accurately location, size, density and skin-to-stone distance, all of which are relevant determinants for treatment decision. With the introduction of technical innovations like dual-energy computed tomography (DECT) acquisition of additional information on chemical stone composition is now possible. The attenuation difference produced by two different x-ray energy spectra is utilized to differentiate uric-acid (UA) calculi from non-uric-acid (non-UA) stones. The post-processing software applied for analysis uses a 3-material decomposition algorithm, which characterizes a calculus as a mixture of UA, calcium and urine. Based on this algorithm, material-specific chromatic image-pixels with an attenuation ratio similar to UA are coloured red, those similar to non-UA stones appear blue. This classification is achieved with high accuracy, which is supported by a reported sensitivity of

* Correspondence: Giuseppe.Magistro@med.uni-muenchen.de
[1]Department of Urology, Ludwig-Maximilians-University of Munich, Marchioninistrasse 15, 81377 Munich, Germany
Full list of author information is available at the end of the article

up to 100% [5–12]. The fact can be decisive for optimal management as in case of UA stones pharmacological chemolitholysis is preferred to interventional approaches [3].

Of note, ureteral stents are also assigned a specific colour according to their material composition on DECT. The imaging of small stones adjacent to a ureteral stent is a common pitfall in the current diagnostic assessment. The option to display stent and stone in contrasting colour may help to optimize the detection. The colour-coded characteristics of calculi based on chemical composition are well documented, whereas for ureteral stents they do not. The determinants underlying the phenomenon of red and blue stents on DECT scans have not been elucidated yet. In the current work it was our main objective to characterize in vitro the appearance of different stents from various manufacturers using DECT.

Methods

In vitro setting

We purchased 36 commonly used stents from 7 manufacturers and analysed them on the third generation SOMATOM® Force Dual Source CT-Scanner (Siemens, Forchheim, Germany). We used a phantom model measuring 45 cm × 20 cm × 20 cm (height x width x depth) and filled it with water at body temperature (36 °C) (Fig. 1). The model itself and experimental settings had no influence on CT performance and analysis. Stents were fixed with clips, spanned throughout the phantom model and consecutive measurements were performed. Each sample was scanned at various tube potentials of 80 and 150 peak kilovoltage (kVp), 90 and 150 kVp and 100 and 150 kVp. We affixed a calculus of 2 mm in diameter of known chemical composition (calcium oxalate monohydrate; blue on DECT scan) to blue and red stents and repeated measurements.

CT protocol and post processing

The images were acquired on a SOMATOM® FORCE Siemens computed tomography (CT) scanner (Siemens, Forchheim, Germany) in dual-energy mode. The patients underwent imaging with 100/Sn150 kVp reflecting our current institutional dual-energy protocol. Continuous non-contrast images were obtained from the level of the diaphragm to the pubic symphysis. A slice thickness of 4 mm and interval of 4 mm were chosen to be consistent with our clinical practice. The images were reconstructed on a multimodality WorkPlace (Siemens) using CT syngo Post-Processing Suite software, version VA 50A (Siemens). Reconstructions used a 0.75-mm slice thickness and 0.7-mm interval, with a QR40 convolution kernel for optimal data analysis. DECT allows differentiating between uric acid (UA) and non-UA stones, which are colour-coded based on a post-processing algorithm. The syngo Post-Processing Suite software program utilizes a 3-material (UA, calcium, and urine) decomposition algorithm to assign colour (red or blue) based on the ratio of X-ray attenuations from the two tube potentials. Materials that more closely resemble the dual-energy characteristics (DEC) of UA stones are depicted in red and those that more closely resemble the DEC of non-UA stones are depicted in blue.

Results

Results are demonstrated in Fig. 2a. All polyurethane-based stents showed a blue appearance on DECT, whereas stents composed of silicone were red. The assigned colours were constant over various kVp values. The determined colour according to material composition of various stents from the same manufacturer was consistent throughout our measurements (Table 1). As shown in Fig. 2b, placing a pure calcium oxalate monohydrate stone (blue) of 2 mm in size next to a ureteral stent of blue colour makes it difficult to discern the fragment on both coronal and sagittal reformatted DECT

Fig. 1 A container was filled with water at body temperature (36 °C). Stents were fixed with clips at both ends and spanned throughout the phantom model for measurements

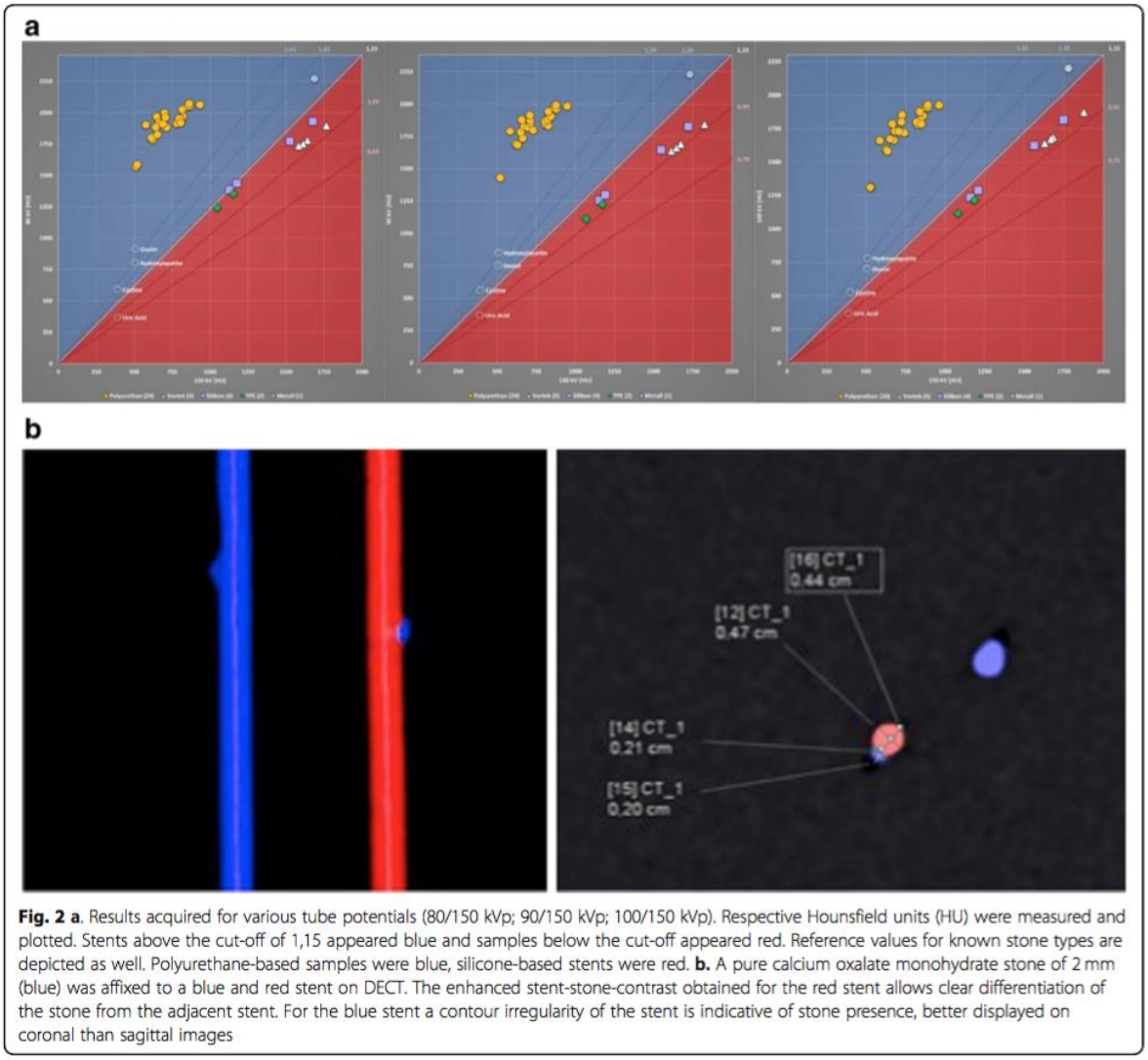

Fig. 2 a. Results acquired for various tube potentials (80/150 kVp; 90/150 kVp; 100/150 kVp). Respective Hounsfield units (HU) were measured and plotted. Stents above the cut-off of 1,15 appeared blue and samples below the cut-off appeared red. Reference values for known stone types are depicted as well. Polyurethane-based samples were blue, silicone-based stents were red. **b.** A pure calcium oxalate monohydrate stone of 2 mm (blue) was affixed to a blue and red stent on DECT. The enhanced stent-stone-contrast obtained for the red stent allows clear differentiation of the stone from the adjacent stent. For the blue stent a contour irregularity of the stent is indicative of stone presence, better displayed on coronal than sagittal images

images. Now, using a silicone-based stent, which appears red on DECT, the presence of the stone could be easily detected due to a clear stent-stone-contrast.

Discussion

Information on chemical stone composition optimizes management of urolithiasis in many ways. As mentioned above, DECT assures identification of UA stones with high accuracy, thus efficient chemolitholysis should be preferred rather than interventional treatment, if it is clinically appropriate and safe. However, the overall incidence of UA stones was estimated to be 11.7% for men and 7% for women [13]. Thus, the clinical impact on management is actually rather low. Furthermore, the unique ability to determine stone types may prevent inefficient treatment options. Extracorporeal shockwave lithotripsy (ESWL) achieves good results for renal stones ≤20 mm, but shockwave-resistant stones composed of calcium oxalate monohydrate or cystine are known negative predictors for success [14]. Both stone types can be identified with high diagnostic accuracy using DECT [15]. In these cases multiple ineffective procedures can be avoided in favour of a more effective treatment modality such as percutaneous nephrolithotomy (PNL).

A distinct appearance of ureteral stents on DECT has been observed, but a systematic analysis of this phenomenon is lacking [16]. In the current study we investigated in vitro a random selection of 36 various samples from 7 manufacturers and we were able to match appearance (blue or red) to material composition

Table 1 A random selection of 36 various stents was purchased from 7 manufacturers. Material composition and reference numbers for each model are displayed. Stents are classified according to their appearance as red or blue on DECT

Manufacturer	RED	BLUE
Uromed		Hydropur (polyurethane, 4640–28) Hydropur (polyurethane, 4687–28) Heparius (polyurethane, 4377–28) Heparius (polyurethane, 4387–28)
Urotech		Yellow-Star (polyurethane, TU-360628) Yellow-Star (polyurethane, EP-360628) Green-Star (polyurethane, EG-480628) White-Star (polyurethane, ES-370628) White-Star (polyurethane, ES-570730)
Cook	C-Flex Towers (TPE, 037732) Universa Soft (TPE, USH-722-T1) Black Silicone (silicone, 133,624)	Universa UFH (polyurethane, UFH-772-T1) Resonance (metal, RMS-060022-R)
Rüsch		Superglide DD (polyurethane, 334,841) Superglide integral (polyurethane, 334,248) Integral Stent Set (polyurethane, 334,201) DD-Ureterstent (polyurethane, 334,801)
Optimed		Optisoft (polyurethane, 3004–2400) Optipur (polyurethane, 3034–2400) Optisplint (polyurethane, 3064–2400) Carbosoft (polyurethane, 3090–2400)
Coloplast/ Porges	Vortek Tumor Stent (Vortek, BCCG75) Vortek (Vortek, ACB576) Vortek Hydrogel (Vortek, BCFA75) Vortek Hydrogel (Vortek, BNFA75) Vortek Mono-J (Vortek, ACA207) Silicone (silicone, AJ4275) Silicone (silicone, AJ4A75) Silikon Pyelostent (silicone, AJ4Y85) Silikon Stenostent (silicone, AJ4W85)	PU-R (polyurethane, AC4D75) PU-R (polyurethane, AC4B75) PU-S (polyurethane, AC4274) Biosoft Duo (polyurethane, BNAA75)
IMP		Tumorstent (polyurethane, S137996070300)

of a stent. In our setting polyurethane-based stents were always blue on DECT, stents composed of silicone appeared always red. We further demonstrated that an enhanced stent-stone-contrast by selecting a stent in a different colour than the adjacent stone facilitates safe and easy detection, even for 2 mm calculi. This enhanced stent-stone-contrast allows clear differentiation in both coronal and sagittal images. Without colour coding, as in NCCT, only a contour irregularity may be suggestive of an adjacent stone, which becomes speculative when calculi decrease in size. This diagnostic obstacle may be overcome using color-coding based on a post-processing algorithm as applied in DECT. We demonstrated that a pure calcium oxalate monohydrate stone (blue) of 2 mm could be clearly differentiated from a silicon-based stent (red). Next to a blue stent, the presence of the stone was indicative by a poorly defined irregularity, which was more prominent on the coronal scan. The analysis of other 2 mm stones with different composition but a distinct colour on DECT scans, could always be detected accurately when the stent appeared in contrasting colour.

This feature may be of value in various clinical scenarios for the management of urolithiasis. The advantage of DECT technology aids urologists in stent selection according to stone appearance and assures accurate monitoring of stone patients. It has to be acknowledged, that stenting is indicated only in case of obstructive pyelonephritis, anuria and analgesia not achieved medically. The impact of our findings still needs to be evaluated for the clinical management.

The early results of DECT imaging for the management of urolithiasis are promising, however, due to the infancy of this technology relevant issues still need to be addressed. Certain pitfalls have been reported including reduced specificity for small calculi < 3 mm and patients with large body habitus [17]. With the development of third-generation scanners and modification of protocol settings and post-processing the capacity and potential of the technology is still advancing [18].

Certain limitations of this study need to be acknowledged. First of all, although we present the analysis of the largest stent collection to date with convincing consistency, we cannot exclude that stents from different manufacturers may display a diverse phenotype. Certain coatings might have a profound impact on appearance on DECT. Second, we present mainly in vitro data. Prospective, clinical trails are necessary to confirm our first results in stone patients and to evaluate the true benefit for management.

Conclusions

Polyurethane-based stents are blue and stents composed of silicone appear red using DECT imaging. The enhanced

stent-stone-contrast using DECT imaging is an additional feature that may be helpful for stent selection. Whenever available, it can contribute to an easy and accurate monitoring of stone patients. The coloured stent-stone-contrast displayed on DECT improves detection, especially of small calculi < 3 mm next to indwelling ureteral stents. Wherever DECT is available, urologists are encouraged to screen for blue and red stents in their institution and to choose ureteral stents according to stone appearance.

Abbreviations
DECT: Dual-energy computed tomography; kVp: peak kilovoltage; NCCT: Non-contrast enhanced computed tomography; PNL: Percutaneous nephrolithotomy; UA: Uric acid

Acknowledgments
None.

Funding
None.

Availability of data and materials
The datasets from this study are available from the corresponding author upon reasonable request.

Authors' contributions
GM: Project development, Data collection and analysis, Manuscript writing. PB: Data collection and analysis. BK: Data collection and analysis. DN: Data collection and analysis. MDA: Data collection and analysis. AG: Data collection and analysis. PW: Data collection and analysis. FS: Data collection and analysis. CGS: Project development, Data collection and management. MS: Project development, Data collection and management. All authors read and approved the final manuscript.

Ethics approval and consent to participate
Not applicable.

Consent for publication
Not applicable.

Competing interests
The authors declare that they have no competing interests.

Publisher's Note

Author details
[1]Department of Urology, Ludwig-Maximilians-University of Munich, Marchioninistrasse 15, 81377 Munich, Germany. [2]Department of Radiology, Ludwig-Maximilians-University of Munich, Munich, Germany. [3]Siemens Healthcare GmbH, Research and Development, Forchheim, Germany. [4]Gemeinschaftspraxis Radiologie München, Munich, Germany.

Received: 21 December 2017 Accepted: 12 April 2019
Published online: 30 April 2019

References

1. Curhan GC. Epidemiology of stone disease. Urol Clin North Am. 2007; 34(3):287–93.
2. Stamatelou KK, Francis ME, Jones CA, Nyberg LM, Curhan GC. Time trends in reported prevalence of kidney stones in the United States: 1976-1994. Kidney Int. 2003;63(5):1817–23.
3. Turk C, Petrik A, Sarica K, Seitz C, Skolarikos A, Straub M, et al. EAU guidelines on diagnosis and conservative Management of Urolithiasis. Eur Urol. 2016;69(3):468–74.
4. Niemann T, Kollmann T, Bongartz G. Diagnostic performance of low-dose CT for the detection of urolithiasis: a meta-analysis. AJR Am J Roentgenol. 2008;191(2):396–401.
5. Primak AN, Fletcher JG, Vrtiska TJ, Dzyubak OP, Lieske JC, Jackson ME, et al. Noninvasive differentiation of uric acid versus non-uric acid kidney stones using dual-energy CT. Acad Radiol. 2007;14(12):1441–7.
6. Spek A, Strittmatter F, Graser A, Kufer P, Stief C, Staehler M. Dual energy can accurately differentiate uric acid-containing urinary calculi from calcium stones. World J Urol. 2016;34(9):1297–302.
7. Boll DT, Patil NA, Paulson EK, Merkle EM, Simmons WN, Pierre SA, et al. Renal stone assessment with dual-energy multidetector CT and advanced postprocessing techniques: improved characterization of renal stone composition--pilot study. Radiology. 2009;250(3):813–20.
8. Eiber M, Holzapfel K, Frimberger M, Straub M, Schneider H, Rummeny EJ, et al. Targeted dual-energy single-source CT for characterisation of urinary calculi: experimental and clinical experience. Eur Radiol. 2012;22(1):251–8.
9. Eliahou R, Hidas G, Duvdevani M, Sosna J. Determination of renal stone composition with dual-energy computed tomography: an emerging application. Semin Ultrasound CT MR. 2010;31(4):315–20.
10. Graser A, Johnson TR, Bader M, Staehler M, Haseke N, Nikolaou K, et al. Dual energy CT characterization of urinary calculi: initial in vitro and clinical experience. Investig Radiol. 2008;43(2):112–9.
11. Hidas G, Eliahou R, Duvdevani M, Coulon P, Lemaitre L, Gofrit ON, et al. Determination of renal stone composition with dual-energy CT: in vivo analysis and comparison with x-ray diffraction. Radiology. 2010;257(2):394–401.
12. Lombardo F, Bonatti M, Zamboni GA, Avesani G, Oberhofer N, Bonelli M, et al. Uric acid versus non-uric acid renal stones: in vivo differentiation with spectral CT. Clin Radiol. 2017;72(6):490–6.
13. Knoll T, Schubert AB, Fahlenkamp D, Leusmann DB, Wendt-Nordahl G, Schubert G. Urolithiasis through the ages: data on more than 200,000 urinary stone analyses. J Urol. 2011;185(4):1304–11.
14. Turk C, Petrik A, Sarica K, Seitz C, Skolarikos A, Straub M, et al. EAU guidelines on interventional treatment for urolithiasis. Eur Urol. 2016; 69(3):475–82.
15. Zhang GM, Sun H, Xue HD, Xiao H, Zhang XB, Jin ZY. Prospective prediction of the major component of urinary stone composition with dual-source dual-energy CT in vivo. Clin Radiol. 2016;71(11):1178–83.
16. Jepperson MA, Thiel DD, Cernigliaro JG, Broderick GA, Parker AS, Haley WE. Determination of ureter stent appearance on dual-energy computed tomography scan. Urology. 2012;80(5):986–9.
17. Jepperson MA, Cernigliaro JG, Sella D, Ibrahim E, Thiel DD, Leng S, et al. Dual-energy CT for the evaluation of urinary calculi: image interpretation, pitfalls and stone mimics. Clin Radiol. 2013;68(12):e707–14.
18. Duan X, Li Z, Yu L, Leng S, Halaweish AF, Fletcher JG, et al. Characterization of urinary stone composition by use of third-generation dual-source dual-energy CT with increased spectral separation. AJR Am J Roentgenol. 2015; 205(6):1203–7.

Journal of Microbiological Methods 154 (2018) 25–32

Contents lists available at ScienceDirect

Journal of Microbiological Methods

journal homepage: www.elsevier.com/locate/jmicmeth

A simple and highly efficient method for gene silencing in *Escherichia coli*

Giuseppe Magistro[a,*], Christiane Magistro[b], Christian G. Stief[a], Sören Schubert[b]

[a] Department of Urology, Ludwig-Maximilians-University, Munich, Germany
[b] Max von Pettenkofer-Institut für Hygiene und Medizinische Mikrobiologie, Munich, Germany

ARTICLE INFO

Keywords:
Gene silencing
RNA interference
Knock down
Escherichia coli

ABSTRACT

Here we present a simple and rapidly achievable protocol for gene silencing in *Escherichia coli* (*E. coli*). In this procedure, antisense RNA (asRNA) of 400-nucleotides (nt) length and absolute complementarity to the target is produced by an expression plasmid. The designed asRNA should ideally cover at least the −10 site of the promoter and the Shine-Dalgarno sequence, and additional 300-bp of the following open reading frame of the target gene. We show that the transcription process of the target is not affected at all, whereas the translation process is impaired. Based on high constitutive expression of asRNA we were able to extend the silencing effect to knock-out levels. By inducible expression, we show that also the modulation is possible. This technique should be widely useful to study gene function in *E. coli* and other bacteria.

1. Introduction

RNA interference (RNAi) via antisense RNA (asRNA) is a cornerstone for controlling the genetic flow in eukaryotic and prokaryotic cells (Khorkova et al., 2014; Saberi et al., 2016; Wagner et al., 2002). Since its discovery, RNAi has become a laboratory standard tool for the modulation of gene function in eukaryotic cell models (Bartel, 2004; Fire et al., 1998; Gregory et al., 2004; Sontheimer, 2005). The modes of action include the interference with transcription, translation and the induction of rapid degradation. Although the presence of asRNAs was firstly documented in bacteria in 1967, its importance remained unappreciated until recent years (Hindley, 1967). One of the first naturally occurring asRNAs was the *micF* RNA identified in *Escherichia coli* and other *Enterobacteriaceae*. The stress response gene *micF* encodes a 93 nt-long asRNA, which impairs expression of the outer membrane protein OmpF by binding *ompF* messenger RNA (mRNA) resulting in both inhibition of translation and degradation (Delihas and Forst, 2001; Green et al., 1986; Guillier et al., 2006). Interest in the field of antisense regulation in bacteria, however, has to be considered rather low in the following period, as by 2001 only twelve chromosomally encoded small RNAs were identified (Saberi et al., 2016). Emerging technologies like RNA-seq have attracted renewed interest and led to the identification of a plethora of regulatory mechanisms involving asRNAs in bacteria.

RNAi as a controlled instrument to modulate gene function as it is established in eukaryotic systems has long been considered impossible in bacteria due to the lack of a machinery similar to the RNA-induced silencing complex (RISC) as found in eukaryotic cells (Hannon and Rossi, 2004). Currently, most of the available protocols to study gene function in bacteria rely on various mutagenesis techniques. Since the discovery of the function of the Clustered Regularly Interspaced Short Palindromic Repeats (CRISPR), which codes for an adaptive immune system in bacteria and archaea (Deltcheva et al., 2011; Ishino et al., 1987; Jinek et al., 2012), it has been widely adopted as a novel tool for targeted genome editing and gene silencing in prokaryotic and eukaryotic cell systems as well (Cho et al., 2013; Cong et al., 2013; Hwang et al., 2013; Jiang et al., 2013; Mali et al., 2013; Qi et al., 2013). For example, by introducing *Cas9* derived from *Streptococcus pyogenes* and an engineered small guide RNA (sgRNA) into the cell system of interest, a versatile toolbox for genomic editing, transcriptional modulation, RNA targeting, and imaging is available (Jiang and Marraffini, 2015; Sternberg and Doudna, 2015). Nevertheless, deciphering the biological function of genes always requires the manipulation of the genetic background of the target organism, either by mutagenesis techniques or the acquisition of various elements that will interfere with cellular processes. These approaches always inherit the risk of off-target effects, genomic rearrangements or polar effects.

Here we describe a simple procedure for gene silencing in the model organism *E. coli*. The approach is based on the concept that the expression of asRNA of absolute complementarity to the target mRNA will specifically knock-down gene function. We determined the length of the asRNA and the critical genetic sites to be addressed for efficient gene silencing. We used either constitutive or inducible expression to evaluate the option to modulate the silencing effect.

* Corresponding author at: Department of Urology, Marchioninistraße 15, 81377 München, Germany.
E-mail address: Giuseppe.Magistro@med.uni-muenchen.de (G. Magistro).

https://doi.org/10.1016/j.mimet.2018.10.003
Received 25 July 2018; Received in revised form 3 October 2018; Accepted 4 October 2018
Available online 05 October 2018

Table 1
Bacterial strains and plasmids.

	Relevant characteristics	Reference
Strains and plasmids		
NU14 wt	O18: K1: H7; cystitis isolate	(Hultgren et al., 1986)
NU14 Δ*ybtA*	*ybtA* deletion mutant	This study
NU14 Δ*ybtA* rec	Complemented mutant, pWKS30-P*ybtA*; Ap	This study
NU14 yRNAi	Wildtype, pHCE-RNAi for *ybtA*; Ap	This study
NU14 vc	Control strain; harbouring empty plasmids pHCE or pTrc99A	This study
NU14 Δ*galU*	*galU* deletion mutant	This study
NU14 Δ*galU* rec	Complemented mutant, pWKS30-P*galU*; Ap	This study
NU14 RNAi-*galU*	Wildtype, pHCE-RNAi for *galU*; Ap	This study
Plasmids		
pKD4	Kanamycin template plasmid	(Datsenko and Wanner, 2000)
pKD46	Lambda red recombinase helper plasmid	(Datsenko and Wanner, 2000)
pCP20	FLP recombinase helper plasmid	(Datsenko and Wanner, 2000)
pWKS30	Low-copy plasmid; Ap	(Wang and Kushner, 1991)
pTrc99A	Plasmid for inducible expression using IPTG; Ap	Pharmacia
pHCE	Plasmid for high constitutive expression; Ap	(Poo et al., 2002)
pWKS30-P*ybtA*	Expressing YbtA under the control of its native promoter; Ap	This study
pRNAi 1	pHCE expressing constituitively *ybtA* antisense RNA; Ap	This study
pRNAi 2	pTrc99A with inducible expression of *ybtA* antisense RNA; Ap	This study
pWKS30-P*galU*	Expressing galU under the control of its native promoter; Ap	This study
pRNAi-*galU*	pHCE expressing constituitively *ybtA* antisense RNA; Ap	This study

2. Material and methods

2.1. Bacterial strains and media

Bacterial strains and plasmids of this study are listed in Table 1. The uropathogenic *E. coli* (UPEC) strain NU14 was isolated from a patient with symptomatic cystitis (Hultgren et al., 1986). Bacteria were cultivated in lysogeny-broth (LB) medium and NBD medium [nutrient broth (NB) supplemented with 200 μM α,α'-dipyridyl (Sigma)]. NBD was used for experiments under iron deplete conditions. Use of antibiotics was provided as necessary [kanamycin 25 μg/ml (Km), ampicillin 100 μg/ml (Ap)].

2.2. Motility assays

Swimming motility was evaluated by using 0.3% LB soft agar plates. A late logarithmic phase culture was adjusted to an OD_{600} = 1.0 and standardised samples were stabbed into the middle of a soft agar plate and incubated at 37 °C. Motility was analysed after 8 h by measuring the diameter of motile bacteria. All experiments were performed in duplicates and repeated at least three times. For statistical analysis a paired *t*-test or the Mann-Whitney *U* test were performed and results were considered statistically significant if the *p*-value was lower than 0.05.

2.3. Construction of isogenic mutants

The isogenic deletion mutant NU14 Δ*ybtA* was generated according to the published protocol by Datsenko and Wanner (Datsenko and Wanner, 2000). Primers with 40-nucleotides (nt) homology extensions to the 5′- and 3′- sites of *ybtA* and 20-nt priming sequences for the template plasmids pKD4 carrying a resistance cassette flanked by FRT recognition target sites were designed (Table 2). The resulting PCR product was transformed into the wild-type strain harbouring the helper plasmid pKD46 with the lambda red recombinase under an arabinose-inducible promoter. In case of successful replacement, Km^R transformants were selected and the correct integration of the resistance cassette was confirmed by PCR.

2.4. Cloning and recombinant DNA techniques

Standard genetic techniques were used mainly as described by Sambrook and Russell (Sambrook, 2001). Enzymes were purchased from Fermentas Thermo Fisher Scientific (St. Leon-Rot, Germany) and used according to the manufacturer's protocol. Primers and plasmids used in this study are listed in Table 2. The plasmid pWKS30-P*ybtA* for complementation of the mutant strain was constructed by PCR amplification of the wild-type gene under the control of its own promoter. The PCR product was purified using a QIAquick PCR purification kit (Qiagen), digested with *KpnI* and *PstI* and cloned into low-copy plasmid pWKS30 (Wang and Kushner, 1991). For the construction of the plasmids pRNAi 1 and 2, both producing antisense RNA for gene silencing of *ybtA*, a 400-nt long fragment starting from the −10 region of the respective promoter was amplified and digested with *Bam*HI and *Sal*I (Fig. 1). The product was cloned into high constitutive expression plasmid pHCE (Poo et al., 2002), resulting in plasmid pRNAi 1. The vector pRNAi 2 is equipped with an IPTG (isopropyl-β-d-thiogalactopyranoside)-inducible *trc* promoter of plasmid pTrc99A. In both plasmids transcription of antisense RNA starts from the original 3'region of *ybtA*. This results in production of antisense RNA that is complementary to the region upstream of the gene of interest and the first 300-nt of the open reading frame of *ybtA*. Hybridization of the antisense RNA to the upstream region of *ybtA* assures covering of the Shine-Dalgarno sequence, which has been shown to be highly sensitive to antisense RNA (Dryselius et al., 2003), and it is supposed to inhibit translation of *ybtA* messenger RNA.

2.5. Western blotting

For detection of protein expression bacterial cultures grown in NBD were collected, corrected to an OD_{600} = 1.0 and finally analysed using rabbit polyclonal antiserum to YbtA (kind gift of A. Rakin) and FyuA (Feldmann et al., 2007). For loading control samples were loaded on a 10% SDS-PAGE and stained with Coomassie-Brilliant-Blue.

2.6. RNA extraction and quantitative real-time PCR (TaqMan)

RNA extraction was performed according to the Trizol (Invitrogen) method (Fu et al., 2013). Total RNA was first treated with DNase I (Fermentas) to remove contaminating genomic DNA. Then, first-strand cDNA was generated using random hexamers and RevertAid H Minus M-MuLV Reverse Transcriptase (Fermentas). PCR reactions were carried out in a final volume of 25 μl containing TaqMan Gene Expression Master Mix (Applied Biosystems), 30 ng of cDNA, primers, and probes.

Table 2
Oligonucleotides.

Genes	Primers and probes	Sequences (5′-3′)
Primers for gene disruption		
ybtA	*ybtA*.KO.for	ATGATGGAGTCACCGCAAACGCAATCTGAAATCTCTATTCACCAGTTGGTGGTCGGTGTAGGCTGGAGCTGCTTC
ybtA	*ybtA*.KO.rev	CATCCCGCGTTTAAAGGTCGAAGGAGTTACGCCAAACTGTTTCTGGAAGGCGGCACATATGAATATCCTCCTTA
galU	*galU*.KO.for	ATGGCTGCCATTAATACGAAAGTCAAAAAAGCCGTTATCCGTGTAGGCTGGAGCTGCTTC
galU	*galU*.KO.rev	TTACTTCTTAATGCCCATCTCTTCTTCAAGCCAGGCTTTACATATGAATATCCTCCTTAG
Primers and probes for TaqMan-PCR		
16SrRNA	*16SrRNA*.for	TTGACGTTACCCGCAGAAGAA
16SrRNA	*16SrRNA*.rev	GCTTGCACCCTCCGTATTACC
16SrRNA	*16SrRNA*.probe	Fam-CGGCTAACTCCGTGCCAGCAGC-Tamra
fyuA	*fyuA*.for	ACACCCGCGAGAAGTTAAATTC
fyuA	*fyuA*.rev	AGCGGTGGTATAGCCGGTACT
fyuA	*fyuA*.probe	Fam-CCTACGACATGCCGACAATGCCTTATTTAA-Tamra
ybtA	*ybtA*.for	GTTGCCTCTCCTGCCACTTC
ybtA	*ybtA*.rev	ATCAGCCAGCAGCAGATCCT
ybtA	*ybtA*.probe	Fam-ACCCGATGGAACGCCAGAAACTG-Tamra
irp2	*irp2*.for	TGGGTGCCGGGTGAATTA
irp2	*irp2*.rev	CGTCCGGGAGCGTCAA
irp2	*irp2*.probe	Fam-ATTTCAACGATCCCCTGCGTAGC-Tamra
Primers for cloning		
ybtA	*PybtA*.KpnI.for	TAGCAGggtaccCTGAATTTCCTGATGAATTT
ybtA	*ybtA*.PstI.rev	TGCATCctgcagGGCCTCTGTCAGGGAGGAGT
RNAi-*ybtA*	RNAi.*ybtA*.SalI.for	TGCAAGgtcgacTGTGAATAATAACCATTATC
RNAi-*ybtA*	RNAi.400.*ybtA*.BamHI.rev	TACGATggatccGTCTGGCGTATGGGTAATGT
RNAi-*ybtA*	RNAi.200.*ybtA*.*Bam*HI.rev	TACGATggatccAACAGCGCAGCAGTTCACC
RNAi-*ybtA*	RNAi.100.*ybtA*.BamHI.rev	TGCATCctgcagGTTTGCGGTGACTCCATCAT
RNAi-*ybtA*	RNAi.50.*ybtA*.BamHI.rev	TGCAAGgtcgacAATAGAACCGAATGGGGTAG
galU	*PgalU*.*Hin*dIII.for	TAGCaagcttATGGCTGCCATTATTACGAA
galU	*PgalU*.BamHI.rev	TGCATCggtaccTTACTTCTTAATGCCCATCT
RNAi-*galU*	RNAi.*galU*.SalI.for	TGCAAGgtcgacGTGGTACTATCGTCGCTATT
RNAi-*galU*	RNAi.400.*galU*.BamHI.rev	TACGATggatccGGCGGACAAATAGACTGCAC

TaqMan PCR was performed on a 7500 Fast Real-Time PCR System (Applied Biosystems). Primers were designed using the Primer Express software (Version 3.0, Applied Biosystems) and probes were labelled with FAM at the 5′-terminus and TAMRA at the 3′-terminus (Table 2). Transcript levels were normalized to 16S rRNA and data were analysed according to the $2^{-\Delta\Delta}$ method (Livak and Schmittgen, 2001).

3. Results

3.1. Analysis of the gene silencing approach on the transcriptional and translational level

The main objective is to generate asRNA with absolute complementarity to the mRNA of interest. Once bound to the target, the gene is silenced by impairment of the ribosome binding to the mRNA as first step of the translation process. With the Shine-Dalgarno sequence being highly sensitive to antisense RNA (Dryselius et al., 2003), we designed fragments covering at least the −10 site of the promoter region of interest. As proof of concept for the gene silencing approach, our target was *ybtA* in the prototypic UPEC isolate NU14. YbtA is a transcriptional regulator of the AraC-like family located on the so-called high-pathogenicity island (HPI). The HPI produces the siderophore yersiniabactin, which represents one highly prevalent iron acquisition system in extraintestinal pathogenic *E. coli* (ExPEC). The regulator YbtA is required for full activation of this pathogenicity island and shows therefore high expression under iron-limited conditions (Perry and Fetherston, 2011; Schubert et al., 1998; Schubert et al., 2002).

In the beginning, it was not clear what the optimal length of the antisense RNA would be to obtain a stable and efficient silencing effect. As a first screening approach we constructed plasmids producing asRNA of different lengths, i.e. 50 nt, 100 nt, 200 nt and 400 nt. Our functional readout was swimming motility, which was recently shown to be supported by the HPI (Magistro et al., 2017). Motility assays were carried out on 0.3% LB soft agar plates and the front of swimming bacteria was measured after 8 h of incubation (Fig. 1B). Only the plasmid expressing 400-nt long asRNA was able to impair significantly motility ($p < .001$). The corresponding sequence was cloned into plasmids with either high constitutive expression (pRNAi 1) or with inducible expression (pRNAi 2). The final plasmid was introduced into the strains to be studied.

The next step was to further analyse this effect on the transcriptional, translational and functional level. Initially we performed qPCR to investigate transcriptional changes between the NU14 wild-type, the NU14 wild-type carrying pRNAi 1 and NU14 Δ*ybtA* under iron starvation using NBD medium (Fig. 2A). Transcript levels of *ybtA* of NU14 wild-type and NU14 with pRNAi 1 displayed no significant difference, indicating that pRNAi does neither affect the transcriptional process nor does it induce the degradation of mRNA. As expected, the *ybtA* deletion mutant showed no transcription of *ybtA*. Gene expression of two further genes located on the HPI was analysed to demonstrate the impact of the *ybtA* knock-down on the transcriptional level. Full transcriptions of *irp2*, coding for a high molecular weight protein (HWMP2) essential for siderophore biosynthesis, and *fyuA*, encoding the designated yersiniabactin receptor, require the regulatory action of YbtA. The promoters of *irp2* and *fyuA* contain specific binding sites termed repeated sequences (RSs). YbtA was shown to bind to these sites as homodimeric complex with yersiniabactin. The importance for transcription of *irp2* and *fyuA* has been demonstrated in previous reports (Anisimov et al., 2005a; Anisimov et al., 2005b; Fetherston et al., 1996; Rakin et al., 1994) and can be confirmed with the almost complete inhibition of gene expression in the *ybtA* mutant. Interestingly, *irp2* and *fyuA* transcript levels were both 20-fold down-regulated in the NU14 strain carrying pRNAi 1 compared to the wild-type strain. This effect is most likely due to the loss of the transcriptional regulator YbtA.

Next, we studied the influence of pRNAi 1 on the protein level (Fig. 2B). Strains were cultivated under iron deplete conditions in NBD medium and samples were subjected to western blotting to detect FyuA and YbtA expression. The *ybtA* deletion mutant demonstrated no FyuA and YbtA expression. Most intriguingly, pRNAi 1 led to a comparable

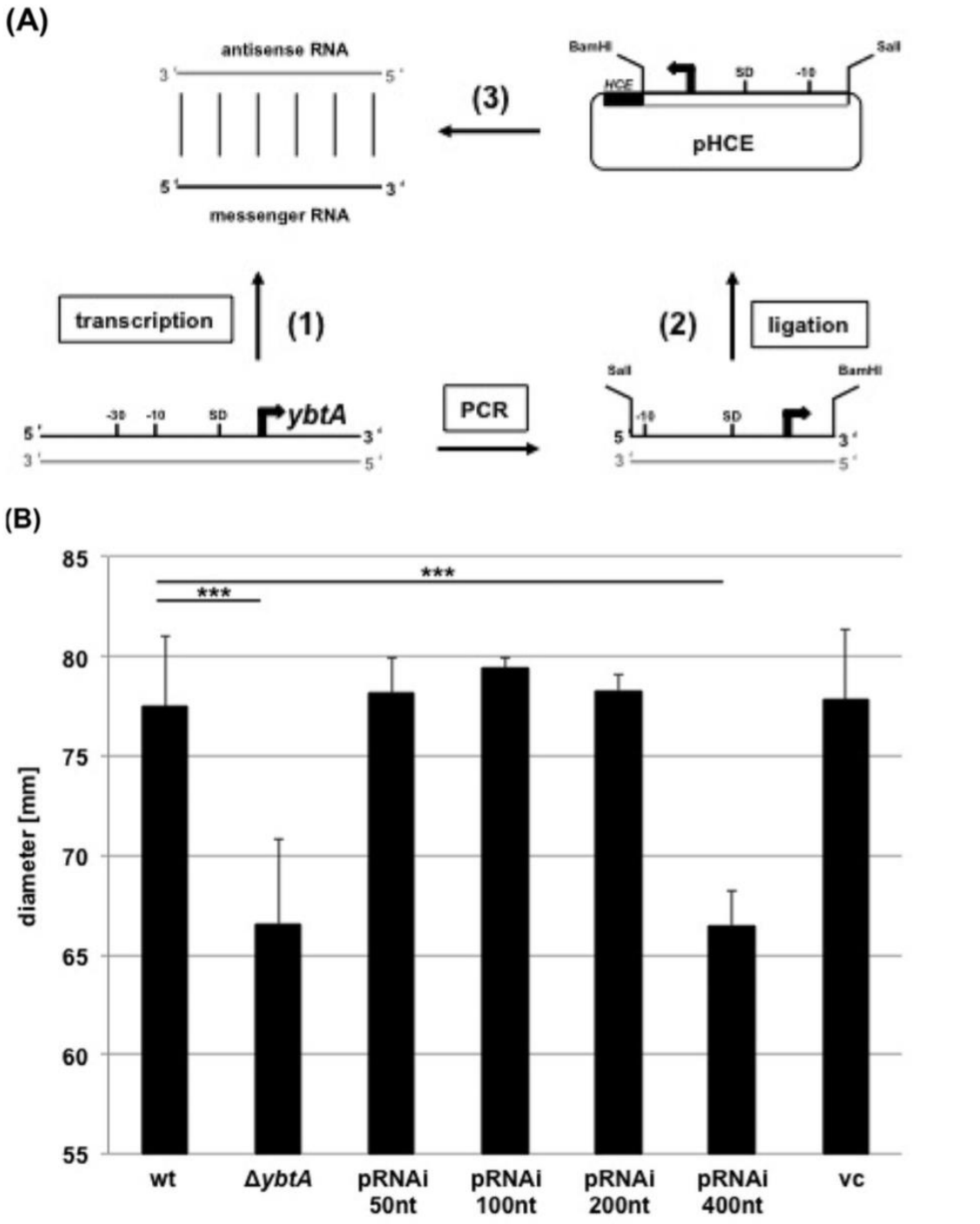

Fig. 1. The rationale of the gene silencing technique.
(A) (Saberi et al., 2016) The physiological initiation of transcription under activating conditions will lead to the generation of messenger RNA. (Khorkova et al., 2014) The asRNA is created by cloning of a fragment in reversed orientation into an expression plasmid (pHCE). Ideally, the designed asRNA covers both the −10 region of the target promoter and the Shine-Dalgarno sequence and in addition up to 300 bp of the open reading frame of the gene of interest. (Wagner et al., 2002) The specifically designed asRNA is produced and it hybridizes to the target messenger RNA with absolute complementarity.

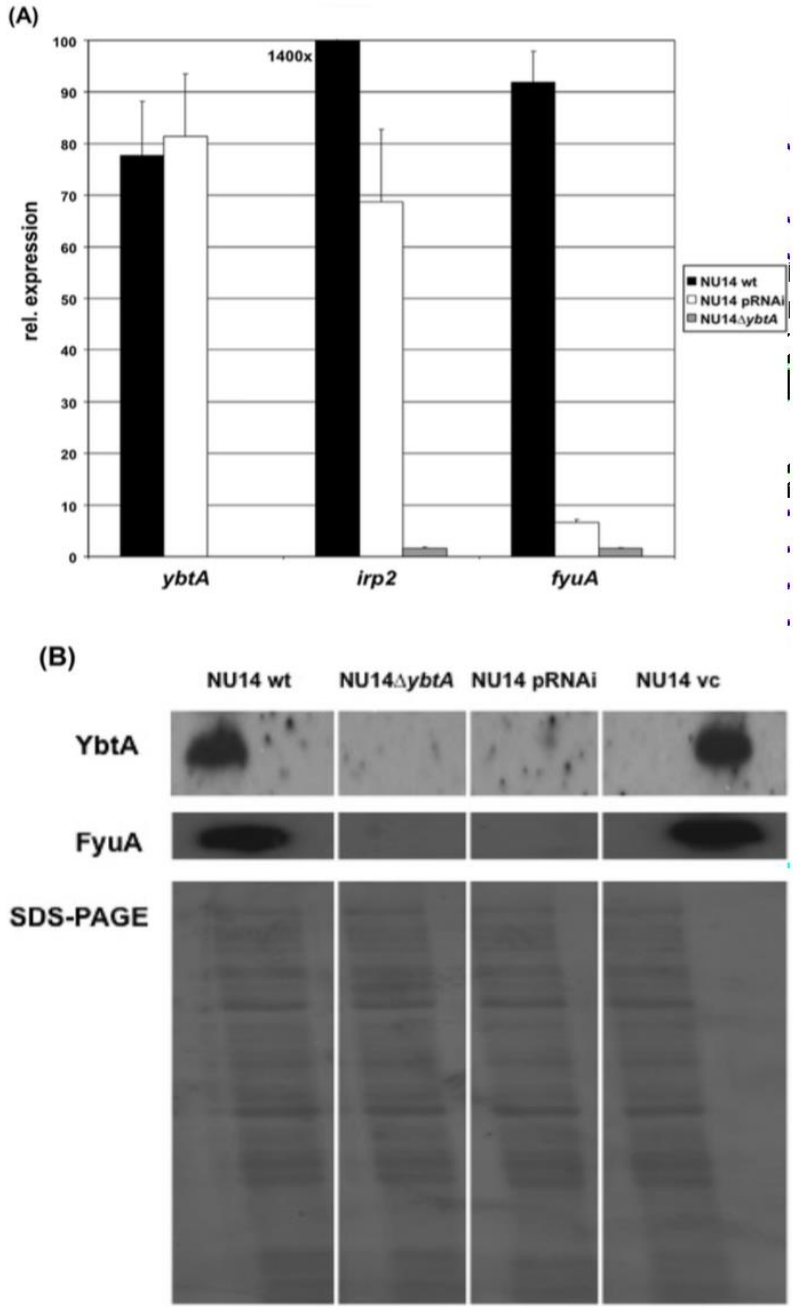

Fig. 2. Transcriptional and translational analysis.
(A) qPCR of HPI genes during growth in iron deplete medium. Expression of asRNA targeting *ybtA* in strain NU14 pRNAi led to no difference in gene expression of *ybtA*, but transcription rates of both *irp2* and *fyuA* were almost 20-fold down-regulated. Data were normalized to 16S rRNA and NU14 wild-type cultivated in iron rich LB medium served as calibrator.
(B) Western blot analysis of FyuA (upper line) and YbtA (lower line) expression under iron deplete conditions. Production of asRNA affected translation comparable to knockout levels. The SDS-PAGE on the bottom served as loading control of the same samples. Lane 1, NU14 wild-type; lane 2, NU14 Δ*ybtA*; lane 3, NU14 pRNAi; lane 4, NU14 vector control.

outcome. This indicates, that translation of *ybtA* mRNA into a protein was almost completely inhibited, explaining the lacking expression of FyuA in the NU14 strain carrying pRNAi 1. Of course, the NU14 wild-type strain and the empty vector control displayed a strong expression of YbtA and FyuA under iron limited conditions. Summing up, these data provide evidence, that pRNAi 1 interferes with the gene function of *ybtA* by inhibition of translation and not on the transcriptional level. We applied this approach in order to confirm the implication of the HPI on flagellum-mediated motility, which was recently shown to promote motility in *E. coli* (Magistro et al., *2017*). Motility assays were carried out on 0.3% LB soft agar plates (Fig. 3A). After 8 h of incubation at 37 °C both the *ybtA* deletion mutant and the wild-type strain expressing asRNA exhibited reduced motility to the same extent, with a 10 mm smaller swimming diameter relative to the wild-type strain and the empty vector control, respectively ($p < .001$). Upon complementation we could restore motility to wild-type levels in the *ybtA* deletion mutant. Overall, these results clearly show that we were able to specifically affect gene function by knocking down *ybtA*.

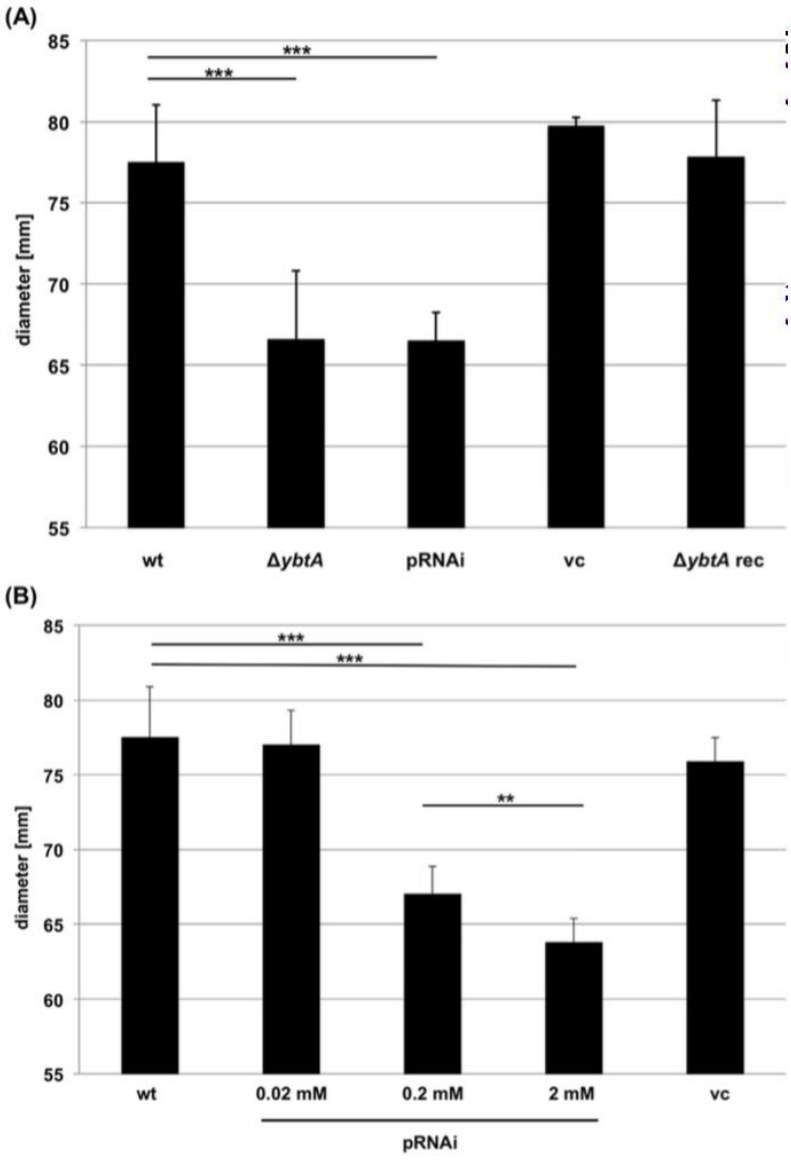

Fig. 3. Functional analysis of *ybtA* knock-downs.
(A) Swimming motility was determined after 8 h of incubation. NU14 Δ*ybtA* and NU14 pRNAi demonstrated equal reduction of motility diameters when high constitutive expression of asRNA was assured. No difference was determined for the vector control and the complemented strain compared to the NU14 wild-type.
(B) Influence of modulated expression of asRNA. An expression plasmid was used for inducible expression of asRNA. Induction with 0.02 mM IPTG led to no change in motility. Rising IPTG concentrations were able to increase silencing efficacy. The strongest silencing was determined for the highest concentration of IPTG. All experiments were performed in triplicates and repeated at least three times. Error bars represent standard deviations. * $p < .05$, ** $p < .01$, *** $p < .001$.

The next step was to evaluate whether the modulation of this gene silencing technique is possible. With plasmid pRNAi 1, constitutive high expression of asRNA is assured. Its functional impact on YbtA was almost identical to the deletion mutant. However, for certain applications a less pronounced impairment of gene function might be desired. In order to modulate the gene silencing, we constructed plasmid pRNAi 2. This plasmid is based on the expression system pTrc99A, which harbours an IPTG - inducible *trc* promoter. The plasmid was introduced into the NU14 wild-type strain and its functional impact was evaluated addressing again the flagella-mediated motility. We applied 0.02 mM, 0.2 mM and 2 mM IPTG for induction. As displayed in Fig. 3B, no significant effect was observed for the lowest concentration. With a log scale increase of IPTG concentration the diameter of motile bacteria was significantly reduced from 77.5 mm (± 3.4 mm) to 68.0 mm (± 3.5 mm) ($p < .001$). Using the highest concentration of 2 mM IPTG this effect was even stronger. The diameter of swimming bacteria on soft agar plates was 62.0 mm (± 4.19 mm) ($p < .001$). The more pronounced effect on motility using 2 mM IPTG compared to 0.2 mM was of statistical significance ($p < .01$). This result clearly shows that the refined expression of highly specific asRNA can be used to modulate the silencing effect on the gene of interest.

Transcriptional regulators such as YbtA tend to be expressed at low levels and therefore, they may be more responsive to asRNA. In order to proof the versatility of the technique we applied our protocol to a highly expressed gene. We selected the glucose-1-phosphate uridylyltransferase GalU, which is known to be implicated in various metabolic and functional processes, among others including flagellum-mediated motility (Caboni et al., 2015; Deng et al., 2010; Hossain et al., 1994; Meyer et al., 2015; Weissborn et al., 1994). According to our protocol we designed 400-nt long asRNA and cloned the respective sequence into plasmid pHCE. We determined its impact on motility in the wild-type strain NU14 after 8 h of incubation (Fig. 4). The *galU* mutant

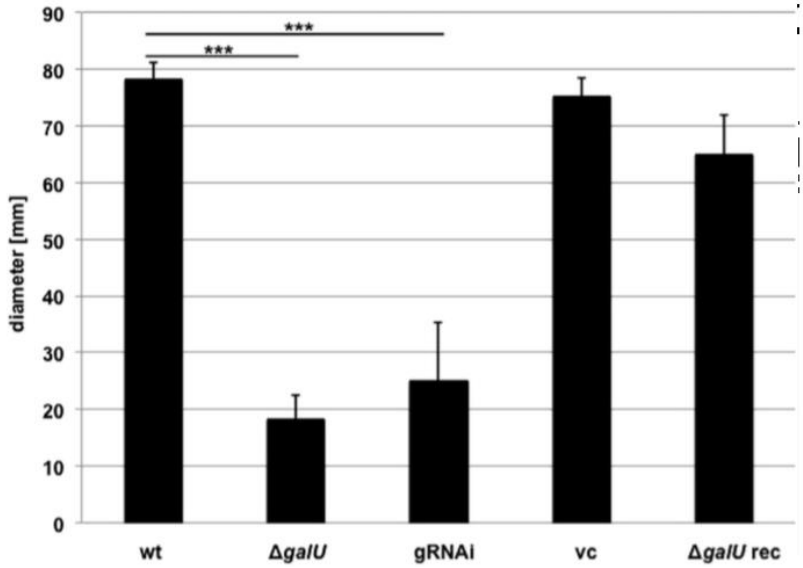

Fig. 4. Gene silencing in *E. coli*.
The gene silencing technique was applied to interfere with the glucose-1-phosphate uridylyltransferase GalU. It is also involved in flagella-mediated motility. A strong reduction of motility was observed for the NU14 Δ*galU* knockout mutant, which could be restored for the complemented strain NU14 Δ*galU* rec. A comparable impact on motility was achieved introducing the asRNA expressing plasmid (gRNAi). All experiments were performed in triplicates and repeated at least three times. Error bars represent standard deviations. * $p < .05$, ** $p < .01$, *** $p < .001$.

displayed a significantly reduced diameter of 60 mm compared to the wild-type ($p < .001$). This phenotype was restored upon complementation, proofing that this phenotype was due to the mutation. NU14 carrying the asRNA expressing plasmid was also impaired significantly with a reduction of 53.3 mm ($p < .001$). Again, this effect was almost comparable to the gene knockout level. This additional experimental set-up provides strong evidence that the presented technique is a valuable tool for gene silencing in *E. coli*.

4. Discussion

The discovery of RNAi must be considered a triumphant advance for molecular science. Since its first description as essential element for genetic regulation in eukaryotic cells, it has become a standard method in laboratories worldwide. Unfortunately, for a very long time this movement went unregarded for the research in prokaryotes like bacteria, as a homologues apparatus was never identified. Nevertheless, the importance of RNAi in bacteria goes beyond any controversy. Numerous examples highlight the fundamental role of asRNA in bacteria for the modulation of transcription and translation, regulation of plasmid replication, plasmid conjugation, bacteriophage development, quorum-sensing, toxin biosynthesis, biofilm formation, metabolite-sensing riboswitches, thermosensing and Hfq-regulated small RNAs (Saberi et al., 2016). But a generally applicable protocol for an easy, safe and self-contained system was still missing. This changed with the development of various toolboxes based on the CRISPR systems. This revolution of specific RNA-directed gene targeting has been exploited in a plethora of applications in both eukaryotes and prokaryotes. The most common procedures are based on CRISPR-Cas9 (Sternberg and Doudna, 2015). Basically, the cells to be investigated are equipped with the Cas9 nuclease or a modified derivate and a chimeric short guide RNA, which hybridizes with the target DNA by Watson-Crick pairing and recruits Cas9 (Hsu et al., 2014; Jinek et al., 2012; Sternberg and Doudna, 2015). Although the versatile potential of this technology has to be acknowledged, introducing this engineered system inherits the potential risk of off-target effects (Fu et al., 2013; Hsu et al., 2014). Especially binding and cleavage specificity of CRISPR-Cas9, chromosomal rearrangements and polar effects in bacterial cell models have yet to be fully determined.

In a plethora of studies RNAi has now been confirmed as a fundamental principle of the regulatory apparatus for the genetic flow in bacteria. But when it comes to practical applications based on asRNA, two main obstacles always have to be overcome (Good and Stach, 2011). First, due to the abundance of natural occurring RNA and its fast decay the sufficient quantity of stable asRNA has to be assured. Second, an efficient delivery system is the key to functionality. There are two general approaches to address both requirements. One relies on the expression of natural asRNA within the cell, the other is supposed to deliver the silencing agent across the tight bacterial cell barriers using biological (transduction, conjugation, transformation), physical (electroporation, laser irridation, sonoporation, heat shock transfer), or chemical methods (peptides, calcium phosphate, lipids, nanoparticles) (Saberi et al., 2016). It may be necessary to stabilize the asRNA transcripts, which is achieved for example by introducing complementary termini creating a stem structure that protects both 5′ and 3′ termini from degradation (Nakashima et al., 2006). When the silencing agent is delivered across membranes, nucleic acid analogs or mimics can be used for protection of the specially designed nucleobase polymer (Geller et al., 2003; Good et al., 2001). As in every protocol developed to interfere specifically with gene function, the knowledge of the target sequence is a prerequisite. Most approaches for asRNA design are consistent with the coverage of at least the ribosome-binding site and the initiation codon of the target gene, but the optimal length of the silencer varies considerably from about 10 to over 100 nt. All these basic principles need to be taken into consideration, when precise and potent gene silencing is applied as a reliable tool.

Here we present a facile and rapidly achievable protocol for gene silencing in bacteria. It is simply based on the concept that asRNA of absolute complementarity to a target mRNA will interfere with the initiation of the respective translation process. The approach was evaluated for the HPI in the prototypic UPEC strain NU14 and the transcriptional, translational and functional analysis clearly demonstrated its efficacy. By introducing an expression plasmid producing highly specific asRNA of at least 400-nt length, we were not only able to knock-down *ybtA* function, but also to modulate the gene silencing. Crucial promoter regions, which have to be covered by the designed asRNA, include the −10 region and the Shine-Dalgarno sequence. Additional coverage of the first 300-bp of the open reading frame of the gene of interest was necessary. Initially, we were not certain about the length of the asRNA. Thus, we evaluated asRNA with various nt-lengths of 50, 100, 200 and 400. A stable silencing effect was observed only for 400 nt. No stabilizing manipulation of the designed asRNA was needed.

The molecular reasons for this requirement are not fully understood. The mechanistic insights underlying this novel protocol were not the scope of this project. As the hybridization process of asRNA and the target sequence is mainly sustained by Watson-Crick pairing, maybe stable binding for sterical inhibition of translation was achieved by only such long asRNA. Using asRNA of 400-nt length with absolute complementarity to a target sequence may reduce the risk of unspecific binding and therefore minimize off-target effects. In our experiments no adverse phenotype was observed. Of course, genome-wide characterization is needed to address the issue of off-target events, but this was not part of this proof of principle study. This protocol was successfully performed for other genes as well. We believe that this protocol should be widely useful. To adapt it to more distantly related bacteria, it should just be necessary to assure asRNA production by established expression plasmids in the respective strain.

Author contributions

G. M. contributed to project development, data collection, data analysis, and manuscript writing.
C. M. contributed to data collection and data analysis.
CG. S. contributed to project development and manuscript writing.
S. S. contributed to project development and manuscript writing.

Conflicts of interest

The authors declare that they have no conflict of interest.

Funding

None.

(B) Screening for the efficient length of asRNA. Plasmids expressing 50 nt, 100 nt, 200 nt or 400 nt asRNA were constructed to knock-down *ybtA*. Motility was assessed after 8 h of incubation to determine the optimal length. Only the construct expressing a 400 nt-long asRNA was able to significantly impair motility. All experiments were performed in triplicates and repeated at least three times. Error bars represent standard deviations. * $p < .05$, ** $p < .01$, *** $p < .001$.

References

Anisimov, R., Brem, D., Heesemann, J., Rakin, A., 2005a. Molecular mechanism of YbtA-mediated transcriptional regulation of divergent overlapping promoters ybtA and irp6 of Yersinia enterocolitica. FEMS Microbiol. Lett. 250 (1), 27–32.
Anisimov, R., Brem, D., Heesemann, J., Rakin, A., 2005b. Transcriptional regulation of high pathogenicity island iron uptake genes by YbtA. Int. J. Med. Microbiol. 295 (1), 19–28.
Bartel, D.P., 2004. MicroRNAs: genomics, biogenesis, mechanism, and function. Cell 116 (2), 281–297.
Caboni, M., Pedron, T., Rossi, O., Goulding, D., Pickard, D., Citiulo, F., et al., 2015. An O antigen capsule modulates bacterial pathogenesis in Shigella sonnei. PLoS Pathog. 11 (3), e1004749.
Cho, S.W., Kim, S., Kim, J.M., Kim, J.S., 2013. Targeted genome engineering in human cells with the Cas9 RNA-guided endonuclease. Nat. Biotechnol. 31 (3), 230–232.
Cong, L., Ran, F.A., Cox, D., Lin, S., Barretto, R., Habib, N., et al., 2013. Multiplex genome engineering using CRISPR/Cas systems. Science 339 (6121), 819–823.
Datsenko, K.A., Wanner, B.L., 2000. One-step inactivation of chromosomal genes in Escherichia coli K-12 using PCR products. Proc. Natl. Acad. Sci. U. S. A. 97 (12), 6640–6645.
Delihas, N., Forst, S., 2001. MicF: an antisense RNA gene involved in response of Escherichia coli to global stress factors. J. Mol. Biol. 313 (1), 1–12.
Deltcheva, E., Chylinski, K., Sharma, C.M., Gonzales, K., Chao, Y., Pirzada, Z.A., et al., 2011. CRISPR RNA maturation by trans-encoded small RNA and host factor RNase III. Nature 471 (7340), 602–607.
Deng, W.L., Lin, Y.C., Lin, R.H., Wei, C.F., Huang, Y.C., Peng, H.L., et al., 2010. Effects of galU mutation on Pseudomonas syringae-plant interactions. Mol. Plant-Microbe Interact. 23 (9), 1184–1196.
Dryselius, R., Aswasti, S.K., Rajarao, G.K., Nielsen, P.E., Good, L., 2003. The translation start codon region is sensitive to antisense PNA inhibition in Escherichia coli. Oligonucleotides 13 (6), 427–433.
Feldmann, F., Sorsa, L.J., Hildinger, K., Schubert, S., 2007. The salmochelin siderophore receptor IroN contributes to invasion of urothelial cells by extraintestinal pathogenic Escherichia coli in vitro. Infect. Immun. 75 (6), 3183–3187.
Fetherston, J.D., Bearden, S.W., Perry, R.D., 1996. YbtA, an AraC-type regulator of the Yersinia pestis pesticin/yersiniabactin receptor. Mol. Microbiol. 22 (2), 315–325.
Fire, A., Xu, S., Montgomery, M.K., Kostas, S.A., Driver, S.E., Mello, C.C., 1998. Potent and specific genetic interference by double-stranded RNA in Caenorhabditis elegans. Nature 391 (6669), 806–811.
Fu, Y., Foden, J.A., Khayter, C., Maeder, M.L., Reyon, D., Joung, J.K., et al., 2013. High-frequency off-target mutagenesis induced by CRISPR-Cas nucleases in human cells. Nat. Biotechnol. 31 (9), 822–826.
Geller, B.L., Deere, J.D., Stein, D.A., Kroeker, A.D., Moulton, H.M., Iversen, P.L., 2003. Inhibition of gene expression in Escherichia coli by antisense phosphorodiamidate morpholino oligomers. Antimicrob. Agents Chemother. 47 (10), 3233–3239.
Good, L., Stach, J.E., 2011. Synthetic RNA silencing in bacteria - antimicrobial discovery and resistance breaking. Front. Microbiol. 2, 185.
Good, L., Awasthi, S.K., Dryselius, R., Larsson, O., Nielsen, P.E., 2001. Bactericidal antisense effects of peptide-PNA conjugates. Nat. Biotechnol. 19 (4), 360–364.
Green, P.J., Pines, O., Inouye, M., 1986. The role of antisense RNA in gene regulation. Annu. Rev. Biochem. 55, 569–597.
Gregory, R.I., Yan, K.P., Amuthan, G., Chendrimada, T., Doratotaj, B., Cooch, N., et al., 2004. The Microprocessor complex mediates the genesis of microRNAs. Nature 432 (7014), 235–240.
Guillier, M., Gottesman, S., Storz, G., 2006. Modulating the outer membrane with small RNAs. Genes Dev. 20 (17), 2338–2348.
Hannon, G.J., Rossi, J.J., 2004. Unlocking the potential of the human genome with RNA interference. Nature 431 (7006), 371–378.
Hindley, J., 1967. Fractionation of 32P-labelled ribonucleic acids on polyacrylamide gels and their characterization by fingerprinting. J. Mol. Biol. 30 (1), 125–136.
Hossain, S.A., Tanizawa, K., Kazuta, Y., Fukui, T., 1994. Overproduction and characterization of recombinant UDP-glucose pyrophosphorylase from Escherichia coli K-12. J. Biochem. 115 (5), 965–972.
Hsu, P.D., Lander, E.S., Zhang, F., 2014. Development and applications of CRISPR-Cas9 for genome engineering. Cell 157 (6), 1262–1278.
Hultgren, S.J., Schwan, W.R., Schaeffer, A.J., Duncan, J.L., 1986. Regulation of production of type 1 pili among urinary tract isolates of Escherichia coli. Infect. Immun. 54 (3), 613–620.
Hwang, W.Y., Fu, Y., Reyon, D., Maeder, M.L., Tsai, S.Q., Sander, J.D., et al., 2013. Efficient genome editing in zebrafish using a CRISPR-Cas system. Nat. Biotechnol. 31 (3), 227–229.
Ishino, Y., Shinagawa, H., Makino, K., Amemura, M., Nakata, A., 1987. Nucleotide sequence of the iap gene, responsible for alkaline phosphatase isozyme conversion in Escherichia coli, and identification of the gene product. J. Bacteriol. 169 (12), 5429–5433.
Jiang, W., Marraffini, L.A., 2015. CRISPR-Cas: New Tools for Genetic Manipulations from Bacterial Immunity Systems. Annu. Rev. Microbiol. 69, 209–228.
Jiang, W., Bikard, D., Cox, D., Zhang, F., Marraffini, L.A., 2013. RNA-guided editing of bacterial genomes using CRISPR-Cas systems. Nat. Biotechnol. 31 (3), 233–239.
Jinek, M., Chylinski, K., Fonfara, I., Hauer, M., Doudna, J.A., Charpentier, E., 2012. A programmable dual-RNA-guided DNA endonuclease in adaptive bacterial immunity. Science 337 (6096), 816–821.
Khorkova, O., Myers, A.J., Hsiao, J., Wahlestedt, C., 2014. Natural antisense transcripts. Hum. Mol. Genet. 23 (R1), R54–R63.
Livak, K.J., Schmittgen, T.D., 2001. Analysis of relative gene expression data using real-time quantitative PCR and the 2(−Delta Delta C(T)) Method. Methods 25 (4), 402–408.
Magistro, G., Magistro, C., Stief, C.G., Schubert, S., 2017. The high-pathogenicity island (HPI) promotes flagellum-mediated motility in extraintestinal pathogenic Escherichia coli. PLoS One 12 (10), e0183950.
Mali, P., Yang, L., Esvelt, K.M., Aach, J., Guell, M., Dicarlo, J.E., et al., 2013. RNA-guided human genome engineering via Cas9. Science 339 (6121), 823–826.
Meyer, C., Hoffmann, C., Haas, R., Schubert, S., 2015. The role of the galU gene of uropathogenic Escherichia coli in modulating macrophage TNF-alpha response. Int. J. Med. Microbiol. 305 (8), 893–901.
Nakashima, N., Tamura, T., Good, L., 2006. Paired termini stabilize antisense RNAs and enhance conditional gene silencing in Escherichia coli. Nucleic Acids Res. 34 (20), e138.
Perry, R.D., Fetherston, J.D., 2011. Yersiniabactin iron uptake: mechanisms and role in Yersinia pestis pathogenesis. Microbes Infect. 13 (10), 808–817.
Poo, H., Song, J.J., Hong, S.P., et al., 2002. Biotechnol. Lett. 24, 1185.
Qi, L.S., Larson, M.H., Gilbert, L.A., Doudna, J.A., Weissman, J.S., Arkin, A.P., et al., 2013. Repurposing CRISPR as an RNA-guided platform for sequence-specific control of gene expression. Cell 152 (5), 1173–1183.
Rakin, A., Saken, E., Harmsen, D., Heesemann, J., 1994. The pesticin receptor of Yersinia enterocolitica: a novel virulence factor with dual function. Mol. Microbiol. 13 (2), 253–263.
Saberi, F., Kamali, M., Najafi, A., Yazdanparast, A., Moghaddam, M.M., 2016. Natural antisense RNAs as mRNA regulatory elements in bacteria: a review on function and applications. Cell. Mol. Biol. Lett. 21, 6.
Sambrook, J.R., 2001. D.W. Molecular Cloning a Laboratory Manual, 3rd edition. .
Schubert, S., Rakin, A., Karch, H., Carniel, E., Heesemann, J., 1998. Prevalence of the "high-pathogenicity island" of Yersinia species among Escherichia coli strains that are pathogenic to humans. Infect. Immun. 66 (2), 480–485.
Schubert, S., Picard, B., Gouriou, S., Heesemann, J., Denamur, E., 2002. Yersinia high-pathogenicity island contributes to virulence in Escherichia coli causing extraintestinal infections. Infect. Immun. 70 (9), 5335–5337.
Sontheimer, E.J., 2005. Assembly and function of RNA silencing complexes. Nat. Rev. Mol. Cell Biol. 6 (2), 127–138.
Sternberg, S.H., Doudna, J.A., 2015. Expanding the Biologist's Toolkit with CRISPR-Cas9. Mol. Cell 58 (4), 568–574.
Wagner, E.G., Altuvia, S., Romby, P., 2002. Antisense RNAs in bacteria and their genetic elements. Adv. Genet. 46, 361–398.
Wang, R.F., Kushner, S.R., 1991. Construction of versatile low-copy-number vectors for cloning, sequencing and gene expression in Escherichia coli. Gene 100, 195–199.
Weissborn, A.C., Liu, Q., Rumley, M.K., Kennedy, E.P., 1994. UTP: alpha-D-glucose-1-phosphate uridylyltransferase of Escherichia coli: isolation and DNA sequence of the galU gene and purification of the enzyme. J. Bacteriol. 176 (9), 2611–2618.

PLOS ONE

RESEARCH ARTICLE

The high-pathogenicity island (HPI) promotes flagellum-mediated motility in extraintestinal pathogenic *Escherichia coli*

Giuseppe Magistro[1]*, Christiane Magistro[2], Christian G. Stief[1], Sören Schubert[2]

1 Department of Urology, Ludwig-Maximilians-Universität, Munich, Germany, **2** Max von Pettenkofer-Institut für Hygiene und Medizinische Mikrobiologie, Munich, Germany

* Giuseppe.Magistro@med.uni-muenchen.de

Citation: Magistro G, Magistro C, Stief CG, Schubert S (2017) The high-pathogenicity island (HPI) promotes flagellum-mediated motility in extraintestinal pathogenic *Escherichia coli*. PLoS ONE 12(10): e0183950. https://doi.org/10.1371/journal.pone.0183950

Editor: Dongsheng Zhou, Beijing Institute of Microbiology and Epidemiology, CHINA

Received: May 20, 2017

Accepted: August 15, 2017

Published: October 10, 2017

Data Availability Statement: All relevant data are within the paper.

Funding: The authors received no specific funding for this work.

Competing interests: The authors have declared that no competing interests exist.

Abstract

The key of success of extraintestinal pathogenic *Escherichia coli* (ExPEC) to colonize niches outside the intestinal tract and to establish infection is the coordinated action of numerous virulence and fitness factors. The so-called high-pathogenicity island (HPI), responsible for synthesis, secretion and uptake of the siderophore yersiniabactin, proved to be an important virulence determinant. In this study we investigated the interaction of the flagellum-mediated motility and the HPI. The impairment of yersiniabactin production by deletion of *irp2* or *ybtA* affected significantly motility. The gain of yersiniabactin production improved motility in both pathogenic and non-pathogenic *E. coli* strains. The loss of flagella expression had no adverse effect on the HPI. Strikingly, external iron abundance was not able to suppress activation of the HPI during motility. The HPI activity of swarming bacteria was comparable to iron deplete conditions, and could even be maximized by supplementing excessive iron. This fact is the first description of a regulatory mechanism, which does not follow the known hierarchical regulation of siderophore systems. Transcriptional reporter fusions of the *ybtA* promoter demonstrated that the entire promoter region with all YbtA binding sites is necessary for complete induction in both HPI-positive and HPI-negative strains. Altogether, these results suggest that the HPI is part of a complex regulatory network, which orchestrates various virulence mechanisms to optimize the overall fitness of ExPEC.

Introduction

Over the last decades the growing body of evidence was helpful to elucidate the pathogenic potential of extraintestinal pathogenic *E. coli* (ExPEC) [1–3]. The orchestrated action of a plethora of virulence and fitness factors enables ExPEC to colonize and to establish infections outside the intestinal tract resulting in diseases like urinary tract infection (UTI), neonatal meningitis, sepsis, intraabdominal infection, pneumonia, osteomyelitis, cellulitis and wound infection. Transcriptomic and proteomic approaches were performed to identify determinants essential to the pathogenesis of UTI [4–6]. It is striking to note that iron acquisition systems always proved to be key players. To face the iron scarcity of the urinary tract, ExPEC has

evolved a multi-factorial strategy to scavenge efficiently for this nutrient [7]. The so-called high pathogenicity island (HPI), responsible for synthesis, secretion and uptake of the siderophore yersiniabactin, represents one of these fundamental iron uptake systems. This pathogenicity island was firstly described in *Yersinia* spp. and spread in a big bang-like moment over a variety of *Enterobacteriaceae*, where it plays a major role in virulence [8–10]. As a pathogenicity island it displays typical features [11–14]: (i) a gene cluster large in size (≥35kb); (ii) location next to a tRNA encoding gene; (iii) a G+C content higher than the host chromosome; (iv) it carries a gene coding for an integrase; (v) the final product contributes to virulence. The genetic organization and regulation of the HPI have been subject of intense research [15]. The mixed-type siderophore yersiniabactin is synthesized by a mixed nonribosomal peptide synthetase (NRPS) / polyketide synthase (PKS) process [16]. YbtA, a transcriptional regulator of the AraC-like family, and the iron master regulator Fur control the transcriptional regulation of the four operons located within the HPI, (i) *ybtA*, (ii) *fyuA*, (iii) *irp2- irp5*, (iv) *irp6-irp9* [17–19]. The promoters of *irp2*, *fyuA*, and the divergent overlapping promoter region between *irp6* and *ybtA* contain specific binding sites termed repeated sequences (RSs). YbtA is proposed to bind to these sites as a homodimeric complex with yersiniabactin. Full expression of Irp2, FyuA and Irp6 depend on the action of YbtA. Here the transcriptional regulator works as an activator. Regarding its own transcription, YbtA shows auto-repression.

Interestingly, the supply of ferric iron to the microbial cell is considered to be the main function, but recent studies indicate the implication of the HPI in various processes apart from just iron acquisition. So Paauw et al. reported that the high binding affinity of yersiniabactin for ferric iron not only promotes bacterial growth by supplying additional iron but also reduces the production of reactive oxygen species by activated immune cells [20]. Furthermore, elements expressed by the HPI for the uptake of ferric yersiniabactin display additional functions. So, the outer membrane receptor FyuA contributes to efficient biofilm formation in human urine and deletion of *fyuA* additionally led to morphological changes of bacteria during biofilm maturation [21]. With FyuA being pathogen-specific, antigenic, surface exposed and *in vivo* expressed it fulfils all essential criteria of a potential vaccine candidate [22]. A multiepitope vaccine containing immunodominant epitopes of iron uptake receptors including FyuA was developed and conveyed protection against ExPEC in a murine model of peritonitis [23; 24]. Another study investigating the primary metabolome of uropathogenic *E. coli* (UPEC) strain UTI89 during growth in minimal medium revealed metabolic changes when genes of the HPI were mutated [25]. An extraordinary observation regarding the HPI function has been reported in UPEC strain CFT073 [26]. This isolate is unable to produce yersiniabactin due to mutations of biosynthetic genes [27; 28]. The fact gives reason to believe, that the deletion of the entire genomic island harbouring the HPI would have no impact on the pathogenicity in a murine model of ascending UTI. Most strikingly, in a co-challenge infection with the wild type strain, the deletion mutant demonstrated a log–scale reduction in colonization of the kidneys.

The versatility of the HPI clearly shows how this acquired iron uptake system became part of a complex network that coordinates various virulence and fitness properties. This multifunctional aspect prompted us to investigate whether additional virulence mechanisms may utilize the HPI. The hostile environment of the urinary tract forces ExPEC to get access to more favourable sites to scavenge for nutrients like iron, as well as to escape the host immune response. In this regard, flagellum-mediated motility has been demonstrated to be of great importance [29–31]. Only a few studies tried to relate the role of siderophore mediated iron uptake to motility. For example, the loss of pyoverdine synthesis in *Pseudomonas putida* abolished completely bacterial surface movement [32]. A functional genomic approach with swarming *Salmonella typhimurium* revealed a strong induction of iron uptake systems during

motility [33]. In the case of *Vibrio parahaemolyticus*, it is known that iron depletion is an essential signal for swarmer cell differentiation [34]. A relevant role of iron homeostasis for motility has also been reported in UPEC [35]. The iron master regulator Fur represses iron uptake systems by binding to specific Fur binding-sites, so called Fur boxes, in complex with ferrous iron under iron abundance. Whenever iron is limited, Fur is inactivated and Fur-regulated genes are de-repressed. Fur boxes were also identified upstream of the activator of flagellar expression *flhD*. Both deletion of *fur* and iron scarcity had a strong impact on motility. Altogether, these examples point towards an important contribution of iron acquisition systems to flagellum-mediated motility. In this work, the main objective is to examine the interaction of the HPI and motility in ExPEC. We present data showing the strong induction of the HPI in motile bacteria and the impact of iron on this interaction.

Material and methods

Bacterial strains and media

Bacterial strains and plasmids used in the present work are listed in Table 1. The prototypic UPEC strain NU14 was isolated from a patient suffering from cystitis [36]. Bacteria were cultured in Luria-Bertani (LB) medium and nutrient broth (NB) [containing per liter: 8 g nutrient broth (Difco), 5 g NaCl] at 37˚C with aeration. NB medium was supplemented with 200 μM α, α'-dipyridyl (Sigma) resulting in NBD medium in order to create iron deplete conditions. Use of antibiotics was provided as necessary (chloramphenicol 20 μg/ml, kanamycin 25 μg/ml, ampicillin 100 μg/ml, tetracycline 12 μg/ml).

Motility assays

Swimming motility was assessed by using 0.3% LB soft agar plates. A late logarithmic phase culture (OD_{600} = 1.0) was stabbed into the middle of a soft agar plate and incubated at 37˚C. Four hours after inoculation motility was quantified every hour by measuring the diameter of swimming bacteria. In order to address the influence of iron excess on motility in a rich medium like LB, soft agar plates were supplemented with different concentrations of additional $Fe(III)Cl_3$ (Fluka AG) as indicated. Samples for β-galactosidase assays, western blotting and quantitative real-time PCR were prepared by scraping bacteria off the edge of a motility ring of strains swarming on a 0.5% LB swarm plate. All experiments were performed in duplicates and repeated at least three times. For statistical analysis a paired t-test or the Mann-Whitney U test were performed and results were considered statistically significant if the *p*-value was lower than 0.05.

Construction of isogenic mutants

Deletion mutants of target genes were generated using the lambda red recombinase approach published by Datsenko and Wanner [37]. Briefly, primers with 40-nt homology extensions to the 5' and 3' regions of the gene of interest and 20-nt priming sequences for the template plasmids pKD3 or pKD4 carrying resistance cassettes flanked by FRT recognition target sites were designed (Table 2). The resulting PCR product was then transformed into strains harbouring the helper plasmid pKD46 with lambda red recombinase under an arabinose-inducible promoter. In case of successful replacement of the specific gene, Km^R or Cm^R transformants were selected. Correct integration of the resistance cassette was confirmed by PCR.

Table 1. Bacterial strains and plasmids.

Strains and plasmids	Relevant characteristics	Reference
NU14 wt	O18: K1: H7; cystitis isolate	[36]
NU14 Δ*ybtA*	*ybtA* deletion mutant	This study
NU14 Δ*irp2*	*irp2* deletion mutant	This study
NU14 Δ*ybtA* rec	complemented mutant, pWKS30-P*ybtA*; Ap	This study
NU14 Δ*irp2* rec	complemented mutant, pWKS30-P*irp2*; Ap	This study
NU14 *hpi*::Kn	entire *hpi* deleted; Kn	This study
CFT073 wt	O6: K2: H1; urosepsis isolate; Ybt negative	[41]
CFT073 Ybt+	Ybt+, Cm	This study
NU14 3RS	wild type, pMP220-3RS; Tet	This study
NU14 2RS+	wild type, pMP220-2RS+FBS; Tet	This study
NU14 2RS	wild type, pMP220-2RS; Tet	This study
NU14 1RS	wild type, pMP220-1RS; Tet	This study
DH5α	*fhuA2 Δ(argF-lacZ)U169 phoA glnV44 Φ80 Δ(lacZ)M15 gyrA96 recA1 relA1 endA1 thi-1 hsdR17*	Stratagene
DH5α Ybt+	Ybt+, Cm	This study
DH5α 3RS	wild type, pMP220-3RS; Tet	This study
DH5α 2RS+	wild type, pMP220-2RS+FBS; Tet	This study
DH5α 2RS	wild type, pMP220-2RS; Tet	This study
DH5α 1RS	wild type, pMP220-1RS; Tet	This study
Plasmids		
pKD3	chloramphenicol template plasmid	[37]
pKD4	kanamycin template plasmid	[37]
pKD46	lambda red recombinase helper plasmid	[37]
pCP20	FLP recombinase helper plasmid	[37]
pWKS30	low-copy plasmid, Ap	[39]
pWKS30-P*ybtA*	expressing YbtA under the control of the native promoter, Ap	This study
pWKS30-P*irp2*	expressing Irp2 under the control of the native promoter, Ap	This study
pCP1	carrying *irp*1-9, *fyuA*, *ybtA* genes and 400 nucleotides of intB, R6K ori; Cm	[42]
pMP220	contains promoterless *lacZ* for transcriptional reporter fusions, Tet	[40]
p3RS	pMP220 carrying entire *ybtA* promoter, Tet	This study
p2RS+	pMP220 carrying two repeated sequences (RS1, RS2) plus Fur binding site, Tet	This study
p2RS	pMP220 carrying two repeated sequences (RS1, RS2) without Fur binding site, Tet	This study
p1RS	pMP220 carrying one repeated sequence (RS2), Tet	This study

https://doi.org/10.1371/journal.pone.0183950.t001

Cloning and recombinant DNA techniques

Standard genetic methods were performed mainly as described by Sambrook and Russell [38]. Enzymes were purchased from Fermentas and used according to the manufacturer's recommendations. Primers and plasmids used in this study are listed in Table 2. Plasmids for complementation of the deleted genes were constructed by PCR amplification of the wild type alleles under the control of their own promoter. The PCR products were purified using a QIAquick PCR purification kit (Qiagen), digested with *KpnI* and *PstI* and cloned into low-copy plasmid pWKS30 [39]. In order to generate transcriptional reporter gene fusions different fragments of the *ybtA* promoter were PCR amplified, digested with *KpnI* and *PstI* and fused with a promoterless *lacZ* gene in plasmid pMP220 [40]. The iron independent YbtA expression was achieved by cloning *ybtA* into plasmid pWKS30 under the control of a *lac* promoter using *KpnI* and *PstI* as restriction enzymes. *YbtA* under the control of a *lac* promoter from plasmid pWKS30-ybtA was PCR amplified, digested with *BamHI* and *SalI* and cloned into the

Table 2. Oligonucleotides.

Primers for gene disruption		
genes	**primers**	**sequences (5'-3')**
irp2	*irp2*.KO.for	CAGCAGTTACATGAAGAGAGCAACCTGATCCAGGCCGGCCTGGAGTGTAGGCTGGAGCTGCTTC
irp2	*irp2*.KO.rev	GTTTGAGTTCACGGAGTAATTCGACGCCGGACCAGTGGCGATGCTCATATGAATATCCTCCTTA
ybtA	*ybtA*.KO.for	ATGATGGAGTCACCGCAAACGCAATCTGAAATCTCTATTCACCAGTTGGTGGTCGGTGTAGGCTGGAGCTGCTTC
ybtA	*ybtA*.KO.rev	CATCCCGCGTTTAAAGGTCGAAGGAGTTACGCCAAACTGTTTCTGGAAGGCGGCACATATGAATATCCTCCTTA
irp2	*irp2*.KO.for	CAGCAGTTACATGAAGAGAGCAACCTGATCCAGGCCGGCCTGGAGTGTAGGCTGGAGCTGCTTC
irp2	*irp2*.KO.rev	GTTTGAGTTCACGGAGTAATTCGACGCCGGACCAGTGGCGATGCTCATATGAATATCCTCCTTA
fliI	*fliI*.KO.for	AGTGTCGCCACTCGCTGGCAAGAACTCTGCCGTCTGGCAGCACCAGGAGTGGTGTAGTGTAGGCTGGAGCTGCTTC
fliI	*fliI*.KO.rev	GATCTTTCAGGGTCGCCAGCGCACCATGTTCTGCCATCTGCCGTTATCTCCTGGGCATATGAATATCCTCCTTA
Primers and probes for TaqMan-PCR		
genes	**primers and probes**	**sequences (5'-3')**
16SrRNA	*16SrRNA*.for	TTGACGTTACCCGCAGAAGAA
16SrRNA	*16SrRNA*.rev	GCTTGCACCCTCCGTATTACC
16SrRNA	*16SrRNA*.probe	FAM-CGGCTAACTCCGTGCCAGCAGC-TAMRA
fyuA	*fyuA*.for	ACACCCGCGAGAAGTTAAATTC
fyuA	*fyuA*.rev	AGCGGTGGTATAGCCGGTACT
fyuA	*fyuA*.probe	FAM-CCTACGACATGCCGACAATGCCTTATTTAA-TAMRA
ybtA	*ybtA*.for	GTTGCCTCTCCTGCCACTTC
ybtA	*ybtA*.rev	ATCAGCCAGCAGCAGATCCT
ybtA	*ybtA*.probe	FAM-ACCCGATGGAACGCCAGAAACTG-TAMRA
Irp2	*Irp2*.for	TGGGTGCCGGGTGAATTA
Irp2	*Irp2*.rev	CGTCCGGGAGCGTCAA
Irp2	*Irp2*.probe	FAM-ATTTCAACGATCCCCTGCGTAGC-TAMRA
fliC	*fliC*.for	CAGGCGATTGCTAACCGTTT
fliC	*fliC*.rev	ATACCATCGTTGGCGTTACGT
fliC	*fliC*.probe	FAM-TTCTAACATTAAAGGCCTGACTCAGGC-TAMRA
fliD	*fliD*.for	GCGTAAGCGCAAGCATCATT
fliD	*fliD*.rev	GCCGGTGTCATTTGATGTGA
fliD	*fliD*.probe	FAM-ACGTGGGTAACGGTGAATATCGTCT-TAMRA
flgK	*flgK*.for	GGGAATAAAACCGCGACGTT
flgK	*flgK*.rev	GGAAAGCTGCGTCACCACAT
flgK	*flgK*.probe	FAM-AAAACCAGTAGCGCCACGCAAGGT-TAMRA
Primers for cloning		
genes	**primers**	**sequences (5'-3')**
ybtA	*PybtA*.KpnI.for	TAGCAGggtaccCTGAATTTCCTGATGAATTT
ybtA	*ybtA*.PstI.rev	TGCATCctgcagGGCCTCTGTCAGGGAGGAGT
Irp2	*Pirp2*.KpnI.for	TAGCACggtaccCCGGGGTCGCGCCCCCCTAA
Irp2	*Irp2*.PstI.rev	TCACTActgcagCTATATCCGCCGCTGACGAC
3RS	*PybtA*.KpnI.for	TAGCAGggtaccCTGAATTTCCTGATGAATTT
3RS	*PybtA*.PstI.rev	TCAGCActgcagGACCTGGTTATCTCCCTGTG
2RS+	*PybtA*.2RS+.KpnI.for	TAGCAGggtaccTGGCGTTCTGAGAATTAATG
2RS+	*PybtA*.PstI.rev	TCAGCActgcagGACCTGGTTATCTCCCTGTG
2RS	*PybtA*.2RS.KpnI.for	TAGCAGggtaccAACTCATCTACCCCATTCGG
2RS	*PybtA*.PstI.rev	TCAGCActgcagGACCTGGTTATCTCCCTGTG
1RS	*PybtA*.1RS.KpnI.for	TAGCAGggtaccTATACCCGCATTGGTCTAAG
1RS	*PybtA*.PstI.rev	TCAGCActgcagGACCTGGTTATCTCCCTGTG

https://doi.org/10.1371/journal.pone.0183950.t002

tetracycline cassette of plasmid pACYC184. A yersiniabactin complemented derivative of the wild type strain CFT073 [41] was constructed by integrating the functional *hpi* core region of *Y. enterocolitica* using plasmid pCP1 [42]. All genetic constructs established in this study were validated by screening PCRs before they were used in experiments.

β-galactosidase assays

β-galactosidase activities of reporter gene fusions were quantified mainly according to standard procedures [43] and expressed as miller units. In order to focus specifically on the regulatory effect of YbtA on its own promoter, a second plasmid pWKS30-*ybtA* expressing YbtA under the control of a *lac* promoter was introduced. All experiments were performed in duplicates and repeated at least three times. For statistical analysis a paired t-test or the Mann-Whitney U test were performed and results were considered statistically significant if the *p*-value was lower than 0.05.

Western blotting

For the detection of flagellar expression bacteria swarming on 0.5% LB swarm plates were scraped off carefully, resuspended in PBS and finally adjusted to an OD_{600} = 1.0. Bacteria from this standardized culture were pelleted by centrifugation and subjected to sodium dodecyl sulfate-polyacrylamide gel electrophoresis (SDS-PAGE) and subsequently transferred to a Protran® nitrocellulose transfer membrane (Whatman). Rabbit polyclonal antiserum to H7 flagellin (kind gift of B. Westerlund-Wikström) was used as primary antibody. For the detection of high pathogenicity island proteins bacterial cultures grown in LB medium or NBD medium were collected, adjusted to an OD_{600} = 1.0 and finally analysed using rabbit polyclonal antiserum to YbtA (kind gift of A. Rakin) and FyuA [44]. The respective samples were loaded on a SDS-PAGE and stained with Coomassie-Brilliant-Blue, which served as loading control.

RNA extraction and quantitative real-time PCR (TaqMan)

Different RNA samples were prepared as described above. RNA extraction was performed using the Trizol (Invitrogen) method [45]. Total RNA was first treated with DNase I (Fermentas) to remove contaminating genomic DNA. Then, first-strand cDNA was synthesized using random hexamers and RevertAid H Minus M-MuLV Reverse Transcriptase (Fermentas) according to the manufacturer's recommendation. TaqMan PCR was run on a 7500 Fast Real-Time PCR System (Applied Biosystems). Primers were designed using the Primer Express software (Version 3.0, Applied Biosystems) and probes were labelled with FAM at the 5'-terminus and TAMRA at the 3'-terminus (Table 2). TaqMan PCR reactions were carried out in a final volume of 25 μl containing TaqMan Gene Expression Master Mix (Applied Biosystems), primers, probe and 30ng of cDNA. Transcript levels were normalized to 16 S rRNA. Data were analyzed by the $2^{-\Delta\Delta}$ method as described by Livak and Schmittgen [46].

Results

The influence of yersiniabactin synthesis on flagellar motility in UPEC

In a first attempt to determine the role of the HPI in flagellum-mediated motility, defined mutations affecting genes involved in the biosynthesis of yersiniabactin were generated in the prototypic UPEC strain NU14. *Irp2*, coding for HMWP2 (high molecular weight protein 2) [47], and *ybtA*, encoding a transcriptional regulator of the AraC-like family [19], were deleted according to the protocol described by Datsenko and Wanner [37]. The functional impact of these deletions on yersiniabactin production was verified in a yersiniabactin detection *luc*

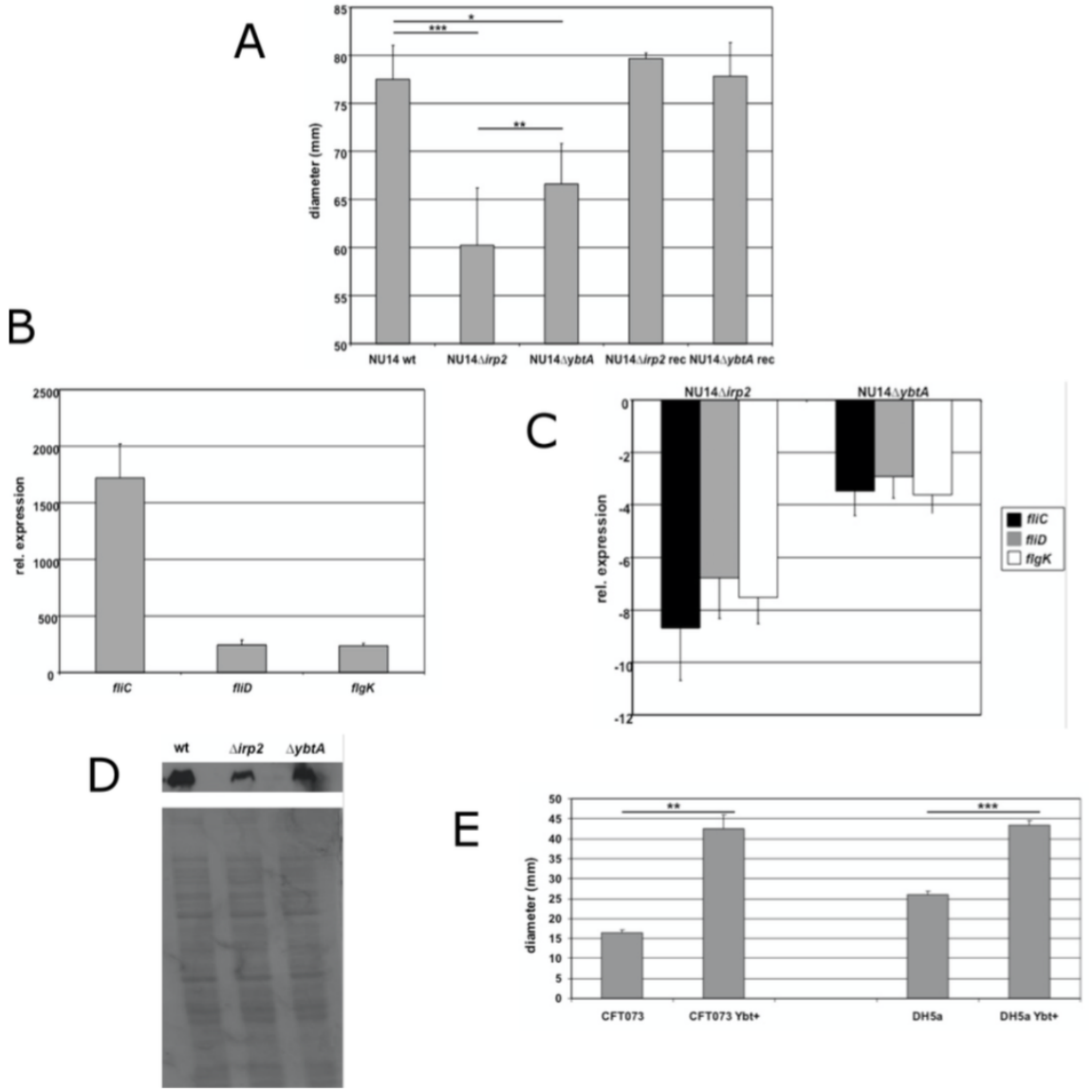

Fig 1. In vitro characterizations of the contribution of the HPI to motility in UPEC strain NU14. (A) Deletions of both *irp2* and *ybtA* resulted in the reduction of the motility diameter on LB soft agar plates (0.3%). Motility was restored in complemented strains. qPCR for flagellar genes during motility in wild type strain NU14 (B) and in HPI mutants (C). Data were normalized to 16S rRNA. Bacteria rotating in LB at 37˚C were used as the calibrator for (B) and wild type strain NU14 during motility served as the calibrator for (C). (D) Detection of flagellin expression using H7 antiserum. Lane 1, NU14 wild type; lane 2, NU14 Δ*irp2*; lane 3, NU14 Δ*ybtA*. (E) The impact of yersiniabactin production on motility in yersiniabactin-negative strains. CFT073 ybt+ and DH5α ybt+ displayed increased motility compared to the respective wild type strains. All experiments were performed in triplicates and repeated at least three times. Error bars represent standard deviations. **p*<0.05, ***p*<0.01, ****p*<0.001.

https://doi.org/10.1371/journal.pone.0183950.g001

[48]. This mutant showed neither induction of flagellar gene expression (Fig 2A) nor detectable expression of flagellin (Fig 2B), and consequently, the mutant was non-motile on LB soft agar plates (Fig 2C). The cultivation of the flagellar mutant under iron deplete conditions (Fig 2D) had no adverse effect on the transcript levels of the HPI genes *ybtA*, *irp2* and *fyuA* ($p>0.05$). Also the detection of FyuA expression by western blot analysis of the *fliI* mutant under iron limited cultivation in NBD medium showed no difference compared to the wild type strain (Fig 2E). Therefore, these data demonstrated that the impairment of the flagellar system does not influence the function of the HPI.

Stimulation of the HPI with additional iron under iron abundance promotes motility

Iron uptake systems are essential to the overall fitness of pathogens and they are supposed to be activated only by scarcity of iron [49]. Strikingly, the HPI contributes to motility under iron rich conditions. Our first step to investigate this phenomenon was to perform transcriptional analysis of the UPEC strain NU14 cultivated in iron deplete medium (NBD medium) and swarming on a LB soft agar plate (Fig 3A). In NBD medium the gene expression of *ybtA*, *irp2* and *fyuA* was strongly induced. Surprisingly, the transcription rate of swarming NU14 showed no significant difference ($p>0.05$), indicating the strong activation of the HPI during motility. This strong induction of transcription prompted us to study whether additional iron may suppress this activation during motility or stimulate even stronger. For that purpose, we supplemented LB soft agar plates with different concentrations of Fe(III)Cl_3. We applied 10 μM, 100 μM and 1 mM of ferric iron. Motility assays indicated a significant increase only for 10 μM Fe(III)Cl_3 compared to standard LB soft agar plates without any additional iron ($p<0.05$) (Fig 3B). Higher concentrations appeared to mediate no relevant benefit for motility. Real-time PCR was further carried out to analyse the gene expression of both the HPI and the flagellar system (Fig 3C). In the case of supplementation with 10 μM of ferric iron we observed a stronger induction of genes of the HPI. *YbtA* increased from 25-fold to 84-fold induction ($p<0.05$), *irp2* showed a rise from 1800-fold to 2800-fold ($p<0.05$), and *fyuA* was upregulated from 28-fold to 70-fold ($p<0.001$). Using higher concentrations of iron we observed a suppression of transcript levels, which finally resulted in the inactivation of the HPI at 1 mM of $FeCl_3$. The transcription of *fliC* could be stimulated with additional iron, but displayed no difference for the various concentrations of iron used. Corresponding results could be obtained by western blotting (Fig 3D). The expression of both YbtA and FyuA increased when 10 μM of ferric iron were added, and diminished at higher concentrations until no expression was detectable. The investigation of flagellin production revealed a rise in expression with additional iron, but according to the qPCR data we could not observe significant changes for different concentrations of $FeCl_3$. At this point, our data clearly prove that the HPI is active during motility under iron rich conditions, and the HPI is even stronger activated when 10 μM of ferric iron is added, instead of being repressed by this excess of iron.

Activation of the *ybtA* promoter during motility

The YbtA-mediated transcriptional regulation of genes like *irp2*, *irp6* and *fyuA* has been elucidated in previous studies [17; 18], which clearly highlighted the essential role of YbtA. The absence of this transcriptional regulator results in a negligible activity of the HPI. But data acquired so far still left a few questions unanswered. With the induction of *ybtA* transcription, representing the starting point for activation of the HPI, our first step was to construct several transcriptional *lacZ* reporter fusions with different fragments of the *ybtA* promoter region (Fig 4A). We fused the entire promoter including all three YbtA binding sites, termed repeated

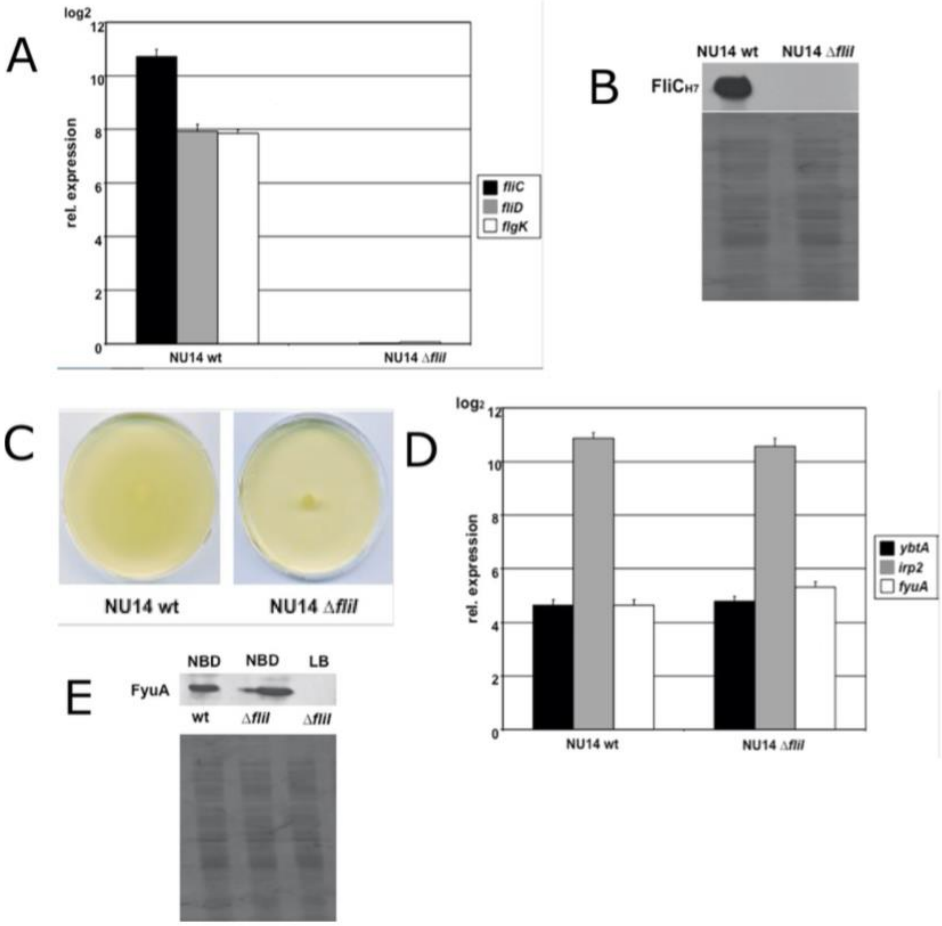

Fig 2. The loss of flagellar expression does not influence the activity of the HPI under iron deplete condition. (A) qPCR for flagellar genes during motility in strains NU14 wild type and flagellar mutant NU14 Δ*flil*. Deletion of *flil* resulted in the loss of flagellar gene expression of *fliC*, *fliD* and *flgK*. Data were normalized to 16S rRNA. Bacteria shaken in LB at 37˚C were used as the calibrator. (B) Detection of flagellin expression using H7 antiserum. Flagellar mutant NU14 Δ*flil* showed no expression of flagellin. (C) Mutant strain NU14 Δ*flil* was non-motile on LB soft agar plates. (D) qPCR for HPI genes of NU14 wild type and NU14 Δ*flil* under iron deplete condition. Transcription rates for *ybtA*, *irp2* and *fyuA* of the flagellar mutant NU14 Δ*flil* displayed no difference relative to the wild type strain NU14 under iron restriction. (E) Detection of FyuA expression in NBD medium. No difference in FyuA expression could be detected between the wild type strain and the flagellar mutant. NU14 Δ*flil* showed no expression of FyuA under iron rich conditions in LB medium.

https://doi.org/10.1371/journal.pone.0183950.g002

sequences (RS), and the Fur box to the *lacZ* gene to confirm the published data concerning *ybtA* regulation. YbtA is supposed to activate the transcription of *irp2*, *irp6* and *fyuA* and represses its own transcription [17–19]. In order to verify the auto-repression of *ybtA* we introduced both plasmid p3RS and plasmid pWKS30-*ybtA* into UPEC strain NU14. PWKS30-*ybtA* contains *ybtA* under the control of a *lac* promoter, so iron independent expression of YbtA is achieved. As depicted in **Fig 4B**, NU14 with additional YbtA expression showed a reduced reporter activity of 330 miller units compared to 540 miller units ($p<0.01$) in the strain carrying the empty

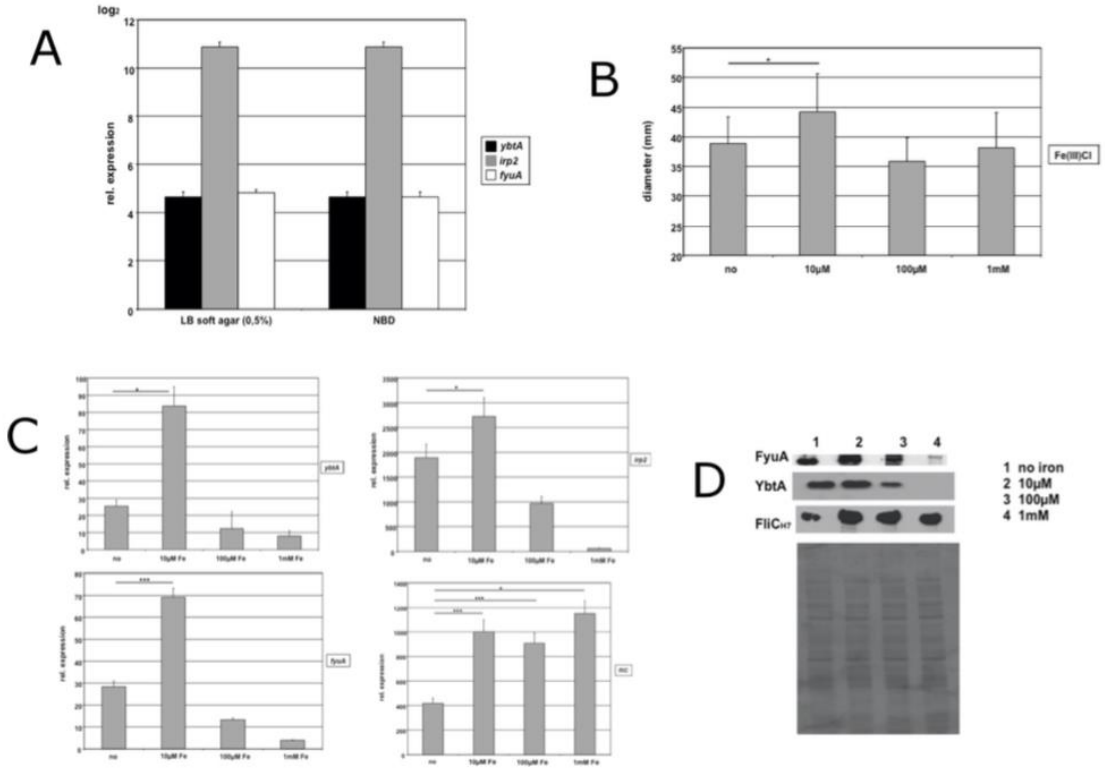

Fig 3. The abundance of iron stimulates the HPI during motility. (A) qPCR for the HPI genes *ybtA*, *irp2* and *fyuA* in NU14 wild type strain showed equal transcription rates for both iron depletion in NBD and during motility on LB soft agar plates. (B) The supplementation of 0.3% LB soft agar plates with 10 µm $Fe(III)Cl_3$ resulted in increased motility (*$p<0.05$). The addition of 100 µM or 1 mM $Fe(III)Cl_3$ did not affect motility diameters significantly. (C) qPCR of swarming NU14 on LB soft agar plates supplemented with different concentrations of $Fe(III)Cl_3$. Only addition of 10 µm $Fe(III)Cl_3$ led to the increased gene expression of the HPI genes *ybtA*, *irp2* and *fyuA*. The transcription of *fliC* was stronger upregulated during motility with the addition of iron, but displayed no difference for various concentration of $Fe(III)Cl_3$. (D) Western blot analysis of the expression of YbtA, FyuA and flagellin on LB soft agar plates supplemented with different concentrations of iron. YbtA and FyuA expression was only increased for 10 µM $Fe(III)Cl_3$. The addition of 1 mM ferric iron repressed almost completely expression of YbtA and FyuA. Rising concentrations of iron led to an overall enhanced expression of flagellin with no difference for various concentrations.

https://doi.org/10.1371/journal.pone.0183950.g003

vector control. We wanted to know whether this expected phenotype could be reproduced in an HPI-negative background, like in K12 *E. coli* DH5α. This setup actually allows the exclusive analysis of the interaction of YbtA with its own promoter, because the influence of all known and still unknown *cis* regulatory elements on the HPI can be excluded. Interestingly, in DH5α the additional expression of YbtA led to an increase in reporter activity of 41% relative to the strain without YbtA expression ($p<0.001$). This surprising observation prompted us to study this effect in the UPEC strain NU14 Δ*hpi*, where the entire HPI has been deleted. Measuring of miller units in the mutant NU14 Δ*hpi* revealed that the extra expression of YbtA indeed induced the reporter activity. We observed an almost 40% increase of miller units when additional YbtA was expressed ($p<0.001$). After all, these promoter studies suggest that YbtA itself activates its own transcription, at least in an HPI-negative genomic background.

We kept on investigating the role of the *ybtA* promoter region in flagellum-mediated motility. The activation of the HPI starts always with the induction of *ybtA* transcription. So we

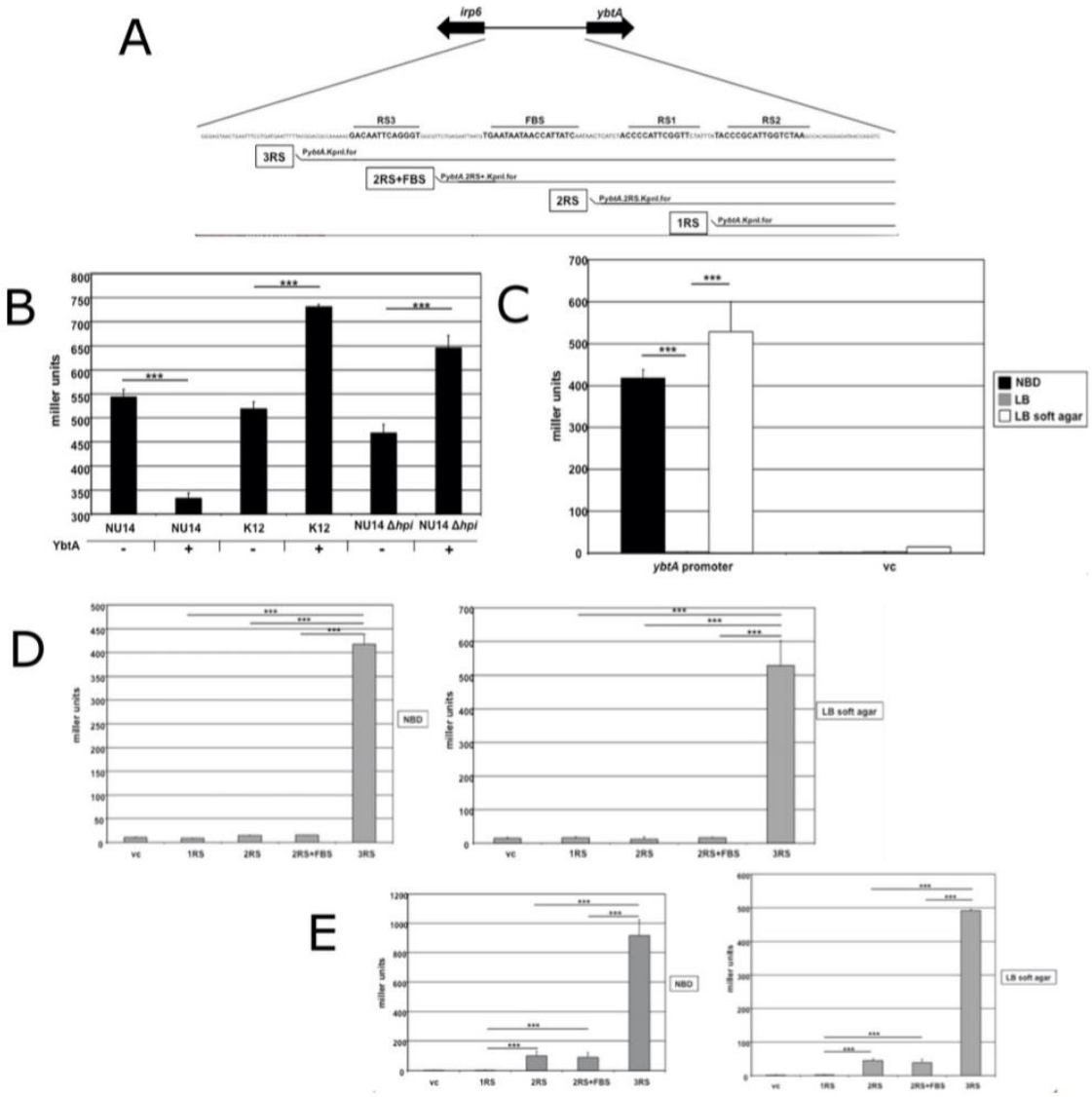

Fig 4. Analysis of the *ybtA* promoter activity under iron depletion and during motility. (A) Construction of transcriptional *lacZ* reporter fusions with different fragments of the *ybtA* promoter region. (B) Influence of the YbtA expression on the *ybtA* promoter activity under iron depletion. The additional expression of YbtA showed a decrease in miller units compared to the empty vector control in NU14 wild type (***$p<0.001$), but increased significantly the reporter signal in the HPI-negative strains DH5α and NU14 Δ*hpi*, respectively (***$p<0.001$). (C) The reporter activity of NU14 wild type strain carrying p3RS cultivated in NBD medium, LB medium and during motility on LB soft agar plates. Elevated miller units could be detected only under iron scarcity and during motility (***$p<0.001$). The reporter activity for different fragments of the *ybtA* promoter region under iron restriction and during motility in UPEC strain NU14 (D) and K12 *E. coli* DH5α (E). In both backgrounds the highest promoter activity was only detected with construct p3RS for both growth in NBD medium and during motility on LB soft agar plates.

https://doi.org/10.1371/journal.pone.0183950.g004

fused different parts of the *ybtA* promoter region to the *lacZ* gene and analyzed the reporter activities of motile bacteria (Fig 4A). The constructs comprised a selection of reporter fusions including the whole promoter region (p3RS), two YbtA binding sites plus the Fur box (p2RS +), two YbtA binding sites without the Fur box (p2RS), only one YbtA binding site (p1RS) and finally a short fragment of the promoter region without any known binding site. Initially, we compared promoter activities in UPEC strain NU14 using reporter plasmid p3RS under different conditions, i.e. cultivation in NBD medium, cultivation in LB medium and swarming NU14 (Fig 4C). As expected, iron depletion activated the *ybtA* promoter compared to the cultivation under iron excess. Consistent with the data presented above, the reporter activity was highly elevated during swarming. Approximately 420 miller units (± 20.1) for bacteria in NBD medium and 530 miller units (± 70.2) for swarming bacteria confirmed, that the HPI is almost equally activated. To determine the role of single promoter fragments containing different regulatory elements, we introduced various reporter constructs into the NU14 wild type strain and compared the reporter signals of bacteria grown under iron starvation with motile bacteria (Fig 4D). The resulting data demonstrated that the entire promoter region with all three YbtA binding sites is necessary to fully activate the *ybtA* promoter. Only the reporter plasmid p3RS displayed a strong signal of 417 miller units (± 20.9). When the swarming UPEC NU14 was examined, we were able to observe the same pattern. Only the wild type strain carrying the reporter construct p3RS including the entire promoter region showed an elevated reporter activity of 528 miller units (± 73.5). To investigate if the observed pattern in UPEC strain NU14 also accounted for a HPI negative strain, reporter activities were detected in K12 *E. coli* strain DH5α carrying also the same reporter constructs (Fig 4E). The cultivation in NBD medium resulted in a strong signal of 490 miller units (± 3.3) for reporter plasmid p3RS. Interestingly, we observed a slight reporter activity for constructs p2RS+ and p2RS, with both containing two YbtA binding sites. Once again, the pattern of reporter activity was identical to the results acquired under iron depletion. Plasmid p3RS displayed the highest rate with 918 miller units (± 100.6), whereas p2RS+ and p2RS produced weak signals. Overall, the promoter studies clearly show that the entire promoter region including all YbtA binding sites is mandatory for complete promoter activity. Furthermore, the *lacZ* reporter activity patterns during motility were similar in the HPI-positive strain NU14 and the HPI-negative strain DH5α suggesting a common mechanism of induction for the HPI, which is independent of YbtA and yersiniabactin production.

Discussion

Numerous studies have been published over the last decades highlighting the fundamental role of iron uptake systems for the overall fitness of pathogenic bacteria [10; 50–53]. The efficient colonization of the urinary tract by UPEC requires the coordination of a plethora of different iron acquisition strategies in order to satisfy the increased need for iron in this hostile environment. Especially the HPI turned out to be essential for the virulence potential of many different pathogens [8–10]. The objective of this present work was to investigate a possible connection between iron acquisition as accomplished by the HPI and motility in UPEC strain NU14. The first results clearly demonstrated that mutations of *ybtA* and *irp2* resulting in the impairment of yersiniabactin production affected flagellar motility. The most interesting aspect of this observation is that motility assays were performed on LB soft agar plates, with LB representing an iron rich condition. External iron excess is supposed to repress transcription of genes involved in iron acquisition through the action of the ferric uptake regulator Fur [49]. However, transcriptional and translational data of HPI mutants motile on LB soft agar plates provided evidence that the reduction of motility is due to a decrease in both transcript levels of

flagellar genes and production of flagellin. The gain of the ability to synthesize yersiniabactin improved the motility in pathogenic and non-pathogenic *E. coli* strains. These results prove that a functional HPI promotes flagellum-mediated motility. We investigated whether this interaction between HPI and flagellar system is mutual. The disruption of flagella expression had no effect on the activity of the HPI under iron deplete cultivation. It appears that induction of flagellum-mediated motility constitutes a stimulus that activates the HPI regardless of the external content of iron. This unexpected phenomenon prompted us to investigate how different concentrations of iron might affect this interaction. Most strikingly, during motility additional iron induced even more both motility and the HPI. Beside the activation of the HPI under iron excess, the further stimulation of a siderophore system with higher amounts of iron under iron excess is quite astonishing. To our knowledge, this is the first report of a higher regulatory mechanism of iron homeostasis that extends beyond the regulation by Fur and external iron content. The cultivation in an iron rich medium like LB shows no induction of iron uptake systems due to the binding of Fur to Fur boxes upstream of iron regulated genes [49]. But as soon as the motility is assessed on LB soft agar plates, UPEC strain NU14 showed a strong activation of the HPI that can even be maximized. With regard to Fur, it could be possible that the ferric uptake regulator itself might be affected or an additional factor prevents binding of Fur to the Fur binding site. Using *lacZ* transcriptional reporter fusions we analysed the *ybtA* promoter activity under different conditions to identify elements of the promoter region necessary for targeting the HPI during motility. We confirm previously published data [17] that all 3 YbtA binding sites are required for full promoter activity under iron scarcity. This also accounts for motility. One surprising finding concerning *ybtA* regulation was the unexpected stimulation of the *ybtA* promoter by YbtA itself. Published reports provided evidence for auto-repression [17; 19], but the HPI background of tested strains was always present in the respective studies. The effect of self-inhibition was confirmed in our experiments when we performed reporter assays in a HPI-positive strain, even in strains with different HPI mutations (data not shown). The exclusive investigation of the influence of YbtA on its own promoter requires the complete deletion of the HPI. In that way, unknown putative *cis*-regulatory elements located on the HPI can be excluded. In an HPI-free background we were able to detect activation of the *ybtA* promoter *lacZ* fusion with the additional expression of YbtA for both pathogenic and non-pathogenic strains. This is not the only interesting observation. It is important to stress, that the binding of YbtA to its promoter can occur in the absence of yersiniabactin. The results for K12 *E. coli* DH5α carrying the YbtA expressing plasmid demonstrated the yersiniabactin-independent interaction of YbtA with its promoter. These new insights complement the current understanding of YbtA-mediated regulation of the HPI. The initial induction of the HPI starts with transcription and translation of YbtA. Small amounts of this regulator will stimulate stronger the expression of YbtA, so that all the other YbtA-dependent operons can be transcribed. This will start the production of yersiniabactin until the HPI is fully activated. At this point, further expression of YbtA may be damped. The molecular mechanism of this inhibition cannot be explained with our experimental set up. But DNA bending mechanisms stabilized through YbtA with or without yersiniabactin, as it is known for the AraC-mediated regulation, may be possible [54]. Further experiments are needed to address this interesting regulatory aspect. As far as the newly discovered HPI-flagella interaction is concerned, the selection of various *ybtA* promoter fragments fused to the *lacZ* reporter gene allowed to examine whether the promoter activity of *ybtA* under iron deplete conditions was comparable to the process of motility. Strikingly, maximum promoter activity was only detected for the entire promoter region of the reporter construct p3RS. This was the case for both UPEC strain NU14 and laboratory strain DH5α. The full activity under iron restriction might be explained by the inactivation of Fur, but the results of motility assays

under iron rich conditions point towards a different mechanism. Fur is supposed to inhibit transcription because of iron abundance. However, a strong signal was measured in both strains. Reporter constructs p2RS+ and p2RS, with a Fur box only included in p2RS+, indicated that Fur might not be the missing link of the flagella-HPI interaction since there is no difference in promoter activity between both reporter plasmids. It is remarkable for the laboratory strain DH5α that neither YbtA nor yersiniabactin can be involved in *ybtA* promoter activity, but there is still a strong signal detectable. Due to the presence of a Fur box in p3RS and p2RS+, the role of Fur for this phenomenon seems to be negligible, otherwise plasmid p2RS + is supposed to display the same activity. The possibility of an unknown factor, maybe another regulator of the AraC-like family, binding to all YbtA binding sites in YbtA-like fashion may be a theory to explain this observation. This hypothesis might also account for the induction of YbtA expression during motility. In both strains NU14 and DH5α, an unknown factor acting alone or in complex with additional elements seems to occupy the entire promoter region in order to activate YbtA expression. It is unclear, whether this missing link is encoded by the *E. coli* core genome, so the same factor is responsible, or whether the mediating factors differ in the strains NU14 and DH5α.

Overall, the data presented in this study clearly showed how the flagellar system activates the HPI by addressing the *ybtA* promoter region. The evasion of important regulatory mechanisms of iron homeostasis seems to be counterbalanced to optimize motility. This work highlights the multi-functional role of the HPI and promotes the concept of a complex but orchestrated network of virulence and fitness factors supporting ExPEC to develop into this successful pathogen.

Author Contributions

Conceptualization: Giuseppe Magistro, Christian G. Stief, Sören Schubert.

Data curation: Giuseppe Magistro, Christiane Magistro.

Formal analysis: Giuseppe Magistro, Christiane Magistro, Christian G. Stief, Sören Schubert.

Writing – original draft: Giuseppe Magistro, Sören Schubert.

Writing – review & editing: Giuseppe Magistro, Sören Schubert.

References

1. Johnson JR. Virulence factors in Escherichia coli urinary tract infection. Clin Microbiol Rev 1991 Jan; 4 (1):80–128. PMID: 1672263
2. Johnson JR, Russo TA. Extraintestinal pathogenic Escherichia coli: "the other bad E coli". J Lab Clin Med 2002 Mar; 139(3):155–62. PMID: 11944026
3. Kaper JB, Nataro JP, Mobley HL. Pathogenic Escherichia coli. Nat Rev Microbiol 2004 Feb; 2(2):123–40. https://doi.org/10.1038/nrmicro818 PMID: 15040260
4. Reigstad CS, Hultgren SJ, Gordon JI. Functional genomic studies of uropathogenic Escherichia coli and host urothelial cells when intracellular bacterial communities are assembled. J Biol Chem 2007 Jul 20; 282(29):21259–67. https://doi.org/10.1074/jbc.M611502200 PMID: 17504765
5. Hagan EC, Lloyd AL, Rasko DA, Faerber GJ, Mobley HL. Escherichia coli global gene expression in urine from women with urinary tract infection. PLoS Pathog 2010; 6(11):e1001187. https://doi.org/10.1371/journal.ppat.1001187 PMID: 21085611
6. Alteri CJ, Mobley HL. Quantitative profile of the uropathogenic Escherichia coli outer membrane proteome during growth in human urine. Infect Immun 2007 Jun; 75(6):2679–88. https://doi.org/10.1128/IAI.00076-07 PMID: 17513849
7. Garenaux A, Caza M, Dozois CM. The Ins and Outs of siderophore mediated iron uptake by extra-intestinal pathogenic Escherichia coli. Vet Microbiol 2011 Nov 21; 153(1–2):89–98. https://doi.org/10.1016/j.vetmic.2011.05.023 PMID: 21680117

8. Heesemann J, Hantke K, Vocke T, Saken E, Rakin A, Stojiljkovic I, et al. Virulence of Yersinia enterocolitica is closely associated with siderophore production, expression of an iron-repressible outer membrane polypeptide of 65,000 Da and pesticin sensitivity. Mol Microbiol 1993 Apr; 8(2):397–408. PMID: 8316088
9. Lawlor MS, O'connor C, Miller VL. Yersiniabactin is a virulence factor for Klebsiella pneumoniae during pulmonary infection. Infect Immun 2007 Mar; 75(3):1463–72. https://doi.org/10.1128/IAI.00372-06 PMID: 17220312
10. Schubert S, Picard B, Gouriou S, Heesemann J, Denamur E. Yersinia high-pathogenicity island contributes to virulence in Escherichia coli causing extraintestinal infections. Infect Immun 2002 Sep; 70 (9):5335–7. https://doi.org/10.1128/IAI.70.9.5335-5337.2002 PMID: 12183596
11. Hacker J, Blum-Oehler G, Muhldorfer I, Tschape H. Pathogenicity islands of virulent bacteria: structure, function and impact on microbial evolution. Mol Microbiol 1997 Mar; 23(6):1089–97. PMID: 9106201
12. Hacker J, Kaper JB. Pathogenicity islands and the evolution of microbes. Annu Rev Microbiol 2000; 54:641–79. https://doi.org/10.1146/annurev.micro.54.1.641 PMID: 11018140
13. Schubert S, Sorsa JL, Cuenca S, Fischer D, Jacobi CA, Heesemann J. HPI of high-virulent Yersinia is found in E. coli strains causing urinary tract infection. Structural, functional aspects, and distribution. Adv Exp Med Biol 2000; 485:69–73. https://doi.org/10.1007/0-306-46840-9_9 PMID: 11109089
14. Schubert S, Rakin A, Heesemann J. The Yersinia high-pathogenicity island (HPI): evolutionary and functional aspects. Int J Med Microbiol 2004 Sep; 294(2–3):83–94. https://doi.org/10.1016/j.ijmm.2004.06.026 PMID: 15493818
15. Perry RD, Fetherston JD. Yersiniabactin iron uptake: mechanisms and role in Yersinia pestis pathogenesis. Microbes Infect 2011 Sep; 13(10):808–17. https://doi.org/10.1016/j.micinf.2011.04.008 PMID: 21609780
16. Miller DA, Luo L, Hillson N, Keating TA, Walsh CT. Yersiniabactin synthetase: a four-protein assembly line producing the nonribosomal peptide/polyketide hybrid siderophore of Yersinia pestis. Chem Biol 2002 Mar; 9(3):333–44. PMID: 11927258
17. Anisimov R, Brem D, Heesemann J, Rakin A. Molecular mechanism of YbtA-mediated transcriptional regulation of divergent overlapping promoters ybtA and irp6 of Yersinia enterocolitica. FEMS Microbiol Lett 2005 Sep 1; 250(1):27–32. https://doi.org/10.1016/j.femsle.2005.06.040 PMID: 16019159
18. Anisimov R, Brem D, Heesemann J, Rakin A. Transcriptional regulation of high pathogenicity island iron uptake genes by YbtA. Int J Med Microbiol 2005 Apr; 295(1):19–28. https://doi.org/10.1016/j.ijmm.2004.11.007 PMID: 15861813
19. Fetherston JD, Bearden SW, Perry RD. YbtA, an AraC-type regulator of the Yersinia pestis pesticin/yersiniabactin receptor. Mol Microbiol 1996 Oct; 22(2):315–25. PMID: 8930916
20. Paauw A, Leverstein-van Hall MA, van Kessel KP, Verhoef J, Fluit AC. Yersiniabactin reduces the respiratory oxidative stress response of innate immune cells. PLoS One 2009; 4(12):e8240. https://doi.org/10.1371/journal.pone.0008240 PMID: 20041108
21. Hancock V, Ferrieres L, Klemm P. The ferric yersiniabactin uptake receptor FyuA is required for efficient biofilm formation by urinary tract infectious Escherichia coli in human urine. Microbiology 2008 Jan; 154 (Pt 1):167–75. https://doi.org/10.1099/mic.0.2007/011981-0 PMID: 18174135
22. Sivick KE, Mobley HL. An "omics" approach to uropathogenic Escherichia coli vaccinology. Trends Microbiol 2009 Oct; 17(10):431–2. https://doi.org/10.1016/j.tim.2009.07.003 PMID: 19758805
23. Wieser A, Romann E, Magistro G, Hoffmann C, Norenberg D, Weinert K, et al. A multiepitope subunit vaccine conveys protection against extraintestinal pathogenic Escherichia coli in mice. Infect Immun 2010 Aug; 78(8):3432–42. https://doi.org/10.1128/IAI.00174-10 PMID: 20498257
24. Wieser A, Magistro G, Norenberg D, Hoffmann C, Schubert S. First multi-epitope subunit vaccine against extraintestinal pathogenic Escherichia coli delivered by a bacterial type-3 secretion system (T3SS). Int J Med Microbiol 2012 Jan; 302(1):10–8. https://doi.org/10.1016/j.ijmm.2011.09.012 PMID: 22000741
25. Lv H, Henderson JP. Yersinia high pathogenicity island genes modify the Escherichia coli primary metabolome independently of siderophore production. J Proteome Res 2011 Dec 2; 10(12):5547–54. https://doi.org/10.1021/pr200756n PMID: 22035238
26. Lloyd AL, Henderson TA, Vigil PD, Mobley HL. Genomic islands of uropathogenic Escherichia coli contribute to virulence. J Bacteriol 2009 Jun; 191(11):3469–81. https://doi.org/10.1128/JB.01717-08 PMID: 19329634
27. Welch RA, Burland V, Plunkett G, III, Redford P, Roesch P, Rasko D, et al. Extensive mosaic structure revealed by the complete genome sequence of uropathogenic Escherichia coli. Proc Natl Acad Sci U S A 2002 Dec 24; 99(26):17020–4. https://doi.org/10.1073/pnas.252529799 PMID: 12471157

28. Henderson JP, Crowley JR, Pinkner JS, Walker JN, Tsukayama P, Stamm WE, et al. Quantitative metabolomics reveals an epigenetic blueprint for iron acquisition in uropathogenic Escherichia coli. PLoS Pathog 2009 Feb; 5(2):e1000305. https://doi.org/10.1371/journal.ppat.1000305 PMID: 19229321

29. Wright KJ, Seed PC, Hultgren SJ. Uropathogenic Escherichia coli flagella aid in efficient urinary tract colonization. Infect Immun 2005 Nov; 73(11):7657–68. https://doi.org/10.1128/IAI.73.11.7657-7668.2005 PMID: 16239570

30. Lane MC, Lockatell V, Monterosso G, Lamphier D, Weinert J, Hebel JR, et al. Role of motility in the colonization of uropathogenic Escherichia coli in the urinary tract. Infect Immun 2005 Nov; 73(11):7644–56. https://doi.org/10.1128/IAI.73.11.7644-7656.2005 PMID: 16239569

31. Lane MC, Alteri CJ, Smith SN, Mobley HL. Expression of flagella is coincident with uropathogenic Escherichia coli ascension to the upper urinary tract. Proc Natl Acad Sci U S A 2007 Oct 16; 104 (42):16669–74. https://doi.org/10.1073/pnas.0607898104 PMID: 17925449

32. Matilla MA, Ramos JL, Duque E, de Dios AJ, Espinosa-Urgel M, Ramos-Gonzalez MI. Temperature and pyoverdine-mediated iron acquisition control surface motility of Pseudomonas putida. Environ Microbiol 2007 Jul; 9(7):1842–50. https://doi.org/10.1111/j.1462-2920.2007.01286.x PMID: 17564617

33. Wang Q, Frye JG, McClelland M, Harshey RM. Gene expression patterns during swarming in Salmonella typhimurium: genes specific to surface growth and putative new motility and pathogenicity genes. Mol Microbiol 2004 Apr; 52(1):169–87. https://doi.org/10.1111/j.1365-2958.2003.03977.x PMID: 15049819

34. McCarter L, Silverman M. Iron regulation of swarmer cell differentiation of Vibrio parahaemolyticus. J Bacteriol 1989 Feb; 171(2):731–6. PMID: 2914871

35. Kurabayashi K, Agata T, Asano H, Tomita H, Hirakawa H. Fur Represses Adhesion to, Invasion of, and Intracellular Bacterial Community Formation within Bladder Epithelial Cells and Motility in Uropathogenic Escherichia coli. Infect Immun. 2016; 84(11):3220–31. https://doi.org/10.1128/IAI.00369-16 PMID: 27572332

36. Hultgren SJ, Schwan WR, Schaeffer AJ, Duncan JL. Regulation of production of type 1 pili among urinary tract isolates of Escherichia coli. Infect Immun 1986 Dec; 54(3):613–20. PMID: 2877947

37. Datsenko KA, Wanner BL. One-step inactivation of chromosomal genes in Escherichia coli K-12 using PCR products. Proc Natl Acad Sci U S A 2000 Jun 6; 97(12):6640–5. https://doi.org/10.1073/pnas.120163297 PMID: 10829079

38. Sambrook J, Russel DW. Molecular Cloning: A Laboratory Manual, Third Edition, Cold Spring Harbor Laboratory Press. 2001

39. Wang RF, Kushner SR. Construction of versatile low-copy-number vectors for cloning, sequencing and gene expression in Escherichia coli. Gene 1991 Apr; 100:195–9. PMID: 2055470

40. Herman P.Spaink, et al. Promoters in the nodulation region of the Rhizobium leguminosarum Sym plasmid pRL1JI. Plant Molecular Biology 1987; 9(1):27–39. https://doi.org/10.1007/BF00017984 PMID: 24276795

41. Mobley HL, Green DM, Trifillis AL, Johnson DE, Chippendale GR, Lockatell CV, et al. Pyelonephritogenic Escherichia coli and killing of cultured human renal proximal tubular epithelial cells: role of hemolysin in some strains. Infect Immun 1990 May; 58(5):1281–9. PMID: 2182540

42. Pelludat C, Hogardt M, Heesemann J. Transfer of the core region genes of the Yersinia enterocolitica WA-C serotype O:8 high-pathogenicity island to Y. enterocolitica MRS40, a strain with low levels of pathogenicity, confers a yersiniabactin biosynthesis phenotype and enhanced mouse virulence. Infect Immun 2002 Apr; 70(4):1832–41. https://doi.org/10.1128/IAI.70.4.1832-1841.2002 PMID: 11895945

43. Miller JH. A short course in bacteria genetics. Cold Spring Harbor Laboratory Press, Cold Spring Harbor, NY. 1992.

44. Feldmann F, Sorsa LJ, Hildinger K, Schubert S. The salmochelin siderophore receptor IroN contributes to invasion of urothelial cells by extraintestinal pathogenic Escherichia coli in vitro. Infect Immun 2007 Jun; 75(6):3183–7. https://doi.org/10.1128/IAI.00656-06 PMID: 17353289

45. Chomczynski P, Sacchi N. Single-step method of RNA isolation by acid guanidinium thiocyanate-phenol-chloroform extraction. Anal Biochem 1987 Apr; 162(1):156–9. https://doi.org/10.1006/abio.1987.9999 PMID: 2440339

46. Livak KJ, Schmittgen TD. Analysis of relative gene expression data using real-time quantitative PCR and the 2(-Delta Delta C(T)) Method. Methods 2001 Dec; 25(4):402–8. https://doi.org/10.1006/meth.2001.1262 PMID: 11846609

47. Gehring AM, Mori I, I, Perry RD, Walsh CT. The nonribosomal peptide synthetase HMWP2 forms a thiazoline ring during biogenesis of yersiniabactin, an iron-chelating virulence factor of yersinia pestis. Biochemistry 1998 Dec 1; 37(48):17104. https://doi.org/10.1021/bi9850524 PMID: 9836605

48. Macnab RM. How bacteria assemble flagella. Annu Rev Microbiol 2003; 57:77–100. https://doi.org/10.1146/annurev.micro.57.030502.090832 PMID: 12730325

49. Andrews SC, Robinson AK, Rodriguez-Quinones F. Bacterial iron homeostasis. FEMS Microbiol Rev 2003 Jun; 27(2–3):215–37. PMID: 12829269

50. Garcia EC, Brumbaugh AR, Mobley HL. Redundancy and specificity of Escherichia coli iron acquisition systems during urinary tract infection. Infect Immun 2011 Mar; 79(3):1225–35. https://doi.org/10.1128/IAI.01222-10 PMID: 21220482

51. Torres AG, Redford P, Welch RA, Payne SM. TonB-dependent systems of uropathogenic Escherichia coli: aerobactin and heme transport and TonB are required for virulence in the mouse. Infect Immun 2001 Oct; 69(10):6179–85. https://doi.org/10.1128/IAI.69.10.6179-6185.2001 PMID: 11553558

52. Watts RE, Totsika M, Challinor VL, Mabbett AN, Ulett GC, De Voss JJ, et al. Contribution of siderophore systems to growth and urinary tract colonization of asymptomatic bacteriuria Escherichia coli. Infect Immun 2012 Jan; 80(1):333–44. https://doi.org/10.1128/IAI.05594-11 PMID: 21930757

53. Gao Q, Wang X, Xu H, Xu Y, Ling J, Zhang D, et al. Roles of iron acquisition systems in virulence of extraintestinal pathogenic Escherichia coli: salmochelin and aerobactin contribute more to virulence than heme in a chicken infection model. BMC Microbiol 2012 Jul 20; 12(1):143.

54. Gallegos MT, Schleif R, Bairoch A, Hofmann K, Ramos JL. Arac/XylS family of transcriptional regulators. Microbiol Mol Biol Rev 1997 Dec; 61(4):393–410. PMID: 9409145

World J Urol (2017) 35:1777–1782
DOI 10.1007/s00345-017-2048-y

ORIGINAL ARTICLE

"Finding the needle in a haystack": oncologic evaluation of patients treated for LUTS with holmium laser enucleation of the prostate (HoLEP) versus transurethral resection of the prostate (TURP)

Annika Herlemann[1] · Kerstin Wegner[1] · Alexander Roosen[2] · Alexander Buchner[1] · Philipp Weinhold[1] · Alexander Bachmann[3] · Christian G. Stief[1] · Christian Gratzke[1] · Giuseppe Magistro[1]

Received: 19 February 2017 / Accepted: 5 May 2017 / Published online: 17 May 2017

Abstract
Purpose To evaluate oncologic parameters of men with bothersome LUTS undergoing surgical treatment with HoLEP or TURP.
Methods Five hundred and eighteen patients undergoing HoLEP ($n = 289$) or TURP ($n = 229$) were retrospectively analyzed for total PSA, prostate volume, PSA density, history of prostate biopsy, resected prostate weight, and histopathological features. Univariate and multivariate logistic regression models were used to identify independent predictors of incidental PCa (iPCa).
Results Men undergoing HoLEP had a significantly higher total PSA (median 5.5 vs. 2.3 ng/mL) and prostate volume (median 80 vs. 41 cc), and displayed a greater reduction of prostate volume after surgery compared to TURP patients (median 71 vs. 50%; all $p < 0.001$). With a prevalence of incidental PCa (iPCa) of 15 and 17% for HoLEP and TURP, respectively, the choice of procedure had no influence on the detection of iPCa ($p = 0.593$). However, a higher rate of false-negative preoperative prostate biopsies was noted among iPCa patients in the HoLEP arm (40 vs. 8%, $p = 0.007$). In multivariate logistic regression, we identified patient age (OR 1.04; 95% CI 1.01–1.07, $p = 0.013$) and PSA density (OR 2.13; 95% CI 1.09–4.18, $p = 0.028$) as independent predictors for the detection of iPCa.
Conclusions Despite differences in oncologic parameters, the choice of technique had no influence on the detection of iPCa. Increased patient age and higher PSA density were associated with iPCa. A higher rate of false-negative preoperative prostate biopsies was noted in HoLEP patients. Therefore, diagnostic assessment of LUTS patients requires a more adapted approach to exclude malignancy, especially in those with larger prostates.

Keywords Benign prostatic hyperplasia · Incidental prostate cancer · Holmium laser enucleation of the prostate · Transurethral resection of the prostate · PSA density

✉ Giuseppe Magistro
giuseppe.magistro@med.uni-muenchen.de

[1] Department of Urology, Ludwig-Maximilians-University of Munich, Marchioninistrasse 15, 81377 Munich, Germany

[2] Department of Urology, Augusta-Kranken-Anstalt gGmbH, Bochum, Germany

[3] alta uro AG, Basel, Switzerland

Introduction

Bothersome lower urinary tract symptoms (LUTS) due to bladder outlet obstruction (BOO) associated with benign prostate enlargement (BPE) represent one of the most common non-malignant conditions considerably affecting the quality of life in aging men. If medical treatment is not able to provide adequate relief of LUTS or causes adverse events, a surgical procedure needs to be considered. Transurethral resection of the prostate (TURP) is still the standard procedure for prostates up to 80 cc [1]. For larger prostate sizes, holmium laser enucleation of the prostate (HoLEP) has been demonstrated to be a safe, efficient, and durable option for symptom relief and functional outcomes of LUTS due to benign prostatic hyperplasia (BPH) [1–11].

Patients at risk for prostate cancer (PCa) due to suspicious results obtained by digital rectal examination (DRE), prostate-specific antigen (PSA) screening, or imaging techniques require prostate biopsy to exclude malignancy prior to surgery [12, 13]. With the introduction of PSA screening,

incidental PCa (iPCa) has been found in histologic specimens without prior diagnosis in 5.9–11.7% of HoLEP patients [14–18] and in 1.4–11.1% of patients treated with TURP [15, 19–24]. Published data indicate that in most of these cases, iPCa is a low-grade disease and active surveillance may be considered as an appropriate treatment strategy for oncologic control [18, 25].

Screening tools including PSA, PSA velocity, and PSA density are constantly re-evaluated to optimize sensitivity and specificity for PCa detection [26–31]. Based on a series of clinical trials, HoLEP should be considered a size-independent technique [32]; however, it is recommended for larger prostates >80 cc according to current guidelines [1].

The accuracy of established screening instruments for detection and prediction of PCa in LUTS patients with clearly enlarged prostates has not been conclusively evaluated yet. Hence, oncologic analysis of this particular subset of patients is of great importance. It is imperative to evaluate basic parameters to optimize the preoperative assessment. Unnecessary overdiagnosis including unwarranted biopsies might be reduced. Therefore, our aim was to evaluate and compare oncologic parameters of iPCa in patients who underwent surgical treatment for LUTS due to BOO with the two reference methods TURP and HoLEP.

Patients and methods

Study design and surgical procedures

A total of 518 patients with BOO due to BPE undergoing surgical treatment with either HoLEP ($n = 289$) or TURP ($n = 229$) at the Department of Urology of the Ludwig-Maximilians-University of Munich, Munich, Germany from January 2013 to December 2014 were retrospectively identified. All procedures were performed by a single senior surgeon or under his direct supervision. HoLEP was always performed for prostate volumes ≥80 cc; TURP was the preferred approach for prostate volumes ≤60 cc. Prostates varying between 60 and 80 cc in volume were treated at the surgeons' discretion. HoLEP was conducted with the VersaPulse® 100 W Holmium Laser (Lumenis Ltd., Yokneam, Israel). We used a frequency setting of 53 Hz and a power setting of 1.2 J. TURP was performed using the Gyrus ACMI PlasmaKinetic SuperPulse™ Generator (Gyrus Medical Ltd., Cardiff, United Kingdom) at a standardized setting of 280 W for cutting and 140 W for coagulation. For both techniques, a 26Fr or 27Fr continuous-flow resectoscope (Karl Storz GmbH & Co, Tuttlingen, Germany) and normal 0.9% saline as irrigation fluid were used. A preoperative transrectal ultrasound-guided biopsy of the prostate was performed whenever indicated due to abnormal digital rectal examination (DRE), and/or elevated total PSA > 4.40 ng/mL (Elecsys® Assay, Roche Diagnostics GmbH, Mannheim, Germany), which was verified after a few weeks using the same assay under standardized conditions. Patients with prior history of PCa or with tissue removal less than 5 g were excluded from the study. The following clinicopathological parameters were evaluated: Patient's age (years), total serum PSA (ng/mL), prostate volume (cc) determined by transrectal ultrasound (TRUS), PSA density (ng/mL/cc), history of prostate biopsy, resected prostate weight (g), percentage (%) of resected tissue relative to preoperative prostate volume [PV (cc) as determined by TRUS related to weight (g) of resected tissue], and histopathological features. All surgical specimens were weighed inside the operating room, immediately sent for histopathology and analyzed by a designated uropathologist, subsequently. Prostate specimens were not totally embedded and a re-review of pathology slides was not performed for the purpose of this study.

Statistical analysis

Patients were divided by surgical approach (HoLEP vs. TURP) and clinicopathological data were collected and compared between groups. Continuous values were presented as the median (interquartile range, IQR). Univariate analyses were performed using the Chi-square test for categorical variables and Mann–Whitney U test for continuous variables. Uni- and multivariate logistic regression analyses were performed on preoperative clinicopathological parameters to identify potential predictors associated with iPCa. Cut-off value for PSA density was 0.15 ng/mL/cc. Based on logistic regression, the probability of iPCa was calculated using the following equation: $p = 1/(1 + \mathrm{EXP}-(b_0 + b_1 \times \mathrm{age} + b_2 \times \mathrm{PSAD})$ with the regression coefficients b_0, b_1, and b_2 (0 or 1 for two PSA density groups). A p value <0.05 was considered statistically significant. All calculations were carried out using SPSS Statistics software, version 24.0 (SPSS, Chicago, IL, USA) and STATISTICA 13 (Dell Statistica, Tulsa, OK, USA).

Results

Clinicopathological characteristics

Patient clinicopathological and oncologic characteristics are displayed in Table 1. A total of 518 consecutive patients [HoLEP ($n = 289$), TURP ($n = 229$)] were included in the final analysis. Median patient age was 71 years (interquartile range (IQR) 65–76) in the HoLEP group and 69 years (IQR 61–75) for TURP patients. Median preoperative total PSA was significantly higher for HoLEP patients (5.5 ng/mL, IQR 3.5–8.8) compared to TURP patients (2.3 ng/mL,

Table 1 Clinicopathological and oncologic parameters stratified by surgical approach (HoLEP vs. TURP)

Variables	HoLEP ($n = 289$)	TURP ($n = 229$)	p value
Age (years)			
Median	71	69	**0.007**
IQR	65–76	61–75	
Total PSA (ng/mL)			
Median	5.5	2.3	**<0.001**
IQR	3.5–8.8	1.2–4.4	
Prostate volume (cc)			**<0.001**
Median	80	41	
IQR	67.3–100	30–55	
PSA density (ng/mL/cc)			
Median	0.063	0.050	**0.001**
IQR	0.042–0.104	0.030–0.095	
≤0.15	253/283 (89%)	204/221 (92%)	0.265
>0.15	30/283 (11%)	17/221 (8%)	
Preoperative prostate biopsy, *n* (%)			
Yes	100/289 (35%)	35/229 (15%)	**<0.001**
No	189/289 (65%)	194/229 (85%)	
Resected prostate weight (g)			
Median	60	20	**<0.001**
IQR	42.8–80	15–35	
Tissue resected (%)			
Median	71	50	**<0.001**
IQR	60.4–85	39–62.8	
Histopathology, *n* (%)			
BPH	242/289 (84%)	189/229 (83%)	0.593
HGPIN	2/289 (1%)	2/229 (1%)	
ASAP	2/289 (1%)	0/229 (0%)	
iPCa	43/289 (15%)	38/229 (17%)	
pT stage, *n* (%)			
pT1a	38/43 (88%)	29/38 (76%)	0.152
pT1b	5/43 (12%)	9/38 (24%)	
Gleason score, *n* (%)			
≤6	37/43 (86%)	32/38 (84%)	0.779
7	4/43 (9%)	5/38 (13%)	
8–10	2/43 (5%)	1/38 (3%)	
iPCa despite negative preoperative prostate biopsy, *n* (%)	17/43 (40%)	3/38 (8%)	**0.007**

Bold values indicate p values <0.05 were considered statistically signficant

Continuous values are given as median (IQR); categorical values are given as number (%)

HoLEP holmium laser enucleation of the prostate, *TURP* transurethral resection of the prostate, *IQR* interquartile range, *PSA* prostate-specific antigen, *BPH* benign prostatic hyperplasia, *HGPIN* high-grade prostatic intraepithelial neoplasia, *ASAP* atypical small acinar proliferation, *iPCa* incidental prostate cancer, *pT stage* pathologic T-stage

IQR 1.2–4.4 ng/mL; $p < 0.001$). As expected, median prostate volume was significantly higher in the HoLEP group (80 cc, IQR 67.3–100) than in men treated with TURP (41 cc, IQR 30–55; $p < 0.001$). Due to an elevated total PSA value and/or abnormal DRE findings, HoLEP patients received preoperative TRUS-guided systematic prostate biopsy more frequently compared to TURP patients (35 vs. 15%; $p < 0.001$). In terms of intraoperative parameters, significantly more tissue removal was obtained by HoLEP compared to TURP (mean resected prostate weight 60 g (IQR 42.8–85) vs. 20 g (IQR 15–35); $p < 0.001$). The original prostate volume was reduced by 71% (IQR 60.4–85) and 50% (IQR 39–62.8) for HoLEP and TURP, respectively ($p < 0.001$).

Oncologic outcomes

On histopathological examination of resected prostate specimens, iPCa was detected in 15% of HoLEP patients and in 17% of patients in the TURP arm ($p = 0.593$). The majority of patients with iPCa were diagnosed with pT1a-stage (88% HoLEP vs. 76% TURP; $p = 0.152$) and a Gleason score ≤6 (86% HoLEP vs. 84% TURP; $p = 0.779$). Stage pT1b adenocarcinoma was detected in 12 and 24% for HoLEP and TURP, respectively ($p = 0.152$). Interestingly, a subgroup analysis of those patients with iPCa revealed a significantly higher rate of false-negative preoperative prostate biopsy results in the HoLEP arm. Seventeen out of forty-three patients (40%) diagnosed with iPCa in enucleated tissue after HoLEP underwent a negative preoperative prostate biopsy compared to 3 out of 38 patients (8%) in the TURP group ($p = 0.007$, Table 1).

Predictors of incidental PCa in LUTS patients

Patient's age, PSA density, preoperative prostate biopsy, % tissue resected, and surgical technique were evaluated as potential predictors for iPCa in a population surgically treated for LUTS (Table 2). In univariate logistic regression, patient age and PSA density were significantly associated with the presence of iPCa in surgical specimens after HoLEP and TURP. In multivariate logistic regression, we found that older patient age (OR 1.04; 95% CI 1.01–1.07; $p = 0.013$) and PSA density >15 ng/mL/cc (OR 2.13; 95% CI 1.09–4.18; $p = 0.028$) were independently associated with the detection of iPCa (Table 2; Fig. 1).

Table 2 Uni- and multivariate logistic regression analyses on clinicopathological parameters associated with incidental prostate cancer after HoLEP and TURP

Variables	Univariate	Multivariate	
	p value	*p* value	OR (95% CI)
Age [continuous] (years)	**0.011**	**0.013**	**1.04 (1.01–1.07)**
PSA density (≤/> 0.15 ng/mL/cc)	**0.023**	**0.028**	**2.13 (1.09–4.18)**
Preoperative prostate biopsy (yes vs. no)	0.760		
Tissue resected [continuous] (%)	0.397		
Surgical technique (HoLEP vs. TURP)	0.594		

Bold values indicate *p* values <0.05 were considered statistically signficant

OR odds ratio, *CI* confidence interval, *HoLEP* holmium laser enucleation of the prostate, *TURP* transurethral resection of the prostate

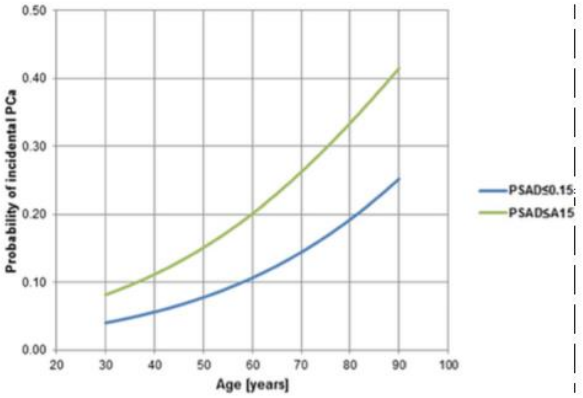

Fig. 1 In uni- and multivariate logistic regression analyses, patient age and PSA density were associated with the detection of incidental PCa. As depicted, a PSA density >0.15 in older patients results in a higher probability for the detection of incidental PCa. *PCa* prostate cancer, *PSA* prostate-specific antigen, *PSAD* PSA density

Discussion

In this study, we evaluated and compared clinicopathological and oncologic parameters of LUTS patients who underwent the "old" (TURP) or "new" (HoLEP) reference method in the repertoire of BPH surgery. As expected, the pre- and perioperative assessment of patients with larger prostates treated with HoLEP revealed significantly elevated values for PSA, prostate volume, and tissue removal compared to patients who underwent TURP. Although more prostatic tissue retrieved by HoLEP is lost due to coagulative and vaporizing effects, histological alteration is comparable between HoLEP and TURP. The ability to detect iPCa is not impaired in either of these two techniques [15]. Here, we provided evidence that the choice of surgical procedure for the management of LUTS due to BOO has no influence on the prevalence of iPCa. Despite diagnostic assessment prior to surgery, according to current guideline recommendations [1], incidental PCa was still detected in 15 and 17% of patients treated with HoLEP and TURP, respectively ($p = 0.593$, Table 1). Our rate of iPCa is slightly higher compared to previously published studies; however, the majority of patients will have pT1a and low-grade disease [14–24]. Therefore, patients with iPCa appear to be adequately followed by active surveillance with an overall survival of 72.8% at 5 years and 63.5% at 10 years [25].

Available screening instruments for the detection of PCa including PSA, PSA density, PSA velocity, PSA doubling time, and free/total PSA ratio provide acceptable accuracy when used within defined limits, but beyond these ranges, they have to be interpreted with caution [13]. With HoLEP becoming the standard

procedure especially for larger prostates, clinicians are faced with a subset of patients in whom diagnostic assessment of LUTS has not been clinically adapted. This is mirrored by our observation that significantly more patients received a prostate biopsy prior to HoLEP (35%) compared to TURP (15%) considering that the prevalence of iPCa was comparable between both study populations. This diagnostic gap stresses the need for modified screening parameters for this indication. The study by Elkoushy et al. [25] evaluated prevalence, predictors, and oncological outcome of patients with iPCa detected at the time of HoLEP. Of 1242 treated patients, 70 (5.64%) were positive for adenocarcinoma in enucleated specimen. Their results suggest that a lower cut-off value of 0.092 ng/mL/cc for PSA density raises the detection of co-existing PCa for this subset of patients. Adapting the reference values for total PSA and PSA density according to prostate volume to maintain a sufficient diagnostic sensitivity was suggested for further clinical studies [30, 33].

Furthermore, patients with elevated PSA levels and larger prostates appear not to be adequately assessed by TRUS-guided systematic biopsy. In this study, patients in the HoLEP treatment arm with a median prostate volume of 80 cc and a negative preoperative prostate biopsy were still positive for PCa in 40% of cases. This finding raises the question whether a saturation biopsy or novel imaging techniques such as multiparametric magnetic resonance imaging (mpMRI)-TRUS-guided fusion biopsy are more appropriate approaches to detect PCa in this selected patient population. Although recent studies reported inferiority of mpMRI-TRUS-guided biopsy to systematic biopsy for overall cancer detection [34], its value for selected LUTS patients presenting with considerably enlarged prostates still needs to be elucidated.

Our multivariate logistic regression analysis further suggests a more adapted approach for LUTS patients to exclude malignancy with available diagnostic instruments. We identified both patient age and PSA density as independent predictors for the detection of incidental PCa for our entire study population (Fig. 1). Increasing age is a well-established risk factor for developing PCa [13]. However, we identified PSA density with a cut-off value of 0.15 ng/mL/cc [28] as an independent predictor of iPCa for LUTS patients at the time of surgery. The study by Elkoushy et al. [25] also demonstrated that patient age and PSA density independently predicted iPCa after HoLEP, although they used a lower cut-off value of 0.092 ng/mL/cc. Results of a recently published cohort of 1272 patients undergoing HoLEP reported iPCa in 103 patients (8.1%) [17]. Based on their multivariate logistic regression analysis, which did not include PSA density, the authors predicted a probability of 20% for co-existing PCa in men older than 80 years. In our cohort, 60 year-old-men were noted to have an approximately 20% risk for the detection of iPCa at the time of surgery when PSA density exceeded 0.15 ng/mL/cc. Conversely, a lower 10% risk for the detection of iPCa was predicted for a PSA density <0.15 ng/mL/cc in the same age cohort (Fig. 1).

Certain limitations of our study need to be acknowledged. First of all, this is a retrospective analysis of LUTS patients treated at a single academic center by a single surgeon. Second, analyzed groups were not matched. Furthermore, various urologists performed systematic 12-core prostate biopsies prior to surgery and a standardized scheme could not be assured. Finally, we did not determine cutoffs for prostate volumes that are not adequately assessed by a 12-core systematic biopsy.

Despite these limitations, our study represents the first comparison of clinicopathological and oncologic parameters in LUTS patients undergoing either HoLEP or TURP. To seek further evidence regarding the clinical value of PSA density as independent predictor for iPCa in LUTS patients, larger, prospective, multicenter trials are needed. Our results suggest that available screening methods require further evaluation and validation for LUTS patients to optimize assessment and to omit overdiagnosis, such as unwarranted preoperative prostate biopsies.

Conclusions

Despite differences in clinicopathological and oncologic parameters of LUTS patients surgically treated with HoLEP in comparison to TURP, our findings suggest that the choice of technique has no influence on the diagnosis of incidental PCa. The majority of patients will have pT1a and low-grade disease. Older patient age and a higher PSA density are independent predictors for the detection of incidental PCa after HoLEP and TURP. However, a higher rate of false-negative preoperative prostate biopsy results was noted in HoLEP patients. Therefore, oncologic evaluation of LUTS patients may require a more adapted diagnostic approach to exclude prostate malignancy, particularly in men with larger size prostates.

Author contributions A. Herlemann: data collection and analysis, and manuscript writing. K. Wegner: data collection and management, and data analysis. A. Roosen: project development and data collection. A. Buchner: data collection and analysis, and manuscript writing. P. Weinhold: data collection and management. A. Bachmann: data collection and management. CG. Stief: Project development, and data collection and management. C. Gratzke: Project development, and data collection and management. G. Magistro: Project development, data collection and analysis, and manuscript writing.

Compliance with ethical standards

Conflict of interest The authors declare that they have no conflict of interest.

Informed consent For this type of study, formal consent is not required. This article does not contain any studies with human participants or animals performed by any of the authors.

References

1. Gravas S et al (2015) Guidelines on the management of non-neurogenic male lower urinary tract symptoms (LUTS), incl. Benign prostatic obstruction (BPO). https://uroweb.org/wp-content/uploads/EAU-Guidelines-Non-Neurogenic-Male-LUTS-Guidelines-2015-v2.pdf
2. Gilling PJ et al (2012) Long-term results of a randomized trial comparing holmium laser enucleation of the prostate and transurethral resection of the prostate: results at 7 years. BJU Int 109(3):408–411
3. Lourenco T et al (2008) Alternative approaches to endoscopic ablation for benign enlargement of the prostate: systematic review of randomised controlled trials. BMJ 337:a449
4. Tan A et al (2007) Meta-analysis of holmium laser enucleation versus transurethral resection of the prostate for symptomatic prostatic obstruction. Br J Surg 94(10):1201–1208
5. Yin L et al (2013) Holmium laser enucleation of the prostate versus transurethral resection of the prostate: a systematic review and meta-analysis of randomized controlled trials. J Endourol 27(5):604–611
6. Elmansy H et al (2012) Holmium laser enucleation versus photoselective vaporization for prostatic adenoma greater than 60 ml: preliminary results of a prospective, randomized clinical trial. J Urol 188(1):216–221
7. Elmansy HM, Kotb A, Elhilali MM (2011) Holmium laser enucleation of the prostate: long-term durability of clinical outcomes and complication rates during 10 years of followup. J Urol 186(5):1972–1976
8. Krambeck AE, Handa SE, Lingeman JE (2013) Experience with more than 1000 holmium laser prostate enucleations for benign prostatic hyperplasia. J Urol 189(1 Suppl):S141–S145
9. Kuntz RM, Lehrich K, Ahyai SA (2008) Holmium laser enucleation of the prostate versus open prostatectomy for prostates greater than 100 grams: 5-year follow-up results of a randomised clinical trial. Eur Urol 53(1):160–166
10. Tooher R et al (2004) A systematic review of holmium laser prostatectomy for benign prostatic hyperplasia. J Urol 171(5):1773–1781
11. van Rij S, Gilling PJ (2012) In 2013, holmium laser enucleation of the prostate (HoLEP) may be the new 'gold standard'. Curr Urol Rep 13(6):427–432
12. Gratzke C et al (2015) EAU Guidelines on the Assessment of Non-neurogenic Male Lower Urinary Tract Symptoms including Benign Prostatic Obstruction. Eur Urol 67(6):1099–1109
13. Mottet N et al (2015) Guidelines on Prostate Cancer; European Association of Urology 2015. http://uroweb.org/wp-content/uploads/09-Prostate-Cancer_LR.pdf
14. Nunez R et al (2011) Incidental prostate cancer revisited: early outcomes after holmium laser enucleation of the prostate. Int J Urol 18(7):543–547
15. Naspro R et al (2004) Holmium laser enucleation versus transurethral resection of the prostate. Are histological findings comparable? J Urol 171(3):1203–1206
16. Kim M et al (2014) Prostate cancer detected after Holmium laser enucleation of prostate (HoLEP): significance of transrectal ultrasonography. Int Urol Nephrol 46(11):2079–2085
17. Bhojani N et al (2015) Coexisting prostate cancer found at the time of holmium laser enucleation of the prostate for benign prostatic hyperplasia: predicting its presence and grade in analyzed tissue. J Endourol 29(1):41–46
18. Rivera ME et al (2014) Holmium laser enucleation of the prostate and perioperative diagnosis of prostate cancer: an outcomes analysis. J Endourol 28(6):699–703
19. Sakamoto H et al (2014) Preoperative parameters to predict incidental (T1a and T1b) prostate cancer. Can Urol Assoc J 8(11–12):E815–E820
20. Otto B et al (2014) Incidental prostate cancer in transurethral resection of the prostate specimens in the modern era. Adv Urol 2014:627290
21. Voigt S et al (2011) Risk factors for incidental prostate cancer-who should not undergo vaporization of the prostate for benign prostate hyperplasia? Prostate 71(12):1325–1331
22. Melchior S et al (2009) Outcome of radical prostatectomy for incidental carcinoma of the prostate. BJU Int 103(11):1478–1481
23. Argyropoulos A et al (2005) Characteristics of patients with stage T1b incidental prostate cancer. Scand J Urol Nephrol 39(4):289–293
24. Jones JS, Follis HW, Johnson JR (2009) Probability of finding T1a and T1b (incidental) prostate cancer during TURP has decreased in the PSA era. Prostate Cancer Prostatic Dis 12(1):57–60
25. Elkoushy MA, Elshal AM, Elhilali MM (2015) Incidental prostate cancer diagnosis during holmium laser enucleation: assessment of predictors, survival, and disease progression. Urology 86(3):552–557
26. Benson MC et al (1993) An algorithm for prostate cancer detection in a patient population using prostate-specific antigen and prostate-specific antigen density. World J Urol 11(4):206–213
27. Carter HB et al (2006) Detection of life-threatening prostate cancer with prostate-specific antigen velocity during a window of curability. J Natl Cancer Inst 98(21):1521–1527
28. Ciatto S et al (2001) Predicting prostate biopsy outcome by findings at digital rectal examination, transrectal ultrasonography, PSA, PSA density and free-to-total PSA ratio in a population-based screening setting. Int J Biol Markers 16(3):179–182
29. Helfand BT et al (2009) Postoperative PSA and PSA velocity identify presence of prostate cancer after various surgical interventions for benign prostatic hyperplasia. Urology 74(1):177–183
30. Kuriyama M et al (1999) Determination of reference values for total PSA, F/T and PSAD according to prostatic volume in japanese prostate cancer patients with slightly elevated serum PSA levels. Jpn J Clin Oncol 29(12):617–622
31. Stephan C et al (2002) Multicenter evaluation of an artificial neural network to increase the prostate cancer detection rate and reduce unnecessary biopsies. Clin Chem 48(8):1279–1287
32. Michalak J, Tzou D, Funk J (2015) HoLEP: the gold standard for the surgical management of BPH in the 21(st) Century. Am J Clin Exp Urol 3(1):36–42
33. Stephan C et al (2005) The ratio of prostate-specific antigen (PSA) to prostate volume (PSA density) as a parameter to improve the detection of prostate carcinoma in PSA values in the range of <4 ng/mL. Cancer 104(5):993–1003
34. Delongchamps NB, Portalez D, Bruguière E, Rouvière O, Malavaud B, Mozer P, Fiard G, Cornud F, MURIELLE Study Group (2016) Are MRI-TRUS-guided targeted biopsies non-inferior to TRUS-guided systematic biopsies for the detection of prostate cancer in patients with a single suspicious focus on multiparametric prostate MRI? Results of a multicentric controlled trial. J Urol 196(4):1069–1075. doi:10.1016/j.juro.2016.04.003

International Journal of Medical Microbiology 307 (2017) 44–56

Contents lists available at ScienceDirect

International Journal of Medical Microbiology

journal homepage: www.elsevier.com/locate/ijmm

Strain-specific impact of the high-pathogenicity island on virulence in extra-intestinal pathogenic *Escherichia coli*

Mounira Smati[a,b,c,1], Giuseppe Magistro[d,1], Sandrine Adiba[e], Andreas Wieser[f], Bertrand Picard[a,b,c], Sören Schubert[f,2], Erick Denamur[a,g,h,*,2]

[a] INSERM, IAME, UMR1137, Paris, France
[b] Univ Paris Nord, IAME, UMR1137, Sorbonne Paris Cité, Bobigny, France
[c] APHP, Hôpitaux Universitaires Paris Seine Saint-Denis, Site Avicenne, Bobigny, France
[d] Department of Urology, Ludwig-Maximilians-University of Munich, Munich, Germany
[e] Institut de Biologie de l'Ecole Normale Supérieure, ENS, CNRS UMR8197, INSERM U1024, Paris, France
[f] Max von Pettenkofer-Institut für Hygiene und Medizinische Mikrobiologie, München, Germany
[g] Univ Paris Diderot, IAME, UMR1137, Sorbonne Paris Cité, Paris, France
[h] APHP, Hôpitaux Universitaires Paris Nord Val de Seine Saint-Denis, Paris, France

ARTICLE INFO

Article history:
Received 10 May 2016
Received in revised form
16 November 2016
Accepted 20 November 2016

Keywords:
Escherichia coli
High pathogenicity island
Experimental virulence
Genetic background

ABSTRACT

In order to clarify the role of the high-pathogenicity island (HPI) in the experimental virulence of *Escherichia coli*, we constructed different deletion mutants of the entire HPI and of three individual genes (*irp2*, *fyuA* and *ybtA*), encoding for three main functions within the HPI. Those mutants were constructed for three phylogroup B2 strains (536-STc127, CFT073-STc73, and NU14-STc95), representative of the main B2 subgroups causing extra-intestinal infections. Transcriptional profiles obtained for the selected HPI genes *irp2*, *fyuA* and *ybtA* revealed similar patterns for all strains, both under selective iron-deplete conditions and in intracellular bacterial communities *in vitro*, with a high expression of *irp2*. Deletion of *irp2* and *ybtA* abrogated yersiniabactin production, whereas the *fyuA* knockout was only slightly impaired for siderophore synthesis. The experimental virulence of the strains was then tested in amoeba *Dictyostelium discoideum* and mouse septicaemia models. No effect of any HPI mutant was observed for the two more virulent strains 536 and CFT073. In contrast, the virulence of the less virulent NU14 strain was dramatically diminished by the complete deletion of the HPI and *irp2* gene whereas a lesser reduction in virulence was observed for the *fyuA* and *ybtA* deletion mutants. The two experimental virulence models gave similar results. It appears that the role of the HPI in experimental virulence is depending on the genetic background of the strains despite similar inter-strain transcriptional patterns of HPI genes, as well as of the functional class of the studied gene. Altogether, these data indicate that the intrinsic extra-intestinal virulence in the *E. coli* species is multigenic, with epistatic interactions between the genes.

1. Introduction

Iron acquisition is critical for the survival of pathogenic bacteria during infection. The high-pathogenicity island (HPI) is a 36- to 43-kb pathogenicity island (PAI), which encodes one of the major bacterial iron uptake systems (Garcia et al., 2011; Garenaux et al., 2011). The structure of the HPI has been extensively studied and several genes of interest have been described: an integrase gene (*int*), the genes *irp1*, *irp2* (iron repressible protein) encoding the siderophore yersiniabactin, the gene *fyuA* encoding the yersiniabactin receptor involved in iron uptake and the regulator gene *ybtA* (Buchrieser et al., 1998; Carniel et al., 1996). The HPI is widely distributed among the *Enterobacteriaceae* (Bach et al., 2000), particularly in *Yersinia*, *Klebsiella*, *Citrobacter*, *Enterobacter*, *Salmonella*, *Serratia* and *Escherichia coli*. It is highly conserved between species with homologies from 98 to 100% between the genes of *Yersinia* and *E. coli* (Dobrindt et al., 2002; Lesic and Carniel, 2005; Schubert et al., 1998). In *E. coli*, the HPI is more common in strains responsible for septicaemia (83%) and urinary tract infections (70%) and in enteroaggregative strains (92%) (Schubert et al., 1998). But it is also found in 27% of strains producing Shiga toxin (STEC) (Karch

* Corresponding author at: IAME, UMR1137, INSERM, Université Paris Diderot, Site Xavier Bichat, 16, rue Henri Huchard, 75018 Paris, France.
E-mail address: erick.denamur@inserm.fr (E. Denamur).
[1] These authors contributed equally to this work.
[2] These authors contributed equally to this work.

http://dx.doi.org/10.1016/j.ijmm.2016.11.004
1438-4221/

Table 1
List of the mutant and complemented strains of *E. coli* 536, CFT073 and NU14, as well as the control strains, with their main characteristics and origins.

Strain ID	Main characteristics	Origin
536	O6 : K15 : H31; pyelonephritis isolate	Berger et al. (1982)
536 ΔHPI	Deletion of the entire *hpi*; St^R	Diard et al. (2010)
536 *irp2*::Kn	Insertional *irp2* mutant; Kn^R	This study
536 *irp2*::Kn rec	Recomplemented mutant, pWKS30-P*irp2*; Kn^R Ap^R	This study
536 *fyuA*::Cm	Isogenic *fyuA* mutant; Cm^R	This study
536 *ybtA*::Kn	Isogenic *ybtA* mutant; Kn^R	This study
536 *ybtA*::Kn rec	Recomplemented mutant, pWKS30-*ybtA*; Kn^R Ap^R	This study
CFT073	O6:K2:H1; pyelonephritis isolate	Mobley et al. (1990)
CFT073 HPI::Cm	Deletion of the entire *hpi*; Cm^R	This study
CFT073 *ybtA*::Kn	Isogenic *ybtA* mutant; Kn^R	This study
NU14	O18 : K1 : H7 ; cystitis isolate	Hultgren et al. (1986)
NU14 HPI::Kn	Deletion of the entire *hpi*; Kn^R	This study
NU14 *irp2*::Kn	Insertional *irp2* mutant; Kn^R	This study
NU14 *irp2*::Cm	Isogenic *irp2* mutant; Cm^R	This study
NU14 Δ*irp2* rec	Recomplemented mutant, pWKS30-irp2; Ap^R	This study
NU14 *irp2*::Cm rec	Recomplemented mutant, pWKS30-P*irp2*; Cm^R Ap^R	This study
NU14 *fyuA*::Cm	Isogenic *fyuA* mutant; Cm^R	This study
NU14 *fyuA*::Cm rec	Recomplemented mutant, pACYC184-*fyuA*; Cm^R Tet^R	This study
NU14 *ybtA*::Kn 1	Isogenic *ybtA* mutant; Kn^R	This study
NU14 *ybtA*::Kn 2	Isogenic *ybtA* mutant; Kn^R	This study
NU14 *ybtA*::Kn rec 1	Recomplemented mutant, pWKS30-*ybtA*; Kn^R Ap^R	This study
NU14 *ybtA*::Kn rec 2	Recomplemented mutant, pCP1; Kn^R Cm^R	This study
DH5α	Laboratory K-12 *E. coli*	Hanahan (1983)
MG1655	Laboratory K-12 *E. coli*	Blattner et al. (1997)
REL 606	Laboratory *E. coli* B	Jeong et al. (2009)
WR1542	*S. enterica* serotype Typhimurium, pACYC5.3L	(Rabsch, Wernigerode)

*St: streptomycin, Kn: kanamycin, Cm: chloramphenicol, Ap: ampicillin, Tet: tetracyclin.

et al., 1999) and in 30% of isolates from faeces of healthy individuals (Bielaszewska et al., 2007).

The *E. coli* species is mainly clonal (Desjardins et al., 1995), with 7 main phylogenetic groups (A, B1, B2, C, D, E, and F) composed of numerous clones grouped in sequence type complexes (STc) or sub-groups (Clermont et al., 2013, 2015). The B2 group is the most diverse with at least 9 phylogenetic subgroups observed (Le Gall et al., 2007) and it is also the most frequently recovered group among the extra-intestinal pathogenic *E. coli* (ExPEC) strains responsible of human infections (Russo and Johnson, 2000). Interestingly, the HPI, which has spread within the *E. coli* species by homologous recombination, is not randomly distributed within the species but overrepresented within the B2 phylogroup (Schubert et al., 2009).

In *E. coli*, the studies on the role of the HPI in experimental virulence gave contrasting results according to strains and models. It appeared critical in some works. Thus, it has an important role during the bacteremic phase in a sepsis model in mouse (Schubert et al., 2002) and for preventing from grazing by the social haploid amoeba *Dictyostelium discoideum* (Adiba et al., 2010) for B2 phylogroup strains IAI51 and IAI52. These isolates belong to the subgroup IV (STc141) infrequently found in extra-intestinal pathologies (Clermont et al., 2014). Similarly, the HPI mutant of the CFT073 strain (B2 subgroup II, STc73) was outcompeted in the kidneys following transurethral competition with the wild type (Lloyd et al., 2009). In contrast, it has no impact in other works. No role has been reported in a neonatal meningitis model in newborn rat for B2 phylogroup strain C5 belonging to the subgroup IX (STc95) (Negre et al., 2004), in a mouse sepsis model (Tourret et al., 2010) and in a nematode (*Caenorhabditis elegans*) model (Diard et al., 2007) for the B2 phylogroup strain 536 (subgroup III, STc127). Lastly, discrepant results were obtained for the same strain 536 in two urinary tract infection (UTI) models: the competition between mutants and wild type in the classical murine model of ascending UTI (Garcia et al., 2011) and the monoinfection in infant mouse UTI followed by sepsis (Brzuszkiewicz et al., 2006).

This variable role of the HPI in experimental virulence could be explained by (i) the type of mutants analysed (deletions of various genes *versus* deletion of all the HPI), (ii) the utilisation in the inoculum of the models of monoinfection *versus* competition of mutant and wild type strains, (iii) the huge genetic diversity of the species in term of gene content, which could modify the effect of the mutations (Touchon et al., 2009) and (iv) the diversity of hosts and routes of inoculation in these experimental models of virulence, although a good correlation has been reported between the mouse, nematode and amoeba models (Adiba et al., 2010).

In order to disentangle these discrepancies in the role of the HPI in experimental virulence, we constructed different mutants of three individual genes (*irp2*, *fyuA* and *ybtA*) representative of the 3 principal functions of the HPI genes as well as of the entire HPI. The respective mutations were introduced in three B2 phylogroup strains representative of the major actual ExPEC subgroups (STc73, STc95 and STc127) of *E. coli*. Gene expression of the HPI under different conditions, as well as yersiniabactin production were analysed in the three prototypic UPEC strains and their respective HPI mutants. The virulence was then tested in two models of experimental virulence corresponding to two levels of integration: the resistance to phagocytosis by the amoeba *D. discoideum* model (Adiba et al., 2010) and a mammal model, the mouse septicaemia (Picard et al., 1999).

2. Materials and methods

2.1. Bacterial strains, media and in vitro growth conditions

Bacterial strains and plasmids used in the present work are listed in Table 1. Three uropathogenic *E. coli* (UPEC) strains of the phylogenetic group B2 were studied belonging to the subgroups II (STc73), III (STc127) and IX (STc95) (Clermont et al., 2015). The complete genome sequences of all three isolates are available. Strain 536 is an uropathogenic *E. coli* strain (O6:K15:H31), which belongs to the subgroup III. This strain was isolated from the urinary

tract of a patient with pyelonephritis (Hacker et al., 1983). It produces siderophores enterobactin, salmochelin and yersiniabactin but does not produce aerobactin. It is a highly virulent strain in the mouse sepsis model (Tourret et al., 2010) and in the nematode *C. elegans* (Diard et al., 2007). Strain CFT073 (O6:K2:H1) belongs to the subgroup II and was isolated from urine and blood of a patient who experienced urinary starting point septicaemia (Mobley et al., 1990). It produces enterobactin, salmochelin and aerobactin but not yersiniabactin despite the presence of the HPI (see below) (Welch et al., 2002). CFT073 is a virulent strain in the mouse model of septicaemia (Johnson et al., 2006) and in the nematode *C. elegans* (Diard et al., 2007). Strain NU14 (O18:K1:H7) belongs to the sub-group IX. The strain was isolated from cystitis. It secretes enterobactin, salmochelin and yersiniabactin but not aerobactin (Johnson et al., 2001).

Three *E. coli* isolates belonging to phylogroup A (K-12 MG1655, DH5α and B REL606) were used as avirulent control strains.

Strains were cultivated in lysogeny broth (LB), nutrient broth (NB) and in NBD medium, *i.e.* nutrient broth supplemented with 0.2 mM α,α'-dipyridyl to create iron depletion. Growth curves in NB and NBD were performed in 50 ml cultures rotating at 37 °C under aeration in 250 ml Erlenmeyer flasks. Overnight cultures were incubated in 50 ml fresh medium to a starting OD_{600nm} of 0.05 and optical density at 600 nm was recorded every 60 min. All experiments were repeated at least three times. Use of antibiotics was provided as necessary (ampicillin 100 μg/ml, chloramphenicol 20 μg/ml, kanamycin 25 μg/ml, tetracyclin 12 μg/ml, streptomycin 100 μg/ml).

2.2. Construction of isogenic mutants and recombinant DNA techniques

Plasmids and primers/probes used in the study are listed in Tables 2 and 3, respectively. Deletion and insertional mutants were generated according to the protocol published by Datsenko et al. (Datsenko and Wanner, 2000). In brief, primers used for gene disruption included at least 40 nucleotides homology extensions to the 5′- and 3′ regions of the target gene and additional 20 nucleotides of priming sequence for amplification of the resistance cassettes on template plasmids pKD3 and pKD4. The PCR product was then transformed into strains carrying the helper plasmid pKD46 expressing the lambda red recombinase under control of an arabinose-inducible promoter. Kn^R or Cm^R resistant transformants were selected and further screened for correct integration of the resistance marker by PCR. For elimination of the antibiotic resistance gene, helper plasmid pCP20 was used according to the published protocol.

Standard genetic protocols were performed mainly as described by Sambrook and Russel (Sambrook and Russell, 2001). Enzymes were purchased from Fermentas (Schwerte, Germany). PCR products were purified using a QIAquick PCR purification kit (Qiagen, Hilden, Germany) and cloned into plasmids pACYC184 and pWKS30 for recomplementation *via* suitable restriction sites. In case of strain NU14 *ybtA*:Kn rec, recomplementation was carried out by integrating a functional HPI core region of *Y. enterocolitica* using plasmid pCP1 (Pelludat et al., 2002).

Table 2
Plasmids used in this work.

Plasmid ID	Main characteristics
pKD3	Chloramphenicol template plasmid
pKD4	Kanamycin template plasmid
pKD46	Lambda red recombinase helper plasmid
pCP20	Helper plasmid for elimination of resistance gene
pACYC184	Medium-copy plasmid; Cm^R Tet^R
pWKS30	Low-copy plasmid; Ap^R
pCP1	Carrying *hpi* core region; transconjugation; Cm^R
pACYC184-*fyuA*	Expressing FyuA
pWKS30-*ybtA*	Expressing YbtA
pWKS30-*irp2*	Expressing Irp2 under lac promoter
pWKS30-*Pirp2*	Expressing Irp2 under native promoter
pACYC5.3L	*fyuA-lux* reporter fusion, *irp6*, *irp7*,*irp8*, *fyuA*, *ybtA*; Cm^R

Table 3
Primers and probes used in this work.

Gene	Primers/Probes	Sequence (5′–3′)
fyuA	*fyuA*.KO.for	GGCGACATGATTAACCCCGCGACGGGAAGCGATGACTTAGGTGTAGGCTGGAGCTGCTTC
	fyuA.KO.rev	CGATATCAAAACGATCGGTTAAATGCCAGGTCAGGTCACTCATATGAATATCCTCCTTA
irp2	Insertional mutant	
	irp2.KO.for	CAGCAGTTACATGAAGAGAGCAACCTGATCCAGGCCGGCCTGGAGTGTAGGCTGGAGCTGCTTC
	irp2.KO.rev	GTTTGAGTTCACGGAGTAATTCGACGCCGGACCAGTGGCGATGCTCATATGAATATCCTCCTTA
	Deletion mutant	
	irp2.full.KO.for	GAGTAATGCTTTTCGGTAAGACGTGCCATCAGGAGGAAGAGTGTAGGCTGGAGCTGCTTC
	irp2.full.KO.rev	GTTCGCGATGGCGTTCCGGGGAAAATCAGTTTGCTTCGCGCATATGAATATCCTCCTTAG
ybtA	*ybtA*.KO.for	ATGATGGAGTCACCGCAAACGCAATCTGAAATCTCTATTCACCAGTTGGTGGTCGGTGTAGGCTGGAGCTGCTTC
	ybtA.KO.rev	CATCCCGCGTTTAAAGGTCGAAGGAGTTACGCCAAACTGTTTCTGGAAGGCGGCACATATGAATATCCTCCTTA
hpi	*hpi*.KO.for	CCTTACCGACGCAAAAATCCGCACCCTCAAGCCTTCTGATAAGTGTAGGCTGGAGCTGCTTC
	hpi.KO.rev	CAGCGTGATTCTTGCGGTACCGAAGCGGCTTAACCAGTCTGTCATATGAATATCCTCCTTAG
16S rRNA	*16SrRNA.for*	TTGACGTTACCCGCAGAAGAA
	16SrRNA.rev	GCTTGCACCCTCCGTATTACC
	16SrRNA.probe	CGGCTAACTCCGTGCCAGCAGC
fyuA	*fyuA.for*	ACACCCGCGAGAAGTTAAATTC
	fyuA.rev	AGCGGTGGTATAGCCGGTACT
	fyuA.probe	CCTACGACATGCCGACAATGCCTTATTTAA
irp2	*irp2.for*	TGGGTGCCGGGTGAATTA
	irp2.rev	CGTCCGGGAGCGTCAA
	irp2.probe	ATTTCAACGATCCCCTGCGTAGC
ybtA	*ybtA.for*	GTTGCCTCTCCTGCCACTTC
	ybtA.rev	ATCAGCCAGCAGCAGATCCT
	ybtA.probe	ACCCGATGGAACGCCAGAAACTG

2.3. Quantitative real-time PCR (TaqMan)

Transcriptional studies were performed as described recently (Magistro et al., 2015). Briefly, RNA was extracted according to the Trizol (Invitrogen, Darmstadt, Germany) method as described by Chomczynski et al. (Chomczynski and Sacchi, 1987). Total RNA was treated with DNase I (Fermentas) to remove residual contaminating genomic DNA. First-strand DNA synthesis was performed using random hexamers and RevertAid H Minus M-MuLV Reverse Transcriptase (Fermentas) following the manufacturer's protocol. TaqMan-PCR was run on a 7500 Fast Real-Time PCR System (Applied Biosystems, Darmstadt, Germany). Primer Express software (Version 3.0, Applied Biosystems) was used to design primers and probes were labelled with FAM (5′) and TAMRA (3′). PCR reactions were carried out in a final volume of 25 μl containing 30 ng of cDNA, primers, probe and TaqMan Gene Expression Master Mix (Applied Biosystems, Darmstadt, Germany). Transcript levels were normalized to that of 16S rDNA. Relative gene expression was analysed according to the $2^{-\Delta\Delta C}{}_{T}$ method (Livak and Schmittgen, 2001). For iron-replete conditions, growth in LB medium served as the calibrator.

For transcriptional studies under iron scarcity, overnight cultures were incubated in 50 ml of fresh NBD medium to a starting OD_{600nm} = 0.05 and cultured in Erlenmeyer flasks rotating at 37 °C under aeration until OD_{600nm} = 0.5 was reached. At last, bacteria were pelleted by centrifugation and total RNA was prepared as described above.

A modified intracellular growth assay was performed to study gene expression of UPEC organized in so called intracellular bacterial communities (IBC). Human urothelial cell line HCV29 (Masters et al., 1986) was seeded into 6-well plates and grown to confluency in RPMI 1640 medium supplemented with 10% fetal bovine serum, L-glutamine, 2 g/l $NaHCO_3$, 10.000 IE penicillin and 10 mg/ml streptomycin (PAN Biotech GmbH, Aidenbach, Germany) at 37 °C, 5% CO_2 and 95% humidity. Prior to infection, HCV29 were gently washed twice with phosphate-buffered saline (PBS) and incubated for 1 h in antibiotic-free supplemented RPMI 1640. Cells were infected with a multiplicity of infection of 1–10 bacteria per host cell (OD_{600nm} = 1.0). Contact with urothelial cells was expedited by centrifugation of plates at 200 x *g* for 3 min. Following incubation for 2 h, cells were washed three times with PBS and then incubated for one hour in fresh medium containing 100 μl/ml gentamicin (Life Technologies, USA) to eliminate any extra-cellular bacteria. Next, cells were gently washed once with PBS and fresh medium supplemented with a limited concentration of 15 μl/ml gentamicin was added to the cells. For this dosage of gentamicin, the antibiotic is supposed to prevent extra-cellular growth and leaching into cells during extended incubation times can be excluded. After 24 h of cultivation, cells were washed twice with PBS and RNAlater (Qiagen, Hilden, Germany) as RNA-stabilizing agent was added to each well. Infected cells harbouring IBCs were finally scraped off thoroughly and subjected to the RNA extraction protocol as described above. The presence of IBCs was confirmed performing fluorescence microscopy on a Leica DM RBE microscope (Fig. S1). Red fluorescent protein (RFP) expressing NU14, 4′,6-diamidino-2-phenylindole (DAPI) (Sigma) for nucleus staining (blue) and phalloidin-FITC dye (green) for labelling of F-actin (Molecular Probes, Invitrogen) were used to visualize the formation of IBCs. All experiments were repeated at least three times.

2.4. Yersiniabatin detection assay

Production of the siderophore yersiniabactin was quantified indirectly using a luciferase reporter assay as described elsewhere (Kakoschke et al., 2014; Martin et al., 2013). Briefly, bacterial strains were cultivated in NBD medium for 24 h at 37 °C. Next, bacteria were pelleted by centrifugation and the supernatant was added to the indicator strain WR 1542 harbouring plasmid pACYC5.3L. All the genes necessary for yersiniabactin uptake are located on the plasmid, i.e. *irp6, irp7, irp8, fyuA, ybtA*. Furthermore, the reporter plasmid is equipped with a fusion of the *fyuA* promoter region with the luciferase reporter gene. The amount of yersiniabactin can be quantified semi-quantitatively, as yersiniabactin-dependant upregulation of *fyuA* expression is determined by luciferase activity of the *fyuA-lux* reporter fusion. After additional 24 h of incubation at 37 °C, the reporter strain was centrifuged and the pellet was resuspended in lysis buffer (100 mM potassium phosphate buffer [pH 7.8], 2 mM EDTA, 1% [wt/vol] Triton X-100, 5 mg/ml bovine serum albumin, 1 mM dithiothreitol, 5 mg/ml lysozyme). Lysis was completed by incubation at room temperature for 20 min and repeated mixing. Next, samples were centrifuged and luciferase reagent (20 mM Tricine-HCl (pH 7.8), 1.07 mM $(MgCO3)4\ Mg(OH)2$, 100 mM EDTA, 470 mM D(−) luciferin, 33.3 mM dithiothreitol, 270 mM Li3 coenzyme A, 530 mM Mg-ATP) was added to the supernatants. Relative light units (RLU) were determined in triplicates using the multimode reader Berthold Tristar LB 941 (Berthold Technologies, Bad Wildbad, Germany). *E. coli* K-12 DH5α and *Samonella enterica* WR1542 strains were the negative control. The cut-off value for positive yersiniabactin production was defined as the value above the mean RLU of the negative control plus twice the standard deviation. Absolute values were corrected by relating luciferase activity to the OD_{600nm} of bacterial cultures grown 24 h in NBD medium. A standard calibration curve was determined using defined concentrations of purified yersiniabactin (EMC Microcollections, Tübingen, Germany) (Fig. S2). All experiments were repeated at least three times.

2.5. D. discoideum *amoeba model*

The social amoeba *D. discoideum* strain AX3 was used for all experiments. This is an axenic strain able to grow using nutrients from the culture medium. The amoeba grows in the HL5 medium and its optimum growth temperature is between 20 and 25 °C. Amoebae are stored at −80 °C in 500 μl of HL5 medium supplemented with 500 μl of dimethylsulfoxide. The method has been described previously (Adiba et al., 2010). Briefly, the bacteria were grown in 10 ml HL5 broth at 37 °C under constant agitation. The cultures were washed in 10 ml of MCPB buffer. Three hundred μL of bacterial culture (10^8 CFU) were inoculated on Petri dishes of 55 mm diameter containing HL5 agar. Seven day long culture of *D. discoideum* grown in 10 ml of HL5 medium at 23 °C were washed with 10 ml of MCPB. Amoebae were then counted in Kovaslide® cell and adjusted to three concentrations corresponding to 10, 10^2 or 10^3 amoebae to 300 μl of suspension. After plating of 300 μl of suspension of amoebae, the dishes were incubated at 23 °C. The dishes were examined at 3, 6 and 9 days to detect the appearance of lysis plaques. The appearance of lysis plaques corresponded to the phagocytosis of the bacteria by the amoeba and defined the grazing sensitive (GS) phenotype. The avirulent strain *E. coli* B REL606 was used as a negative control with the appearance of plaques to 10, 10^2, 10^3 amoebae. Conversely, virulent strains were resistant to phagocytosis by the amoeba, defining the grazing resistant (GR) phenotype. Three replicates were made by strain, and all experiments were done twice.

2.6. Septicaemia mouse model

Female mice OF1 of 14–16 g (4 week-old) from Charles River® (L'Arbresle, France) were used. Bacteria in exponential growth phase were obtained after culture in LB for 16 h at 37 °C and were washed twice in 0.9% NaCl. They were suspended in saline solution before injection at a concentration of 10^9 CFU/ml. Ten to 20 mice

per strain received a subcutaneous injection of 0.2 ml of bacterial suspension in the neck. Time to death was recorded during the following 7 days. Mice surviving more than 7 days were considered cured and sacrificed (Picard et al., 1999). In each experiment, the CFT073 strain was used as a positive control killing all the inoculated mice whereas the *E. coli* K-12 MG1655 strain was used as a negative control for which all the inoculated mice survive (Johnson et al., 2006). All animal experimentation was conducted following European (Directive 2010/63/EU on the protection of animals used for scientific purposes) and national recommendations (French Ministry of Agriculture and French Veterinary Services, accreditation A 75-18-05). The protocol used was approved by the Animal Welfare Committee of the Veterinary Faculty in Lugo, University of Santiago de Compostela (AE-LU-002/12/INV MED.02/OUTROS 04).

2.7. Statistical analysis

For analysis of gene expression and siderophore production the *t*-test was used. Kaplan-Meier estimates of mouse survival were performed through XLSTAT® software. Survival differences were estimated by Log-Rank test. Survival differences were considered significant if the *P*-value was lower than 0.05. For the amoeba model, the data were compared using a Wilcoxon/Krustal-Wallis test. Differences were considered significant if the *P*-value was lower than 0.05.

3. Results

3.1. Transcriptional analysis of the HPI

The first step to evaluate the impact of the HPI on virulence was to study gene expression profiles in all three prototypic UPEC strains 536, CFT073 and NU14 (Fig. 1). Transcript levels of *ybtA*, *irp2* and *fyuA* coding for the HPI specific transcriptional regulator, an essential synthesis gene and the specific yersiniabactin receptor, respectively, were quantified using real-time PCR. All strains harbour the complete HPI, however, strain CFT073 is not able to produce yersiniabactin due to in-frame stop codons in biosynthetic genes. Bacteria grown in NBD medium showed a similar pattern of response to iron limitation on the transcriptional level, with *irp2* being the most up-regulated gene (Fig. 1A). This pattern was also observed for CFT073 with an almost 3-fold induction and only a weak increase of transcripts for the marker genes *ybtA* and *fyuA*. Compared to cultivation in LB medium *ybtA, irp2 and fyuA* were up-regulated 2-fold, 12-fold and 4-fold, respectively, in strain 536. For NU14 a slight induction of gene expression for *ybtA* and *fyuA* was observed, whereas a strong 42-fold increase was detected for *irp2*.

UPEC were shown to form intracellular bacterial communities (IBC) in urothelial cells (Mulvey et al., 2001). The exact role of siderophore systems for this important step in the pathogenesis of urinary tract infections still remains elusive, especially for the HPI. Thus, we performed a modified gentamicin protection assay using the urothelial cell line HCV29 to investigate the activation of the HPI of intracellular bacteria *in vitro* (Fig. 1B). After 24 h of persistence in an intracellular niche (Fig. S1), bacteria were harvested and gene expression of the marker genes *ybtA, irp2* and *fyuA* was determined. Interestingly, a similar profile was observed in all UPEC strains as for the growth in NBD medium, with *irp2* being the most up-regulated gene. But the transcription rate was significantly higher in the cell culture assay than for the growth in NBD medium. In strain 536 we observed a 203-fold ($p < 0.001$), 48-fold ($p = 0.01$) and 87-fold ($p < 0.05$) increase for *ybtA, irp2* and *fyuA* compared to strict iron deplete condition, respectively. Similar results were obtained for CFT073 showing a 55-fold ($p < 0.001$), 119-fold ($p = 0.001$) and 93-fold ($p = 0.01$) upregulation of *ybtA, irp2* and *fyuA* compared to cultivation in NBD medium, respectively. Gene expression of *ybtA, irp2* and *fyuA* in strain NU14 increased 154-fold ($p < 0.001$), 14-fold ($p < 0.01$) and 20-fold ($p < 0.001$), respectively. These data suggest that the HPI is highly activated when UPEC are organized in an intracellular niche over an extended period of time.

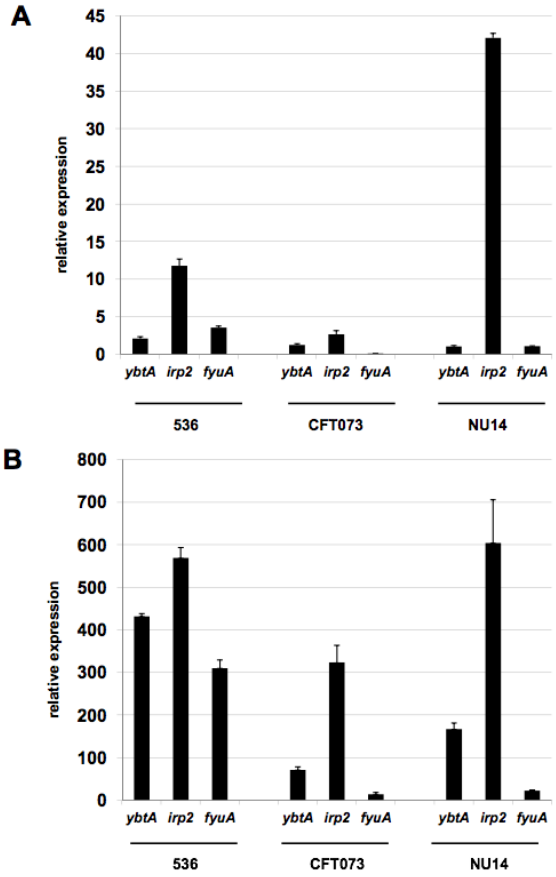

Fig. 1. Transcriptional analysis of high-pathogenicity island genes under iron limited condition (A) and in intracellular bacterial communities (IBC) *in vitro* (B). (A) Gene expression of *ybtA, irp2* and *fyuA* was quantified during cultivation in NBD medium. A similar expression profile was detected in all UPEC strains. *irp2* was the most upregulated gene. (B) Transcription rates of UPEC forming intracellular bacterial communities (IBC) in urothelial cell line HCV29 *in vitro*. Again, *irp2* showed the strongest induction. Transcription of HPI genes was significantly higher than in NBD medium ($p < 0.001$). Strains grown in LB medium served as calibrator. Data were normalized to 16S rRNA. All experiments were repeated at least three times, and error bars indicate standard deviations.

3.2. Yersiniabactin production of different HPI mutants

Mutants with impaired HPI function and the respective complemented derivatives were generated for 536, CFT073 and NU14 to evaluate the impact of the HPI on virulence in different genetic backgrounds (Table 1). Gene disruptions were constructed for *irp2, fyuA* and *ybtA*. First, we tested the mutants for their ability to produce the siderophore yersiniabactin using a luciferase reporter assay as described previously (Fig. 2) (Kakoschke et al., 2014; Martin et al., 2013). As expected, deletion of essential biosynthetic genes like *irp2* abrogated yersiniabactin production. This was demonstrated for strains 536 (536 *irp2*:Kn), NU14 (NU14 *irp2*:Cm) and the natural *irp2* mutant CFT073 ($p < 0.001$). Interestingly,

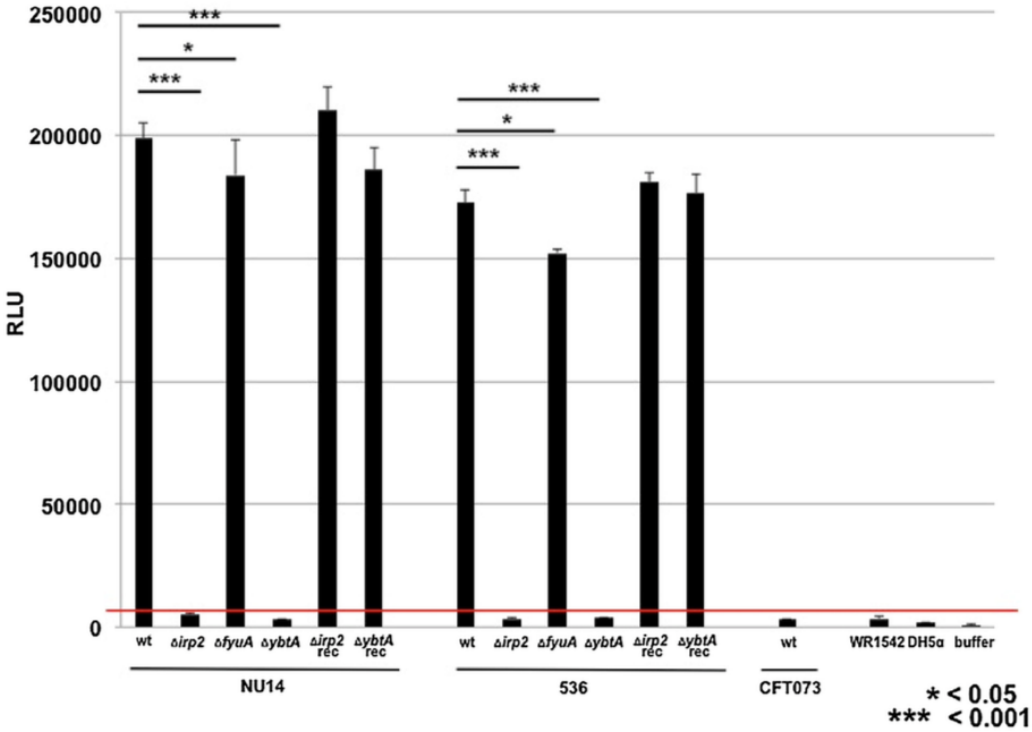

Fig. 2. Yersiniabactin production of HPI mutants under iron limited conditions. Yersiniabactin production of different HPI mutants was measured using a luciferase reporter assay. Deletion of *irp2* resulted in no detectable yersiniabactin in all UPEC backgrounds. Yersiniabactin production was also abrogated in the *ybtA* mutant strains. Plasmidal complementation of *irp2* and *ybtA* restored the ability to synthesize the siderophore. Deletion of *fyuA* coding for the specific receptor showed a significant reduction of yersiniabactin ($p < 0.05$). The reporter strain WR1542 and K-12 *E. coli* DH5α are not able to produce yersiniabactin and were used as negative controls. Horizontal bar close to zero indicates the cut off level in the experiments. All experiments were repeated at least three times, and error bars indicate standard deviations.

deletions of the transcriptional regulator *ybtA*, also resulted in no detectable amounts of yersiniabactin in mutants 536 *ybtA*:Kn and NU14 *ybtA*:Kn ($p < 0.001$). Complementation *in trans* for *irp2* (536 *irp2*:Kn rec; NU14 *irp2*:Cm rec) and *ybtA* (536 *ybtA*:Kn rec; NU14 *ybtA*:Kn rec 1) restored the ability to produce yersiniabactin. *FyuA*, encoding the specific yersiniabactin receptor, sappeared to have a moderate impact on synthesis. Compared to the wild type strains NU14 (2.0×10^5 RLU, ±5989) and 536 (1.7×10^5 RLU, ±5522), the *fyuA* mutants were slightly impaired for production in NU14 *fyuA*:Cm (1.8×10^5 RLU, ±14272) and 536 *fyuA*:Cm (1.5×10^5 RLU, ±1647) (both $p < 0.05$).

Our next step was to evaluate the contribution of yersiniabactin to growth under iron deplete condition. Growth experiments were carried out in NB for the three wild type strains and the *irp2* mutants of strains 536 (536 *irp2*:Kn) and NU14 (NU14 *irp2*: Cm), both lacking yersiniabactin synthesis. As depicted in Fig. 3A, under iron rich conditions no significant difference in growth could be determined, neither for the wild type strains 536, CFT073 and NU14, nor for the respective yersiniabactin deficient mutants. The supplementation of NB with dipyridyl creates iron limitation resulting in strong activation of the HPI, as shown above. Growth under iron deplete condition caused a significant impairment for all three wild type strains compared to cultivation in nutrient broth (Fig. 3B and C). Under these specific conditions the growth of the wild type strains differed significantly (all $p < 0.05$). The shortest generation time was shown for the yersiniabactin negative strain CFT073 (91.07 min ± 4.61), followed by NU14 (139.89 min ± 3.68) and last 536 (159.47 min ± 1.94) (Fig. 3C). The deletion of *irp2* caused a significant growth reduction of 57.2% and 29,6% in mutant strains (536 *irp2*:Kn) and (NU14 *irp2*: Cm), respectively (both $p < 0.05$) (Fig. 3B). Complementation *in trans* was able to restore growth of the mutant strains 536 *irp2*:Kn rec and NU14 *irp2*:Cm rec to wild type levels (Fig. 3B). These data clearly show that growth under selective iron limiting conditions differs between prototypic UPEC strains. The ability to produce yersiniabactin is considered a relevant fitness factor, as its impairment results in a substantial growth deficit under iron depletion.

3.3. Amoeba model of virulence

We first compared the virulence of the wild type strains in an unicellular model mimicking a macrophage, *i.e.* the amoeba (Steinert and Heuner, 2005). The strains 536, CFT073 and NU14 were all resistant to the amoeba phagocytosis showing no lysis plaque (GR phenotype) at densities of 10, 10^2 and 10^3 amoebae per 10^8 CFU of bacteria whereas the control strain REL606 gave large lysis plaques (GS phenotype) with the formation of fruity bodies by the amoeba (Fig. 4A–C).

We then tested the various mutants of the HPI. The strain 536 deleted for the entire HPI (536ΔHPI) revealed the same GR phenotype as the wild type strain being therefore virulent in the amoeba model. Similarly, 536 mutants of *irp2*, *fyuA* and *ybtA* (536 *irp2*:Kn, 536 *fyuA*:Cm and 536 *ybtA*:Kn, respectively) showed an identical GR phenotype. The deletion of the complete HPI in CFT073 (CFT073 HPI:Cm) or of the *ybtA* gene (CFT073 *ybtA*:Kn) led to an identical GR phenotype compared to the wild type, as expected. The deletion of

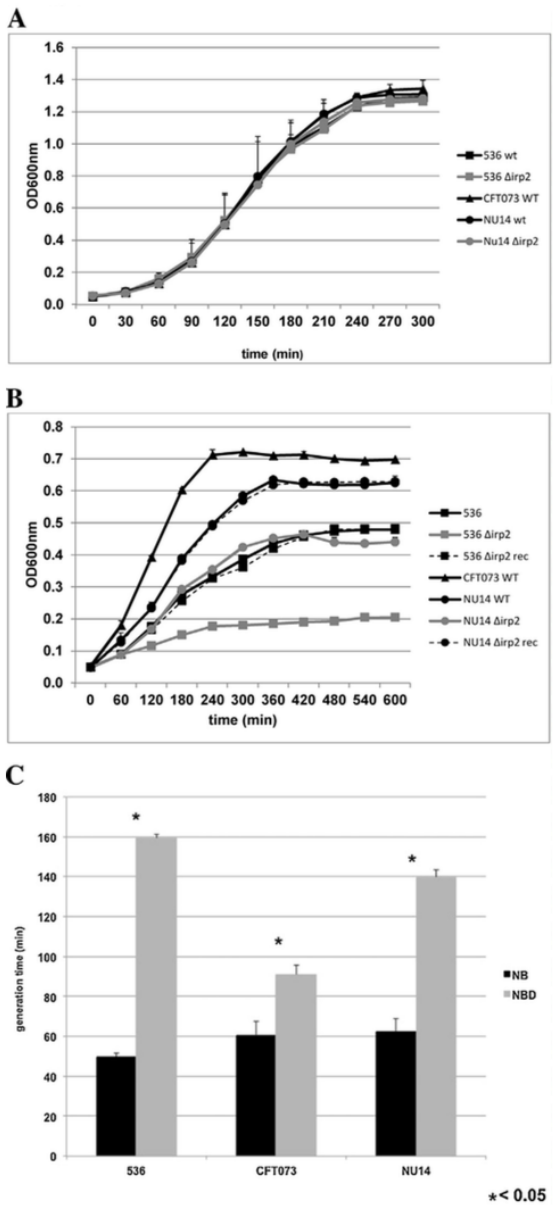

Fig. 3. Growth curves of prototypic UPEC strains and their respective yersiniabactin deficient mutants. A) Wild type strains and *irp2* mutants cultured in NB medium revealed no difference for growth under iron abundance. B) Growth under iron deplete conditions in NBD impaired growth for all three wild type strains compared to cultivation in nutrient broth. The *irp2* mutants displayed a significant growth deficit relative to the wild type strains. Complementation *in trans* restored growth completely in the yersiniabactin deficient strains to wild type level. C) Generation time determined for wild type strains cultivated in NB and NBD medium. All experiments were repeated at least three times, and error bars indicate standard deviations.

Table 4
Virulence phenotypes of the *E. coli* NU14 wild type and derivative strains, as well as the *E. coli* B REL 606 control strain, in the *D. discoideum* amoeba model.

Strains	Amoeba inoculum		
	10	10^2	10^3
REL 606	SSSSSS[a]	SSSSSS	SSSSSS
NU14	RRRRRR	RRRRRR	RRRRRR
NU14 HPI:Kn	RRRRRR	SSSSRR	SSSSSS
NU14 *irp2*:Kn	SSSRRR	SSSRRR	SSSSSS
NU14Δ*irp2* rec	RRRRRR	RRRRRR	RRRRRS
NU14 *fyuA*:Cm	RRRRRR	RRRRRR	SSSSSS
NU14 *fuyA*:Cm rec	RRRRRR	RRRRRR	RRRRRR
NU14 *ybtA*:Kn (1 and 2)	RRRRRR	RRRRRR	SSSSSS
NU14 *ybtA*:Kn rec 2	RRRRRR	RRRRRR	RRRRRS

[a] S corresponds to a grazing sensitive phenotype (presence of lysis plaques) in one replicate. R corresponds to a grazing resistant phenotype (absence of lysis plaques) in one replicate. Three replicates were made by strain, and the experiment was done twice, thus generating 6 letters. The strain REL606 is the control strain for grazing sensitivity.

the complete HPI in NU14 evidenced a GS phenotype with small lysis plaques appearing at a density of 10^2 amoebae ($p = 0.0002$) (Table 4). The two independent deletion mutants of *irp2* in *E. coli* NU14 (NU14 *irp2*:Kn and NU14 *irp2*:Cm) showed a GS phenotype already at density of 10 amoebae ($p < 0.0001$). The mutant of the gene *fyuA* (NU14 *fyuA*:Cm) led to a GS phenotype of amoebae at a density of only 10^3 ($p = 0.008$). Similarly, the two independent mutants of *ybtA* (NU14 *ybtA*:Kn 1 and 2) exhibited a GS phenotype with small lysis plaques at an amoebae density of only 10^3 ($p = 0.008$) (Fig. 4D). Thus, when taking into account the amoebae inoculum, two levels in diminishing of virulence can be distinguished according to the mutants: a high decrease of virulence for the HPI and *irp2* mutants and a lower reduction of virulence for the *fyuA* and *ybtA* mutants.

We then performed complementation experiments for those gene mutants of NU14 showing a significant loss of virulence compared to the wild type. For this we introduced both chromosomal and plasmid complementation. In these complementation experiments, a selective pressure was maintained using the corresponding antibiotics (chloramphenicol, ampicillin or tetracycline) in the culture medium. The virulent GR phenotype of the wild strain was restored by the pWKS30 plasmid bearing *irp2* (NU14Δ*irp2* pWKS30-*irp2*). Mediated plasmid complementation was obtained with the plasmid pACYC184 for the *fyuA* gene (NU14 *fyuA*:Kn pACYC184-fyuA). However, complementation of the *ybtA* mutant with the plasmid pWKS30-*ybtA* was not successful, whereas we achieved a chromosomal complementation by introduction of the suicide vector pCP1 restoring the wild type GR phenotype (NU14 *ybtA*:Kn rec 2) (Fig. 4E and Table 4).

3.4. Mouse model of virulence

We next tested the effect on virulence of the HPI by using the same strategy in a mammalian model, *i.e.* the mouse sepsis model (Picard et al., 1999). We first compared the virulence of the wild type strains. Kaplan-Meier survival curves of mice inoculated with 536, CFT073 and NU14 strains showed significantly different patterns (Fig. 5) ($p < 0.001$). Strain 536 was the most virulent, killing all inoculated mice in less than 20 h (95% in less than 16 h), followed by strain CFT073 that killed all mice in about 2 days. Lastly, the strain NU14 killed 90% of the mice in about 4 days and can be considered as a "slow killer".

We then tested deletion mutant strains. The *E. coli* strain 536ΔHPI had previously been tested (Diard et al., 2010), showing killing of mice identical to that of the wild type strain. Given these results, the other gene deletion mutants of the HPI have not been tested in mice for ethical reasons. The strain CFT073 ΔHPI:Cm and

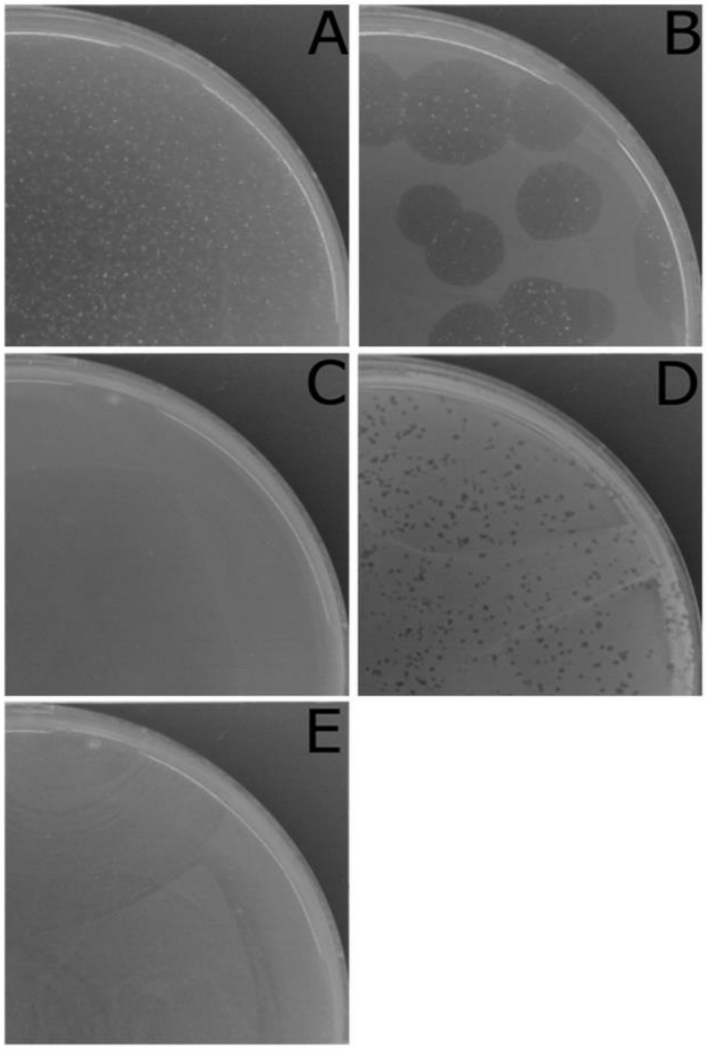

Fig. 4. Examples of virulence phenotypes observed in the *D. discoideum* amoeba model. 10^8 CFU bacteria were plated on Petri dishes containing HL5 agar with *D. discoideum* at variable concentrations and examined at day 6. (A) *E. coli* B REL606 with 10^3 amoebae. Amoebae fed the lawn of bacteria, and once the bacteria are depleted, amoebae trigger a developmental program: cells aggregate and form fruity bodies (white dots). (B) *E. coli* B REL 606 with 10^2 amoebae. Large lysis plaques are observed with also some fruity bodies inside plaques. (A) and (B) represent the grazing sensitive (GS) phenotype. (C) *E. coli* NU14 with 10^3 amebae. Only a lawn of bacteria is visible, with no lysis plaque, corresponding to the grazing resistance (GR) phenotype. (D) *E. coli* NU14 *ybtA*:Kn with 10^3 amoebae. Amebae form small lysis plaques, indicating a GS phenotype. (E) *E. coli* NU14 *ybtA*:Kn rec 2 with 10^3 amoebae. Amebae did not form lysis plaque, indicating a GR phenotype. The complementation abolishes the GS phenotype observed in (D).

CFT073 Δ*ybtA*:Kn revealed no statistically different survival curves compared to the wild strain ($p = 0.276$). In view of these results, the *fyuA* deletion mutant has not been tested in mice. However, the NU14 ΔHPI:Kn mutant showed a dramatic decrease in virulence (10% mortality versus 90% for the wild strain) ($p < 0.00001$) (Fig. 6). Likewise, the two *irp2* deletion mutants of strain NU14 constructed in two independent mutagenesis experiments (NU14 *irp2*:Cm and NU14 *irp2*:Kn) were devoid of virulence as they killed none of the mice. There was no statistically significant difference in the killing phenotype between the *irp2* mutants and the complete HPI mutant ($p = 0.157$). The NU14 *fyuA*:Cm mutant strain was less virulent than the wild type, killing 50% of the mice ($p < 0.001$). Similarly, two NU14 deletion mutants of *ybtA* constructed in two separate experiments (NU14 *ybtA*:Kn 1 and NU14 *ybtA*:Kn 2) were less virulent than the wild type strain showing only 60% mortality ($p = 0.015$) (Fig. 6).

We were not able to complement the *irp2*, *fyuA* and *ybtA* deletion mutants of the strain NU14, neither by cloning the respective deleted gene on a plasmid nor by a chromosomal insertion of the entire HPI introduced by the suicide vector pCP1 (Table 1). Indeed, we evidenced *in vivo* during the infection a loss of the plasmid or the chromosomal insert. Strains re-isolated from spleens of dead animals proved to have lost their antibiotic resistance markers as shown by plating on appropriate antibiotic containing media (data not shown).

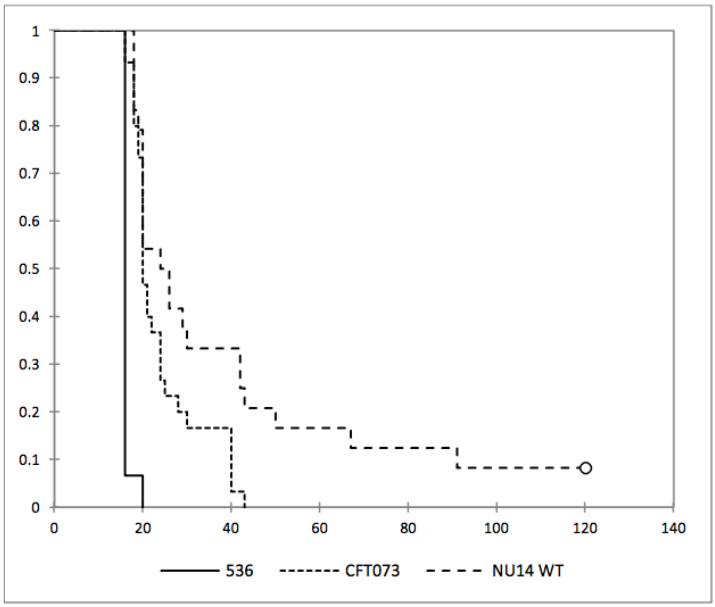

Fig. 5. Kaplan-Meir survival curves of mice injected with wild type *E. coli* strains 536 (continuous line), CFT073 (dotted line) and NU14 (dashed line) showing the three distinct patterns of virulence ($p < 0.001$).

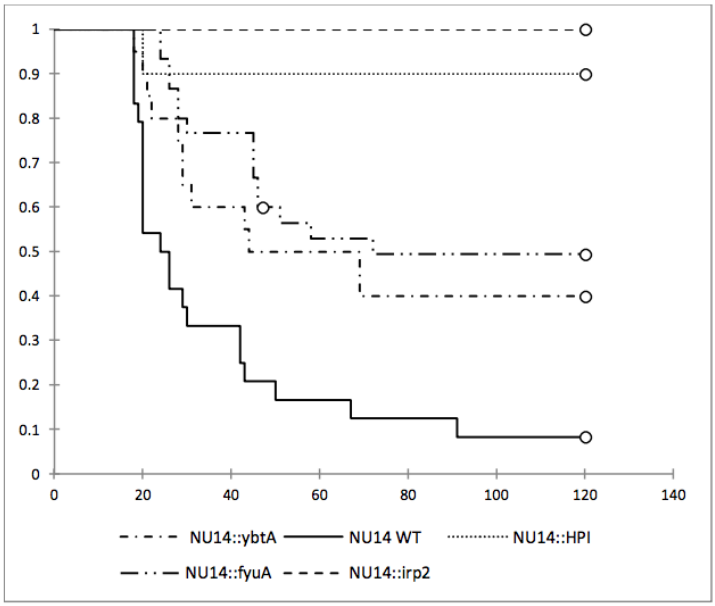

Fig. 6. Kaplan-Meir survival curves of mice injected with *E. coli* NU14 strains. Wild type (continuous line), complete deletion of the HPI (dotted line), *irp2* deletion (dashed line), *ybtA* deletion (dash-dotted line) and *fyuA* deletion (dash-dotted-dotted line).

4. Discussion

Discrepant results have been described in the literature with respect to the role of the HPI in *E. coli* as determined using various models and strains. To unravel the contribution of the HPI to *E. coli* virulence, we compared the basic regulatory patterns of the HPI expression and the experimental virulence of three B2 phylogroup UPEC strains in two validated models, *i.e.* an amoebae model (Adiba et al., 2010) and a mouse sepsis model (Johnson et al., 2006), using mutants of the entire HPI as well as of each of its three main functional classes of genes (*irp2*, *fyuA* and *ybtA*).

4.1. HPI function in different UPEC backgrounds

A growing body of evidence has been published on the contribution of the HPI to virulence in pathogenic bacteria. This has been mainly attributed to its function as ferric iron uptake system. Interestingly, recent reports provided insight into the multi-faceted spectrum of HPI function. According to its biochemical features yersiniabactin has to be considered an universal metallophore able to form stable complexes with various metal ions (Bobrov et al., 2014; Koh et al., 2015). Its affinity to bind ferric iron, copper and zinc were shown to be essential for pathogenicity in different infection models. Protection from copper toxicity and redox-based phagocytic processes underlines the outstanding role among other siderophores (Chaturvedi et al., 2012). Furthermore, the innate immune system counteracts siderophore-mediated iron uptake by the secretion of lipocalin 2, which sequesters the catecholate siderophore enterobactin. Evasion of lipocalin 2 through secretion of yersiniabactin is a further feature of the HPI promoting infectious diseases (Bachman et al., 2011). Further intriguing discoveries revealed that single elements of the HPI support additional virulence features. For example, FyuA is required for efficient biofilm formation (Hancock et al., 2008) and turned out to be a promising vaccine candidate in a murine model of urinary tract infection (Brumbaugh et al., 2013). Additional data indicated the complex interaction of the HPI with other biosynthetic and metabolic pathways (Lv and Henderson, 2011; Martin et al., 2013; Yan et al., 2015). Altogether, this highlights the multi-functionality of the HPI.

The beneficial effect of the HPI as an iron acquisition system is well documented in the literature. Especially the contribution of yersiniabactin under iron deplete conditions or in the presence of iron chelating compounds including lactoferrin, transferrin and lipocalin 2 has been extensively studied *in vitro* (Bachman et al., 2011; Hancock et al., 2008; Paauw et al., 2009). In the present work we confirm again the role of the HPI as fitness factor under iron scarcity for ExPEC (Fig. 3). When abundance of iron is available, there is no need for the synthesis of yersiniabactin. Growth curves performed in NB demonstrated neither a difference between wild type strains nor between wild type strains and their respective *irp2* mutants. Under selective iron deplete conditions, however, a functional HPI turned out to be of great importance. The yersiniabactin deficient *irp2* mutants were significantly impaired for growth in NBD medium respective to their wild type strains 536 and NU14. Successful complementation to wild type level proved that this phenotype could be attributed to the deletion of *irp2*. Determination of the generation time for the various growth conditions revealed apparent differences among the three prototypic UPEC strains. The natural HPI mutant CFT073 is deficient for yersiniabactin, but is able to synthesize the catecholates enterobactin and salmochelin and the hydroxamate aerobactin (Henderson et al., 2009). Both strain 536 and NU14 are equipped with functional siderophore systems for enterobactin, salmochelin and yersiniabactin. Growth curves in NBD clearly showed that CFT073 has the shortest generation time among the wild types tested, indicating that it is the best-adapted strain for this specific setting. ExPEC has evolved a plethora of various uptake systems for ferric and ferrous iron and iron-bound heme uptake as well (Subashchandrabose and Mobley, 2015). The set-up and coordination of various iron scavenging systems do not follow a common pattern. They are highly adapted in every single pathogen according to their specialized niches. This aspect is illustrated by the growth characteristics of the three prototypic UPEC strains cultivated in NBD, which differ significantly (Fig. 3B and C). Although a virulence factor like the HPI may be common in UPEC, its contribution to overall virulence needs to be evaluated and interpreted specifically and may not account to all UPEC in general.

In the present study we started to investigate whether regulatory patterns on the transcriptional level vary between different UPEC isolates in response to iron limitation. Transcription rates of selected marker genes *irp2*, *fyuA* and *ybtA* were increased in all prototypic UPEC strains during growth in NBD medium. The *irp2* gene was highly up-regulated indicating that biosynthesis of yersiniabactin is induced. Although *E. coli* CFT073 is not able to produce yersiniabactin, a transcriptional response to iron limitation was detectable. The consistent reaction on the transcriptional level speaks in favour of general regulatory events applying to the HPI independent from the UPEC specific background. With regard to regulation of the HPI for iron scavenging purpose, the three prototypic UPEC strains belonging to different phylogenetic sub-groups were comparable, even though the relative induction of the *irp2* gene appeared to be more prominent in *E. coli* NU14 strain compared to 536 and CFT073 strains. However, it is difficult to compare the induction directly between the respective *E. coli* strains due to the experimental setting of the gene expression assays (Fig. 1A).

With the finding that UPEC can persist in intracellular compartments of urothelial cells, several virulence and fitness factors are necessary to adapt to the hostile environment. Both, scarcity of nutrients and immunologic responses dedicated to eliminate the pathogen have to be faced by UPEC. The formation of intracellular bacterial communities in umbrella cells seems to be an essential step to overcome these challenges. Iron uptake systems have been shown to be highly up-regulated in IBCs (Berry et al., 2009; Reigstad et al., 2007). Exposing three UPEC isolates to the same experimental setting, we analysed the activation of the HPI after 24 h in IBCs *in vitro*. The same transcriptional profile was confirmed for the cell culture assay as observed for cultivation in NBD medium (Fig. 1B). Of note, the transcription rate was significantly higher in IBC suggesting a stronger activation of the HPI. Interestingly, the natural HPI mutant *E. coli* CFT073 reacted as did the *E. coli* isolates harbouring a functional HPI. In this study we did not evaluate changes on the translational level, so the final outcome of the transcriptional events is not clear. Comparison of *E. coli* CFT073 *with E. coli* strains NU14 and 536 suggests that the high induction of the HPI in IBCs may not be exclusively attributed to iron uptake. The activation of siderophore systems in NBD medium is significantly stronger at the transcriptional level than growth in the medium used for cell culture experiments (data not shown). Thus, the highly induced gene expression in IBCs may be explained by additional signals targeting the HPI, not only for iron uptake. *In vivo* studies are warranted to confirm this strong activation of the HPI in IBCs. Published data on the contribution of the HPI in the natural mutant CFT073 revealed a relevant role for colonizing the kidneys in a murine model of urinary tract infection (Lloyd et al., 2009). This phenotype points towards additional functions of the HPI supporting pathogenicity and overall fitness of the pathogen.

The impact of specific gene mutations on yersiniabactin production was analysed using a luciferase reporter assay for quantification. As expected, gene disruption of biosynthetic genes like *irp2* resulted in undetectable levels of yersiniabactin. This is consistent with published data for *E. coli* and other HPI-positive species (Henderson et al., 2009; Perry et al., 1999). YbtA, the HPI-specific transcriptional regulator belonging to the family of AraC-like regulators, was shown to be a negative regulator of its own expression and a transcriptional activator of *irp2*, *fyuA* and *ybtP* promoters (Perry and Fetherston, 2011). In concert with yersiniabactin, YbtA is supposed to be required for full activation of the HPI. Published data provided evidence for a significant down-regulation of YbtA-regulated genes in a *ybtA* deletion mutant (Fetherston et al., 1996, 1999; Perry et al., 2003). In this work, results clearly demonstrated that yersiniabactin production is strongly dependant on the action of YbtA. No detectable siderophore production was observed in NU14 and 536 mutants. The exact role of YbtA has not been defined

for *E. coli*. This pronounced effect on the HPI suggests a particular function in *E. coli*, which warrants further experiments to elucidate this effect. Data on the impact of FyuA on HPI function are heterogeneous. On the one hand reports revealed a positive effect on transcription in *Yersinia pestis* (Perry et al., 2003), on the other hand mutations of *fyuA* lead to a reduced expression of biosynthetic proteins HMWP 1 and 2 in *Yersinia enterocolitica* (Pelludat et al., 1998). The data obtained in this study provide evidence for a slight impairment in siderophore production in UPEC, which reached statistical significance ($p < 0.05$). Since this mutant is not able to take up yersiniabactin, a relevant feedback is missing, which restricts the expensive biosynthesis of the siderophore. Among the tested UPEC isolates, the observed phenotypes of different HPI mutants were consistent for NU14 and 536 and could be restored upon complementation (only shown for *irp2* and *ybtA*) (Fig. 2). Differences in HPI function in an UPEC specific background must be taken into consideration. Further studies are warranted to identify UPEC-specific regulatory features of the HPI.

4.2. The two experimental virulence models gave similar results

As previously described (Adiba et al., 2010), we observed a clear correlation between the virulence in amoebae and mice. No effect of the HPI was evidenced for *E. coli* strains 536 and CFT073. In contrast we observed a significant impact of the HPI and the respective HPI encoded genes on virulence of *E. coli* strain NU14. This effect could be demonstrated in both experimental models. The amoebae model appeared inexpensive, easy to perform and devoid of ethical problems, allowing to test a large number of mutants. Moreover, it allows performing easily complementation of the mutants by maintaining a selection pressure with addition of antibiotics to the culture medium.

However, the amoeba model encompasses several limitations. First, it explores only one step of the virulence process, the phagocytosis by professional phagocytes such as macrophages and granulocytes. Second, the temperature of the experiment is at 24 °C, whereas the optimal temperature of growth and virulence gene expression in *E. coli* is 37 °C (Konkel and Tilly, 2000; Maurelli et al., 1984), the central temperature of the mouse.

4.3. The effect of the HPI is strain-specific

The data of both virulence models provided evidence that different effects of the HPI on virulence do exist. Both strain CFT073 of subgroup II (STc73) and strain 536 of subgroup III (STc127) were not affected in their virulence properties by the deletion of the entire HPI or one of the HPI genes. Strain CFT073, which is a natural mutant of *irp2* cannot produce yersiniabactin but possesses a full HPI. Its deletion had no effect in the two experimental models. The *E. coli* strain 536, which produces siderophores enterobactin, salmochelin and yersiniabactin, is not affected by the deletion of HPI in its virulence. This observation is further corroborated by previous studies reporting no relevant attenuation of a complete deletion of the HPI in strain 536 in a murine model of septicaemia (Tourret et al., 2010). However, this phenotype is in contrast to reports providing evidence that the HPI is a relevant virulence and fitness factor in UPEC strain 536 in a murine model of cystitis, pyelonephritis and bacteremia (Brumbaugh et al., 2015). One explanation for this discrepancy may be that both animal models assess different aspects relevant to the pathogenesis of infection. In contrast, the NU14 strain of subgroup IX (STc95), which produces the same panel of siderophores as strain 536, exhibited a significant decrease of virulence by deletion of the full HPI or one of its genes. The main characteristic of NU14 compared to *E. coli* 536 is having a lower level of intrinsic virulence in mice (Fig. 5). In strain 536, even extensive deletion of seven PAIs, including the HPI, was not able to decrease the intrinsic virulence in mice at the tested inoculum (Tourret et al., 2010). Thus, the less virulent strain NU14 unmasks more easily the impact of the loss of a single virulence factor. This is probably due to the huge genomic diversity in the *E. coli* gene content that allows multiple combinations of genes with genetic interactions conditioning the virulence phenotype (Touchon et al., 2009). Altogether, these results suggest the influence of the genetic background within *E. coli* species on the virulence mediated by the HPI.

4.4. The genes of different functions within the HPI differentially affect the virulence phenotype

The pattern of virulence of the NU14 wild type and its HPI mutant allowed us to explore further the role of the three main functional classes of genes present on the HPI, *i.e.* biosynthesis, internalisation and regulation. The mutant carrying a deleted *irp2* synthesis gene, thus not producing yersiniabactin was avirulent, as was the mutant of the full HPI. In contrast, mutants carrying a deleted *fyuA* receptor or *ybtA* regulator genes, were both only slightly attenuated (Fig. 6 and Table 4). The mutant of the receptor gene synthesizes yersiniabactin but cannot internalize the siderophore complexed with iron, although one cannot exclude the hypothesis of an entry by an alternative pathway unknown for now. The mutant of the regulator gene has a drastic effect on the yersiniabactin production in UPEC. Without YbtA, no yersiniabactin was detectable, but in terms of virulence it was only slightly impaired. If iron acquisition is considered to be the main contribution to pathogenicity, then the *irp2, ybtA* and the complete HPI deletion were supposed to be avirulent, since no yersiniabactin is produced. But this was not the case. The HPI may be part of a complex network, which promotes additional functions optimizing the virulence potential and overall fitness of UPEC.

It is surprising that different UPEC backgrounds influence the HPI function. Comparative genomic analysis revealed only minor differences between UPEC strains. The genome of 536 is only 292 kb smaller than CFT073 and genomic variations were limited to features of pathogenicity islands (Brzuszkiewicz et al., 2006). The fact, that the prototypic UPEC strains in this work are specialized to different sites of the urinary tract and belong to different phylogenetic sub-groups, gives rise to the concept, that the genetic background of a strain may influence considerably the function of single pathogenicity factors.

5. Concluding remarks

For the first time, we provide evidence that basic regulatory patterns of the HPI are common to various UPEC strains when selective iron limitation was analysed. But when overall experimental virulence was investigated, mutations of the HPI lead to drastic differences between UPEC strains. It remains unclear whether this is caused by genomic variations or interactions of single elements of the HPI with unknown factors. Nevertheless, it indicates that the intrinsic extra-intestinal virulence in the *E. coli* species is multigenic, with epistatic interactions. Furthermore, we show that the contribution of the HPI to virulence cannot be exclusively attributed to iron uptake.

Acknowledgment

This work was partly supported by a grant from the "Centre de cooperation Universitaire Franco-Bavarois/Bayerisch-Französisches Hochschulzentrum" Az. FK-26/10.

Appendix A. Supplementary data

Supplementary data associated with this article can be found, in the online version, at http://dx.doi.org/10.1016/j.ijmm.2016.11.004.

References

Adiba, S., Nizak, C., van Baalen, M., Denamur, E., Depaulis, F., 2010. From grazing resistance to pathogenesis: the coincidental evolution of virulence factors. PLoS One 5, e11882.

Bach, S., de Almeida, A., Carniel, E., 2000. The Yersinia high-pathogenicity island is present in different members of the family Enterobacteriaceae. FEMS Microbiol. Lett. 183, 289–294.

Bachman, M.A., Oyler, J.E., Burns, S.H., Caza, M., Lepine, F., Dozois, C.M., Weiser, J.N., 2011. Klebsiella pneumoniae yersiniabactin promotes respiratory tract infection through evasion of lipocalin 2. Infect. Immun. 79, 3309–3316.

Berger, H., Hacker, J., Juarez, A., Hughes, C., Goebel, W., 1982. Cloning of the chromosomal determinants encoding hemolysin production and mannose-resistant hemagglutination in Escherichia coli. J. Bacteriol. 152, 1241–1247.

Berry, R.E., Klumpp, D.J., Schaeffer, A.J., 2009. Urothelial cultures support intracellular bacterial community formation by uropathogenic Escherichia coli. Infect. Immun. 77, 2762–2772.

Bielaszewska, M., Zhang, W., Mellmann, A., Karch, H., 2007. Enterohaemorrhagic Escherichia coli O26:H11/H-: a human pathogen in emergence. Berl. Munch. Tierarztl. Wochenschr. 120, 279–287.

Blattner, F.R., Plunkett 3rd, G., Bloch, C.A., Perna, N.T., Burland, V., Riley, M., Collado-Vides, J., Glasner, J.D., Rode, C.K., Mayhew, G.F., et al., 1997. The complete genome sequence of Escherichia coli K-12. Science 277, 1453–1462.

Bobrov, A.G., Kirillina, O., Fetherston, J.D., Miller, M.C., Burlison, J.A., Perry, R.D., 2014. The Yersinia pestis siderophore, yersiniabactin, and the ZnuABC system both contribute to zinc acquisition and the development of lethal septicaemic plague in mice. Mol. Microbiol. 93, 759–775.

Brumbaugh, A.R., Smith, S.N., Mobley, H.L., 2013. Immunization with the yersiniabactin receptor, FyuA, protects against pyelonephritis in a murine model of urinary tract infection. Infect. Immun. 81, 3309–3316.

Brumbaugh, A.R., Smith, S.N., Subashchandrabose, S., Himpsl, S.D., Hazen, T.H., Rasko, D.A., Mobley, H.L., 2015. Blocking yersiniabactin import attenuates extraintestinal pathogenic Escherichia coli in cystitis and pyelonephritis and represents a novel target to prevent urinary tract infection. Infect. Immun. 83, 1443–1450.

Brzuszkiewicz, E., Bruggemann, H., Liesegang, H., Emmerth, M., Olschlager, T., Nagy, G., Albermann, K., Wagner, C., Buchrieser, C., Emody, L., 2006. How to become a uropathogen: comparative genomic analysis of extraintestinal pathogenic Escherichia coli strains. Proc. Natl. Acad. Sci. U. S. A. 103, 12879–12884.

Buchrieser, C., Brosch, R., Bach, S., Guiyoule, A., Carniel, E., 1998. The high-pathogenicity island of Yersinia pseudotuberculosis can be inserted into any of the three chromosomal asn tRNA genes. Mol. Microbiol. 30, 965–978.

Carniel, E., Guilvout, I., Prentice, M., 1996. Characterization of a large chromosomal high-pathogenicity island in biotype 1 B Yersinia enterocolitica. J. Bacteriol. 178, 6743–6751.

Chaturvedi, K.S., Hung, C.S., Crowley, J.R., Stapleton, A.E., Henderson, J.P., 2012. The siderophore yersiniabactin binds copper to protect pathogens during infection. Nat. Chem. Biol. 8, 731–736.

Chomczynski, P., Sacchi, N., 1987. Single-step method of RNA isolation by acid guanidinium thiocyanate-phenol-chloroform extraction. Anal. Biochem. 162, 156–159.

Clermont, O., Christenson, J.K., Denamur, E., Gordon, D.M., 2013. The Clermont *Escherichia coli* phylo-typing method revisited: improvement of specificity and detection of new phylo-groups. Environ. Microbiol. Rep. 8, 58–65.

Clermont, O., Christenson, J.K., Daubie, A.S., Gordon, D.M., Denamur, E., 2014. Development of an allele-specific PCR for Escherichia coli B2 sub-typing, a rapid and easy to perform substitute of multilocus sequence typing. J. Microbiol. Methods 101, 24–27.

Clermont, O., Gordon, D., Denamur, E., 2015. Guide to the various phylogenetic classification schemes for Escherichia coli and the correspondence among schemes. Microbiology 161, 980–988.

Datsenko, K.A., Wanner, B.L., 2000. One-step inactivation of chromosomal genes in Escherichia coli K-12 using PCR products. Proc. Natl. Acad. Sci. U. S. A. 97, 6640–6645.

Desjardins, P., Picard, B., Kaltenbock, B., Elion, J., Denamur, E., 1995. Sex in Escherichia coli does not disrupt the clonal structure of the population: evidence from random amplified polymorphic DNA and restriction-fragment-length polymorphism. J. Mol. Evol. 41, 440–448.

Diard, M., Baeriswyl, S., Clermont, O., Gouriou, S., Picard, B., Taddei, F., Denamur, E., Matic, I., 2007. Caenorhabditis elegans as a simple model to study phenotypic and genetic virulence determinants of extraintestinal pathogenic Escherichia coli. Microbes Infect. 9, 214–223.

Diard, M., Garry, L., Selva, M., Mosser, T., Denamur, E., Matic, I., 2010. Pathogenicity-associated islands in extraintestinal pathogenic Escherichia coli are fitness elements involved in intestinal colonization. J. Bacteriol. 192, 4885–4893.

Dobrindt, U., Blum-Oehler, G., Nagy, G., Schneider, G., Johann, A., Gottschalk, G., Hacker, J., 2002. Genetic structure and distribution of four pathogenicity islands (PAI I(536) to PAI IV(536)) of uropathogenic Escherichia coli strain 536. Infect. Immun. 70, 6365–6372.

Fetherston, J.D., Bearden, S.W., Perry, R.D., 1996. YbtA, an AraC-type regulator of the Yersinia pestis pesticin/yersiniabactin receptor. Mol. Microbiol. 22, 315–325.

Fetherston, J.D., Bertolino, V.J., Perry, R.D., 1999. YbtP and YbtQ: two ABC transporters required for iron uptake in Yersinia pestis. Mol. Microbiol. 32, 289–299.

Garcia, E.C., Brumbaugh, A.R., Mobley, H.L., 2011. Redundancy and specificity of Escherichia coli iron acquisition systems during urinary tract infection. Infect. Immun. 79, 1225–1235.

Garenaux, A., Caza, M., Dozois, C.M., 2011. The ins and outs of siderophore mediated iron uptake by extra-intestinal pathogenic Escherichia coli. Vet. Microbiol. 153, 89–98.

Hacker, J., Hughes, C., Hof, H., Goebel, W., 1983. Cloned hemolysin genes from Escherichia coli that cause urinary tract infection determine different levels of toxicity in mice. Infect. Immun. 42, 57–63.

Hanahan, D., 1983. Studies on transformation of Escherichia coli with plasmids. J. Mol. Biol. 166, 557–580.

Hancock, V., Ferrieres, L., Klemm, P., 2008. The ferric yersiniabactin uptake receptor FyuA is required for efficient biofilm formation by urinary tract infectious Escherichia coli in human urine. Microbiology 154, 167–175.

Henderson, J.P., Crowley, J.R., Pinkner, J.S., Walker, J.N., Tsukayama, P., Stamm, W.E., Hooton, T.M., Hultgren, S.J., 2009. Quantitative metabolomics reveals an epigenetic blueprint for iron acquisition in uropathogenic Escherichia coli. PLoS Pathog. 5, e1000305.

Hultgren, S.J., Schwan, W.R., Schaeffer, A.J., Duncan, J.L., 1986. Regulation of production of type 1 pili among urinary tract isolates of Escherichia coli. Infect. Immun. 54, 613–620.

Jeong, H., Barbe, V., Lee, C.H., Vallenet, D., Yu, D.S., Choi, S.H., Couloux, A., Lee, S.W., Yoon, S.H., Cattolico, L., et al., 2009. Genome sequences of escherichia coli B strains REL606 and BL21(DE3). J. Mol. Biol. 394, 644–652.

Johnson, J.R., Weissman, S.J., Stell, A.L., Trintchina, E., Dykhuizen, D.E., Sokurenko, E.V., 2001. Clonal and pathotypic analysis of archetypal Escherichia coli cystitis isolate NU14. J. Infect. Dis. 184, 1556–1565.

Johnson, J.R., Clermont, O., Menard, M., Kuskowski, M.A., Picard, B., Denamur, E., 2006. Experimental mouse lethality of Escherichia coli isolates, in relation to accessory traits, phylogenetic group, and ecological source. J. Infect. Dis. 194, 1141–1150.

Kakoschke, T., Kakoschke, S., Magistro, G., Schubert, S., Borath, M., Heesemann, J., Rossier, O., 2014. The RNA chaperone Hfq impacts growth, metabolism and production of virulence factors in Yersinia enterocolitica. PLoS One 9, e86113.

Karch, H., Schubert, S., Zhang, D., Zhang, W., Schmidt, H., Olschlager, T., Hacker, J., 1999. A genomic island, termed high-pathogenicity island, is present in certain non-O157 Shiga toxin-producing Escherichia coli clonal lineages. Infect. Immun. 67, 5994–6001.

Koh, E.I., Hung, C.S., Parker, K.S., Crowley, J.R., Giblin, D.E., Henderson, J.P., 2015. Metal selectivity by the virulence-associated yersiniabactin metallophore system. Metallomics 7, 1011–1022.

Konkel, M.E., Tilly, K., 2000. Temperature-regulated expression of bacterial virulence genes. Microbes Infect. 2, 157–166.

Le Gall, T., Clermont, O., Gouriou, S., Picard, B., Nassif, X., Denamur, E., Tenaillon, O., 2007. Extraintestinal virulence is a coincidental by-product of commensalism in B2 phylogenetic group Escherichia coli strains. Mol. Biol. Evol. 24, 2373–2384.

Lesic, B., Carniel, E., 2005. Horizontal transfer of the high-pathogenicity island of Yersinia pseudotuberculosis. J. Bacteriol. 187, 3352–3358.

Livak, K.J., Schmittgen, T.D., 2001. Analysis of relative gene expression data using real-time quantitative PCR and the 2(-delta C(T)) method. Methods 25, 402–408.

Lloyd, A.L., Henderson, T.A., Vigil, P.D., Mobley, H.L., 2009. Genomic islands of uropathogenic Escherichia coli contribute to virulence. J. Bacteriol. 191, 3469–3481.

Lv, H., Henderson, J.P., 2011. Yersinia high pathogenicity island genes modify the Escherichia coli primary metabolome independently of siderophore production. J. Proteome Res. 10, 5547–5554.

Magistro, G., Hoffmann, C., Schubert, S., 2015. The salmochelin receptor IroN itself, but not salmochelin-mediated iron uptake promotes biofilm formation in extraintestinal pathogenic Escherichia coli (ExPEC). Int. J. Med. Microbiol. 305, 435–445.

Martin, P., Marcq, I., Magistro, G., Penary, M., Garcie, C., Payros, D., Boury, M., Olier, M., Nougayrede, J.P., Audebert, M., et al., 2013. Interplay between siderophores and colibactin genotoxin biosynthetic pathways in Escherichia coli. PLoS Pathog. 9, e1003437.

Masters, J.R., Hepburn, P.J., Walker, L., Highman, W.J., Trejdosiewicz, L.K., Povey, S., Parkar, M., Hill, B.T., Riddle, P.R., Franks, L.M., 1986. Tissue culture model of transitional cell carcinoma: characterization of twenty-two human urothelial cell lines. Cancer Res. 46, 3630–3636.

Maurelli, A.T., Blackmon, B., Curtiss 3rd, R., 1984. Temperature-dependent expression of virulence genes in Shigella species. Infect. Immun. 43, 195–201.

Mobley, H.L., Green, D.M., Trifillis, A.L., Johnson, D.E., Chippendale, G.R., Lockatell, C.V., Jones, B.D., Warren, J.W., 1990. Pyelonephritogenic Escherichia coli and killing of cultured human renal proximal tubular epithelial cells: role of hemolysin in some strains. Infect. Immun. 58, 1281–1289.

Mulvey, M.A., Schilling, J.D., Hultgren, S.J., 2001. Establishment of a persistent Escherichia coli reservoir during the acute phase of a bladder infection. Infect. Immun. 69, 4572–4579.
Negre, V.L., Bonacorsi, S., Schubert, S., Bidet, P., Nassif, X., Bingen, E., 2004. The siderophore receptor IroN, but not the high-pathogenicity island or the hemin receptor ChuA, contributes to the bacteremic step of Escherichia coli neonatal meningitis. Infect. Immun. 72, 1216–1220.
Paauw, A., Leverstein-van Hall, M.A., van Kessel, K.P., Verhoef, J., Fluit, A.C., 2009. Yersiniabactin reduces the respiratory oxidative stress response of innate immune cells. PLoS One 4, e8240.
Pelludat, C., Rakin, A., Jacobi, C.A., Schubert, S., Heesemann, J., 1998. The yersiniabactin biosynthetic gene cluster of Yersinia enterocolitica: organization and siderophore-dependent regulation. J. Bacteriol. 180, 538–546.
Pelludat, C., Hogardt, M., Heesemann, J., 2002. Transfer of the core region genes of the *Yersinia enterocolitica* WA-C serotype O:8 high-pathogenicity island to *Y. enterocolitica* MRS40, a strain with low levels of pathogenicity, confers a yersiniabactin biosynthesis phenotype and enhanced mouse virulence. Infect Immun. 70 (4), 1832–1841.
Perry, R.D., Fetherston, J.D., 2011. Yersiniabactin iron uptake: mechanisms and role in Yersinia pestis pathogenesis. Microbes Infect. 13, 808–817.
Perry, R.D., Balbo, P.B., Jones, H.A., Fetherston, J.D., DeMoll, E., 1999. Yersiniabactin from Yersinia pestis: biochemical characterization of the siderophore and its role in iron transport and regulation. Microbiology 145, 1181–1190 (Pt 5).
Perry, R.D., Abney, J., Mier Jr., I., Lee, Y., Bearden, S.W., Fetherston, J.D., 2003. Regulation of the Yersinia pestis Yfe and Ybt iron transport systems. Adv. Exp. Med. Biol. 529, 275–283.
Picard, B., Garcia, J.S., Gouriou, S., Duriez, P., Brahimi, N., Bingen, E., Elion, J., Denamur, E., 1999. The link between phylogeny and virulence in Escherichia coli extraintestinal infection. Infect. Immun. 67, 546–553.
Reigstad, C.S., Hultgren, S.J., Gordon, J.I., 2007. Functional genomic studies of uropathogenic Escherichia coli and host urothelial cells when intracellular bacterial communities are assembled. J. Biol. Chem. 282, 21259–21267.
Russo, T.A., Johnson, J.R., 2000. Proposal for a new inclusive designation for extraintestinal pathogenic isolates of Escherichia coli: ExPEC. J. Infect. Dis. 181, 1753–1754.
Sambrook, J.R., Russell, D.W. (Eds.), 2001. Molecular Cloning: A Laboratoty Manual. , 3rd edition. Cold Spring Harbor Laboratory Press.
Schubert, S., Rakin, A., Karch, H., Carniel, E., Heesemann, J., 1998. Prevalence of the high-pathogenicity island of Yersinia species among Escherichia coli strains that are pathogenic to humans. Infect. Immun. 66, 480–485.
Schubert, S., Picard, B., Gouriou, S., Heesemann, J., Denamur, E., 2002. Yersinia high-pathogenicity island contributes to virulence in Escherichia coli causing extraintestinal infections. Infect. Immun. 70, 5335–5337.
Schubert, S., Darlu, P., Clermont, O., Wieser, A., Magistro, G., Hoffmann, C., Weinert, K., Tenaillon, O., Matic, I., Denamur, E., 2009. Role of intraspecies recombination in the spread of pathogenicity islands within the Escherichia coli species. PLoS Pathog. 5, e1000257.
Steinert, M., Heuner, K., 2005. Dictyostelium as host model for pathogenesis. Cell Microbiol. 7, 307–314.
Subashchandrabose, S., Mobley, H.L., 2015. Virulence and fitness determinants of uropathogenic Escherichia coli. Microbiol. Spectr 3.
Touchon, M., Hoede, C., Tenaillon, O., Barbe, V., Baeriswyl, S., Bidet, P., Bingen, E., Bonacorsi, S., Bouchier, C., Bouvet, O., et al., 2009. Organised genome dynamics in the Escherichia coli species results in highly diverse adaptive paths. PLoS Genet. 5, e1000344.
Tourret, J., Diard, M., Garry, L., Matic, I., Denamur, E., 2010. Effects of single and multiple pathogenicity island deletions on uropathogenic Escherichia coli strain 536 intrinsic extra-intestinal virulence. Int. J. Med. Microbiol. 300, 435–439.
Welch, R.A., Burland, V., Plunkett 3rd, G., Redford, P., Roesch, P., Rasko, D., Buckles, E.L., Liou, S.R., Boutin, A., Hackett, J., 2002. Extensive mosaic structure revealed by the complete genome sequence of uropathogenic Escherichia coli. Proc. Natl. Acad. Sci. U. S. A. 99, 17020–17024.
Yan, L., Nie, W., Lv, H., 2015. Metabolic phenotyping of the Yersinia high-pathogenicity island that regulates central carbon metabolism. Analyst 140, 3356–3361.

EUROPEAN UROLOGY 69 (2016) 286–297

available at www.sciencedirect.com
journal homepage: www.europeanurology.com

European Association of Urology

Platinum Priority – Collaborative Review – Pelvic Pain

Editorial by Thomas M. Kessler on pp. 298–299 of this issue

Contemporary Management of Chronic Prostatitis/Chronic Pelvic Pain Syndrome

Giuseppe Magistro[a,*], *Florian M.E. Wagenlehner*[b], *Magnus Grabe*[c], *Wolfgang Weidner*[b], *Christian G. Stief*[a], *J. Curtis Nickel*[d]

[a] *Department of Urology, Campus Großhadern, Ludwig-Maximilians-Universität München, Munich, Germany;* [b] *Clinic for Urology, Pediatric Urology and Andrology, Justus-Liebig-University Giessen, Giessen, Germany;* [c] *Department of Urology, Skåne University Hospital, Malmö, Sweden;* [d] *Department of Urology, Queen's University, Kingston, Ontario, Canada*

Article info

Article history:
Accepted August 31, 2015

Associate Editor:
James Catto

Keywords:
Chronic prostatitis
Chronic pelvic pain syndrome
Monotherapies
Phenotypically directed multimodal management

EU ACME
www.eu-acme.org/europeanurology

Please visit www.eu-acme.org/europeanurology to read and answer questions on-line. The EU-ACME credits will then be attributed automatically.

Abstract

Context: Chronic prostatitis/chronic pelvic pain syndrome (CP/CPPS) is a common condition that causes severe symptoms, bother, and quality-of-life impact in the 8.2% of men who are believed to be affected. Research suggests a complex pathophysiology underlying this syndrome that is mirrored by its heterogeneous clinical presentation. Management of patients diagnosed with CP/CPPS has always been a formidable task in clinical practice. Due to its enigmatic etiology, a plethora of clinical trials failed to identify an efficient monotherapy.
Objective: A comprehensive review of published randomized controlled trials (RCTs) on the treatment of CP/CPPS and practical best evidence recommendations for management.
Evidence acquisition: Medline and the Cochrane database were screened for RCTs on the treatment of CP/CPPS from 1998 to December 2014, using the National Institutes of Health Chronic Prostatitis Symptom Index as an objective outcome measure. Published data in concert with expert opinion were used to formulate a practical best evidence statement for the management of CP/CPPS.
Evidence synthesis: Twenty-eight RCTs identified were eligible for this review and presented. Trials evaluating antibiotics, α-blockers, anti-inflammatory and immune-modulating substances, hormonal agents, phytotherapeutics, neuromodulatory drugs, agents that modify bladder function, and physical treatment options failed to reveal a clear therapeutic benefit. With its multifactorial pathophysiology and its various clinical presentations, the management of CP/CPPS demands a phenotypic-directed approach addressing the individual clinical profile of each patient. Different categorization algorithms have been proposed. First studies applying the UPOINTs classification system provided promising results. Introducing three index patients with CP/CPPS, we present practical best evidence recommendations for management.
Conclusions: Our current understanding of the pathophysiology underlying CP/CPPS resulting in this highly variable syndrome does not speak in favor of a monotherapy for management. No efficient monotherapeutic option is available. The best evidence-based management of CP/CPPS strongly suggests a multimodal therapeutic approach addressing the individual clinical phenotypic profile.
Patient summary: Chronic prostatitis/chronic pelvic pain syndrome presents a variable syndrome. Successful management of this condition is challenging. It appears that a tailored treatment strategy addressing individual patient characteristics is more effective than one single therapy.

* Corresponding author. Department of Urology, Campus Großhadern, Ludwig-Maximilians-Universität München, Marchioninistraße 17, München, 81377 Germany.
E-mail address: giuseppe.magistro@med.uni-muenchen.de (G. Magistro).

http://dx.doi.org/10.1016/j.eururo.2015.08.061
0302-2838/

CrossMark

1. Introduction

Lower urinary tract symptoms (LUTS) and pelvic pain due to pathologies of the prostate have always considerably affected quality of life of men of all ages. Epidemiologic data suggest that the prevalence of prostatitis-like symptoms is comparable with ischemic heart disease and diabetes mellitus. The rate of prostatitis-like symptoms ranges from 2.2% to 9.7%, with a mean prevalence of 8.2% [1].

In the late 1990s, the National Institutes of Health (NIH) established a consensus definition and classification system for prostatitis [2]. It has been accepted internationally in both clinical practice and research (Table 1). Prostatitis syndromes comprise infectious forms (acute and chronic), the chronic pelvic pain syndrome (CPPS), and asymptomatic prostatitis [2]. In <10% of patients with prostatitis syndrome, a causative uropathogenic organism can be detected. An acute bacterial episode will lead to chronic bacterial prostatitis in 10% and to CPPS in a further 10% [3]. CPPS accounts for most of the prostatitis-like symptoms in >90% of men.

The National Institutes of Health Chronic Prostatitis Symptom Index (NIH-CPSI) presents an objective assessment tool and outcome measure for prostatitis-like symptoms [4,5]. The introduction of a generally accepted classification system and an objective outcome measure led to a plethora of clinical trials that made one particular point clear. Although the treatment of bacterial prostatitis obviously relies on the adequate use of antimicrobial agents, successful management of CPPS has always been a formidable task. The complex and heterogeneous pathophysiology of CPPS is poorly understood. Consequently, an effective monotherapy is not available, which makes the management of CPPS challenging for both physicians and patients. Clinical trials were not able to identify a monotherapy with significant clinical efficacy. A meta-analysis evaluating data of randomized controlled trials (RCTs) using the NIH-CPSI as a common outcome measure failed to derive a guideline statement on the treatment of this bothersome condition [6,7].

The dilemma of limited success of clinical trials prompted us to provide a comprehensive review with expert interpretations of the available literature to formulate best practice recommendations. Introducing index patients diagnosed with CPPS, we demonstrate how these recommendations might be applied in clinical practice. The main objective of this review is to present best practice recommendations for the management of CPPS (NIH type III).

Table 1 – National Institutes of Health classification system for prostatitis syndromes

Category	Nomenclature
I	Acute bacterial prostatitis
II	Chronic bacterial prostatitis
III	Chronic prostatitis/chronic pelvic pain syndrome
IIIA	Inflammatory
IIIB	Noninflammatory
IV	Asymptomatic prostatitis

2. Evidence acquisition

2.1. Search strategy

We performed a systematic review of the literature in the PubMed and Cochrane database according to the Preferred Reporting Items for Systematic Reviews and Meta-analysis statement [8]. We searched for RCTs and meta-analyses on the treatment of chronic prostatitis CP/CPPS from January 1988 to December 2014. A detailed description of the search strategy is presented in Supplementary Table 1 and Supplementary Figure 1. In addition, references of review articles were screened for possibly missed articles.

2.2. Inclusion criteria

RCTs published in English were selected if they met the following criteria: (1) RCTs (comparisons; placebo or sham controlled; no invasive procedures), (2) patients were classified as CP category IIIA or IIIB according to the NIH consensus definition, (3) at least 10 individuals were evaluated per treatment arm, and (4) the NIH-CPSI score was utilized as an outcome measure for CP/CPPS. Articles were first reviewed independently by two authors to determine their eligibility for inclusion. With consensus the article moved on to the next round, and if the first two reviewers disagreed, a third reviewer was included to reach unanimous agreement (Fig. 1).

2.3. Interpretation of data

The systematic literature review revealed 28 RCTs for the therapy of CPPS eligible for inclusion. Two performed meta-analyses published in the last 4 yr on this subject [6,7] were not able to provide any relevant useful information for clinical practice. We realized that no significant clinical data from recently published RCTs could be included since the last meta-analyses were performed (Supplementary Table 1, Supplementary Fig. 1). Another attempt to evaluate the available clinical data would add nothing to the literature and not provide any more guidance to practicing urologists. Consequently, we present the available literature on treatment modalities to outline the scientific dilemma and formulate best practice statements that used published data in concert with expert opinion. This does not use formal meta-analysis. We attempted to outline the complete management of CPPS including diagnostic assessment and treatment.

The introduction of index patients demonstrates how to implement the presented recommendations in clinical practice. After the conception of each index patient, the relevant symptoms were identified and treatment options were discussed. For this purpose, every author received the different case presentations and independently analyzed symptoms, treatment targets, and therapeutic options. The results were returned to G.M., who collected responses and

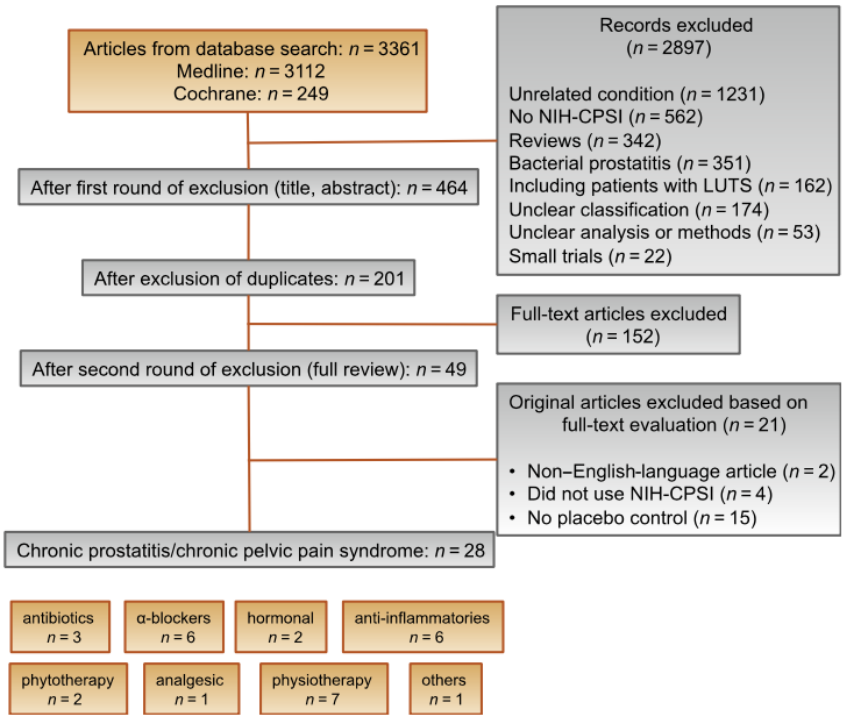

Fig. 1 – Flowchart of study selection.
LUTS = lower urinary tract symptoms; NIH-CPSI = National Institutes of Health Chronic Prostatitis Symptom Index.

pointed out discrepancies. After discussions we agreed on the points presented in tables.

3. Evidence synthesis

3.1. *Chronic prostatitis/chronic pelvic pain syndrome*

CP/CPPS (NIH category III) is defined as urologic pain or discomfort in the pelvic region, associated with urinary symptoms and/or sexual dysfunction, lasting for at least 3 of the previous 6 mo. Differential diagnoses of pelvic pain such as urinary tract infection, cancer, anatomic abnormalities, or neurologic disorders need to be excluded. CP/CPPS is subclassified as an inflammatory type (NIH category IIIA) and a noninflammatory type (NIH category IIIB) according to the presence of leukocytes in prostatic samples [2].

3.1.1. *Clinical presentation*

Patients with prostatitis-like symptoms report perineal, testicular, and penile discomfort. Pain may also be accompanied by LUTS and sexual dysfunction. Symptoms persist for at least 3 mo. CP/CPPS is often associated with negative cognitive, behavioral, sexual, or emotional consequences that should be addressed as part of the medical history. The correct classification demands a systematic diagnostic assessment.

3.1.2. *Diagnosis*

The first step is to assess the severity and impact of symptoms by utilizing the NIH-CPSI (level of evidence 2b; grade of recommendation B) [9]. The NIH-CPSI presents an objective assessment tool and outcome measure for prostatitis-like symptoms [4,5]. The symptom-scoring questionnaire is a reliable tool for basic evaluation and therapeutic monitoring. This self-administered questionnaire asks nine questions that are scored in three domains: pain, urinary symptoms, and the impact on quality of life. Severity categories have been proposed, and a 6-point decline from the baseline total score is considered the threshold for a positive therapeutic response. In addition, the International Prostate Symptom Score [10] and the International Index of Erectile Function [11] present optional valuable outcome measures to evaluate the current condition and course of disease in response to treatment.

Physical examination of the abdomen, genitalia, perineum, and prostate is mandatory. Additional evaluation of myofascial trigger points and/or musculoskeletal dysfunction of the pelvis and pelvic floor may be helpful.

Microbiologic localization cultures are the standard laboratory method for identifying chronic bacterial prostatitis (NIH type II). The four-glass test according to Meares and Stamey is recommended [12]. First voided urine, midstream urine, expressed prostatic secretion, and post–prostate

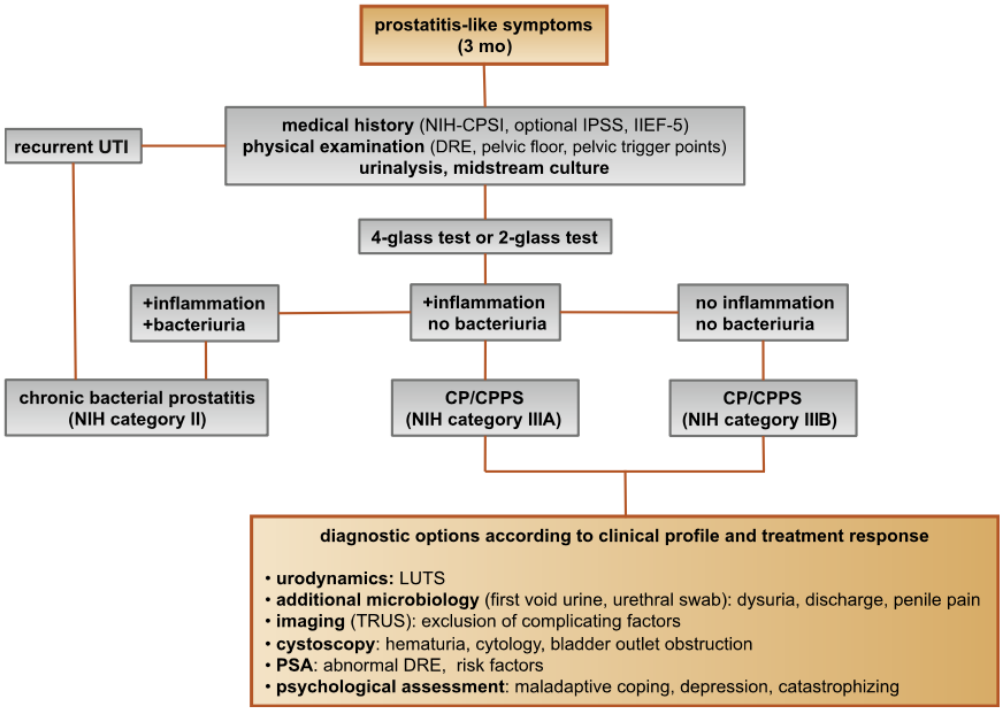

Fig. 2 – Diagnostic algorithm for patients with chronic prostatitis-like symptoms.
CP/CPPS = chronic prostatitis/chronic pelvic pain syndrome; DRE = digital rectal examination; IIEF = International Index of Erectile Function; IPSS = International Prostate Symptom Score; LUTS = lower urinary tract symptoms; NIH-CPSI = National Institutes of Health Chronic Prostatitis Symptom Index; PSA = prostate-specific antigen; TRUS = transrectal ultrasound.

massage urine are analyzed for identification and quantification of pathogens and inflammation. A simpler two-glass test is also possible as a reasonably accurate screen for initial evaluation. It involves the investigation of pre– and post–prostate massage urine. It was shown to correlate well with the four-glass test [13]. The four-glass test or two-glass test are used to exclude bacterial infection. Although the detection of leukocytes confirms CP/CPPS type IIIA, in type IIIB no signs of inflammation are observed. The clinical value of this categorization has never been validated. Semen cultures of the ejaculate alone are not sufficient for diagnosis.

Laboratory testing including complete blood count, inflammatory parameters, and serum prostate-specific antigen (PSA) is not recommended to diagnose CP/CPPS. PSA may be considered if patients are at risk for prostate cancer. Transrectal ultrasound is not useful for the diagnosis, unless there is a specific indication in selected patients such as intraprostatic abscess, calcification, or dilatation of seminal vesicles.

Urodynamic studies may be considered in selected patients with voiding/storage symptoms suggestive of bothersome LUTS. Cystoscopy or retrograde urethrography may be considered to rule out bladder outlet obstruction. Figure 2 shows a diagnostic algorithm for patients with prostatitis-like symptoms [9,14].

3.1.3. Treatment of chronic prostatitis/chronic pelvic pain syndrome

Due to the heterogeneity and the still elusive pathophysiology of CP/CPPS, the establishment of effective treatment modalities remains challenging. A multitude of clinical trials failed to identify an efficient primary treatment. Here we present published randomized placebo- or sham-controlled clinical trials using the NIH-CPSI as an objective outcome measure (Table 2).

3.1.3.1. Antibiotics. Antibiotics have been proposed as an option for the treatment of CP/CPPS. But recommendations were based on empirical experience rather than evidence-based studies. Three RCTs were eligible for inclusion. Six-week courses of therapy with ciprofloxacin (500 mg 2 times per day) [15] or levofloxacin (500 mg 4 times per day) [16] did not result in a statistically significant treatment response measured by the NIH-CPSI compared with placebo. Both studies were of good quality but apparently underpowered. The clinical trial by Zhou et al compared the efficiency of a treatment with tetracycline (500 mg 2 times per day) over 12 wk versus placebo [17]. Despite some quality issues, the authors report a significant mean decrease of 18.5 points in the NIH-CPSI after treatment. Altogether the available RCTs failed to support the recommendation to use antimicrobial agents as a primary treatment option.

Table 2 – Included randomized clinical trials for treatment of chronic prostatitis/chronic pelvic pain syndrome

Treatment	Duration	Patients, *n*	Basic mean NIH-CPSI total score	Mean change	Significance	Jadad total score	Reference
Antibiotics							
Ciprofloxacin	6 wk	49	24.2	−6.2	No ($p > 0.05$)		
vs							
tamsulosin		49	24.6	−4.4			
vs						≥3	[15]
combination		49	25.3	−4.1			
vs							
placebo		49	25.0	−.4			
Levofloxacin	6 wk	45	24.4	−5.6	No ($p > 0.05$)	≥3	[16]
vs							
placebo		35	21.3	−3.1			
Tetracycline	12 wk	24	35.6	−8.5	Yes ($p < 0.01$)	<3	[17]
vs							
placebo		24	NR	NR			
α-Blockers							
Tamsulosin	6 wk	27	26.4	−9.1	Yes ($p < 0.05$)	≥3	[19]
vs							
placebo		30	26.2	−5.5			
Alfuzosin	12 wk	138	23.8	−7.1	No ($p > 0.05$)	≥3	[20]
vs							
placebo		134	25.1	−6.5			
Silodosin 8 mg	12 wk	45	26.8	−10.2	Yes ($p < 0.05$)		
vs							
silodosin 4 mg		52	26.0	−12.1		≥3	[18]
vs							
placebo		54	27.9	−8.5			
Doxazosin	24 wk	30	23.1	−10.6	Yes ($p < 0.001$)		
vs							
DIT		30	21.9	−10.2		<3	[23]
vs							
placebo		30	22.9	−0.7			
Terazosin	14 wk	43	25.1	−14.3	Yes ($p = 0.01$)		
vs						<3	[22]
placebo		43	27.2	−10.2			
Alfuzosin	24 wk	17	26.0	−9.9	Yes ($p = 0.01$)		
vs						<3	[21]
placebo		20	23.0	−3.8			
Anti-inflammatories							
Rofecoxib 25 mg	6 wk	53	22.5	−4.9	No ($p > 0.05$)		
vs							
rofecoxib 50 mg		49	20.5	−6.2		≥3	[24]
vs							
placebo		59	22.9	−4.2			
Prednisolone	4 wk	9	25.5	NR	No ($p > 0.05$)		
vs						≥3	[26]
placebo		12	23.4				
Celecoxib	6 wk	32	23.9	−8.0	Yes ($p < 0.015$)		
vs						≥3	[27]
placebo		32	24.3	−4.8			
Tanezumab	Single dose	30	25.0	−4.3	No ($p > 0.05$)		
vs						<3	[25]
placebo		32	26.0	−2.8			
Zafirlukast	4 wk	10	22.4	−4.6	No ($p > 0.05$)		
vs						≥3	[28]
placebo		7	23.4	−8.1			
OM-89	12 mo	94	21.8	−10.4	No ($p > 0.05$)		
vs						≥3	[29]
placebo		91	23.0	−9.8			
Hormonal agents							
Finasteride	24 wk	33	20.1	−3.0	No ($p > 0.05$)		
vs						≥3	[30]
placebo		31	22.5	−0.8			
Mepartricin	60 d	13	25.0	−15.0	Yes ($p < 0.01$)		
vs						≥3	[31]
placebo		13	25.0	−5.0			
Phytotherapy							
Cernilton	12 wk	70	19.3	−7.7	Yes ($p < 0.05$)		
vs						≥3	[33]
placebo		69	20.3	−5.2			

Table 2 (*Continued*)

Treatment	Duration	Patients, *n*	Basic mean NIH-CPSI total score	Mean change	Significance	Jadad total score	Reference
Quercetin	4 wk	15	21.0	−7.9	Yes ($p < 0.01$)	≥3	[32]
vs placebo		13	20.2	−1.4			
Neuromodulation							
Pregabalin	6 wk	218	26.2	−6.5	No ($p > 0.05$)	≥3	[34]
vs placebo		106	25.9	−4.3			
Modulation of bladder physiology							
Pentosan polysulfate	16 wk	51	27.1	−5.9	No ($p > 0.05$)	≥3	[36]
vs placebo		49	25.8	−3.2			
Physical therapy							
GTM	10 wk	11	25.8	−6.8	No ($p > 0.05$)	≥3	[37]
vs MPT		12	33.5	−14.4			
PTNS	12 wk	45	23.6	−13.4	Yes ($p < 0.001$)	<3	[38]
vs sham		44	22.8	−1.4			
Acupuncture	10 wk	44	24.8	−10.3	Yes ($p < 0.05$)	≥3	[39]
vs sham		45	25.2	−6.2			
Electroacupuncture	6 wk	12	26.9	−9.5	Yes ($p < 0.001$)	≥3	[40]
vs sham		12	25.5	−3.5			
vs control		12	28.0	−3.5			
ESWT	4 wk	30	23.2	−3.5	Yes ($p < 0.05$)	≥3	[41]
vs sham		30	25.1	−0.1			
Aerobic exercise	18 wk	52	21.9	−7.4	Yes ($p < 0.05$)	<3	[43]
vs sham		51	23.0	−4.8			
SEMT	16 wk	30	25.8	−7.2	No ($p > 0.05$)	≥3	[42]
vs sham		30	25.2	−4.6			

DIT = doxazosin plus ibuprofen plus thiocolchicoside; ESWT = extracorporeal shock wave therapy; GTM = global therapeutic massage; MPT = myofascial physical therapy; NIH-CPSI = National Institutes of Health Chronic Prostatitis Symptom Index; PTNS = posterior tibial nerve stimulation; SEMT = sono-electromagnetic therapy.

3.1.3.2. α-Blockers. Seven RCTs investigating the benefit of a monotherapy with α-adrenergic receptor blockers versus placebo met the criteria for inclusion [15,18–23]. The outcomes regarding clinical efficiency determined by NIH-CPSI were quite heterogeneous. Smaller trials evaluating a course of at least 12 wk with different α-blockers provided evidence for positive clinical response [18,21–23], whereas most studies analyzing a shorter duration of 6 wk did not confirm a therapeutic benefit. Of note, clinical trials testing the α-blocker tamsulosin versus placebo over 6 wk in a comparable study population with similar baseline characteristics revealed different clinical outcomes. On the one hand, the study by Alexander et al [15] failed to prove clinical efficiency; on the other hand, the trial by Nickel and colleagues supported the use of tamsulosin [19]. Due to the heterogeneity of published data, α-blockers cannot be recommended as first-line monotherapy. However, a prolonged treatment of 12 wk in patients with bothersome LUTS and no prior treatment with α-blockers may be considered in a multimodal therapeutic regimen.

3.1.3.3. Anti-inflammatories. A role of inflammation and immune dysfunction has been proposed for the pathophysiology of CPPS and appears to be evident for CP/CPPS NIH category IIIA. Five RCTs have been included that evaluated the therapeutic effect of anti-inflammatory agents [24–29]. Various approaches have been subjected to clinical trials. Interestingly, only two studies exclusively analyzed category type IIIA. Among the two trials investigating the cyclooxygenase-2 inhibitors rofecoxib (25 mg or 50 mg 4 times per day) [24] and celecoxib (200 mg 4 times per day) [27] over 6 wk compared with placebo, only the study by Zhao et al was able to reveal clinical efficiency of celecoxib in patients diagnosed with CPPS type IIIA. But this treatment response was limited to the duration of therapy. Two weeks after treatment, no clinical improvement was observed.

A reducing course of oral prednisolone over 4 wk failed to demonstrate therapeutic efficiency [26]. Neither tanezumab [25], a humanized monoclonal antibody directed against nerve growth factor, nor zafirlukast [28], a leukotriene antagonist, were able to demonstrate superiority over

placebo. In addition, OM-89, a modified preparation of lysed pathogenic *Escherichia coli*, was evaluated as an immunostimulating agent for the treatment of patients with CP/CPPS [29]. Again, no statistically significant difference was observed between treatment arm and placebo group with regard to clinical efficacy. To conclude, clinical trials strongly suggest that a monotherapy with anti-inflammatory or immunomodulating agents is not effective.

3.1.3.4. Hormonal agents. Two RCTs investigating the impact of hormonal modulation on prostatitis-like symptoms in patients diagnosed with CP/CPPS were selected for inclusion. The clinical trial by Nickel et al evaluated the efficiency of the specific type II 5α-reductase inhibitor finasteride versus placebo in patients with CP/CPPS category IIIA [30]. It represents a standard treatment for LUTS in patients with BPH, but finasteride (5 mg 4 times per day) over 6 mo was not able to significantly improve the clinical outcome in this study population. Another clinical trial by De Rose et al investigated the role of mepartricin, a compound known to decrease estrogen levels in the prostate [31]. This small trial reported a significant clinical improvement measured by the NIH-CPSI after a course of 60 d with mepartricin (40 mg 4 times per day) compared with placebo. Hormonal first-line treatment cannot be recommended according to published data in patients with CP/CPPS.

3.1.3.5. Phytotherapy. Only two RCTs studying the potential role of phytotherapeutic agents were eligible for inclusion. A small trial by Shoskes et al tested the clinical efficiency of quercetin, a bioflavonoid with antioxidative properties [32]. Quercetin (500 mg 2 times per day) over 4 wk provided significant symptomatic amelioration compared with placebo as determined by the NIH-CPSI. Another clinical trial analyzed the therapeutic benefit of cernilton, a standardized pollen extract [33]. A 12-week course of cernilton (two capsules every 8 h) led to a significant improvement of the NIH-CPSI score compared with placebo. Therefore, clinical evidence qualifies certain phytotherapeutic agents as a treatment modality. With only very few side effects, they can be recommended as primary therapy or a combination in multimodal treatment regimens.

3.1.3.6. Neuromodulatory therapy. Because pain is the dominant symptom in CP/CPPS, analgesic neuromodulatory agents appear to be a promising approach. Only one RCT investigated the benefit of an oral course of pregabalin in increasing dosages (from 150 mg to 600 mg daily) over 6 wk [34]. An adequate treatment response was confirmed by NIH-CPSI for the pain subdomain, but at the same time neurologic side effects were more frequent in the pregabalin group. This therapeutic regimen failed to demonstrate a significant clinical benefit over placebo based on an analysis of the primary end point, although important secondary outcomes were positive [35]. Thus published data do not recommend pregabalin as a first-line single treatment of CP/CPPS.

3.1.3.7. Modulation of bladder physiology. On the assumption of a common pathophysiologic origin of conditions causing pelvic pain syndromes like interstitial cystitis/bladder pain syndrome (IC/BPS) and CP/CPPS, one RCT evaluated the effect of pentosan polysulfate (300 mg 3 times per day), a medication indicated for IC/BPS, over 16 wk compared with placebo in patients diagnosed with CP/CPPS [36]. This trial observed a positive treatment response in the treatment arm with regard to NIH-CPSI domains, but it did not reach statistical significance compared with the placebo group. According to clinical evidence, pentosan polysulfate cannot be recommended as a first-line treatment of patients with CP/CPPS.

3.1.3.8. Physical therapy. Physiotherapeutic approaches have been shown to provide moderate clinical relief in pain syndromes associated with skeletal muscle dysfunction. With regard to CP/CPPS, various modalities like myofascial physical therapy [37], percutaneous posterior tibial nerve stimulation (PTNS) [38], acupuncture or electroacupuncture [39,40], perineal extracorporeal shock wave therapy (ESWT) [41], sono-electro-magnetic therapy (SEMT) [42], or aerobic exercise [43] have been evaluated in randomized sham-controlled trials. A randomized feasibility trial of myofascial physical therapy by Fitzgerald et al included both patients diagnosed with IC/BPS and CP/CPPS [37]. Myofascial physical therapy displayed a relevant mean decrease of 14.4 points in the NIH-CPSI total score after 10 wk of direct physiotherapy. Compared with an unspecific global therapeutic massage (sham group), this change did not reach statistical significance.

Trials evaluating the clinical benefit of perineal ESWT and PTNS in patients diagnosed with CP/CPPS type IIIB indicated a statistically relevant improvement measured by the NIH-CPSI total score. SEMT showed no significant difference in the NIH-CPSI total score after 16 wk compared with the placebo procedure, but it revealed a therapeutic benefit for the quality-of-life subscore as a secondary outcome.

Acupuncture proved to be efficient after 10 wk of treatment versus the sham group, but this first improvement appeared not to be durable in the course of follow-up. Electroacupuncture suggested a statistically significant benefit in the pain subdomain compared with the control group. However, no relevant change was observed for the total NIH-CPSI score.

Another trial investigated the influence of a course of 18 wk of physical training on the clinical outcome of a patient diagnosed with CP/CPPS. A specific aerobic exercise and an unspecific stretching and motion exercise (sham control) were established and evaluated. Aerobic exercise turned out to be superior to the control group as measured by a validated Italian version of the NIH-CPSI questionnaire. Pain in particular was significantly improved in the group performing aerobic exercise. The heterogeneity of clinical data available and methodologic difficulties in conducting RCTs for this kind of treatment modality do not allow to give a recommendation for specific physiotherapeutic options as a primary intervention. More sham-controlled studies are needed. Nevertheless, published results suggest that at least subgroups of patients diagnosed with CP/CPPS may profit from physical therapy.

3.1.3.9. Combination therapy. The previous discussion revealed quite impressively our dilemma with randomized controlled studies evaluating the effectiveness of monotherapies we considered to be helpful. Clinical trials of good quality but apparently underpowered reported the traditional first-line treatments as failures. Interestingly, randomized controlled studies investigating uncommon approaches like phytotherapies confirmed significant clinical efficacy. Only a few trials addressed the impact of combination therapies. The trial by Alexander et al investigated the influence of a monotherapy with ciprofloxacin (500 mg 2 times per day) or tamsulosin (0.4 mg 4 times per day) or a combination of ciprofloxacin and tamsulosin versus placebo [15]. After a treatment course of 6 wk, neither the monotherapies nor the combination were superior to placebo.

The placebo-controlled trial by Tugcu et al randomized 90 patients diagnosed with CP/CPPS category IIIB to receive doxazosin (4 mg 4 times per day), a triple therapy consisting of doxazosin (4 mg 4 times per day), the anti-inflammatory ibuprofen (400 mg 4 times per day), and the muscle relaxant thiocolchicoside (12 mg four times per day), or a placebo once per day [23]. After a therapy course of 6 mo, the single treatment with doxazosin was equally effective as the triple therapy. Both treatment arms were significantly superior to the placebo group, and clinical outcome was stable after an additional 6 mo of follow-up.

3.1.3.10. Meta-analysis. Throughout this review readers might wonder why well-conducted clinical trials evaluating the same therapeutic options result in this heterogeneity of clinical outcomes. How can a general recommendation be formulated for the successful management of CP/CPPS? Published data of randomized placebo/sham-controlled trials were pooled and subjected to meta-analysis [6,7]. No recommendations for monotherapies can be made based on these results. Data suggest that the combination of α-blockers and antibiotics may have a decent therapeutic effect with regard to symptom scores for selected patients [6]. However, certain limitations have to be taken into account when data synthesis in the form of a meta-analysis is performed. Some studies represent small single-center trials with inadequate control groups and blinding. According to basic characteristics, duration of disease and prior treatments are not documented. This makes the interpretation of this heterogeneous pool of data difficult and needs to be considered when recommendations are formulated.

3.1.3.11. Phenotypically directed multimodal management: UPOINTs. UPOINT represents a novel 6-point clinical phenotyping system for the management of CP/CPPS. It profiles patients and indicates individual treatment targets to implement an individualized multimodal therapeutic regimen. The six UPOINT domains comprise *U*rinary symptoms, *P*sychological dysfunction, *O*rgan-specific symptoms, *I*nfection, *N*eurologic/systemic conditions, and *T*enderness of muscles (Fig. 3) [44–47]. UPOINT is able to discriminate clinical phenotypes, and positive domains appear to correlate with symptom severity and duration of disease [45]. Clinical results indicate a correlation between the number of positive UPOINT domains and total NIH-CPSI score [48,49]. With sexual dysfunction as a common condition affecting 40–70% of men with CP/CPPS [50–54], the inclusion of an additional domain for *S*exual dysfunction was proposed and evaluated. The modified UPOINTs algorithm has been suggested to support an optimized stratification of individual phenotypic profiles. However, clinical studies attempting to confirm an improved correlation between positive UPOINTs domains and symptom severity revealed heterogeneous results [48,55–57].

Most clinical trials conducted so far speak in favor of the extended UPOINTs approach. First studies suggest that the multimodal treatment guided by UPOINT leads to a significant improvement of symptoms and quality of life [58]. In a prospective study including a cohort of 100 men positive for a minimum of three UPOINT domains, clinical response to a phenotypically directed multimodal treatment was evaluated by a change in NIH-CPSI score. Almost 84% of patients met the primary end point of at least a 6-point change in total NIH-CPSI score with a median follow-up of 50 wk. All NIH-CPSI subdomains comprising scores for pain, urinary symptoms, and quality of life were significantly improved (each $p < 0.0001$). Although first results are promising, further clinical RCTs are warranted for a complete validation of the UPOINTs approach. Categorization and treatment options directed by UPOINTs phenotype are depicted in Figure 3.

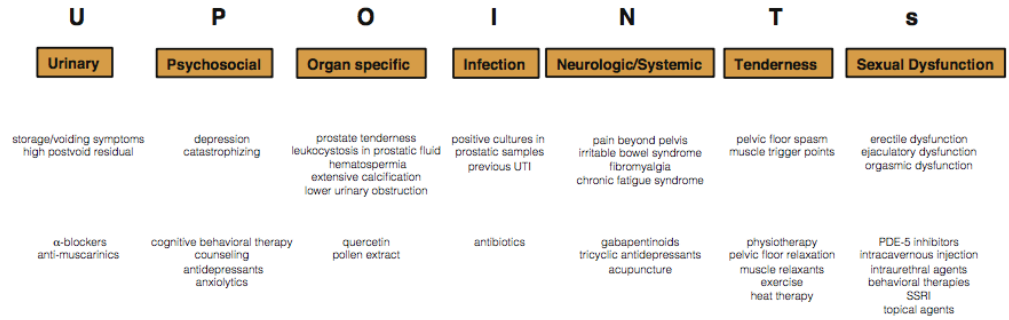

Fig. 3 – Phenotypically directed multimodal management UPOINTs. Adapted with permission from Springer [47].
PDE5 = phosphodiesterase type 5; SSRI = selective serotonin reuptake inhibitor.

3.2. *Clinical practice*

In this section we introduce three index patients diagnosed with CP/CPPS. This selection may represent the most frequent clinical presentations in daily routine. Applying the UPOINTs algorithm, we have formulated our best practice recommendations based on published data in concert with expert opinion.

3.2.1. *Case 1*

A 42-year-old man presents with modest perineal discomfort radiating to both testicles. He complains about hesitancy and a slow stream. In the last 2 yr he had two episodes of an acute bacterial prostatitis that were treated with an antimicrobial for 2 wk each time. The patient explains that sometimes his symptoms flare up and resolve partially on antibiotics. On digital rectal examination (DRE), the prostate feels slightly enlarged, and the patient reports moderate tenderness to palpation. Laboratory testing including PSA and C-reactive protein (CRP) was normal. A two-glass test is performed, and no pathogen is detected. Post–prostatic massage urine is positive for leukocytes, and microscopy shows an inflammatory pattern. Prostate volume as determined by transrectal ultrasonography is about 30 ml. Peak urinary flow rate is 14 ml/s with a voided urine volume of 300 ml. Postvoid residual urine volume is 80 ml. The patient is on no regular medication.

Table 3 shows the phenotypic evaluation according to UPOINTs and the resulting treatment plan.

3.2.2. *Case 2*

A 46-year-old man presents with modest perineal discomfort. The patient complains about hesitancy and a slow stream, which has been increasing in recent years along with an increase in perineal pain. He wakes up at least three times a night to urinate. He is sexually active and describes post-ejaculatory pain. On DRE the prostate feels normal, but the patient reports moderate tenderness to palpation. Laboratory testing including PSA and CRP is normal. A two-glass test is performed, but no signs of inflammation or bacterial infection are detected. Prostate volume as determined by transrectal ultrasonography is about 30 ml. Peak urinary flow rate is 12 ml/s with a voided urine volume of 250 ml. Postvoid residual urine volume is 120 ml. The patient is on no regular medication.

Table 4 shows the phenotypic evaluation according to UPOINTs and the resulting treatment plan.

Table 3 – Phenotypic evaluation and recommendations on treatment

Diagnosis	CP/CPPS category IIIA
UPOINTs	
U	Hesitancy, weak stream
P	NA
O	Tenderness to palpation, flares
I	NA
N	NA
T	NA
s	NA
Treatment	
U	α-Blockers
O	Pollen extract and/or quercetin, NSAID for flares

CP/CPPS = chronic prostatitis/chronic pelvic pain syndrome; NA = not applicable; NSAID = nonsteroidal anti-inflammatory drug.

Table 4 – Phenotypic evaluation and recommendations on treatment

Diagnosis	CP/CPPS category IIIB
UPOINTs	
U	Hesitancy, weak stream
P	NA
O	Tenderness to palpation, perineal discomfort
I	NA
N	NA
T	Perineal and pelvic muscle tenderness
s	NA
Treatment	
U	α-Blockers
O	Pollen extract and/or quercetin
T	Local heat therapy (cushion, pads), physiotherapy/pelvic floor relaxation

CP/CPPS = chronic prostatitis/chronic pelvic pain syndrome; NA = not applicable.

Table 5 – Phenotypic evaluation and recommendations on treatment

Diagnosis	CP/CPPS category III B
UPOINTs	
U	NA
P	Depression, catastrophizing
O	NA
I	NA
N	Neuropathic pain
T	Perineal and pelvic muscle tenderness
s	NA
Treatment	
P	Psychological support, referral to psychologist (cognitive behavioral therapy), tricyclic antidepressants
N	Pregabalin, tricyclic antidepressants, acupuncture
T	Physiotherapy/pelvic floor relaxation, muscle relaxants

CP/CPPS = chronic prostatitis/chronic pelvic pain syndrome; NA = not applicable.

3.2.3. *Case 3*

A 42-year-old man presents with modest perineal discomfort. Burning sensations are radiating to the abdomen and his back. The patient is anxious about his symptoms and fears a malignant process. His worries and doubts have been progressing in recent years. It started with his diagnosis of irritable bowel syndrome. The development of chronic fatigue syndrome and intermediate episodes of migraine headaches are secondary findings that emerged in the last 3 yr. The patient admits that depressive episodes have become more frequent since the perineal pain started. On DRE the prostate feels normal. The pelvic floor is tender to touch. Laboratory testing including PSA and CRP is normal.

A two-glass test is performed, but no signs of inflammation or bacterial infection are detected. The patient is on no regular medication.

Table 5 shows the phenotypic evaluation according to UPOINTs and the resulting treatment plan.

4. Conclusions

In this comprehensive review we presented our current understanding of best practice management of symptomatic CP/CPPS based on published data in concert with expert opinion. We have not been able to decipher the pathophysiology underlying CP/CPPS to identify common key targets for treatment. This has made the management of this bothersome condition very challenging for both clinicians and patients. Our inability to formulate recommendations with a high grade of evidence for efficient monotherapies reflects the main problem. Scientific reports do not speak in favor of a common etiology applying to all forms of CP/CPPS. A multifactorial genesis appears to contribute to an individual multifaceted complex of symptoms for every patient diagnosed with CP/CPPS. The current understanding of the management of CP/CPPS strongly suggests a multimodal therapeutic approach addressing the individual clinical phenotypic profile. More RCTs are warranted for validation of this phenotype-directed treatment. Although its role for the management of CP/CPPS has still to be defined, it appears to be a promising and effective alternative to the current empirical sequential monotherapy.

Author contributions: Giuseppe Magistro had full access to all the data in the study and takes responsibility for the integrity of the data and the accuracy of the data analysis.

Study concept and design: Magistro, Nickel.
Acquisition of data: Magistro, Wagenlehner, Nickel.
Analysis and interpretation of data: Magistro, Wagenlehner, Grabe, Weidner, Stief, Nickel.
Drafting of the manuscript: Magistro, Wagenlehner, Grabe, Weidner, Stief, Nickel.
Critical revision of the manuscript for important intellectual content: Magistro, Wagenlehner, Grabe, Weidner, Stief, Nickel.
Statistical analysis: None.
Obtaining funding: None.
Administrative, technical, or material support: None.
Supervision: Magistro, Wagenlehner, Nickel.
Other (specify): None.

Financial disclosures: Giuseppe Magistro certifies that all conflicts of interest, including specific financial interests and relationships and affiliations relevant to the subject matter or materials discussed in the manuscript (eg, employment/affiliation, grants or funding, consultancies, honoraria, stock ownership or options, expert testimony, royalties, or patents filed, received or pending), are the following: J. Curtis Nickel is a consultant/researcher for Pfizer, Astellas, Ferring, Farr Laboratories, Taris, Allergan, Aquinox, Lilly, NIH/NIDDK, and CIHR. Florian M.E. Wagenlehner is a consultant/researcher for Astellas, Astra-Zeneca, Bionorica, Calixa, Cerexa, Cernelle, Cubist, Galenus, Leo-Pharma, Merlion, OM-Pharma, Pierre Fabre, Rosen Pharma, and Zambon. The other authors having nothing to disclose.

Funding/Support and role of the sponsor: None.

Appendix A. Supplementary data

Supplementary data associated with this article can be found, in the online version, at http://dx.doi.org/10.1016/j.eururo.2015.08.061.

References

[1] Krieger JN, Lee SW, Jeon J, Cheah PY, Liong ML, Riley DE. Epidemiology of prostatitis. Int J Antimicrob Agents 2008;31(Suppl 1):S85–90.
[2] Krieger JN, Nyberg Jr L, Nickel JC. NIH consensus definition and classification of prostatitis. JAMA 1999;282:236–7.
[3] Yoon BI, Kim S, Han DS, et al. Acute bacterial prostatitis: how to prevent and manage chronic infection? J Infect Chemother 2012;18:444–50.
[4] Litwin MS, McNaughton-Collins M, Fowler Jr FJ, et al. The National Institutes of Health chronic prostatitis symptom index: development and validation of a new outcome measure. Chronic Prostatitis Collaborative Research Network. J Urol 1999;162:369–75.
[5] Wagenlehner FM, Van Till JW, Magri V, et al. National Institutes of Health Chronic Prostatitis Symptom Index (NIH-CPSI) symptom evaluation in multinational cohorts of patients with chronic prostatitis/chronic pelvic pain syndrome. Eur Urol 2013;63:953–9.
[6] Anothaisintawee T, Attia J, Nickel JC, et al. Management of chronic prostatitis/chronic pelvic pain syndrome: a systematic review and network meta-analysis. JAMA 2011;305:78–86.
[7] Cohen JM, Fagin AP, Hariton E, et al. Therapeutic intervention for chronic prostatitis/chronic pelvic pain syndrome (CP/CPPS): a systematic review and meta-analysis. PLoS One 2012;7:e41941.
[8] Moher D, Liberati A, Tetzlaff J, Altman DG. Preferred reporting items for systematic reviews and meta-analyses: the PRISMA statement. J Clin Epidemiol 2009;62:1006–12.
[9] Engeler D, Baranowski AP, Borovicka J, et al. Guidelines on chronic pelvic pain. European Association of Urology Web site. http://uroweb.org/wp-content/uploads/26-Chronic-Pelvic-Pain_LR.pdf. Updated 2015.
[10] Badia X, Garcia-Losa M, Dal-Re R. Ten-language translation and harmonization of the International Prostate Symptom Score: developing a methodology for multinational clinical trials. Eur Urol 1997;31:129–40.
[11] Rosen RC, Riley A, Wagner G, Osterloh IH, Kirkpatrick J, Mishra A. The international index of erectile function (IIEF): a multidimensional scale for assessment of erectile dysfunction. Urology 1997;49:822–30.
[12] Meares EM, Stamey TA. Bacteriologic localization patterns in bacterial prostatitis and urethritis. Invest Urol 1968;5:492–518.
[13] Nickel JC, Shoskes D, Wang Y, et al. How does the pre-massage and post-massage 2-glass test compare to the Meares-Stamey 4-glass test in men with chronic prostatitis/chronic pelvic pain syndrome? J Urol 2006;176:119–24.
[14] Grabe M, Bartoletti R, Bjerklund Johansen TE, et al. Guidelines on urological infections. European Association of Urology Web site. http://uroweb.org/wp-content/uploads/19-Urological-infections_LR2.pdf. Updated 2015.
[15] Alexander RB, Propert KJ, Schaeffer AJ, et al. Ciprofloxacin or tamsulosin in men with chronic prostatitis/chronic pelvic pain syndrome: a randomized, double-blind trial. Ann Intern Med 2004;141:581–9.
[16] Nickel JC, Downey J, Clark J, et al. Levofloxacin for chronic prostatitis/chronic pelvic pain syndrome in men: a randomized placebo-controlled multicenter trial. Urology 2003;62:614–7.
[17] Zhou Z, Hong L, Shen X, et al. Detection of nanobacteria infection in type III prostatitis. Urology 2008;71:1091–5.

[18] Nickel JC, O'Leary MP, Lepor H, et al. Silodosin for men with chronic prostatitis/chronic pelvic pain syndrome: results of a phase II multicenter, double-blind, placebo controlled study. J Urol 2011; 186:125–31.
[19] Nickel JC, Narayan P, McKay J, Doyle C. Treatment of chronic prostatitis/chronic pelvic pain syndrome with tamsulosin: a randomized double blind trial. J Urol 2004;171:1594–7.
[20] Nickel JC, Krieger JN, McNaughton-Collins M, et al. Alfuzosin and symptoms of chronic prostatitis-chronic pelvic pain syndrome. N Engl J Med 2008;359:2663–73.
[21] Mehik A, Alas P, Nickel JC, Sarpola A, Helstrom PJ. Alfuzosin treatment for chronic prostatitis/chronic pelvic pain syndrome: a prospective, randomized, double-blind, placebo-controlled, pilot study. Urology 2003;62:425–9.
[22] Cheah PY, Liong ML, Yuen KH, et al. Terazosin therapy for chronic prostatitis/chronic pelvic pain syndrome: a randomized, placebo controlled trial. J Urol 2003;169:592–6.
[23] Tugcu V, Tasci AI, Fazlioglu A, et al. A placebo-controlled comparison of the efficiency of triple- and monotherapy in category III B chronic pelvic pain syndrome (CPPS). Eur Urol 2007;51:1113–7.
[24] Nickel JC, Pontari M, Moon T, et al. A randomized, placebo controlled, multicenter study to evaluate the safety and efficacy of rofecoxib in the treatment of chronic nonbacterial prostatitis. J Urol 2003;169:1401–5.
[25] Nickel JC, Atkinson G, Krieger JN, et al. Preliminary assessment of safety and efficacy in proof-of-concept, randomized clinical trial of tanezumab for chronic prostatitis/chronic pelvic pain syndrome. Urology 2012;80:1105–10.
[26] Bates SM, Hill VA, Anderson JB, et al. A prospective, randomized, double-blind trial to evaluate the role of a short reducing course of oral corticosteroid therapy in the treatment of chronic prostatitis/chronic pelvic pain syndrome. BJU Int 2007;99:355–9.
[27] Zhao WP, Zhang ZG, Li XD, et al. Celecoxib reduces symptoms in men with difficult chronic pelvic pain syndrome (category IIIA). Braz J Med Biol Res 2009;42:963–7.
[28] Goldmeier D, Madden P, McKenna M, Tamm N. Treatment of category III A prostatitis with zafirlukast: a randomized controlled feasibility study. Int J STD AIDS 2005;16:196–200.
[29] Wagenlehner FM, Ballarini S, Naber KG. Immunostimulation in chronic prostatitis/chronic pelvic pain syndrome (CP/CPPS): a one-year prospective, double-blind, placebo-controlled study. World J Urol 2014;32:1595–603.
[30] Nickel JC, Downey J, Pontari MA, Shoskes DA, Zeitlin SI. A randomized placebo-controlled multicentre study to evaluate the safety and efficacy of finasteride for male chronic pelvic pain syndrome (category IIIA chronic nonbacterial prostatitis). BJU Int 2004;93: 991–5.
[31] De Rose AF, Gallo F, Giglio M, Carmignani G. Role of mepartricin in category III chronic nonbacterial prostatitis/chronic pelvic pain syndrome: a randomized prospective placebo-controlled trial. Urology 2004;63:13–6.
[32] Shoskes DA, Zeitlin SI, Shahed A, Rajfer J. Quercetin in men with category III chronic prostatitis: a preliminary prospective, double-blind, placebo-controlled trial. Urology 1999;54:960–3.
[33] Wagenlehner FM, Schneider H, Ludwig M, Schnitker J, Brahler E, Weidner W. A pollen extract (Cernilton) in patients with inflammatory chronic prostatitis-chronic pelvic pain syndrome: a multicentre, randomised, prospective, double-blind, placebo-controlled phase 3 study. Eur Urol 2009;56:544–51.
[34] Pontari MA, Krieger JN, Litwin MS, et al. Pregabalin for the treatment of men with chronic prostatitis/chronic pelvic pain syndrome: a randomized controlled trial. Arch Intern Med 2010;170:1586–93.
[35] Aboumarzouk OM, Nelson RL. Pregabalin for chronic prostatitis. Cochrane Database Syst Rev 2012:CD009063.
[36] Nickel JC, Forrest JB, Tomera K, et al. Pentosan polysulfate sodium therapy for men with chronic pelvic pain syndrome: a multicenter, randomized, placebo controlled study. J Urol 2005;173:1252–5.
[37] FitzGerald MP, Anderson RU, Potts J, et al. Randomized multicenter feasibility trial of myofascial physical therapy for the treatment of urological chronic pelvic pain syndromes. J Urol 2009;182:570–80.
[38] Kabay S, Kabay SC, Yucel M, Ozden H. Efficiency of posterior tibial nerve stimulation in category IIIB chronic prostatitis/chronic pelvic pain: a Sham-Controlled Comparative Study. Urol Int 2009;83: 33–8.
[39] Lee SW, Liong ML, Yuen KH, et al. Acupuncture versus sham acupuncture for chronic prostatitis/chronic pelvic pain. Am J Med 2008;121:79–87.
[40] Lee SH, Lee BC. Electroacupuncture relieves pain in men with chronic prostatitis/chronic pelvic pain syndrome: three-arm randomized trial. Urology 2009;73:1036–41.
[41] Zimmermann R, Cumpanas A, Miclea F, Janetschek G. Extracorporeal shock wave therapy for the treatment of chronic pelvic pain syndrome in males: a randomised, double-blind, placebo-controlled study. Eur Urol 2009;56:418–24.
[42] Kessler TM, Mordasini L, Weisstanner C, et al. Sono-electromagnetic therapy for treating chronic pelvic pain syndrome in men: a randomized, placebo-controlled, double-blind trial. PLoS One 2014;9:e113368.
[43] Giubilei G, Mondaini N, Minervini A, et al. Physical activity of men with chronic prostatitis/chronic pelvic pain syndrome not satisfied with conventional treatments–could it represent a valid option? The physical activity and male pelvic pain trial: a double-blind, randomized study. J Urol 2007;177:159–65.
[44] Nickel JC, Shoskes D. Phenotypic approach to the management of chronic prostatitis/chronic pelvic pain syndrome. Curr Urol Rep 2009;10:307–12.
[45] Shoskes DA, Nickel JC, Dolinga R, Prots D. Clinical phenotyping of patients with chronic prostatitis/chronic pelvic pain syndrome and correlation with symptom severity. Urology 2009;73:538–42.
[46] Shoskes DA, Nickel JC, Rackley RR, Pontari MA. Clinical phenotyping in chronic prostatitis/chronic pelvic pain syndrome and interstitial cystitis: a management strategy for urologic chronic pelvic pain syndromes. Prostate Cancer Prostatic Dis 2009;12:177–83.
[47] Shoskes DA, Nickel JC. Classification and treatment of men with chronic prostatitis/chronic pelvic pain syndrome using the UPOINT system. World J Urol 2013;31:755–60.
[48] Magri V, Wagenlehner F, Perletti G, et al. Use of the UPOINT chronic prostatitis/chronic pelvic pain syndrome classification in European patient cohorts: sexual function domain improves correlations. J Urol 2010;184:2339–45.
[49] Hedelin HH. Evaluation of a modification of the UPOINT clinical phenotype system for the chronic pelvic pain syndrome. Scand J Urol Nephrol 2009;43:373–6.
[50] Magri V, Perletti G, Montanari E, Marras E, Chiaffarino F, Parazzini F. Chronic prostatitis and erectile dysfunction: results from a cross-sectional study. Arch Ital Urol Androl 2008;80:172–5.
[51] Beutel ME, Weidner W, Brahler E. Chronic pelvic pain and its comorbidity [in German]. Urologe A 2004;43:261–7.
[52] Trinchieri A, Magri V, Cariani L, et al. Prevalence of sexual dysfunction in men with chronic prostatitis/chronic pelvic pain syndrome. Arch Ital Urol Androl 2007;79:67–70.
[53] Mehik A, Hellstrom P, Sarpola A, Lukkarinen O, Jarvelin MR. Fears, sexual disturbances and personality features in men with prostatitis: a population-based cross-sectional study in Finland. BJU Int 2001;88:35–8.
[54] Lee SW, Liong ML, Yuen KH, et al. Adverse impact of sexual dysfunction in chronic prostatitis/chronic pelvic pain syndrome. Urology 2008;71:79–84.

[55] Davis SN, Binik YM, Amsel R, Carrier S. Is a sexual dysfunction domain important for quality of life in men with urological chronic pelvic pain syndrome? Signs "UPOINT" to yes. J Urol 2013;189:146–51.
[56] Samplaski MK, Li J, Shoskes DA. Inclusion of erectile domain to UPOINT phenotype does not improve correlation with symptom severity in men with chronic prostatitis/chronic pelvic pain syndrome. Urology 2011;78:653–8.
[57] Zhao Z, Zhang J, He J, Zeng G. Clinical utility of the UPOINT phenotype system in Chinese males with chronic prostatitis/chronic pelvic pain syndrome (CP/CPPS): a prospective study. PLoS One 2013;8:e52044.
[58] Shoskes DA, Nickel JC, Kattan MW. Phenotypically directed multimodal therapy for chronic prostatitis/chronic pelvic pain syndrome: a prospective study using UPOINT. Urology 2010;75:1249–53.